Original Research Article

Development and validation of an HPLC-UV method for analysis of methylphenidate hydrochloride and loxapine succinate in an activated carbon disposal system

Pooja Bakshi [a], Andrew Korey [b], William Fowler [b], Ajay K. Banga [a,*]

[a] Department of Pharmaceutical Sciences, Mercer University, Atlanta, GA 30341, USA
[b] Verde Environmental Technologies, 12900 Whitewater Drive, Minnetonka, MN 55343, USA

ABSTRACT

Unused medications have the possibility of being abused, causing serious harm to individuals who were not prescribed the drug. The Food and Drug Administration (FDA) recommends the proper disposal of unused prescribed medications to maintain safety and prevent environmental hazards. However, many of the current disposal techniques do not properly address safety. A drug disposal pouch containing granular activated carbon offers a unique disposal method to deactivate residual or expired medication in a convenient, effective, and safe manner. A robust and validated method for methylphenidate hydrochloride and loxapine succinate was developed using high-performance liquid chromatography (HPLC) and the deactivation efficiency of the disposal system was tested. Methylphenidate hydrochloride was analyzed on a C_{18} analytical column (250 mm × 4.60 mm, 100Å) using acetonitrile-water (0.05% (v/v) trifluoroacetic acid) as the mobile phase at a flow rate of 1.0 mL/min with a run time of 15 min and retention time of 7.8 min. Loxapine succinate was separated on a C_8 100Å (250 mm × 4.6 mm, 5 μm) column maintained at 25 °C using a flow rate of 1.0 mL/min. The run time was 10 min and the retention time of the drug was around 4.6 min. Mobile phase was composed of acetonitrile and water (0.3% triethylamine) at pH 3.0 as 40:60 (v/v). Reference standard solutions (100 μg/mL) for both drugs were prepared by dissolving in mobile phases. These methods provide good linearity ($R^2 = 0.999$) over the range of 5–100 μg/mL for methylphenidate hydrochloride and 0.1–100 μg/mL for loxapine succinate. The assay methods were successfully applied to study the deactivation of these drugs.

© 2018 Xi'an Jiaotong University. Production and hosting by Elsevier B.V. This is an open access article under the CC BY-NC-ND license (http://creativecommons.org/licenses/by-nc-nd/4.0/).

1. Introduction

Proper disposal of unused prescription medications has become a significant problem. Storage of expired and unwanted medications can lead to either accidental exposure or intentional use or abuse of prescription medications. The potential for misuse and addiction to prescription medications, such as those for pain, is a national health concern that has social and economic implications. In 2015, over 33,000 Americans died as a result of opioid overdose or substance abuse disorders related to prescription of opioid pain medications, and 591,000 suffered from addiction to heroin [1,2]. Although prescription medications play an important role in the treatment of severe and acute chronic pain conditions, due to their over prescription or prescription without adequate safeguards, their misuse can have devastating effects. According to the National Survey on Drug Use and Health, fewer than four percent of people who had

used prescription painkillers non-medically started using heroin within five years [1]. Thus, the proper disposal of prescription medication is important. In the present study, we focused on the disposal of two psychoactive medications, methylphenidate hydrochloride (MPH) and loxapine succinate.

MPH is a common prescription medication used for treating attention-deficit hyperactivity disorder (ADHD), and affects the dopamine balance in the brain by stimulating the nervous system [3]. The pharmacological action of MPH through the intranasal route is similar to that of cocaine, which causes rapid release of dopamine [4]. It is listed as a Schedule II, federally-controlled substance because of its high potential for abuse, which is similar to morphine and may lead to severe physiological dependence. This effect of intensely gratifying euphoria makes MPH very addictive [5]. Another drug which has potential for abuse is loxapine succinate. It is a tricyclic, antipsychotic prescription medication, which is used for treating schizophrenia. Loxapine succinate exerts its action by blocking the action of dopamine, and is thus used to manage emotions and actions that are usually accompanied with schizophrenia. Loxapine succinate has a potential of being abused,

as it only provides temporary relief and is used for the management of schizophrenia [6]. Both drugs are prescribed frequently and thus have increased the potential for abuse.

Since MPH and loxapine succinate have a high potential for abuse, we wanted to investigate their deactivation profile using drug disposal system. The analytical accuracy of the method developed for both drugs was also tested. In the literature, there are few analytical methods reported for the determination of MPH [7,8] and loxapine succinate [9]. All the available methods are time consuming and expensive and use liquid chromatography–mass spectrometry (LC–MS) or high-performance liquid chromatography (HPLC) with multiple solvents as mobile phases. Consequently, there is a need to develop a simple, sensitive, economical, and time-efficient method for the determination of MPH and loxapine succinate in dosage forms (tablets and capsules). Therefore, we developed an easy and reproducible reverse-phase HPLC (RP-HPLC) for the estimation of MPH and loxapine succinate in dosage forms by following the International Council for Harmonization (ICH) of Technical Requirements for Registration of Pharmaceuticals for Human Use validation guidelines [10]. This method allowed us to investigate deactivation of MPH and loxapine succinate in the presence of activated carbon, as well as test the stability of the drug under different storage conditions.

One of the ways by which accidental exposure of unneeded medicines can be avoided is through the "medicine take back program." This program offers safe disposal of most types of unneeded prescription medicines [11]. If no medicine takeback programs or DEA-authorized collectors are available, the easiest way to dispose of these medications in household trash is by mixing these medications with an unpalatable substance such as dirt, cat litter, or coffee grounds. Medications that pose a potential threat can be flushed down the toilet. To minimize the accidental exposure and misuse of these prescription medications, the Food and Drug Administration (FDA) has developed several guidelines to encourage the proper disposal of these medicines, as mentioned in the FDA recommendations for drug disposal [12]. Still, there are some medicines, for example, fentanyl patches, that may be harmful, and, in some cases, fatal with just one dose, especially if they are used by someone other than the person for whom the medicine was prescribed [13]. All the above mentioned procedures do not actually make the drug inactive, and have harmful effects on the environment as the mixing of these medications with the cat litter or coffee grounds cannot deactivate the drug, and can lead to contamination of the water system [14].

Activated carbon is one of the best alternatives to dispose of medications, as it attracts and holds the organic compounds by the adsorption process [15]. Due to its property of material porosity, active pharmaceutical ingredient (API) easily sticks to the surface area [16]. However, this technology has not been explored to address the drug disposal problem, and there is a pressing need for more research on effective disposal techniques for highly addictive prescription medications.

In the present study, we aimed to evaluate the deactivation efficiency of the activated carbon-based drug disposal system, Deterra®. This drug deactivation system is based on MAT$_{12}$® Molecular Adsorption Technology, which deactivates the API by a physical adsorption process [17]. The term "deactivates" is used to signify the irreversible physical adsorption process between active substance and activated carbon. We investigated the drug disposal of two model psychoactive prescription medications which have a potential of abuse, MPH and loxapine succinate.

The proposed drug deactivation system offers a unique disposal method to deactivate unused, residual or expired medications by using granular activated carbon within a pouch that is convenient, safe and effective. This study is aimed to investigate the deactivation profile of MPH and loxapine succinate using an activated carbon disposal system. Successful method development and validation of MPH and loxapine succinate was performed to test the efficiency of this system precisely.

2. Experimental

2.1. Chemicals and reagents

MPH and loxapine succinate were purchased from Sigma-Aldrich (St. Louis, MO, USA). Dosage forms: generic MPH (20 mg, CorePharma) tablets and loxapine succinate (20 mg, Lannett) capsules were provided by Verde Environmental Technologies Inc. (Minnetonka, MN, USA). The Deterra® drug deactivation system (the pouch containing 15 g of granular activated carbon within a water soluble film reservoir) was also provided by Verde Environmental Technologies Inc. Acetonitrile (ACN), methanol and trifluoroacetic acid (TFA), of HPLC grade, were obtained from Fisher Scientific (Pittsburgh, PA, USA). Nylon filters (0.22 μm) used for sample filtration were purchased from Medsupply Partners (Atlanta, GA, USA). Deionized water (DI) (MQ res: 18.2 MΩ·cm, permC: 7.4 μS/cm) was generated with a Milli-Q Direct 8 (Millipore, Bedford, MA, USA). All other reagents used were of HPLC or ACS grade.

2.2. Instrumentation

The analysis was carried out using a Waters Alliance HPLC system (e2695 separating module) (Waters Co., Milford, MA, USA) with photodiode array detector (Waters 2996) with an autosampler and column heater. Data were collected and processed using Empower™ software (Version 2) from Waters. RP-HPLC methods were used for the quantification of all samples.

2.3. Chromatographic conditions

The assay method for MPH and loxapine succinate was developed, validated and applied to study the drug deactivation profile of both drugs. This method was also used to predict the storage stability of MPH and loxapine succinate in water. The mobile phase was filtered through a 0.2 μm filter (GNWP 0.2 μm; Millipore, Bedford, MA, USA) and degassed using sonication.

MPH was analyzed using a C$_{18}$ Phenomenex Kinetex, biphenyl (250 mm × 4.6 mm, 100 Å) column set at 25 °C with methanol (0.1% formic acid (FA)) and water (0.1% FA, pH 6.8 adjusted using ammonium hydroxide) (50:50 v/v) as the mobile phase. A flow rate of 1 mL/min with an injection volume of 25 μL and an absorption wavelength of 258 nm were used. The run time was 15 min and the retention time of the drug was around 7.8 min.

For the analysis of loxapine succinate, the compound was separated on a C$_8$ Phenomenex Luna (250 mm × 4.6 mm, 5 μm) at an ambient temperature with acetonitrile (ACN) and water (0.3% (v/v), trimethylamine, pH 3) (40:60 v/v) as the mobile phase. A sample volume of 10 μL was injected at a flow rate of 1 mL/min and analyzed at an absorption wavelength of 211 nm. The run time was 12 min and the retention time of the drug was around 4.6 min.

2.4. Preparation of stock and working standards solutions

All standard solutions for MPH and loxapine succinate were prepared using deionized water to give a working standard in the range of 5–100 μg/mL and 0.1–100 μg/mL, respectively. Stock standard solutions of MPH and loxapine succinate were prepared at a concentration of 1 mg/mL in deionized water and stored at 4 °C. Working standard solutions of MPH and loxapine succinate

were prepared by diluting the standard stock solution with deionized water to yield concentrations of 0.1, 0.25, 0.5, 1, 2.5, 5, 10, 25, 50 and 100 μg/mL. Quality control (QC) concentrations were then prepared at 50, 75 and 100 μg/mL for MPH and 25, 50 and 100 μg/mL for loxapine succinate control samples.

2.5. Method validation

HPLC methods were validated to ensure consistent, reliable, and accurate results to determine the levels of two psychoactive medications in all samples. The HPLC methods were validated in terms of sensitivity, linearity, accuracy, precision, specificity and robustness. Method validations for both drugs were performed over a 3-day period.

2.5.1. Determination of the limit of detection (LOD) and limit of quantification (LOQ)

The LOD was determined by injecting lower concentrations of MPH and loxapine succinate sequentially until a signal (peak)-to-noise ratio was obtained. The LOQ, which is the lowest quantifiable concentration, was also determined from the range of concentrations analyzed for the LOD determination.

2.5.2. Evaluation of linearity

Standard solutions were evaluated for the linearity within a concentration range of 5–100 μg/mL for MPH and 0.1–100 μg/mL for loxapine succinate. The peak area was plotted against drug concentration and the linearity was thus calculated by the linear regression equation $y = mx + c$, where y represents the peak area and x represents either the MPH or loxapine succinate concentration in μg/mL. A correlation coefficient of approximately 0.999 or more was considered as desirable for all calibration curves.

2.5.3. Determination of accuracy and precision

The inter-day validation was conducted with three sets of three QC samples of different concentrations for MPH (50, 75 and 100 μg/mL) and loxapine succinate (25, 50 and 100 μg/mL). These samples were evaluated for three days by generating a calibration curve for each day. As for the intra-day validation, six sets of three different drug samples were assayed and evaluated with reference to one calibration curve on the same run. The accuracy and precision values were calculated using a standard formula, as per the ICH guidelines. The accuracy and precision of the methods were determined for both intra-day and inter-day variations using multiple analyses of different concentrations of samples on three different days.

2.5.4. Specificity

The specificity of each assay was determined by comparing the chromatograms of the blank solution (water) with that of the drug standard solution (drug in water) of varying concentrations. Furthermore, the specificity of the improved HPLC method was determined by analyzing the MPH and loxapine succinate dosage forms in activated carbon. Observations were made for any interfering peaks generated during the analysis.

2.5.5. Robustness

Robustness is a measure of method's capacity to remain unaffected by small deliberate changes. The chromatogram resolution and retention behavior were evaluated for any changes in flow rate ($\pm$ 0.05 mL/min), organic solvent ratio ($\pm$ 5% methanol), and pH ($\pm$ 0.5).

2.6. Stability

The short-term stability of MPH and loxapine succinate under storage conditions was evaluated using three standard concentrations (10, 25 and 50 μg/mL) ($n = 3$) stored for one week at varying temperatures of 4 °C, 25 °C, and −20 °C. All stored standard solutions were analyzed using freshly prepared calibration standards. The stability of MPH and loxapine succinate was assessed by comparing the concentration of both drugs in each solution before and after the storage period.

2.7. Deactivation of pharmaceutical dosage forms using an activated carbon disposal system

The assay method was applied to support the deactivation profile of MPH and loxapine succinate in the presence of an activated carbon drug disposal system. The system consisted of a pouch containing 15 g of granular activated carbon packaged within a water soluble inner film reservoir. The deactivation of tablets and capsules as dosage forms were examined over 28 days using the model psychoactive medications. Ten MPH and loxapine succinate tablets (20 mg each) were placed into individual pouches separately followed by addition of 50 mL of warm tap water at a temperature of about 43 °C. To mix the activated carbon and warm water properly, pouches were shaken for 10 s at a rate of one shake per second. This was followed by a waiting period of 30 s to release the air bubbles from the charcoal. After ensuring that all of the medications settled to the bottom of the pouch, the pouches were sealed, stored upright, and left undisturbed at room temperature. Separate pouches were set up for each time point at 8 h, 1, 2, 4, 7, 14, 21 and 28 days and samples were collected from pouches to examine deactivation of drug during the study. Before taking samples, pouches were mildly shaken from side to side to ensure the medications were mixed homogenously in the pouch. Samples were then filtered with a 0.22 μm nylon filter and analyzed by the validated HPLC methods. The deactivation rate was calculated as follows:

% Deactivated = [(Initial amount of drug in pouch – Final amount of drug in pouch)/ Initial amount of drug in pouch] × 100.

2.8. Desorption study

At the end of the adsorption study (28 days), the pouch contents were transferred to 500 mL bottles, and 200 mL of tap water was added to each bottle. The samples were shaken for 1 h at 150 rpm, stored upright for 23 h at room temperature, then filtered and analyzed by HPLC. The water was then completely replaced with 250 mL of 30% ethanol, shaken for an additional hour, and stored for 23 h at room temperature. After that, samples were taken from the container, filtered and analyzed by HPLC.

3. Results

3.1. Method development and optimization

The most suitable isocratic condition to resolve MPH with a C_{18} column, after the chromatographic conditions were optimized for specificity, resolution and retention time, was a mobile phase consisting of methanol (0.1% FA) and water (0.1% FA, pH 6.8) (50:50, v/v). For loxapine succinate, analyte was separated on a C_8 column and the mobile phase consisted of ACN and water (0.3% (v/v) triethylamine, pH 3) (40:60, v/v). When the pH of the mobile phase was increased or when a higher percentage of organic solvent was used, the resultant chromatogram had an increase either in background noise or peaks indicating the tailing effect. Thus,
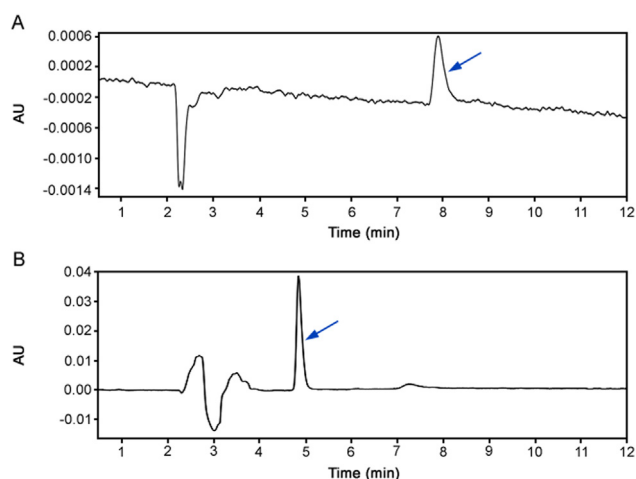
Fig. 1. Representative chromatograms of (A) methylphenidate hydrochloride standard (25 μg/mL) and (B) loxapine succinate standard (25 μg/mL). Arrow indicates drug peak.

based on the above mentioned parameters, MPH and loxapine succinate eluted at a retention time of 7.8 and 4.6 min, respectively, as shown in Fig. 1. Table 1 depicts the chromatographic parameters applied for the method.

3.2. Method validation

The method was validated according to the validation of analytical procedures provided in the ICH guidelines and draft guidance for the industry: analytical procedures and methods validation.

3.2.1. Linearity and range

A linear relationship was obtained between the peak area for both drugs and corresponding concentrations. The mean standard calibration curves are presented in Fig. 2. The calibration curves exhibit linearity over the concentration range of 5–100 μg/mL for MPH and 0.1–100 μg/mL for loxapine succinate with regression coefficient values greater than 0.999. The methods ($R^2 = 0.999$) provided a good correlation between the peak area and drug concentration.

3.2.2. Sensitivity

The LOD was evaluated by determining the minimum levels of concentration for MPH and loxapine succinate that could be detected using this analytical method. The LOQ was studied by estimating the minimum concentration that could be quantified with acceptable accuracy and precision. The LOD values for MPH and loxapine succinate were determined to be 1.38 μg/mL and 0.07 μg/mL, and the LOQ values were 4.17 μg/mL and 0.20 μg/mL, respectively.
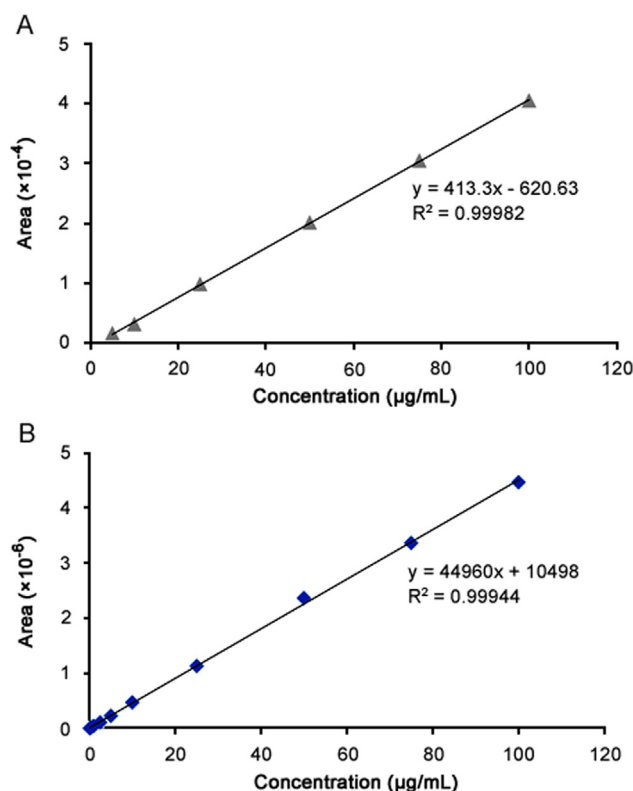

Fig. 2. Linearity of the HPLC method for analysis of (A) methylphenidate hydrochloride and (B) loxapine succinate.

3.2.3. Accuracy and precision

The intra-day and inter-day accuracy and precision of the assay method were studied by analyzing replicates at 3 different concentration levels: 50, 75 and 100 μg/mL (MPH) and 25, 50 and 75 μg/mL (loxapine succinate) (Table 2). The intra-day and inter-day variation was found to be within 0.8%–6%. The intra-day and inter-day accuracy was found to be within 90%–110%.

Under the stated experimental conditions, the precision (RSD) values were a maximum of 6% and the accuracy values were within a range of 94%–99% for MPH and the precision (RSD) values were at a maximum of 4.31% and the accuracy values were within a range of 98%–105% for loxapine succinate.

3.2.4. Robustness

The robustness of the method was determined by deliberately changing the experimental conditions. The resolution of MPH and loxapine succinate was evaluated and the effects of changes in flow rate ± 0.05 mL/min, mobile phase composition ± 5% (for methanol), and pH ± 0.5 were evaluated. Both the analytes, MPH and loxapine succinate, were adequately resolved under varied chromatographic conditions. Tables 3 and 4 demonstrate all the varied chromatographic conditions performed in the methods, and the % recovery for the MPH and loxapine succinate standard

Table 1
HPLC isocratic method for methylphenidate hydrochloride and loxapine succinate.

Parameter	Methylphenidate hydrochloride	Loxapine succinate
Column	Kinetex Biphenyl C$_{18}$ 100Å (5 μm, 250 mm × 4.6 mm)	Phenomenex Luna C$_8$ 100Å (5 μm, 250 mm × 4.6 mm)
Mobile phase	Methanol (0.1% formic acid) and water (0.1% formic acid) at pH 6.8 and a composition of 50:50 (v/v)	Acetonitrile and water (0.3% triethylamine) at pH 3.0 and a composition of 40:60 (v/v)
Flow rate (mL/min)	1.0	1.0
Injection volume (μL)	25	10
Wavelength (nm)	258	211
Retention time (min)	7.8	4.6

Table 2
Intra-day and inter-day accuracy and precision of HPLC assay for methylphenidate hydrochloride and loxapine succinate.

Medications	Reference value (μg/mL)	Intra-day (n = 6)			Inter-day (n = 3)		
		Mean ± SD (μg/mL)	Precision (%)	Accuracy ± SD (%)	Mean ± SD (μg/mL)	Precision (%)	Accuracy ± SD (%)
Methylphenidate hydrochloride	50	48.59 ± 2.09	4.31	97.19 ± 3.52	49.33 ± 1.76	3.57	98.66 ± 4.19
	75	73.05 ± 2.92	4.00	97.40 ± 3.57	74.11 ± 2.68	3.61	98.81 ± 3.90
	100	94.56 ± 5.70	6.03	94.56 ± 4.76	97.10 ± 4.76	4.90	97.10 ± 5.70
Loxapine succinate	25	24.90 ± 0.20	0.81	99.59 ± 0.80	24.98 ± 0.27	1.07	99.94 ± 1.06
	50	52.29 ± 0.49	0.94	104.57 ± 0.98	50.37 ± 2.04	4.05	100.74 ± 4.08
	75	74.25 ± 0.86	1.16	99.90 ± 1.15	73.90 ± 0.74	1.00	98.53 ± 0.99

Table 3
Robustness of the method for methylphenidate hydrochloride.

Parameter	Changes	Retention time (min)	Area	Concentration (μg/mL)
Flow rate (mL/min)	0.95	8.2	11,852	27.47
	1.00	7.8	11,958	27.70
	1.05	7.4	10,985	25.59
% of methanol in MP	45	10.7	11,608	26.94
	50	7.8	11,958	27.70
	55	6.0	11,430	26.56
pH	6.3	7.8	12,034	27.86
	6.8	7.8	11,958	27.70
	7.3	7.8	12,953	29.85

Table 4
Robustness of the method for loxapine succinate.

Parameter	Changes	Retention time (min)	Area	Concentration (μg/mL)
Flow rate (mL/min)	0.95	4.6	2,686,615	29.37
	1.00	4.4	2,584,496	27.97
	1.05	4.2	2,445,796	26.73
% of methanol in ACN	35	6.0	2,448,612	26.76
	40	4.4	2,458,234	26.87
	45	3.7	2,588,303	28.29
pH	2.5	4.8	2,505,610	27.39
	3.0	4.4	2,458,234	26.87
	3.5	5.0	2,478,983	27.09

concentration, 25 μg/mL, was found to be within an acceptable range of 80%–120%.

3.2.5. Specificity

Specificity was used to test the ability of the assay method to eliminate the effects of all interfering substances on MPH and loxapine succinate peak results, specifically by comparing the chromatograms to the blank samples. The validated method showed that the drug contents eluted with no interfering peaks generated by the excipients in the marketed products.

3.3. Stability

Three concentrations (10, 25 and 100 μg/mL) of MPH and loxapine succinate in water (n = 3) were analyzed to assess the stability. The stability was assessed after storage for one week at different storage temperatures. Stability assessments indicated that both drugs were stable in water for 1 week at room temperature (25 °C), 4 °C and −20 °C. The % accuracies for the MPH and loxapine succinate standard concentrations were found to be within acceptable ranges of 92%–107% and 95%–105%, respectively (Fig. 3).

3.4. Deactivation study

The deactivation of MPH and loxapine succinate with a drug disposal system was observed over 28 days. After the addition of the dosage forms and water into the pouches, adsorption started immediately. As shown in Fig. 4, 96.9% of loxapine succinate and 99.9% of MPH were adsorbed and deactivated by the drug disposal system at the end of 8 h. Both drugs continued to be adsorbed over time, and at the end of 28 days, 100% drug deactivation was achieved. The deactivation profiles for both drugs are presented in Fig. 4.

3.5. Desorption study

A desorption or washout study was performed following the deactivation study in order to determine the potential for leaching of the active ingredients from activated carbon in the presence of water and alcohol. To test the robustness of the system, desorption was examined in the presence of a larger volume of water (250 mL) followed by 30% ethanol (250 mL). The results show that after 28 days, no drug leached out after one day of desorption in the presence of water, and only 1% of the drug was leached out from the activated carbon in the presence of the organic solvent ethanol (Table 5).

4. Discussion

Lack of awareness of the need for proper disposal of prescription medication leads to abuse and environmental contamination, and this problem has been increasing steadily [18]. Thus, the potential for abuse of prescription medications should be addressed in the medical community and by primary care practitioners.

MPH and loxapine succinate are examples of two commonly abused drugs, and we investigated their deactivation efficiency by using an activated carbon disposal system. MPH and loxapine succinate were successfully detected with RP-HPLC, utilizing buffered water and organic solvents (Fig. 1).

In the present study, as MPH (logP: 2.2) and loxapine (logP: 3.6) are lipophilic compounds, C_{18} reverse-phase column was used for MPH analysis and C_8 for loxapine. MPH and loxapine succinate are weak bases with pKa values of 8.8 and 7.1, respectively. MPH was separated using methanol and water as the mobile phase, and the pH was adjusted to 6.8. Similarly, loxapine was separated using ACN and water as the mobile phase with the pH adjusted to 3. More than 99% ionization was achieved for both drugs at their respective pH values, with corresponding log D value of 0. The concentrations of methanol and acetonitrile were optimized to give a symmetric peak with a reasonable run time. A detailed layout of the HPLC parameters used in the developed method is discussed in Table 1. The reliability and sensitivity of the validated methods were ensured with good linearity, accuracy, and precision within the ICH and FDA limits for the method validation of analytical samples.
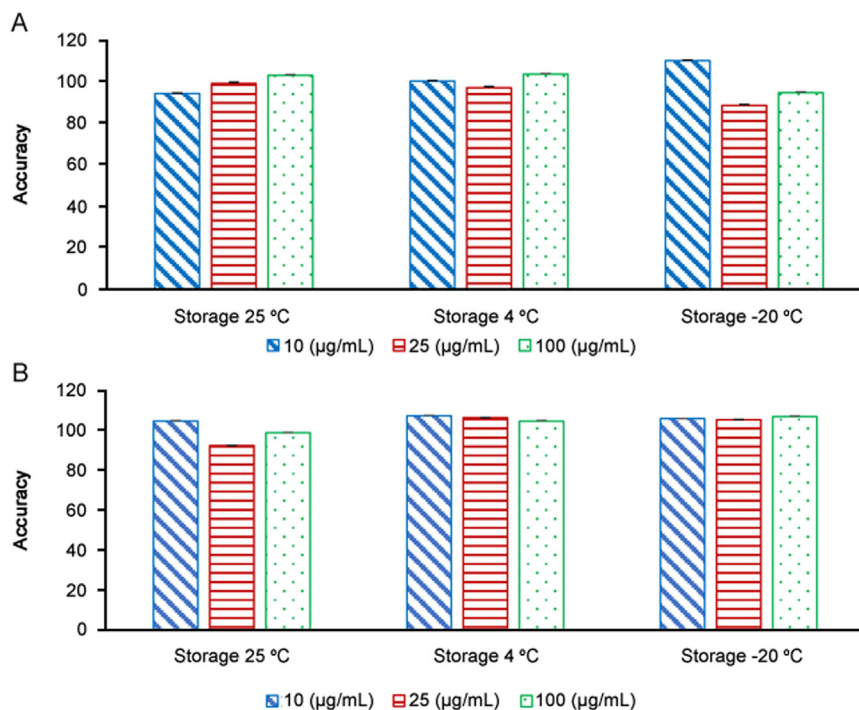
Fig. 3. Stability of (A) methylphenidate hydrochloride standards (10, 25 and 100 μg/mL) and (B) loxapine succinate standards (10, 25 and 100 μg/mL) at different temperatures, 25 °C, 4 °C and − 20 °C for one week.

In addition, analysis of the marketed preparation of MPH and loxapine succinate with the validated assay methods showed that the drug contents eluted with no interfering peaks generated by the excipients in the marketed products. Results for robustness are summarized in Tables 3 and 4, and the methods were found to remain unaffected by changing the method parameters. The study also presented that both MPH and loxapine succinate were stable in water at different temperatures, 25 °C, 4 °C and −20 °C, for the storage over the period of one week. Both validated methods were applied to examine the ability of the disposal system to deactivate two commonly abused prescription drugs, MPH and loxapine succinate.

According to the FDA guidelines, all medications being deposed of in household trash should be mixed with unpalatable substances such as cat litter or coffee grounds, or should be flushed

Table 5
Amount of the drug leached from activated carbon during desorption study.

Medication	% leached in water	% leached in ethanol
Methylphenidate hydrochloride	0.0	1.0
Loxapine succinate	0.0	0.0
Average	0	0.5

down the toilet [11]. However, these procedures do not deactivate the drug, and the drug is still available in the active form; this can lead to contamination of the environment and the water system. Our studies were consistent with the studies performed by Harwadkar et al. [15], in which various deactivating agents were tested, and activated carbon was found to be the most efficacious deactivation agent, causing complete deactivation for various
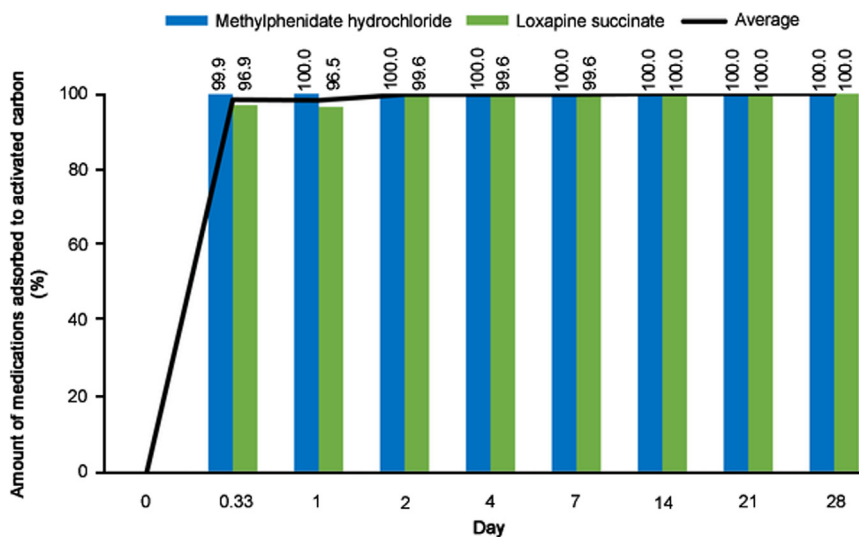

Fig. 4. Deactivation profile of methylphenidate hydrochloride and loxapine succinate dosage forms.

dosage forms of medications such as dexamethasone tablets and amoxicillin capsules.

Using activated carbon is an effective technique to remove contaminants or pollutants from the water or air, but various factors can influence the adsorption capacity. Generally, factors such as the pH of the solution, pKa, hydrophobicity and molecular weight of the compound, and type of the activated carbon used may influence the adsorption of molecules to the activated carbon, and thus affect the deactivation capability of the system. The activated carbon present in our disposal system pouch is specific for the molecular size, as it is based on MAT$_{12}$® Molecular Adsorption Technology [19]. This renders the drug irretrievable by binding to it through a physical adsorption process [20].

The pH of the drug disposal system, comprising of activated carbon in water, was close to neutral (pH 6.8), and was found to remain unaffected by the addition of drugs (MPH and loxapine succinate). It has been reported that the optimal pH for maximum adsorption capacity is near 7 [21]. The results obtained in our study are in accordance with this, as more than 95% deactivation of the drugs was achieved within 8 h.

The hydrophobicity of the compound is another factor that determines the adsorption efficiency of the activated carbon, and thus affects the hydrophobic interaction between the activated carbon and the adsorbent [22,23]. Westerhoff et al. [24] observed that the removal efficiency of the contaminants was dependent on the logK$_{ow}$ values, which are indicators of the hydrophobicity of the molecules. In addition, another study found that the hydrophobic character of the compound also influences the uptake rate of the compound [25]. The study determined that the adsorbent (polar compounds) and adsorbate (activated carbon) displayed van der Waals force of interaction toward each other, thus leading to a better adsorption capacity. Thus, hydrophobicity not only determines the adsorption capacity, but also influences the rate of adsorption to the activated carbon. In our study, MPH (logP: 2.2) [26] and loxapine (logP: 3.6) [27] were both moderately lipophilic compounds, and hence showed more than 99% deactivation after 24 h of interaction with the activated carbon (Fig. 4). Our results were consistent with the previous studies presented in the literature [28].

The MPH used were in tablet form; this could have led to faster adsorption to activated carbon compared to that of capsules. Solid dosage forms like capsules may require more dissolution time in water before adsorption can occur; this could cause a slight delay in the rate of adsorption of loxapine succinate capsules compared to that of MPH tablets. Previous research has noted the influence of molecular weight and hydrophobicity of the adsorbate on the adsorption capacity of activated carbon. In our study, we did not observe any significant differences in the adsorption capacity of the disposal system between these two model drugs.

The efficiency of the deactivation system to retain the adsorbed drug was further tested by examining the desorption. This study was aimed to simulate landfill situations which provide exposure to large volumes of water and some organic solvents. Our results showed that the activated carbon used in our study was efficient in adsorbing the drug, and did not release on exposure to these stress conditions. In the desorption study, we observed that no drug was leached out in the presence of water and, on an average, less than 1% of the drug was leached out in the presence of ethanol (Table 5).

The findings of the research indicated that the adsorption efficiency of the activated carbon was good, and it would not release the drug back into the environment when the contents of the pouch were present in the landfill, thereby providing a safer disposal method compared to other traditional alternative methods suggested by the FDA for drug disposal. This drug disposal pouch would therefore eliminate the risk of abuse of unused prescriptions, and also solve the problem of environmental and water pollution. Hence, the Deterra® activated carbon disposal system provides a simple and convenient way to dispose of these medications in normal trash, without causing any environmental or safety risks.

5. Conclusions

An isocratic RP-HPLC method for the determination of MPH and loxapine succinate was developed, and is precise and reliable. The regression line equation is capable of reliably predicting the drug concentration in the range of 5–100 µg/mL and 0.1–100 µg/mL for MPH and loxapine succinate, respectively, from the peak area obtained. The stability assessments revealed that both drugs were stable in water at 25 °C, 4 °C and −20 °C for one week. The method was successfully validated and allowed the reliable, sensitive, robust, and specific detection of MPH and loxapine succinate in a common marketed preparation.

This method was then used to test the efficiency of an activated carbon-based drug disposal system for adsorption of MPH and loxapine succinate from dosage forms to activated carbon. The system was very efficient, with more than 99% drug deactivation achieved after 24 h, and less than 0.5% of the drug was released from activated carbon by an extraction protocol that mimicked a landfill situation.

Thus, this drug disposal system offers a simple and safe method to be used by patients. These results are encouraging, and provide the basis of an environmentally friendly method of drug disposal.

Conflicts of interest

The authors declare that there are no conflicts of interest.

Acknowledgments

References

[1] lynne walsh, Reports and Detailed Tables From the 2015 National Survey on Drug Use and Health (NSDUH), 2016. 〈https://www.samhsa.gov/samhsa-data-outcomes-quality/major-data-collections/reports-detailed-tables-2015-NSDUH〉.

[2] R.A. Rudd, P. Seth, F. David, et al., Increases in drug and opioid-involved overdose deaths - United States, 2010–2015, MMWR Morb. Mortal. Wkly. Rep. 65 (2016) 1445–1452.

[3] T.D. Challman, J.J. Lipsky, Methylphenidate: its pharmacology and uses, Mayo Clin. Proc. 75 (2000) 711–721.

[4] N.D. Volkow, G.J. Wang, S.J. Gatley, et al., Temporal relationships between the pharmacokinetics of methylphenidate in the human brain and its behavioral and cardiovascular effects, Psychopharmacology 123 (1996) 26–33.

[5] W.A. Morton, G.G. Stockton, Methylphenidate abuse and psychiatric side effects, Prim. Care Companion J. Clin. Psychiatry 2 (2000) 159–164.

[6] L. Sperry, B. Hudson, C.H. Chan, Loxapine abuse, N. Engl. J. Med. 310 (1984) 598.

[7] A. Seçilir, L. Schrier, Y.A. Bijleveld, et al., Determination of methylphenidate in plasma and saliva by liquid chromatography/tandem mass spectrometry, J. Chromatogr. B Anal. Technol. Biomed. Life Sci. 923–924 (2013) 22–28.

[8] S.J. Soldin, Y.P. Chan, B.M. Hill, et al., Liquid-chromatographic analysis for methylphenidate (Ritalin) in serum, Clin. Chem. 25 (1979) 401–404.

[9] J.S. Zimmer, S.R. Needham, C.D. Christianson, et al., Validation of HPLC–MS/MS methods for analysis of loxapine, amoxapine, 7-OH-loxapine, 8-OH-loxapine and loxapine N -oxide in human plasma, Bioanalysis 2 (2010) 1989–2000.

[10] ICH, Q2 (R1) Validation of analytical procedures: text and methodology, in: Proceedings of the International Conference on Harmonization, 1996.

[11] U.S. Food and Drug, Safe Disposal of Medicines - Disposal of Unused Medicines: What You Should Know. ⟨http://www.fda.gov/Drugs/ResourcesForYou/Consumers/BuyingUsingMedicineSafely/EnsuringSafeUseofMedicine/SafeDisposalofMedicines/ucm186187.htm⟩.

[12] O. of the Commissioner, Consumer Updates - How to Dispose of Unused Medicines. ⟨http://www.fda.gov/ForConsumers/ConsumerUpdates/ucm101653.htm⟩.

[13] T.J. Cicero, M.S. Ellis, A. Paradis, et al., Determinants of fentanyl and other potent μ opioid agonist misuse in opioid-dependent individuals, Pharmacoepidemiol. Drug Saf. 19 (2010) 1057–1063.

[14] That Drug Expiration Date May Be More Myth Than Fact, NPR.Org. ⟨http://www.npr.org/sections/health-shots/2017/07/18/537257884/that-drug-expiration-date-may-be-more-myth-than-fact⟩.

[15] A. Herwadkar, N. Singh, C. Anderson, et al., Development of disposal systems for deactivation of unused/residual/expired medications, Pharm. Res. 33 (2016) 110–124.

[16] Z. Jeirani, C.H. Niu, J. Soltan, Adsorption of emerging pollutants on activated carbon, Rev. Chem. Eng. 33 (2016), ⟨http://dx.doi.org/10.1515/revce-2016-0027⟩.

[17] Verde Technologies Introduces Deterra® Drug Deactivation System | Deterra System. ⟨http://deterrasystem.com/2015/02/verde-technologies-introduces-deterra-drug-deactivation-system⟩.

[18] L. Simoni-Wastila, H.K. Yang, Psychoactive drug abuse in older adults, Am. J. Geriatr. Pharmacother. 4 (2006) 380–394.

[19] V. Technologies, Deterra™ Drug Deactivation System Introduces Consumer Solution to Fighting Prescription Drug Abuse Epidemic. ⟨http://www.prnewswire.com/news-releases/deterra-drug-deactivation-system-introduces-consumer-solution-to-fighting-prescription-drug-abuse-epidemic-300060612.html⟩.

[20] New Deterra system deactivates discarded medications | The Westerly Sun. ⟨http://www.thewesterlysun.com/news/latestnews/7493956-129/new-deterra-pouch-system-deactivates-discarded-medications.html⟩.

[21] R. Leyva-Ramos, Effect of temperature and pH on the adsorption of an anionic detergent on activated carbon, J. Chem. Technol. Biotechnol. 45 (1989) 231–240.

[22] B. Li, Z. Lei, Z. Huang, Surface-treated activated carbon for removal of aromatic compounds from water, Chem. Eng. Technol. 32 (2009) 763–770.

[23] E.F. Mohamed, C. Andriantsiferana, A.M. Wilhelm, et al., Competitive adsorption of phenolic compounds from aqueous solution using sludge-based activated carbon, Environ. Technol. 32 (2011) 1325–1336.

[24] P. Westerhoff, B. Nalinakumari, P. Pei, Kinetics of MIB and geosmin oxidation during ozonation, Ozone Sci. Eng. 28 (2006) 277–286.

[25] J. Lladó, C. Lao-Luque, B. Ruiz, et al., Role of activated carbon properties in atrazine and paracetamol adsorption equilibrium and kinetics, Process Saf. Environ. Prot. 95 (2015) 51–59.

[26] Pubchem, methylphenidate | C14H19NO2 - PubChem. ⟨https://pubchem.ncbi.nlm.nih.gov/compound/methylphenidate⟩.

[27] DrugBank, ed., Loxapine, DrugBank, 2017. ⟨https://www.drugbank.ca/drugs/DB00408⟩.

[28] Y. Song, M. Manian, W. Fowler, et al., Activated carbon-based system for the disposal of psychoactive medications, Pharmaceutics 8 (2016) 31.

Original Research Article

LC and LC–MS/MS studies for the identification and characterization of degradation products of acebutolol

Uday Rakibe [a], Ravi Tiwari [b,*], Anand Mahajan [c], Vipul Rane [a], Pravin Wakte [a]

[a] Department of Chemical Technology, Dr. Babasaheb Ambedkar Marathwada University, Aurangabad, Maharashtra, India
[b] Department of Pharmaceutical Sciences, SVKM's NMIMS, Shirpur, Dist. Dhule, Maharashtra, India
[c] Department of Pharmaceutical Analysis, Goa College of Pharmacy, Panjim, Goa, India

A B S T R A C T

The aim of the present investigation was to demonstrate an approach involving use of liquid chromatography (LC) and liquid chromatography-mass spectrometry (LC–MS) to separate, identify and characterize very small quantities of degradation products (DPs) of acebutolol without their isolation from the reaction mixtures. The drug was subjected to oxidative, hydrolytic, thermal and photolytic stress conditions as per International Conference on Harmonization (ICH) guideline Q1A(R2). Among all the stress conditions the drug was found to be labile in hydrolytic (acidic & basic) and photolytic stress conditions, while it was stable in water-induced hydrolysis, oxidative and thermal stress conditions. A total of four degradation products were formed. A C_{18} column was employed for the separation of all the DPs on a gradient mode by using high-performance liquid chromatography (HPLC). All the DPs were characterized with the help of their fragmentation pattern and the masses obtained upon LC–MS/MS and MS^n analysis. All the hitherto unknown degradation products were identified as 1-(2-(2-hydroxy-3-(isopropylamino)propoxy)-5-(amino)phenyl)ethanone (DP-I), N-(4-(2-hydroxy-3-(isopropylamino)propoxy)-3-acetylphenyl)acrylamide (DP-II), 1-(2-(2-hydroxy-3-(isopropylamino)propoxy)-5-(hydroxymethylamino)phenyl)ethanone (DP-III) and 1-(6-(2-hydroxy-3-(isopropylamino)propoxy)-2,3-dihydro-2-propylbenzo[d]oxazol-5-yl)ethanone (DP-IV). Finally the in-silico carcinogenicity and hepatotoxicity predictions of the drug and all the DPs were performed by using toxicity prediction softwares viz., TOPKAT, LAZAR and Discovery Studio ADMET. The results of in-silico toxicity studies revealed that acebutolol (0.967) and DP-I (0.986) were found to be carcinogenic, while acebutolol (0.490) and DP-IV (0.437) were found to be hepatotoxic.

1. Introduction

Acebutolol hydrochloride is a selective, hydrophilic beta-adrenoreceptor blocker which is used to treat hypertension and ventricular arrhythmias. Other beta-adrenergic agents are atenolol, betaxolol, celiprolol, bisoprolol, esmolol, metoprolol, nebivolol, etc. Chemically acebutolol (Fig. 1) is N-[3-Acetyl–4-[2–hydroxy–3-[(1–methylethyl)amino]propoxy]-butanamide [1]. There exist various reports on investigation and analysis of acebutolol by using different analytical techniques such as high-performance liquid chromatography (HPLC), thin layer chromatography, ion pair HPLC, liquid chromatography with tandem mass spectrometry (LC–MS/MS), voltammetry, and polarography. The drug is reported for the enantioselective determination of its active metabolite diacetolol in

spiked human plasma samples by LC–MS/MS [2–6], determination in pharmaceutical formulations and biological fluids by voltammetric method [7], and major metabolite determination in infant's blood circulation and breast milk by a stereospecific HPLC assay method [8]. There are HPLC methods reported for acebutolol doping analysis and toxicological investigations of fatal cases of acebutolol self-poisoning [9,10]. A literature report is also available on comparative HPLC and LC–MS analysis of antiepileptic with beta-blocking drugs [11]. Acebutolol is also explored by ion-pair HPLC method for its determination in pharmaceuticals [12]. However, very few reports are on acebutolol stability studies and its determination in acid induced degradation products (DPs) and identification of radio-degradation products by irradiation of high dose ionizing radiation emitted by beam of high energy electrons [13–15].

Hence, the endeavor of the present study was to separate, identify and characterize DPs of acebutolol formed under ICH Q1A (R2) [16] recommended stress conditions of hydrolysis (acid, base and neutral), oxidation, dry heat and photolysis. Moreover, the parallel objective of this study was to explore comprehensive
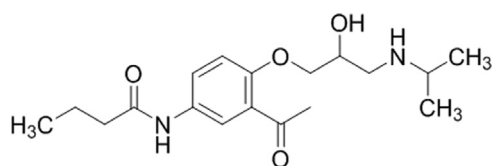

Fig. 1. Structure of acebutolol.

information on the degradation pathway of the drug. To achieve this task a systematic outline of the study includes (i) degradation study of acebutolol under conditions of oxidation, hydrolysis, thermal and photolysis, (ii) separation of DPs and validation of the developed LC method, (iii) characterization of DPs by LC–MS/MS and MS^n studies, (iv) proposal of degradation pathway of the drug, and (v) prediction of in-silico carcinogenicity and hepatotoxicity of the drug and DPs by different models.

2. Experimental

2.1. Drug and reagents

Pure acebutolol was purchased from Sigma-Aldrich (Mumbai, India). Analytical reagent (AR) grade sodium hydroxide (NaOH), ammonium formate (NH$_4$HCO$_2$), formic acid (HCOOH) and HPLC grade methanol were purchased from Merck Specialities Pvt. Ltd. (Mumbai, India). AR grade hydrochloric acid (HCl) and 30% hydrogen peroxide were purchased from Qualigens Fine Chemicals Pvt. Ltd. (Mumbai, India) and S.D. Fine-Chem. Ltd. (Mumbai, India), respectively. Ultra-pure double distilled HPLC grade water obtained from Labsil Instruments (Bangalore, India) was used throughout the studies.

2.2. Equipments

An HPLC system (Shimadzu Corporation, SPD-M20A, Kyoto, Japan) equipped with LC Solution software was used for LC studies equipped with a photo-diode array (PDA) detector, sample injector with 20 μL loop, and on-line degasser containing binary pump. The output signals were assessed on a Dell computer using LC Solution software. Stress degradation studies were carried out using precision water bath (Meta-Lab Ltd., Mumbai, India) containing a thermostat for temperature control. A hot air oven (Scientico Ltd., Mumbai, India) was used to perform solid state thermal stress studies. Photodegradation studies were executed in a photostability chamber (Thermolab Scientific Equipments Pvt. Ltd., Mumbai, India), where the temperature was adjusted to 25 ± 2 °C during the study. The measurement of visible and near UV illumination energy was carried out by using a calibrated lux and UV meter (Thermolab Scientific Equipments Pvt. Ltd., Mumbai, India) [17]. The LC–MS system controlled by Xcalibur software (version 2.0) consisted of LCQ Fleet and TSQ Quantum Access with Surveyor Plus HPLC System (Thermo, San Jose, USA). All the separation studies were carried out using a C$_{18}$ column (150 mm × 4.6 mm i. d., particle size 5 μm) Kromasil (Eka Chemicals AB, Bohus, Sweden). A pH meter (Controlled Dynamics, Vadodara, India) was used to adjust the pH of mobile phase and all other solutions used during the study. Other equipments used during the study were weighing balance (Shimadzu, AUX220, Kyoto, Japan), sonicator (Spectralab UCB 30, Mumbai, India) and analytical balance (Precissa XR 205 SMDR, Moosmattstrasse Dietikon, Switzerland).

2.3. Forced degradation studies

The objective of forced degradation studies was to achieve 10%–15% degradation of the drug. The drug was subjected to oxidative, hydrolytic, thermal and photolytic stresses. The results were obtained by comparing four samples of every stress condition viz., untreated blank sample, stressed blank sample, untreated standard drug sample and stressed drug sample solution. In case of thermal and photolytic stress conditions only two samples were generated viz., sample exposed to stress condition and control sample.

2.3.1. Hydrolytic degradation

The hydrolytic decomposition was performed in acidic, alkaline and neutral conditions. Samples were prepared by taking 1 mL of stock solution of drug (1000 μg/mL) and 1 mL of hydrolytic agent (1 M HCl, 1 M NaOH and water) in 10 mL volumetric flask. If required, the samples were heated at constant temperature on water bath at 80 °C for specified time intervals. The samples were neutralized by using equal strength of acid or alkali before injected into HPLC system.

2.3.2. Oxidative degradation

Oxidative degradation was carried out by using hydrogen peroxide. Samples were prepared by taking 1 mL of stock solution of the drug (1000 μg/mL) and 1 mL of hydrogen peroxide (30%) in 10 mL volumetric flask. If required, the samples were heated on constant temperature water bath at 80 °C for specified time intervals. After required exposure samples were diluted up to the mark by using diluent and subjected for HPLC analysis.

2.3.3. Thermal degradation

Drug sample of 10 mg each was taken in two 10 mL volumetric flasks and sealed. One flask was exposed to dry heat in hot air oven for specified temperature and time interval and the other was kept as control. After required exposure two separate solutions were prepared by weighing appropriate amounts of the sample exposed to thermal stress and control to produce concentration of 100 μg/mL. The samples were diluted up to the mark with the help of diluent and injected separately into HPLC.

2.3.4. Photodegradation

The drug layer of 1 mm thickness was prepared in a petri dish and exposed to ICH recommended photostability conditions with the overall illumination of not less than 1.2 million lx h along with the integrated near ultraviolet energy of not less than 200 W h/m^2. Another petri dish containing the drug (1 mm layer thickness) was wrapped with aluminum foil and kept as control. After required exposure two separate solutions were prepared by weighing appropriate amounts of the sample exposed to stress and control to produce concentration of 100 μg/mL. The samples were diluted up to the mark with the help of diluent and injected separately into HPLC.

Photodegradation of the drug was also carried out in solution phase. Two solutions with the concentration of 100 μg/mL were prepared in 10 mL volumetric flask by using methanol as diluent. One was exposed to ICH dose of light and the other was kept as control.

2.4. HPLC method development

HPLC studies were carried out individually on all the reaction solutions and then on the mixture of those solution in which the degradation was observed. A duplicate sample of each stress condition was injected into HPLC system along with a separate blank stress sample to achieve an optimum degradation. To accomplish an appropriate separation and to resolve all the polar

DPs overlapping/merging, various HPLC trials were conducted. The separation was executed using different proportions of acetonitrile (ACN), methanol (MeOH) and ammonium formate buffer (10 mM) by varying the pH of buffer with formic acid. The detection wavelength, injection volume and flow rate were 235 nm, 20 μL and 1 mL/min, respectively.

2.5. HPLC method validation

The developed LC method was validated by covering various parameters outlined in the ICH guidelines Q2(R1) [18]. The selected validation parameters included linearity, precision (inter-day and intra-day), accuracy, specificity, and selectivity.

2.5.1. Linearity
Linearity of the method was established by using solutions containing 50–250 μg/mL of the drug. Each linearity sample was injected in triplicate into the HPLC column by keeping the injection volume constant.

2.5.2. Precision
A precision study was carried out by injecting the drug with three different concentrations (100, 150 and 200 μg/mL) in triplicate into the HPLC on the same day and the next day. The values of standard deviation (SD) and percent relative standard deviation (% RSD) were calculated for both intra-day and inter-day precision.

2.5.3. Accuracy
The accuracy of the method was established by conducting recovery studies of pure drug from degradation samples by standard addition method. The mixtures of stressed samples were spiked with the drug with concentrations of 80, 120 and 160 μg/mL.

2.5.4. Specificity and selectivity
The specificity of the method was investigated through establishment of resolution factor between the drug peak and the nearest resolving peak, and also among other peaks. Selectivity was confirmed through peak purity studies using a PDA detector. A mixture of degradant was produced by mixing an equal amount of solutions generated during different stress conditions and subjected for HPLC analysis.

2.6. Mass spectral studies on the drug

Mass spectral studies were performed in positive electrospray ionization (ESI) mode in the mass range of 50–1000 Da to establish the fragmentation pattern of the drug. In order to get clear mass spectrum without any background noise, the drug at a concentration of 5 μg/mL in methanol:water (50:50, v/v) was directly infused using a syringe pump into the mass spectrometer. The mass parameters were appropriately tuned to get clear molecular ion peak of the drug. High purity nitrogen was used as the nebulizer and auxiliary gas. The drug was further subjected to MS/MS analysis in positive ESI mode to explore the origin of each individual fragment.

2.7. LC–MS/MS studies

The degraded drug samples were subjected to LC–MS/MS analysis in positive ESI mode using the previously developed gradient LC method. A satisfactory separation of degradation products was achieved by using C$_{18}$ column. For structure elucidation of the DPs, the samples with maximum degradation were subjected to LC–MS analysis. The structural identity of each DP was performed with the LC–MS fragmentation analysis.

2.8. In-silico toxicity studies

The drug and all its degradation products were subjected to in-silico carcinogenicity and hepatotoxicity predictions by using different models. Carcinogenicity prediction was performed by using Toxicity Prediction by Komputer Assisted Technology (TOPKAT) version 6.2, Lazar Toxicity Prediction software version 1.1.2 building on top of the OpenTox framework and adopting DSSTox database, TOPKAT Extensible built with Bayesian models and partial least square (PLS) technique. Hepatotoxicity prediction was carried out by using Discovery Studio ADMET. The model was developed from available literature data of 382 compounds known to exhibit liver toxicity or trigger dose-related elevated aminotransferase levels in more than 10% of the human population [19].

3. Results and discussion

3.1. Degradation behaviour

The chromatogram in Fig. 2 reveals the degradation behaviour of acebutolol. A total of four degradation products were generated from the drug (denoted as I-IV according to the elution order in the chromatogram). A major degradation product (DP-I) was formed in both acid and alkaline stress conditions, while the other major degradation product (DP-IV) was generated only in alkaline stress condition. Two minor degradation products, DP-II and DP-III, were formed only in photolytic stress condition. This shows that the acebutolol is photo labile to a certain extent and an indication for the bulk drug substance and generic drug product manufacturers to optimize the critical quality attributes (CQA) to avoid the significant light exposure during the manufacturing process. Apart from the above listed stress conditions the drug was found to be stable in neutral (heating in water), oxidative and thermal stress conditions.
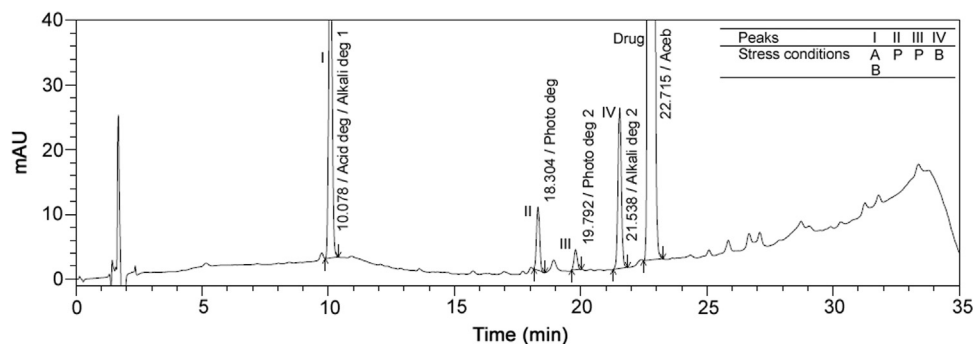

Fig. 2. HPLC chromatogram of all the acebutolol products (I-IV) and acebutolol.
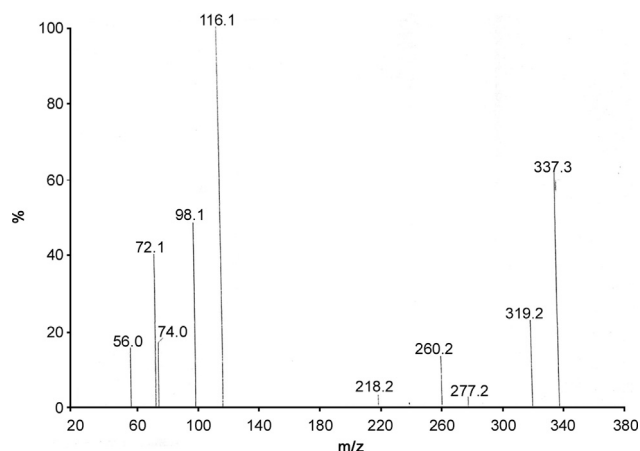
Fig. 3. Line spectrum of acebutolol obtained in MS study.

3.2. Fragmentation pathway of the drug

As shown in Fig. 3, a total of 10 fragments were formed from the drug. Molecular ion fragment of the drug (numbered as 0) had the mass of 337.21, which followed a parallel fragmentation pathway. The two fragments of m/z 116.11 and m/z 319.20 were formed from the drug due to the cleavage of ether linkage of the side chain and loss of hydroxyl group, respectively (Fig. 4). Two types of fragment ions can be easily identified in Fig. 4, viz., side chain fragment ions and cyclic structure fragment ions. The fragment with m/z 116.11 on loss of isopropyl resulted in ion with m/z 74.06, in which lone pair of electrons of nitrogen succeeded in cyclic structure (m/z 72.04) formation with the terminal hydroxyl group. In the alternate fragmentation pathway of ion with m/z 116.11, the ions with m/z 98.10 and m/z 56.05 were formed on loss of hydroxyl and isopropyl groups, respectively. In this fragmentation part, the bond cleavages took place between carbon and heteroatom linkages, which are considered to be loose links as
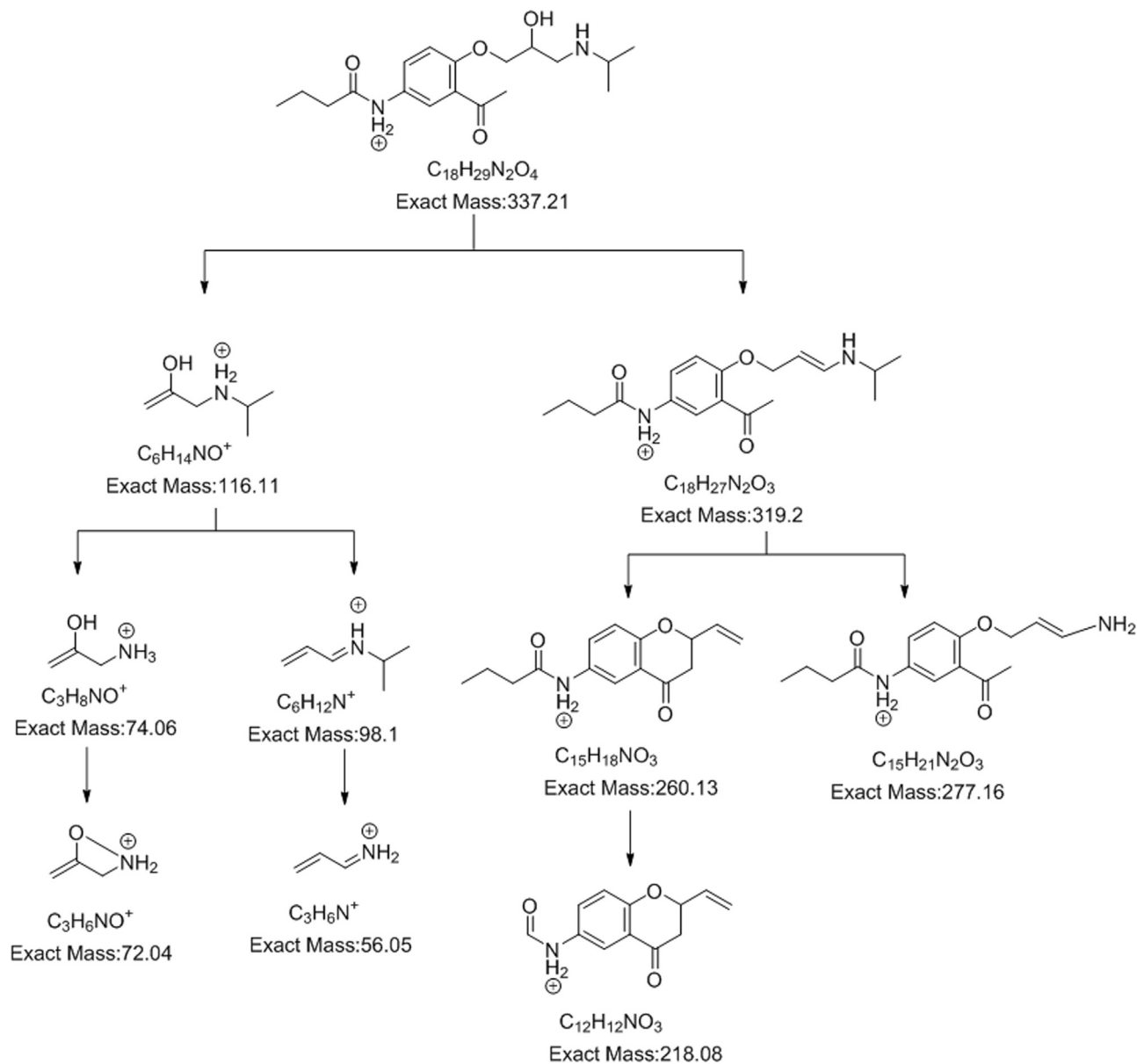

Fig. 4. Fragmentation pathway of acebutolol.

Table 1
Interpretation of MS/MS data of fragments of acebutolol.

Peak no.	Experimental mass	Best possible molecular formulae	Theoretical mass	RDB[a]	Possible parent fragment	Difference from parent ion	Possible losses corresponding to difference
0	337.30	$C_{18}H_{29}N_2O_4^+$	337.21	5.5			
1	319.20	$C_{18}H_{27}N_2O_3^+$	319.20	6.5	0	18.00	H_2O
2	277.20	$C_{15}H_{21}N_2O_3^+$	277.16	6.5	1	42.04	C_3H_6
3	260.20	$C_{15}H_{18}NO_3^+$	260.13	7.5	1	59.04	C_3H_9N
4	218.20	$C_{12}H_{12}NO_3^+$	222.11	6.5	3	42.08	C_3H_6
5	116.10	$C_6H_{14}NO^+$	116.11	0.5	0	220.97	$C_{12}H_{15}NO_3$
6	98.10	$C_6H_{12}N^+$	98.10	1.5	5	18.14	H_2O
7	74.00	$C_3H_8NO^+$	74.06	0.5	6	42.05	C_3H_6
8	72.10	$C_3H_8NO^+$	72.04	1.5	7	2.20	H_2
9	56.00	$C_3H_6N^+$	56.05	1.5	8	42.05	C_3H_6

[a] RDB: ring plus double bonds.

compared to C–C bond. On the other hand, the fragment with m/z 319.20 was formed from the drug on loss of hydroxyl group, and then in the subsequent step the fragment with m/z 319.20 underwent cleavage of isopropyl amine and isopropyl entities from the terminal side chain to form a cyclic fragment ion with m/z 260.13 and m/z 277.16, respectively. Finally, the fragment with m/z 260.13 on loss of a propyl group from the side chain led to the ion with m/z 218.08. The interpretation of MS/MS data of fragments of

the drug is shown in Table 1, and the complete fragmentation pathway of the drug is shown in Fig. 4.

3.3. LC–MS/MS studies on stressed samples

The mass spectra of all the four degradation products, DP-I-IV, are shown in Fig. 5. The experimental masses, best possible molecular formulae, theoretical mass, RDB (ring plus
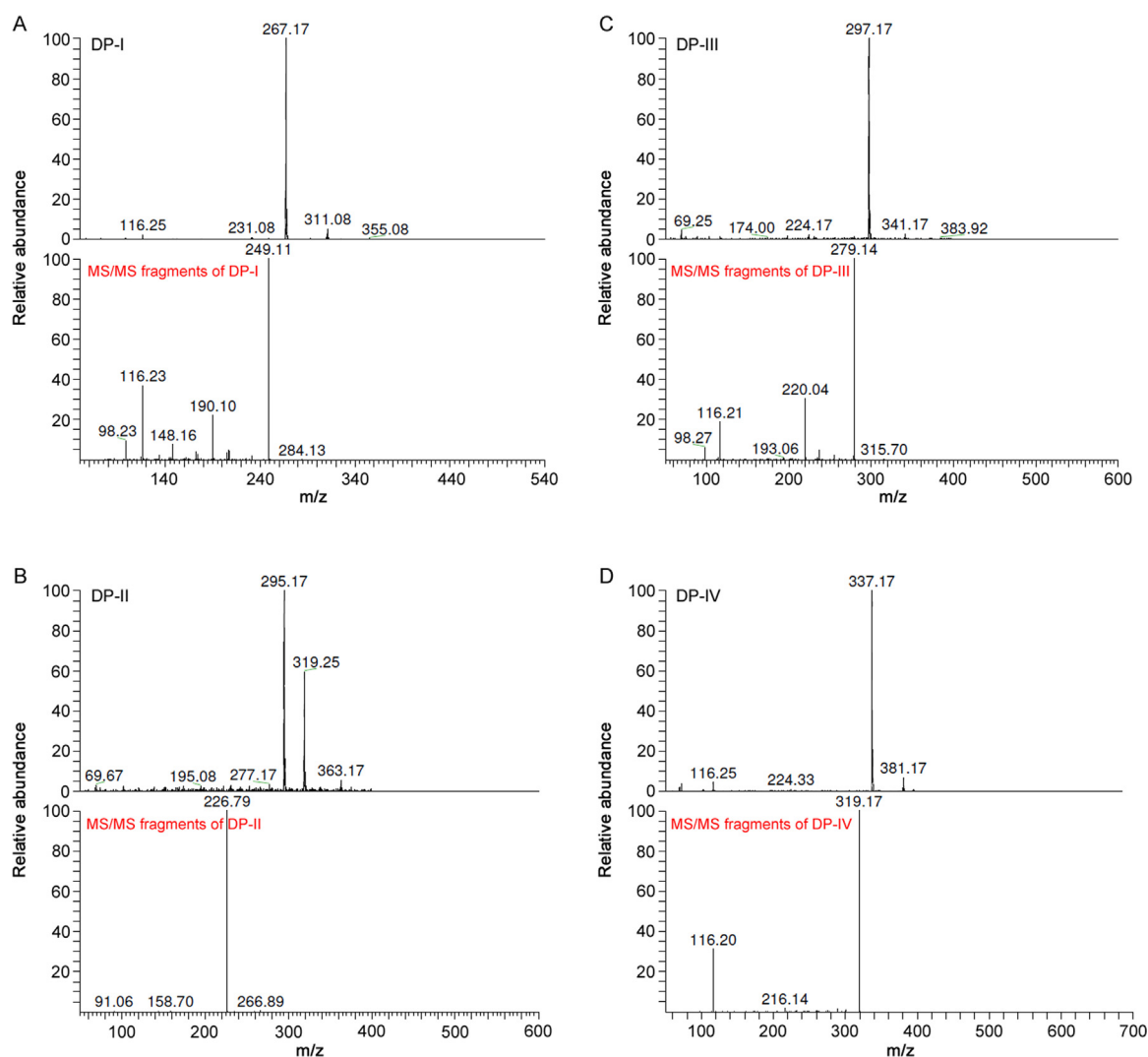

Fig. 5. Line spectra of degradation products: (A) DP-I, (B) DP-II, (C) DP-III and (D) DP-IV obtained in LC–MS/MS studies.

Table 2
LC–MS/MS data of DPs (I-IV) along with their possible molecular formulae and major fragments.

DPs	Experimental mass	Best possible molecular formula	Theoretical mass	RDB[a]	Major fragments (chemical formula)
I	267.17	$C_{14}H_{23}N_2O_3^+$	267.17	4.5	249.11 ($C_{14}H_{21}N_2O_2^+$), 190.10 ($C_{11}H_{12}NO_2^+$), 148.16 ($C_8H_6NO_2^+$), 116.23 ($C_6H_{14}NO^+$), 98.23 ($C_6H_{12}N^+$)
II	319.25	$C_{17}H_{23}N_2O_4^+$	319.17	5.5	295.17 ($C_{15}H_{23}N_2O_4^+$), 277.17 ($C_{14}H_{17}N_2O_4^+$), 266.79 ($C_{14}H_{20}NO_4^+$), 226.79 ($C_{11}H_{18}N_2O_3^+$), 195.08 ($C_{11}H_{19}N_2O^+$)
III	297.17	$C_{15}H_{25}N_2O_4^+$	297.18	4.5	279.14 ($C_{15}H_{23}N_2O_3^+$), 224.17 ($C_{11}H_{14}NO_4^+$), 220.04 ($C_{12}H_{14}NO_3^+$), 193.06 ($C_{11}H_{13}O_3^+$)
IV	337.17	$C_{18}H_{29}N_2O_4^+$	337.21	5.5	319.17 ($C_{18}H_{27}N_2O_3^+$), 224.33 ($C_{12}H_{18}NO_3^+$), 216.14 ($C_{12}H_{10}NO_3^+$), 116.20 ($C_6H_{14}NO^+$)

[a] RDB: ring plus double bonds.

double bonds) and major fragments of all the DPs are listed in Table 2.

3.4. Identification of degradation products

The identification of all the degradation products was achieved with the help of their fragments obtained in LC–MS/MS studies and comparison with fragmentation pattern of the drug obtained in MS/MS and MS^n analysis.

3.4.1. DP-I (m/z 267.17)

As shown in the mass spectrum of DP-I in Fig. 5A, the fragmentation pathway of DP-I was established and the same is shown in Fig. 6. The mass spectrum of DP-I revealed the formation of formate ion adduct with m/z 311.08, which had ~ 44 Da mass units higher than DP-I. This adduct was observed in all the DPs and formed due to ammonium formate mobile phase used during HPLC separation studies. In the initial positive ESI LC–MS analysis of DP-I, a total of three fragments were formed viz., m/z 267.17, 231.08 and 116.25, which could not provid sufficient information about the source of fragment ions. Hence, in the subsequent analysis, ion with m/z 267.17 was fragmented in ion trap MS system, which led to the formation of source ions with m/z 249.11, 190.10, 148.16, 116.23 and 98.23. A similar approach was applied to explore the sources of ions for rest of the DPs. The base peak of fragment with m/z 267.17 (DP-I) was formed as an amide hydrolysis product with the cleavage of butyraldehyde moiety from the drug. The fragment with m/z 267.17 underwent a loss of water molecule and resulted in the formation of ion with m/z 249.11. This ion (m/z 249.11) underwent a parallel pathway and led to the

formation of the other two daughter ions of m/z 231.08 and m/z 116.23 on loss of a water molecule and 1-(3-aminophenyl) ethanone, respectively. The ion with m/z 231.08 on loss of ethenamine (C-N cleavage) resulted in daughter ion with m/z 190.10. This parallel pathway was concluded with the loss of an acetyl moiety from ion with m/z 109.10 and led to the formation of daughter ion with m/z 148.16. Finally loss of water molecule from ion with m/z 116.25 resulted in the formation of ion with m/z 98.23.

3.4.2. DP-II (m/z 319.17)

As per the mass spectrum of DP-II shown in Fig. 5B, and its fragmentation pattern depicted in Fig. 6, a formation of formate ion adduct with m/z 363.17 was observed which had ~ 44 Da mass units higher than DP-II. Under photolytic conditions as recommended by ICH Q1B, a direct light catalyzed oxidation resulted in loss of a terminal methyl group along with two protons, leading to the formation of DP-II with m/z 319.17. In the subsequent pathway, DP-II resulted in the formation of several daughter ions viz., m/z 295.17, 277.17, 266.89, 226.79, and 195.08. The few remaining ions viz., m/z 158.70, 91.06 and 69.67 might result from background noise; hence they were not considered in the fragmentation pathway. A loss of propan-2-amine and ethene moiety led to the formation of fragments with m/z 266.89 and m/z 295.17, respectively. The fragment with m/z 295.17 on multiple cleavages viz., formaldehyde, water molecule and methyl group led to the formation of ion with m/z 195.08. On the other side, fragment with m/z 277.17 was formed on loss of a methyl group and to compensate this loss, lone pair of electrons of nitrogen underwent cyclization with the terminal methyl to form aziridine ring. The fragment with m/z 226.79 was also formed from m/z 295.17 in a
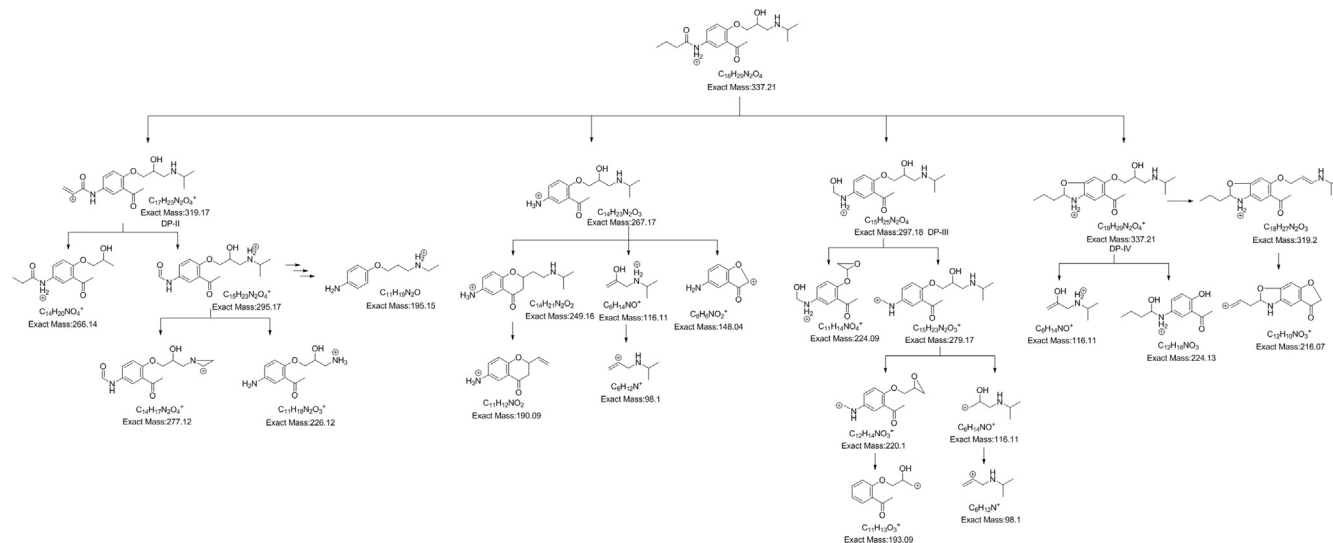

Fig. 6. Fragmentation pathway of DP-I-IV.

Table 3
Linearity data for acebutolol.

Conc. (µg/mL)	Injection 1	Injection 2	Injection 3	Average area	Slope	Correlation coefficient (r)
50	4,527,102	4,443,534	4,485,356	4,485,331		
100	8,773,153	8,533,928	8,619,327	8,642,136		
150	12,401,889	12,472,518	12,437,144	12,437,184	86,347	0.998
200	17,237,409	17,540,180	17,388,815	17,388,801		
250	21,703,531	21,694,116	21,698,824	21,698,824		

two-step process, which involved an initial loss of methyl group followed by cleavage of isopropyl entity. The proposed structures and fragmentation pathways are outlined in Fig. 6.

3.4.3. DP-III (m/z 297.17)

The mass spectrum of DP-III shown in Fig. 5C, revealed the formation of formate ion adduct with m/z 341.17 which had ~44 Da mass units higher than DP-III. A direct cleavage of propyl group from amide side chain of the drug resulted in the formation of enol form of DP-III with m/z 297.17. DP-III on loss of N-methylpropan-2-amine moiety enabled the newly generating fragment to exhibit epoxide ring moiety which was evident in the ion fragment with m/z 224.17, while DP-III on loss of water molecule led to the formation of ion fragment with m/z 279.14. There onwards fragments ion (m/z 279.14) followed a parallel pathway of fragmentation with the loss of isopropyl amino group and 1-(2-hydroxy-5-(methylamino) phenyl)ethanone to form daughter ions with m/z 220.04 and m/z 116.21, respectively. A cleavage of methyl amino group from ion fragment m/z 220.04 resulted in ion with m/z 193.06, while loss of water molecule from m/z 116.21 led to the formation of ion with m/z 98.27. The proposed structures and fragmentation pathways are outlined in Fig. 6.

3.4.4. DP-IV (m/z 337.17)

As the line spectra shown in Fig. 5D and fragmentation pathway depicted in Fig. 6 for DP-IV, DP-IV had the mass similar to the drug (m/z 337.21) along with formate ion adduct of ~ 44 Da that other DPs also showed. Based on the similarity of mass, DP-IV was considered as a structural isomer of acebutolol. The side chain carbonyl oxygen underwent cyclization with adjacent phenyl ring to form DP-IV with m/z 337.17. In the subsequent steps, DP-IV on loss of side chain hydroxyl group resulted in the formation of fragment with m/z 319.17 which in the later step led to the loss of N-isopropylprop-1-en-1-amine and resulted in the formation of another cyclic fragment with m/z 216.14. On the other hand, a cleavage on ether linkage of the side chain and loss of 1-(iso-propylamino)propan-2-ol from DP-IV led to the formation of ions with m/z 116.25 and 224.33, respectively.

3.5. Method development and validation

The drug and all its degradation products were found to show an acceptable separation by using acetonitrile (A) and ammonium formate buffer (B) (10 mM) with the pH 3.5 in a linear gradient mode (Tmin/A:B: T0/5:95; $T$10/25:75; $T$30/55:45; $T$35/5:95). The LC method validation was performed with respect to the parameters such as linearity, precision, accuracy, specificity and selectivity. In linearity studies, the selected drug concentrations showed an appropriate linear response, and the sensitivity of the method viz., limit of detection (LOD) and limit of quantitation (LOQ), was established from the linearity data. The values of slope and correlation coefficient (r) were 86,347 and 0.998, respectively, whereas the theoretical calculated concentrations for LOD and LOQ were found to be 13.44 µg/mL and 40.74 µg/mL, respectively.

Table 4
Method specificity and peak purity data.

Drug/degradation products	Relative retention time	Peak purity	Single point threshold	Resolution
DP-I	0.227	0.9998	0.9979	0.000
DP-II	0.705	0.9973	0.9924	29.921
DP-III	0.796	0.9960	0.9918	6.031
DP-IV	0.918	0.9994	0.9982	7.909
Acebutolol	1.000	0.9999	0.9999	4.682

The linearity data obtained for the concentrations from 50 µg/mL to 250 µg/mL is shown in Table 3. For inter-day and intra-day precision studies, the % RSD values were 0.73%–1.88% and 0.12%–1.03%, respectively. The accuracy study revealed the percent recovery of the spiked drug in the mixture of stressed samples in the range of 101.07% – 101.58% with the mean recovery of 101.32%. The three known concentrations of the spiked drug were 80, 120 and 160 µg/mL. The developed LC method was found to be specific for each peak with respect to peak purity data obtained using a PDA detector. The relative retention time, peak purity, resolution and single point threshold data of drug and DPs are shown in Table 4. The developed method could be applied to other synthetic small molecules having similar physicochemical properties for the assay, identification and characterization of drug substance and degradation products without their isolation from the reaction mixtures. The developed method and the characterization technique are suitable for the quantification and identification of acebutolol bulk drug substance containing the degradants/impurities reported in this article.

3.6. Degradation pathway of the drug

The degradation pathway of the drug under various stress conditions is shown in Fig. 7. DP-I was formed as an amide hydrolysis product on loss of butyraldehyde moiety from the drug, while DP-II was the product obtained on cleavage of acetyl moiety from the drug. DP-III was formed from the drug on loss of propyl group along with a water molecule and DP-IV was obtained as a dehydration product from the drug.

3.7. In-silico carcinogenicity and hepatotoxicity

The carcinogenicity results obtained from TOPKAT, Lazar Toxicity and TOPKAT Extensible model software revealed that the drug (0.967) and DP-I (0.986) were found to be carcinogenic, while DP-II to DP-IV were non-carcinogenic. As per TOPKAT model assessment the values below 0.3 indicate non-carcinogen and above 0.7 signify carcinogen, while the values between 0.3 and 0.7 are considered in intermediate zone. All the compounds under investigation (acebutolol and its DPs) were found to be non-carcinogenic (inactive) as per Lazar Toxicity Prediction model and TOPKAT Extensible model. The results obtained in hepatotoxicity study by using Discovery Studio ADMET model revealed that the
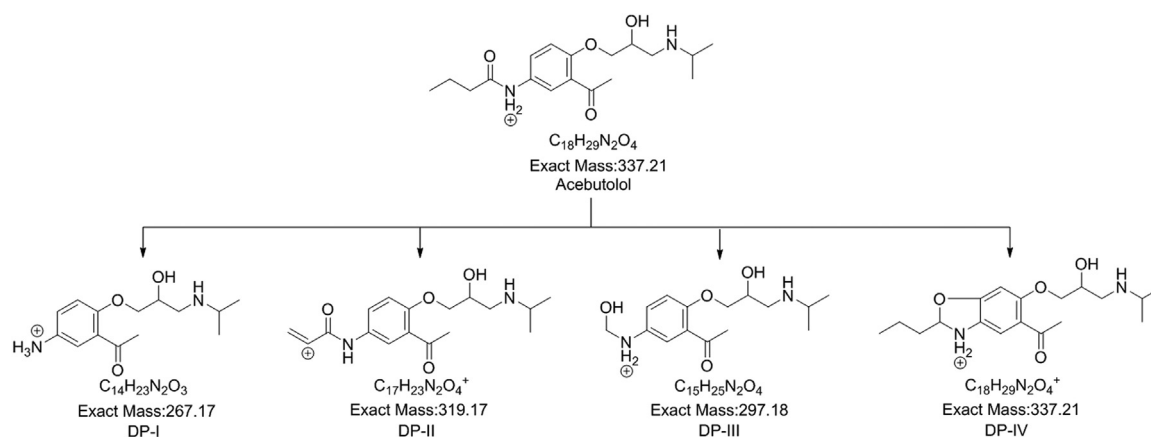
Fig. 7. Degradation pathway of acebutolol.

Table 5
In-silico carcinogenicity and hepatotoxicity study data of acebutolol and its DPs.

Drug/DPs	TOPKAT	Lazar toxicity	TOPKAT extensible	Discovery studio
Acebutolol	0.967 (carcinogen)	Inactive	0.435 (non-carcinogen)	0.490 (nontoxic)
DP-I	0.986 (carcinogen)	Inactive	0.514 (non-carcinogen)	0.397 (nontoxic)
DP-II	0.000 (non-carcinogen)	Inactive	0.000 (non-carcinogen)	0.000 (nontoxic)
DP-III	0.000 (non-carcinogen)	Inactive	0.000 (non-carcinogen)	0.000 (nontoxic)
DP-IV	0.000 (non-carcinogen)	Inactive	0.469 (non-carcinogen)	0.437 (nontoxic)

drug and all DPs were non-toxic. As per Discovery Studio ADMET, the computed probabilities for toxic and non-toxic values were 0.5 or more and 0.5 or less, respectively. But the results obtained for drug (0.490) and DP-IV (0.437) indicated high probability of hepatotoxic potential. The in-silico carcinogenicity and hepatotoxicity results are depicted in Table 5.

4. Conclusions

A forced degradation study on acebutolol was performed to determine its labile behaviour under respective stress condition. The drug was labile to acidic, alkaline and photolytic stresses, while it was stable in other neutral, oxidative and thermal conditions. The LC separation studies revealed the formation of four degradation products from the drug. DP-I was formed in acidic and basic conditions and DP-IV was generated only in basic condition. The two remaining minor DPs, DP-II and DP-III, were the products of photolytic degradation. The structures of all these degradants were resolved with the help of MS, MS^n, and LC–MS/MS analysis. The complete degradation pathway of the drug was established. The in-silico carcinogenicity study explored the carcinogenic potential of the drug and DP-I, while the values obtained by Discovery Studio software for the drug and DP-IV revealed a high probability of hepatotoxic potential.

Conflicts of interest

The authors declare that there are no conflicts of interest.

References

[1] A.C. Moffat, M.D. Osselton, B. Widdop, Clarke's Analysis of Drugs and Poisons, Pharmaceutical Press, London, 2005: 569.

[2] H. Jiang, C. Randlett, H. Junga, et al., Using supported liquid extraction together with cellobiohydrolase chiral stationary phases-based liquid chromatography with tandem mass spectrometry for enantioselective determination of acebutolol and its active metabolite diacetolol in spiked human plasma, J. Chromatogr. B 877 (2009) 173–180.

[3] J. Szymura-Oleksiak, M. Walczak, J. Bojarski, et al., Enantioselective high performance liquid chromatographic assay of acebutolol and its active metabolite diacetolol in human serum, Chirality 11 (1999) 267–271.

[4] R.B. Miller, A validated, high-performance liquid chromatographic method for the determination of acebutolol and diacetolol in human plasma, J. Liq. Chromatogr. Relat. Technol. 15 (1992) 3233–3245.

[5] M. Piquette-Miller, R.T. Foster, F.M. Pasutto, et al., Stereospecific high-performance liquid chromatographic assay of acebutolol in human plasma and urine, J. Chromatogr. 526 (1990) 129–137.

[6] M.G. Sankey, A. Gulaid, C.M. Kaye, Preliminary study of the disposition in man of acebutolol and its metabolites, diacetolol using a new stereoselective HPLC method, J. Pharm. Pharmacol. 36 (1984) 276–277.

[7] A.F. Al-Ghamdi, M.M. Hefnawy, A.A. Al-Majed, et al., Development of square-wave adsorptive stripping voltammetric method for determination of acebutolol in pharmaceutical formulations and biological fluids, Chem. Cent. J. 6 (2012) 1–8.

[8] S.A. Mostafavi, D.A. Stinson, K. Dooly, et al., Excretion of acebutolol and its major metabolite diacetolol into infant blood circulation and the breast milk, Iran. J. Pharm. Res. 2 (2003) 141–144.

[9] M.S. Leloux, F. Dost, Doping analysis of beta-blocking drugs using high-performance liquid chromatography, Chromatographia 32 (1991) 429–435.

[10] A. Tracqui, P. Kintz, P. Wendling, et al., Toxicological findings in a fatal case of acebutolol self-poisoning, J. Anal. Toxicol. 16 (1992) 398–400.

[11] M.E. Abdel-Hamid, Comparative LC–MS and HPLC analyses of selected antiepileptics and beta-blocking drugs, Farmaco 55 (2000) 136–145.

[12] A. Levent, Development of an ion-pair HPLC method for determination of acebutolol in pharmaceuticals, Anal. Lett. 43 (2010) 1448–1456.

[13] J. Krzek, A. Kwiecień, M. Żylewski, Stability of atenolol, acebutolol and propranolol in acidic environment depending on its diversified polarity, Pharm. Dev. Technol. 11 (2006) 409–416.

[14] A. El-Gindy, A. Ashour, L. Abel-Fattah, et al., First derivative spectrophotometric, TLC-densitometric, and HPLC determination of acebutolol HCL in presence of its acid-induced degradation product, J. Pharm. Biomed. Anal. 24 (2001) 527–534.

[15] M. Ogrodowczyk, K. Dettlaff, P. Kachlicki, et al., Identification of radio-degradation product of acebutolol and alprenolol by HPLC/MS/MS, J. AOAC Int. 98 (2015) 46–50.

[16] ICH Q1A(R2) Guideline: Stability testing of new drug substances and products (2003) International Conference on Harmonisation (ICH), IFMPA, Geneva, Switzerland.

[17] ICH Q1B Guideline: Stability testing: Photostability testing of new drug substances and products International Conference on Harmonisation (ICH), IFPMA, Geneva, Switzerland, 1996.

[18] ICH Q2(R1) Guideline: Validation of Analytical Procedures: Text and Methodology International Conference on Harmonization (ICH), IFPMA, Geneva, Switzerland, 2005.

[19] P. Szymański, M. Markowicz, E. Mikiciuk-Olasik, Adaptation of high-throughput screening in drug discovery-toxicological screening test, Int. J. Mol. Sci. 13 (2012) 427–452.

Original Research Article

Detection and determination of undeclared synthetic caffeine in weight loss formulations using HPLC-DAD and UHPLC-MS/MS

Carine Viana [a,b,*], Gabriela M. Zemolin [a], Thaís R. Dal Molin [a], Luciana Gobo [c],
Sandra Maria Ribeiro [a], Gabriela C. Leal [a], Gabriela Z. Marcon [a], Leandro M. de Carvalho [a,c]

[a] Graduate Program in Pharmaceutical Sciences, Federal University of Santa Maria (UFSM), Santa Maria-RS, Brazil
[b] Center of Health Sciences, Federal University of Santa Maria (UFSM), Santa Maria-RS, Brazil
[c] Department of Chemistry, Federal University of Santa Maria (UFSM), Santa Maria-RS, Brazil

ARTICLE INFO

ABSTRACT

Caffeine is present in products marketed for weight loss, with the purpose of increasing thermogenesis and lipid metabolism. The dosage declared by the product manufacturer, or even its presence, is not always correctly described on the label. This work aimed to investigate the undeclared synthetic caffeine in weight loss formulations by a high-performance liquid chromatography with diode array detection (HPLC-DAD) method. From one hundred products purchased through Brazilian e-commerce, seventeen contained caffeine, either naturally or synthetically added to formulation. The caffeine-containing samples were confirmed by an ultra-high performance liquid chromatography-tandem mass spectrometry (UHPLC-MS/MS) method, and adulteration was clearly proven in five products. The content highest caffeine contained 448.8 mg per dose. Other irregularities were also found; nevertheless, the most serious was the addition of synthetic drugs without asking the consumers. Additional drugs expose the consumer to more possible side-effects as well as deleterious drug interactions. Intentional adulteration with any unlabeled substance is typically motivated by a desire to increase or alter the claimed effect of the marketed product to gain a commercial advantage.

1. Introduction

Products marketed for weight loss often contain high amounts of caffeine from natural or synthetic sources in order to increase thermogenesis and lipid metabolism. Caffeine has been shown to heighten resting energy expenditure in adult humans (both normal and overweight) in a dose-dependent manner. Caffeine increases the metabolic rate through the inhibition of phosphodiesterase (PDE) and stimulation of adenosine receptors. This leads to an accumulation of intracellular 3,5-cyclic-adenosine monophosphate (cAMP), which is metabolically excitatory for cells [1,2].

The caffeine content of drinks varies according to the product. In eight ounces of coffee, for example, the content varies from 60 mg in espresso to 125 mg in brewed coffee. Soft drinks, mainly colas, range in caffeine 23–31 mg per 8-ounce bottle [3]. Except for pregnant women, 400 mg of caffeine is the recommended daily allowance for an average person [4]. High doses of caffeine may produce insomnia, heart palpitations, anxiety, nausea, vomiting,

increased blood pressure, muscle twitching, tremors, and increased cholesterol levels [5]. Doses over 600 mg/day can cause significant side effects, including tachycardia, tremors, insomnia, nervousness, chest pain, and arrhythmias [6,7]. The chronic use of high doses can lead to dependence and tolerance, thus requiring larger doses in order to produce the same effect. In these subjects, the abrupt discontinuation might cause a clinical situation called caffeine withdrawal syndrome. The American Psychiatry Association accepts "caffeine withdrawal" as a clinical diagnosis. Its symptoms include headache, marked fatigue or drowsiness, dysphoria, depressed mood or irritability, difficulty concentrating, and flu-like symptoms [8]. The adverse effects might have distinct clinical relevance at different dosages according to a population group. Caffeine intakes from all sources of up to 200 mg per day by pregnant women do not raise safety concerns for the fetus. However, considering the reduced maternal clearance and prolonged half-life during pregnancy along with the exposure of the fetus to maternal caffeine plasma levels, the unborn child is the most vulnerable group for adverse effects due to caffeine among the general population. Subjects with hypertension and/or advanced atherosclerosis have an increased risk for cardiovascular diseases. The administration of a single dose of 200 mg of caffeine significantly increases blood pressure and decreases myocardial

---

blood, and such changes could increase the risk of acute cardiovascular events in these population groups [4].

The US FDA has defined traditional pharmacy compounding as "the combining or altering of ingredients by a licensed pharmacist in response to a licensed practitioner's prescription for an individual patient, which produces a medication tailored to that patient's special medical needs" [9]. In Brazil, this sector is regulated by the National Health Surveillance Agency (ANVISA), and the definition is the same as that of the American agency [10]. There are approximately 8200 compounding pharmacies registered in the country, representing about 10% of the country's drug market [11]. Nevertheless, as it is a highly competitive market, the pharmacies use digital technologies to increase sales. Phones, websites, drive-thru systems, message ordering, and cell phone applications have been applied to interact with customers.

Adulteration with synthetic drugs is a recurring problem with so-called natural medicines [12]. Cases of adverse effects resulting from the intentional addition of synthetic drugs in herbal medicines have been reported [13]. For example, fenproporex, chlordiazepoxide and fluoxetine were identified as adulterants in prescription diet pills, and users reported headaches, palpitations, chest pain, nausea, insomnia and fatigue [13,14]. The clinical consequences can be serious and sometimes life-threatening. This is especially true when patients use medications with potential interactions or when patients have other predisposing medical conditions. These incidents emphasize the importance of detecting the presence of undeclared synthetic drugs in herbal medicines to ensure their safety. Food supplements, pharmaceuticals, and compounded drugs are under distinct regulations, and all are potential targets for adulterations [12,14–19].

This work aimed to investigate the addition of undeclared caffeine as an adulterant in compounded formulations for weight loss. Since caffeine may be present naturally in some vegetable raw materials of the formulations, all of the components were also analyzed separately. A high-performance liquid chromatography with diode array detection (HPLC-DAD) method was developed to analyze the undeclared synthetic caffeine present in different pharmaceutical products. The presence and content of caffeine were confirmed using a comparative ultra-high performance liquid chromatography-tandem mass spectrometry (UHPLC-MS/MS) method. The quality and safety requirements of health products have been a recurrent matter among regulatory agencies. Accordingly, this study also aims to highlight the critical points concerning the regulation of compounded and industrialized products containing caffeine.

2. Materials and method

2.1. Instrumentation and apparatus

The chromatographic separations were carried out on a Knauer (Berlin, Germany) HPLC system, which consisted of a Smartline Pump 1000 coupled to a Smartline Manager 5000, and a multichannel UV spectrophotometer detector based on diode array technology (Smartline UV Detector 2600) equipped with ChromGate® (Knaeur) software (Version 3.3.1). The chromatographic runs were conducted at room temperature ($21 \pm 2\,°C$) using a reverse-phase C_{18} column (4.6 mm × 250 mm, 5 μm; Thermo Scientific) with an Acclaim® 120 C_{18} guard cartridge (4.3 mm × 10 mm, 5 μm; Dionex Corporation, Sunnyvale, USA). Samples were injected using a sample injector equipped with a 20 μL loop. The detection was performed at 220 nm.

Mass spectrometry experiments were performed on an Agilent 1260 Infinity LC-MS chromatograph with automatic injection and an Agilent 6430 triple quadrupole mass detector (Santa Clara, CA,

United States). The chromatographic column was a Poroshell 120 EC-C_{18} (3.0 mm × 100 mm) with a 2.7 μm particle size. An electrospray ionization source (ESI) was used to ionize the chromatographic effluent generated until 7.0 min. The parameters for ESI were optimized to give the best response and signal stability of the analyte. The final optimized parameters were a nitrogen gas flow of 11 L/min, a nebulizer pressure of 30 psi, a capillary voltage of ± 2.4 kV and a drying gas temperature of 250 °C (N_2). The ionized compounds were subsequently analyzed in an Agilent 6430 triple quadrupole mass spectrometer operating in the multiple reaction monitoring (MRM) mode with a resolution of 0.7 m/z (FWHM). The quantification transitions were divided into three temporal segments of acquisition, and the dwell time for each transition was optimized to 20 ms. High purity nitrogen (99.999%) obtained from Linde (Munich, Germany) was used as the collision-inducing gas. The ions monitored in ESI-MS/MS for the qualitative confirmation of caffeine were m/z 195.10 (precursor ion) and m/z 138.2 (product ion).

2.2. Reagents and solutions

The certified reference material caffeine was purchased from Sigma-Aldrich (Germany) with a declared purity of 99.0%. A stock solution of caffeine (1.0 g/L) was prepared in ultrapure water, and working solutions were obtained by dilutions of the stock solution with water.

Phaseolus vulgaris, *Caralluma fimbriata*, *Cassia nomame*, *Fucus vesiculosus*, *Equisentum* sp., *Plantago psyllium*, *Cordia ecalyculata*, green tea (*Camellia sinensis*), *Spirulina maxima*, *Passiflora sp.*, *Rhamnus purshiana*, *Garcinia cambogia*, *Citrus aurantium*, Glucomannan (*Amorphophallus konjak*), Ma Huang (*Ephedra* sp.), *Paullinia cupana*, chitosan, and *Cassia augustifolia* were obtained from local compounding pharmacies, and all were raw materials in their bulk forms.

HPLC-grade solvents methanol (MeOH) and acetonitrile (ACN) were obtained from the Tedia Company (USA). Orthophosphoric acid (H_3PO_4) (85%, m/v) was purchased from Merck (Darmstadt, Germany). The methanol for analysis by UHPLC-MS/MS was of Chromasolv LC-MS grade and supplied by Sigma-Aldrich (St. Louis, MO, United States).

2.3. Sample source

The samples were acquired from pharmacies that announced herbal weight loss products in nine different Brazilian states (i.e., Ceará, Distrito Federal, Goiás, Minas Gerais, Parana, Rio de Janeiro, Rio Grande do Sul, Santa Catarina, and São Paulo). The samples were purchased by contacting the pharmacies by email, telephone or via their websites. A pool of 20 capsules was prepared for both the determination of caffeine by the HPLC-DAD method and confirmatory analysis by UHPLC-MS/MS.

2.4. HPLC condition

The HPLC determination of caffeine was carried out by using a constant eluent composition of 0.1% phosphoric acid-ACN (70:30, v/v) and a gradient flow rate from 0.8 to 1.5 mL/min. The flow rate conditions were as follows: 0.8 mL/min (0–4.4 min), 0.5 mL/min (4.5–5 min), 0.5–1.5 mL/min (5–10 min), and 1.5 mL/min (10 min). The total run time was 10 min. A re-equilibration period of 5 min was used between individual runs. Before the daily chromatographic experiments, the C_{18} column was conditioned with the mobile phase for 45 min.

The equivalent weight of one capsule was dissolved in 25 mL of hot water (90 °C) in a volumetric flask in order to perform the HPLC-DAD analysis. After extracting the caffeine by infusion and

sonication for 30 min, the quantitative determination was performed in triplicate. All extracts were diluted forty times and filtered through a 0.45 μm cellulose acetate membrane prior to injection into the HPLC system. For studying the caffeine content in bulk raw plant extracts, 36 herbal materials were acquired from different compounding pharmacies in Southern Brazil (Rio Grande do Sul). The herbal extracts were analyzed by the same procedure as the herbal weight loss pharmacy-compounded products aforementioned.

2.5. UHPLC-MS/MS condition

For confirmatory analysis by UHPLC-MS/MS, an isocratic elution was performed using 0.1% acetic acid/methanol (50:50, v/v) under a flow rate of 0.4 mL/min. The injection volume was 5 μL, and the column was maintained at 30 °C. The ESI ionization source was used in the positive mode. The drying gas was under a flow of 13 L/min at 350 °C. The nebulizer pressure was 40 psi, and the capillary voltage was 4000 V.

The equivalent weight of one capsule was dissolved in 25 mL of methanol. Methanol was the best choice for sample extraction because it is more protic than acetonitrile, facilitating the ionization and increasing the caffeine signal. The sample was then sonicated for 15 min in an ultrasonic bath. All extracts were diluted 100 times, filtered through a 0.2 μm hydrophilic membrane and transferred to the vials for analysis.

2.6. Validation of HPLC-DAD method

The HPLC-DAD method was validated by determining the following operational characteristics: specificity, linearity, limits of quantification (LOQ) and detection (LOD), precision and accuracy [20,21].

The method specificity was evaluated by studying the interference of other amines (L-tyrosine, *p*-octopamine, *p*-synephrine, tyramine, and hordenine) in caffeine analysis. *Phaseolus vulgaris*, *Caralluma fimbriata*, *Cassia nomame*, *Fucus vesiculosus*, *Equisentum* sp., *Plantago psyllium*, *Cordia ecalyculata*, green tea *(Camellia sinensis)*, *Spirulina maxima*, *Passiflora sp.*, *Rhamnus purshiana*, *Garcinia cambogia*, *Citrus aurantium*, Glucomannan *(Amorphophallus konjak)*, Ma Huang *(Ephedra* sp.), *Paullinia cupana*, chitosan and *Cassia augustifolia* were also used to determine the specificity of the method. These bulk raw materials were treated in the same way as the samples of compounded formulations.

The method linearity was evaluated by six-point calibration curves performed on three different days. The LOD and LOQ were calculated using the following equations: LOD = 3.3 × Sa/b and LOQ = 10 × Sa/b, where Sa is the intercept standard deviation and b is the slope. The precision was expressed by the variation coefficients expressed as the relative standard deviation (RSD) of results obtained in triplicate for three different analyte concentrations. The accuracy was evaluated as a percentage of recovery obtained from analyzing samples spiked with known amounts of a reference substance at three different levels. The percentage recovery was calculated using the formula proposed by the AOAC [22].

3. Results and discussion

3.1. Determination of caffeine by HPLC-DAD and UHPLC-MS/MS

In the present work, validation experiments were carried out for the determination of caffeine in different pharmacy-compounded products. The caffeine can be selectively determined in formulations for weight loss containing different plant materials,
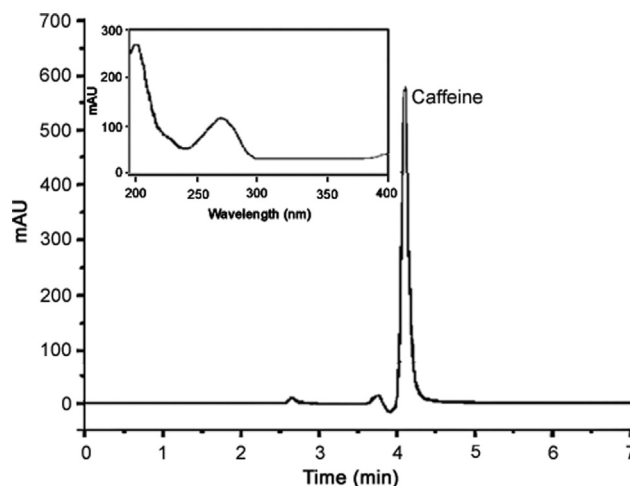

Fig. 1. HPLC-DAD chromatogram obtained for caffeine.

as observed in Fig. 1. An HPLC method using acetonitrile/0.1% H_3PO_4 (30:70, v/v) as the mobile phase and a gradient elution method with a programmed flow rate was optimized. The method showed to be selective for the determination of caffeine without interference from any other biogenic amines, such as synephrine, tyramine, L-tyrosine, p-octopamine, and hordenine.

The presence of caffeine was confirmed by a UHPLC-ESI-MS/MS comparative method. As can be observed in Fig. 2, for sample "O", caffeine can be determined in formulations containing plant materials and other components. The confirmation measurement was based on the MRM mode by evaluating the ion fragments at 195.1 *m/z* (molecular ion) 138.1 *m/z* (quantifier ion) and 110.1 *m/z* (qualifier ion). The samples analyzed by the UHPLC-ESI-MS/MS confirmatory method were selected after the screening step by the validated HPLC-DAD method.

3.2. Validation of HPLC-DAD method for caffeine determination

The optimized method was validated based on the principal analytical validation parameters. Linearity data, analysis of variance (ANOVA), LOD and LOQ for determination of caffeine by the developed HPLC-DAD method are concise in Table 1. No interfering peaks were found in the chromatogram due to sample excipients. The linearity data were validated using ANOVA, which demonstrated significant linear regression ($p < 0.05$) and no significant deviation from linearity ($p < 0.10$). The sensitivity of the chromatographic system employed was assessed by determining the LOD and LOQ; the results were considered low and demonstrated good sensitivity for the method. Precision and accuracy data are summarized in Table 2. The low RSD obtained for all of the samples spiked with standards indicated good precision and repeatability for the method. The accuracy of the method was acceptable, as it was 97.2% with an SD value less than 2.2.

3.3. Sampling

In the present study, we searched websites of compounding pharmacies that advertised weight loss formulations. A total of 190 compounding pharmacies were contacted by email, telephone, via the pharmacy website or personally to request any available natural weight loss products. The appealing practice by pharmacies e-commerce could be observed, once the websites offer benefits that do not always correspond to the compounded product. Alluring claims such as "Belly's dry", "Miracle weight loss formula", and "Lymphatic drainage in capsules" as well as the use of images that demonstrate the quick and effective weight loss are often
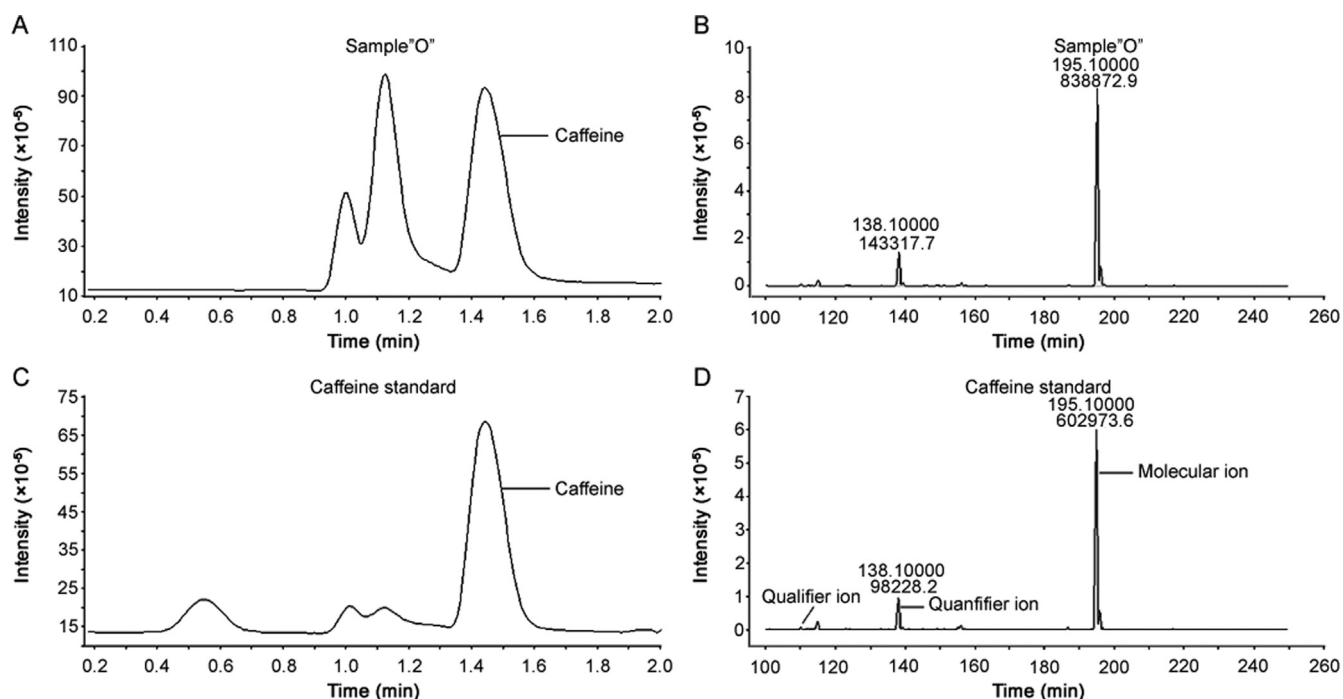
Fig. 2. Total ion chromatograms (TIC) and ESI-MS/MS spectrum obtained for the caffeine analysis of (A and B) compounded formulation containing *Citrus aurantium*, L-carnitine, green tea, and chitosan (sample "O") in comparison to (C and D) caffeine standard by UHPLC-ESI-MS/MS.

Table 1
Linearity data, analysis of variance, LOD and LOQ for determination of caffeine by the developed HPLC-DAD method.

Parameters	Results[a]
Linearity	
Concentration range (μg/mL)	1.0–20.0
Slope $\pm$ standard error	192706.6 $\pm$ 9846.3
Intercept $\pm$ standard error	623.0 $\pm$ 101986.4
Correlation coefficient (r)	0.998
Analysis of variance	
Linear regression	5702.1 (4.96)[b]
Linearity deviation	3.76 (4.69)[c]
LOD (μg/mL)	0.05
LOQ (μg/mL)	0.16

[a] Data obtained from 3 six-point calibration curves.
[b] Values in parentheses are the corresponding critical values for F at $P = 0.05$.
[c] Values in parentheses are the corresponding critical values for F at $P = 0.10$.

Table 2
Precision and recovery for determination of caffeine by the developed HPLC-DAD method.

Level/added conc. (μg/mL)	Precision (%RSD)	Recovery (mean $\pm$ SD, %)
1	1.8	98.6 $\pm$ 2.2
10	3.1	101.2 $\pm$ 0.7
20	1.0	91.7 $\pm$ 0.9
Mean		97.2

$n = 3$ in each level or concentration.

used by pharmacy websites. Such claims have been employed with the unique purpose of improving sales, consequently promoting an indiscriminate use of these products.

One hundred weight loss compounded formulations were received from seventy pharmacies. In disagreement with the regulations, all formulations were suggested without requiring any

medical prescription [10]. In addition, about 40% of the acquired formulations had brand names on their labels, such as "Compound for Reducing Body Size", "Weight Loss Compound", "Weight Loss Compound IV", "Weight Loss Compound Magri II", "Plus La Santa Slimming", "Fine Fit M", "Compound for Reducing Fat Mass", "Slimming Compound", "Compound for Reducing Appetite", "Slimming Vegetable Compound", "Oriental Cleaning", and "Super Fat Burners M". The names given to the products acquired in this work were appealing, with the clear purpose of stimulating consumption. A compounded product must contain only its formulation detailed on the label.

According to Brazilian regulations, industrialized capsules containing caffeine have been commercialized under "food for athletes" as a product category and can be sold with a brand name. The caffeine supplements for athletes should state the highlighted and bold warning, "This product should not be consumed by children, pregnant women, the elderly, and those who are sick". Their labels cannot induce the consumer to ingest a product, which does not have any action for weight loss, definition or the gain of muscle mass. The terms "anabolic", "muscular hypertrophy", "muscle mass", "fat burning", "fat burners", "increased sexual ability", "anticatabolic", "anabolic", or similar terms cannot be present on the packaging [23]. However, these requirements are not always followed by manufacturers, and some products end up being removed from the market [24–26]. Warnings required for industrialized products do not exist for pharmacy-compounded capsules containing caffeine, once they are prescription-only healthcare products.

The pharmaceutical regulation is very diverse around the world, and the harmonization of such regulations is a subject of discussion among the main global regulatory agencies. The sampling is a useful tool to analyze merchant compliance with applicable regulations. In the USA, concerns have been also raised that some pharmacies were going beyond traditional drug compounding for individual patients and selling large quantities of drugs without meeting safety and other requirements applicable [9,27].

Table 3
Labeled vegetal compounds in all weight loss compounded formulations ($n = 100$), their frequency and caffeine content in each component.

Compound	Frequency	Caffeine* (mg/kg $\pm$ RSD)
Caralluma fimbriata	26	–
Rhamnus purshiana	25	–
Fucus vesiculosus	21	–
Garcinia cambogia	20	–
Centella asiatica	17	–
Citrus aurantium	15	–
Cordia ecalyculata	14	43,100.7 $\pm$ 2.1
Phaseolus vulgaris	14	–
Cynara scolymus	14	–
Amorphophallus konjak	12	–
Spirulina maxima	12	–
Equisentum sp.	12	–
Cassia angustifolia	10	727.8 $\pm$ 4.6
Chitosan	9	–
Slendesta®	8	–
Passiflora sp.	7	–
Green tea (*Camellia sinensis*)	7	28,152.0 $\pm$ 3.9
Baccharis trimera	6	–
Gymnema silvestris	5	–
Gelidium corneum	4	–
Plantago psyllium	4	–
Ptychopetalum uncinatum	4	–
Cyamopsis sp.	2	–
White tea (*Camellia sinensis*)	2	6100.0 $\pm$ 2.8
Cassia nomame	1	8546.6 $\pm$ 2.1
Valeriana officinalis	1	–
Paullinia cupana	1	21,549.9 $\pm$ 4.7
Echinodorus macrophyllus	1	–
Persea americana	1	–
Ginkgo biloba	1	–
Arctostaphylos uvaursi	1	–
Cordia salicifolia	1	–
Phytolacca decandra	1	–
Ephedra sinica	1	–
Erythrina mulungu	1	–
Chlorella pyrenoidosa	1	–

* $n = 3$; (-) values below LOD.

3.4. Determination of caffeine in compounded formulations for weight loss

Table 3 shows the vegetal compounds present in all of the weight loss products analyzed in this study ($n=100$), their frequency, and caffeine content by using the proposed HPLC-DAD method. Caffeine was present only in the following components: *Cordia ecalyculata*, *Cassia angustifolia*, green tea (*Camellia sinensis*), white tea (*Camellia sinensis*), *Cassia nomame*, and *Paullinia cupana*. Green tea (*Cammelia sinensis*) and *Paullinia cupana* had caffeine concentrations equivalent to those already described in the literature [28–30]. In contrast, white tea (*Cammelia sinensis*) presented levels lower than those reported in the literature (43.080 mg/kg) [31,32], which represents about seven-fold more caffeine than the level found in this work. However, batch to batch variations are common in raw materials of plant origin. The presence of caffeine in *Cassia angustifolia* and *Cassia nomame* has not been previously reported. Herein, it is important to emphasize the possibility that both the herbal materials analyzed were not, in fact, the vegetal species that were declared in the product. In this case, our research tried to have access to the same bulk raw materials normally used in the weight loss formulations by the studied compounding pharmacies. Thus, we consider that the sellers are acquiring the herbal materials they really intend to use in terms of the natural active principle. Thus, *C. angustifolia* and *C. nomame* were considered as the species that the manufacturers really use for compounding the studied weight loss formulations.

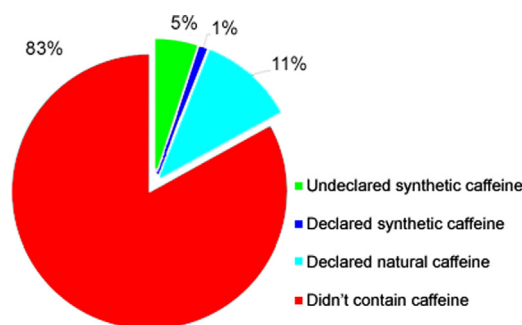*Cordia ecalyculata* presented a compatible caffeine content or

Fig. 3. Incidence of caffeine in the analyzed samples.

one that was even higher than those presented by *Camellia sinensis* and *Paullinia cupana*, species that recognizably have high levels of this substance. This data may justify its frequent use in weight loss formulations.

All weight loss pharmacy-compounded products ($n = 100$) were analyzed with regard to the caffeine content by using the validated HPLC-DAD method. Fig. 3 shows the incidence of caffeine in the analyzed products; this substance was detected either from natural or synthetic sources in 17 samples. Although the differentiation between natural and added caffeine can be somewhat hampered by the possible batch-to-batch variability of caffeine contents in raw materials, levels much higher than those expected from natural sources (e.g., Table 3) may be attributed to the intentional addition of a synthetic drug. Table 4 presents the formulation description, brand name, dose and caffeine content of those analyzed formulations that contained caffeine. The caffeine presence was qualitatively confirmed by monitoring the ions produced in ESI with m/z values of 195.10 (precursor ion) and 138.2 (product ion) in the comparative UHPLC-ESI-MS/MS method. In five analyzed samples (samples E, F, I, N, and O), the adulteration with synthetic caffeine was obvious, as the contents found were not declared on the labels and could not be attributed to any product of natural origin. Twelve percent of the samples had either the natural or synthetic caffeine content as stated on the label.

The samples with the highest caffeine content were sample I and sample N. After analyzing both samples, it is possible to note that the caffeine content does not come from the natural raw materials present in the formulations. Sample I contained 224.4 mg of caffeine per dose, and its recommended labeled dosage is two doses per day, which represents a daily intake of 448.8 mg caffeine. The sources of caffeine in this formulation are *Cordia ecalyculata* and *Cassia nomame*, which together could provide approximately 10.3 mg of caffeine per dose. In sample N, 70.8 mg of caffeine per dose was found, and the pharmacy recommended three doses a day, which represents an intake of 212 mg of caffeine per day. White tea could provide a caffeine content of 1.2 mg per dose considering the value determined in this study.

The problem is that the consumers of these products are not aware of the risks associated with the caffeine added illegally. The user can present typical symptoms of this substance and even interactions of it with other drugs. The caffeine may increase sleep latency and reduce sleep duration in some adult individuals, particularly when consumed close to bedtime [4]. Individual sensitivity to the effects of caffeine is well recognized [33]. However, caffeine consumption can cause adverse effects such as increases in blood pressure, a rapid heartbeat, and tremors, and the caffeine-induced hypokalemia could contribute to ventricular arrhythmias [4,33].

Another irregularity found in the sampling process was the presence of hydrochlorothiazide (sample G), a potent diuretic, and benzocaine (sample M), an analgesic. Even if stated on the label, their inclusion can be considered an illegal practice since pharmacies inserted these drugs into the formulations deliberately. The

Table 4
Description of compounded formulation, brand name, doses and caffeine content of those analyzed pharmacy-compounded products that contained caffeine ($n = 17$).

Sample	Formulation	Brand name	Basal content of caffeine[a,b,c] (mg/dose)	Determined caffeine (mg/dose $\pm$ RSD)	Dose/day[d]	Intake (mg/day)
A	*Faseolus vulgaris* 200 mg; *Caralluma fimbriata* 200 mg; *Cassia nomame* 100 mg; White tea 100 mg; *Fucus vesiculosus* 100 mg; Equisetum 100 mg; Psylium 200 mg	Compound for Reducing Body Size	6.9	6.8 $\pm$ 2.2	3	20.5
B	*Cordia ecalyculata* 300 mg	Pholia Magra	12.9	2.0 $\pm$ 0.3	2	4.0
C	*Cordia ecalyculata;* Green tea; *Garcinia cambogia*	Weight Loss Compound	***	1.5 $\pm$ 1.0	3	4.7
D	*Faseolus vulgaris; Caralluma fimbriata; Citrus aurantium;* Green tea	Weight Loss Compound IV	***	3.0 $\pm$ 0.3	2	6.0
E	*Cassia angustifolia* 350 mg	Weight Loss Compound Magri II	0.2	13.5 $\pm$ 2.0	2	27.0
F	*Cordia ecalyculata* 200 mg; Slendesta® 200 mg; Green tea 150 mg	–	12.8	37.4 $\pm$ 4.6	2	74.8
G	*Fucus vesiculosus* 80 mg; *Centella asiatica* 80 mg; Spirulina 80 mg; Passiflora 50 mg; *Rhamnus purshiana* 100 mg; Caffeine 30 mg; Hydrochlorothiazide 10 mg	Weight Loss Compound	30	32.1 $\pm$ 4.5	2	64.3
H	*Centella asiática* 200 mg; *Fucus vesiculosus* 200 mg; Green tea 100 mg; Advantra Z® (*Citrus aurantium*) 400 mg	–	2.8	4.4 $\pm$ 0.6	2	8.8
I	Mahuang 250 mg; *Cordia ecalyculata* 200 mg; Slendesta® 300 mg; *Cassia nomame* 200 mg; *Citrus aurantium* 300 mg; Chromium picolinate 100 mcg; *Faseolus vulgaris* 350 mg; Citrin extract® 200 mg; *Garcinia cambogia* 100 mg	Plus La Santa Slimming	10.3	224.4 $\pm$ 5.2	2	448.7
J	Green tea 250 mg	–	7.0	2.5 $\pm$ 0.5	2	5.1
K	*Fucus vesiculosus* 90 mg; *Centella asiatica* 150 mg; *Rhamnus purshiana* 5 mg; *Citrus aurantium* 80 mg	Fine Fit "M"	–	2.1 $\pm$ 0.6	2	4.2
L	*Cordia ecalyculata* 300 mg	Pholia Magra	12.9	3.7 $\pm$ 0.3	3	11.2
M	Green tea 200 mg; *Garcinia cambogia* 500 mg; Advantra Z® (*Citrus aurantium*) 200 mg; Glucomanann 200 mg; Benzocaine 30 mg	–	5.6	1.9 $\pm$ 0.3	2	3.8
N	*Faseolus vulgaris* 100 mg; *Caralluma fimbriata* 200 mg; White tea 200 mg	Appetite Suppressant	1.2	70.8 $\pm$ 4.7	3	212.4
O	*Citrus aurantium* 200 mg; L-carnitina 100 mg; Green tea 100 mg; Chitosan 100 mg	Compound for Reducing Fat Mass	8.4	32.0 $\pm$ 3.4	3	96.1
P	*Zingiber officinale;* Green tea; *Cinnamomum zeylanicum; Capsicum frutensens*	Slimming Compound	***	1.0 $\pm$ 0.6	3	3.1
R	Green tea 500 mg	–	14.0	15.0 $\pm$ 1.3	3	45.0

[a] calculated from the values described in Table 2.
[b] (***) Non-declared amounts of the components don't permit to establish a relationship of the basal content of caffeine per dose.
[c] (-) Formulations that have no caffeine or caffeine-containing compounds declared on the label.
[d] Suggested by manufacturer in the formulation label.

addition of synthetic drugs, without first asking or warning the consumer, occurs in order to satisfy the consumer and ensure that the product works as intended as well as to provide quicker effects. In fact, for weight-loss products, consumers tend to quit using the products if they do not realize any initial effects. In contrast, if the product quickly succeeds in providing the desired results, more units are likely to be sold, thus increasing the pharmacy's profit. However, this practice exposes the user to potential drug side-effects and drug interactions.

A final comparison with the industrialized dietary supplements would be relevant. It is noteworthy to point out that caffeine supplements for athletes cannot contain any other substances and must declare the dosage, which must be between 210 and 420 mg per serving [23]. However, this does not guarantee that the dietary supplements available on the market adhere to these concentrations. Several product recalls have already been made for these reasons [17,18,33,34].

4. Conclusion

An HPLC-DAD method for the separation and identification of caffeine in compounded formulations was validated. From one hundred analyzed samples, this substance was present in seventeen. The adulteration was proven in five products by UHPLC-MS/ MS method. The users of these products reported here could have increased sleep latency and a reduced sleep duration, particularly when consumed close to bedtime. Caffeine consumption acutely increases blood pressure and may also present adverse effects such as increases in a rapid heartbeat, tremors and arrhythmias. Moreover, the consumer may use other substances and/or medicines, and interactions deleterious to the health of consumers can occur. Other irregularities were also indicated such as formulations assigned a brand name, appealing labels, alluring claims by websites in order to improve the sales, and the addition of synthetic drugs without first asking the user. Lastly, it is noteworthy that due to the exponential increase in connectivity by the Internet, people involved in the manufacturing and marketing of intentionally adulterated health products have gained access to a wide marketplace. In countries that have very weak or non-existent health surveillance systems, adulteration can have an even bigger impact. This background plus the growing consumption of weight loss formulations indicates the need to take enforcement measures by competent health authorities in order to detect possible adulterations.

Conflicts of interest

The authors declare that there are no conflicts of interest.

References

[1] G.H. Kamimori, C.S. Karyekar, R. Otterstetter, et al., The rate of absorption and relative bioavailability of caffeine administered in chewing gum versus capsules to normal healthy volunteers, Int. J. Pharm. 234 (2002) 159–167.

[2] R. Vaughan, Effects of Dietary Stimulators of Metabolism and Mitochondrial Biogenesis In Vitro And in Vivo: Implications for Metabolic Disease, Thesis of Doctoral Degree, University of New Mexico, Mexico, 2014.

[3] Z. Gardner, M. McGuffin, American Herbal Products Association's Botanical Safety Handbook, Second edition, CRC Press, Boca Raton, 2013.

[4] EFSA Panel on Dietetic Products, Nutrition and Allergies, Scientific Opinion on the safety of caffeine, EFSA J. 13 (2015) 4102–4122. Available from: ⟨http://onlinelibrary.wiley.com/doi/10.2903/j.efsa.2015.4102/epdf⟩ (accessed 1 October 2017).

[5] A. Roberts, Caffeine: An Evaluation of the Safety Database. Nutraceuticals: Efficacy, Safety and Toxicity, Academic Press, San Diego, 2016: 417–434.

[6] M. Cannon, C.T. Cooke, J.S. McCarthy, Caffeine-induced cardiac arrhythmia: an unrecognised danger of health food products, Med. J. Aust. 174 (2001) 520–521.

[7] H.R. Lierberman, W.J. Tharion, B. Shukitt-Hale, et al., Effects of caffeine, sleep loss, and stress on cognitive performance and mood during U.S. Navy SEAL training, Psychopharmacol 164 (2002) 250–261.

[8] S. Ferré, Mechanisms of the psychostimulant effects of caffeine: implications for substance use disorders, Psychopharmacol 233 (2016) 1963–1979.

[9] United States Government Accountability Office (U.S. GAO), Drug Compounding: FDA Has Taken Steps to Implement Compounding Law, but Some States and Stakeholders Reported Challenges. GAO-17 − 64, 2016. Available from: ⟨http://www.gao.gov/products/GAO-17-64⟩ (accessed 12 October 2017).

[10] Brazil, Agência Nacional de Vigilância Sanitária (ANVISA), Resolução nº 67, de 8 de outubro de 2007, Diário Oficial da União, 2007.

[11] Brazil, Federal Council of Pharmacy, Number of Magistral Pharmacies, data, 2015. Available from: ⟨http://www.cff.org.br/pagina.php?Id=801&menu=801&titulo=Dados+2015+⟩ (accessed 1 October 2017).

[12] L.M. De Carvalho, P.A. Cohen, C.V. Silva, et al., A new approach to determining pharmacologic adulteration of herbal weight loss products, Food Addit. Contam. Part A 29 (2012) 1661–1667.

[13] E. Williamson, S. Driver, K. Baxter, Interações Medicamentosas de Stockley - Plantas Medicinais e Medicamentos Fitoterápicos, Artmed, Porto Alegre, 2012.

[14] P.A. Cohen, Imported fenproporex-based diet pills from Brazil: a report of two cases, J. Gen. Int. Med. 24 (2009) 430–433.

[15] P.A. Cohen, C. Benner, D. McCormick, Use of a pharmaceutically adulterated dietary supplement, Pai You 485Guo, among Brazilian-born women in the United States, J. Gen. Int. Med. 27 (2012) 51–56.

[16] M.I. Avigan, R.P. Mozersky, L.B. Seeff, Scientific and Regulatory Perspectives in Herbal and Dietary Supplement Associated Hepatotoxicity in the United States, Int. J. Mol. Sci. 17 (2016) 331–361.

[17] D.B.J. Neves, E.D. Caldas, Determination of caffeine and identification of undeclared substances in dietary supplements and caffeine exposure assessment, Food Chem. Toxicol. 105 (2017) 194–202.

[18] C. Viana, G.M. Zemolin, L. Müller, et al., High-performance liquid chromatographic analysis of biogenic amines in pharmaceutical products containing *Citrus aurantium*, Food Add. Contam. Part A 30 (2013) 634–642.

[19] J. Gudeman, M. Jozwiakowski, J. Chollet, et al., Potential risks of pharmacy compounding, Drugs RD 13 (2013) 1–8.

[20] I.C.H. Q2B (R1) Validation of analytical procedures: text and methodology, Proceedings of the International Conference on Harmonization, November 2005.

[21] The United States Pharmacopeial Convention, U.S. Pharmacopeia 39/National Formulary 34, 2015.

[22] AOAC, Official Methods of Analytical Chemists of AOAC International, Washington, DC, 1990.

[23] Brazil, Agência Nacional de Vigilância Sanitária (ANVISA). Resolução n° 18, de 27 de abril de 2010, Diário Oficial da União, 2010.

[24] Brazil, ANVISA, Resolução nº 1349, de 23 de maio de 2016, Diário Oficial da União, 2016.

[25] Brazil, ANVISA, Resolução nº 81, de 05 de novembro de 2008, Diário Oficial da União, 2008.

[26] Brazil, ANVISA, Anvisa alerta para o risco de consumo de suplemento alimentar. Available from: ⟨http://portal.anvisa.gov.br/wps/content/anvisa+portal/anvisa/sala+de+imprensa/assunto+de+nteresse/noticias/anvisa+alerta+para+risco+de+con-sumo+de+suplemento+alimentar%2⟩ (Accessed 1 October 2017).

[27] US Food and Drug Administration (FDA). Pharmacy Compounding of Human Drug Products Under Section 503A of the Federal Food, Drug, and Cosmetic Act: Guidance, June 9, 2016. Available from: ⟨https://www.fda.gov/downloads/Drugs/GuidanceComplianceRegulatoryInformation/Guidances/UCM469119.pdf⟩ (accessed 11 October 2017).

[28] L.L. Sombra, M.R. Gómez, R. Olsina, et al., Comparative study between capillary electrophoresis and high-performance liquid chromatography in 'guarana' based phytopharmaceuticals, J. Pharm. Biomed. Anal. 36 (2005) 989–994.

[29] M. Friedman, C.E. Levin, S.H. Choi, et al., Changes in the composition of raw tea leaves from the Korean Yabukida plant during high-temperature processing to pan-fried kamairi-cha green tea, J. Food Sci. 74 (2009) 406–412.

[30] I.K. Bae, H.M. Ham, M.H. Jeong, et al., Simultaneous determination of 15 phenolic compounds and caffeine in teas and mate using RP-HPLC/UV detection: method development and optimization of extraction process, Food Chem. 172 (2015) 469–475.

[31] U.J. Unachukwu, S. Ahmed, A. Kavalier, et al., White and green teas (*Camellia sinensis* var. sinensis): variation in phenolic, methylxanthine, and antioxidant profiles, J. Food Sci. 75 (2010) C545–C548.

[32] Y. Zhao, P. Chen, L. Lin, et al., Tentative identification, quantification, and principal component analysis of green pu-erh, green and white teas using UPLC/DAD/MS, Food Chem. 126 (2011) 1269–1277.

[33] B.J. Guller, S.C. Steelman, S.L. Thomas, Multi- ingredient, caffeine-containing dietary supplements: history, safety, and efficacy, Clin. Ther. 37 (2015) 275–301.

[34] C.A. Haller, M. Duan, N.L. Benowitz, et al., Concentrations of Ephedra alkaloids and caffeine in commercial dietary supplements, J. Anal. Toxicol. 28 (2004) 145–151.

Original Research Article

Gas chromatography-mass spectrometry method for determination of β-propiolactone in human inactivated rabies vaccine and its hydrolysis analysis

Shuo Lei [a], Xun Gao [a], Yang Sun [b], Xiangyong Yu [c], Longshan Zhao [a],*

[a] School of Pharmacy, Shenyang Pharmaceutical University, Shenyang 110016, China
[b] Liaoning Medical Device Test Institute, Shenyang 110179, China
[c] Shenyang Wellwolf Pharmaceutical Science and Technology Co. Ltd, Shenyang 110022, China

ABSTRACT

A simple method was established for the determination of β-propiolactone (BPL) in human inactivated rabies vaccine by gas chromatography-mass spectrometry (GC-MS). The determination was performed on an Agilent HP-INNOWAX (30 m × 0.32 mm i.d., 0.25 μm) capillary column at the temperature of 80 °C. Electrospray ionization (ESI) was used by selective ion detection at m/z 42. The temperature for ESI source and inlet was set at 230 °C and 200 °C, respectively. Helium was used as the carrier gas at a flow rate of 25.1 mL/min. The total run time was 8 min. Acetonitrile and other components in the sample did not interfere with the determination of BPL. The results showed good linearity of BPL in the range of 0.50–10.01 μg/mL, with the limit of detection and the limit of quantification of 0.015 μg/mL and 0.050 μg/mL, respectively. Satisfactory precision was achieved for the current developed method. The method was applied to detect 6 batches of vaccine samples, and the results indicated that the target analyte BPL was present in three batches of unpurified samples, but was not detected in the purified samples, indicating the test samples were qualified. The established method was proved to be simple, versatile and sensitive, which can meet the requirements of quality control of BPL in human inactivated rabies vaccine.

© 2018 Xi'an Jiaotong University. Production and hosting by Elsevier B.V. This is an open access article under the CC BY-NC-ND license (http://creativecommons.org/licenses/by-nc-nd/4.0/).

1. Introduction

Vaccines represent great triumphs of medicine against various infectious diseases [1] such as rabies, measles, diphtheria, whooping cough and hepatitis B. Among them, rabies is considered as a highly lethal encephalomyelitis caused by rabies virus (RABV) [2,3]. Although it is highly lethal with few effective therapies, rabies can be prevented by vaccination [4]. However, vaccines made from pathogenic microorganisms and their metabolites always show safety risks [5,6]. In order to ensure their safety and effectiveness, it is of great significance to choose appropriate virus inactivator. β-propiolactone (BPL), an excellent virus inactivation reagent, can act directly on viral nucleic acid [7,8] to cause mutation and block replication of virus [9]. Although BPL has a powerful reactivity with virus nucleic acid, it does not damage structure and function of the fusion protein on the surface of virus [10] and has no effect on the viral capsid protein or immunogenicity of inactivated virus [9].

What's more, BPL can be easily hydrolyzed to 3-hydroxypropionic acid which is non-toxic [7,9,11]. Therefore, it has been widely applied in inactivation of various vaccines [12–14]. However, it is reported that BPL is a carcinogen [7,11], which should be paid more attention to in clinic. From the structure of BPL (top of Fig. 1B), it can be seen that BPL contains two types of activated carbon atoms [15], carbonyl carbon atom and β-carbon atom, which can be reacted with a variety of nucleophiles [14,16,17] and may cause toxicity in human body. Thus it is necessary to establish a high-sensitivity method to detect BPL in vaccines.

It has been reported that there are several analytical methods for the determination of BPL in vaccines, such as high performance liquid chromatography (HPLC) [18,19] and gas chromatography (GC) [7,9,11,20,21]. However, due to weak ultraviolet (UV) absorption of BPL [9], it is not advocated to be determined by HPLC with UV-detector. Afterwards, it was reported that GC method for determination of BPL could achieve more faithful results [7,11]. In order to avoid hydrolysis, the thinning water should be kept at 2–8 °C, and the investigation required rapid operation in ice boxes, which was tedious and had a high demand for experiment operators. To overcome the drawbacks mentioned above, a modified method was developed for the determination of residual BPL in

---

Peer review under responsibility of Xi'an Jiaotong University.
* Corresponding author.
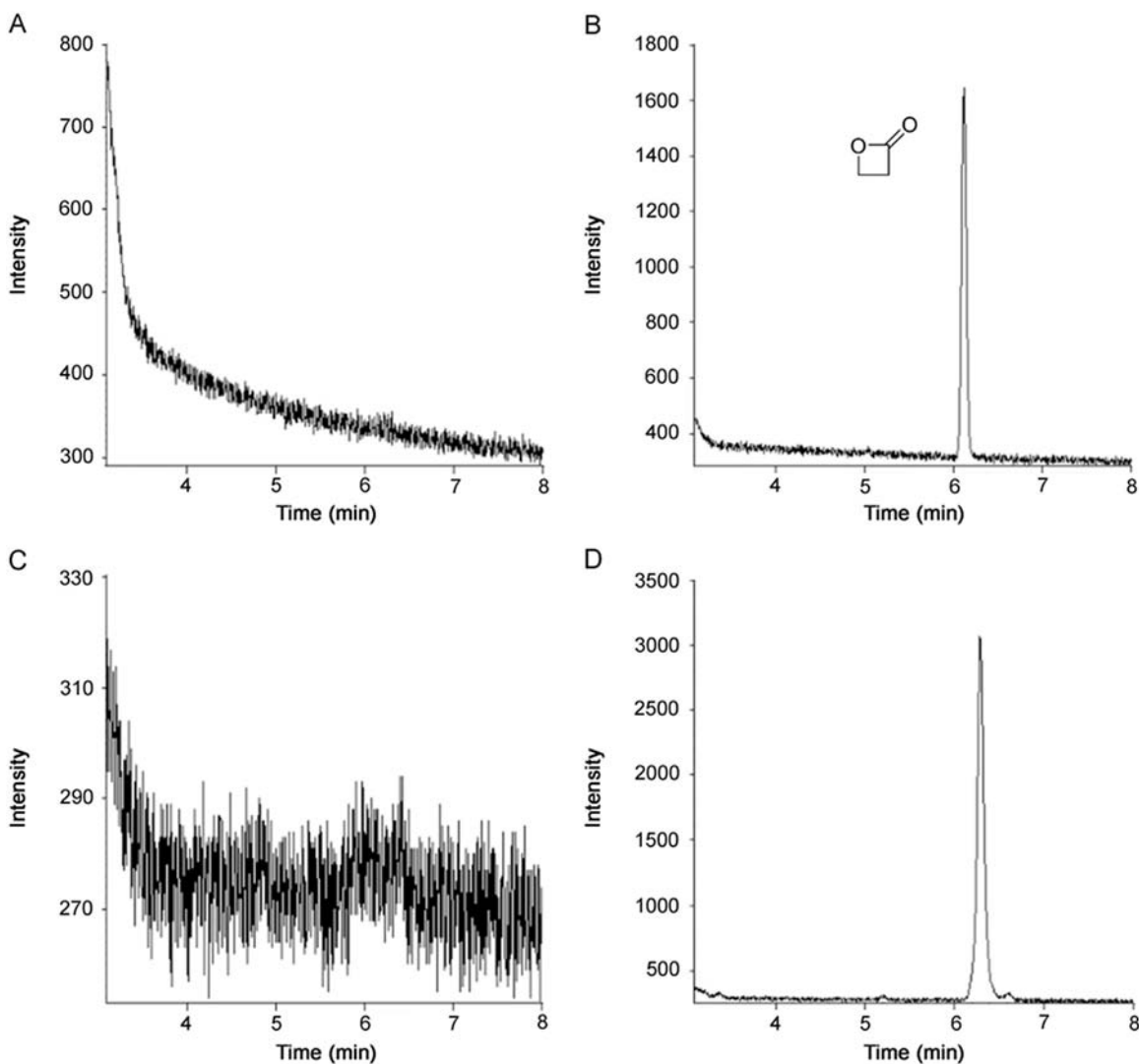 E-mail address: longshanzhao@163.com (L. Zhao).

Fig. 1. Chromatograms of blank solvent, BPL reference and samples for (A) blank solvent (acetonitrile), (B) BPL reference substance, (C) sample MPV20170401-G25, and (D) sample MPV20170401-Mie.

rabies virus concentrate by gas chromatography [9], using acetonitrile as reference attenuant dissolvent. In order to further optimize the determination of trace amount of BPL, an analytical method with much lower limit of detection based on gas chromatography-mass spectrometry (GC-MS) was developed and validated in this study. In addition, when BPL is used as a sterilizing agent, more attention should be paid to ensure that it is rapidly and completely hydrolyzed into its decomposition product 3-hydroxypropionic acid, which is perfectly compatible and harmless. In order to confirm the safety of vaccines and provide a reference for the research of vaccine safety, hydrolysis experiment was also carried out to verify the degradation of BPL in lyophilized human inactivated rabies vaccine (LHIRV).

2. Experimental

2.1. Chemicals and reagents

BPL and LHIRV were supplied by Chengda Biological Technology Co., Ltd (Shenyang, China). Acetonitrile of HPLC grade was bought from Fisher (Fair lawn, NJ, USA). Chromatographic-grade water was prepared with a Milli-Q Reagent Water System (Millipore, Bedford, MA). Sodium hydroxide of analytical grade was

purchased from Tianjin Aopusheng Chemical Reagent Co., Ltd. (Tianjin, China).

2.2. Instrumentation and conditions

An Agilent 6890N-5973 System was applied with an HP-IN-NOWAX capillary column (30 m × 0.32 mm i.d., 0.25 μm) at the temperature of 80 °C. Helium was used as carrier gas with a total flow rate of 25.1 mL/min. The temperature for ESI source and inlet was set at 230 °C and 200 °C, respectively. Electrospray ionization (ESI) was used by selective ion scanning (SIM) at *m/z* 42.

2.3. Preparation of standard solution

BPL standard stock solution (1001 μg/mL) was prepared in acetonitrile (HPLC grade) and kept in amber bottles at −20 °C, which was used for the preparation of working solutions and calibration curves by further dilution with acetonitrile.

2.4. Preparation of samples

Unpurified LHIRV included MPV20170401-Mie, MPV20170402-Mie and MPV20170501-Mie, while purified LHIRV included MPV20170401-G25, MPV20170402-G25 and MPV20170501-G25.

The samples were diluted by acetonitrile to concentration of about 3.0 μg/mL and then filtered through 0.45 μm nylon membrane syringe filters.

2.5. Method validation

In order to prove the reliability of the method, this experiment verified the methodology from selectivity, linearity, recovery and other aspects. The selectivity of the method was investigated by analyzing blank solvent (acetonitrile), BPL standard solution, sample MPV20170401-Mie and sample MPV20170401-G25. The blank solvent and sample MPV20170401-G25 should have no interference peaks around the peak of the analyte. Linearity of the method was established at 0.50, 1.00, 2.00, 5.00 and 10.01 μg/mL. Calibration curve was generated using linear regression analysis. The linearity obtained was assumed satisfactory with the correlation coefficients (r^2) higher than 0.99. The analytical limits were shown on the basis of limit of detection (LOD) and limit of quantification (LOQ) for BPL, which were calculated at the lowest concentration as 3 and 10 times of signal-to-noise (S/N), respectively.

The precision was evaluated by measuring the standard solution for six times, and was expressed as the relative standard deviations (RSDs) of retention time and peak area. The standard solution was prepared by diluting the stock solution to 3.00 μg/mL. To evaluate the stability of BPL, BPL standard solution and samples spiked with BPL were placed at room temperature for 4 h and determined every 2 h. Stability was checked by comparing the measured results with the results obtained at 0 h, expressed as RSD. The BPL in standard solution and samples could be regarded as stable with RSDs lower than 3.0%. The repeatability of the method was assessed by the determination of RSD values of BPL content in samples. The recovery was evaluated by determining spiked LHIRV samples at three levels (2.4, 3.0 and 3.6 μg/mL) in triplicate.

2.6. Application of the established method in LHIRV injection

The established method was applied in LHIRV injection, including LHIRV purified samples and unpurified samples.

2.7. BPL hydrolyzation experiments

In our research, in order to accelerate the hydrolysis of BPL, the aqueous solution was heated by water bath at 37 °C. The aqueous solution was prepared at concentration of 1.00 μg/mL. The amount of BPL was determined per 30 min, and hydrolysis curve of BPL was made.

3. Results

3.1. Method validation

3.1.1. Specificity
From Fig. 1, it can be seen that the retention time of the target compound was 6.12 min. The blank solvent and sample MPV20170401-G25 had no interferences, suggesting that the specificity of the developed method was satisfactory.

3.1.2. Linearity
The calibration curve of BPL was $y = 49220x + 3469.2 (n = 5)$ in the range of 0.50–10.01 μg/mL and the correlation coefficients (r^2) was 0.9999, indicating the obtained linearity was satisfactory.

3.1.3. LOD and LOQ
The analytical limits were shown on the basis of LOD and LOQ for BPL. The LOD and LOQ of BPL were 0.015 μg/mL and 0.050 μg/mL, respectively, which was sufficient to determine trace amount of BPL in matrix.

3.1.4. Precision
The precision was expressed as the RSD of retention time and peak area. The results showed good precision with the RSD of retention time less than 1% and RSD of peak area less than 3%, respectively.

3.1.5. Stability and repeatability
The results showed that the RSDs of BPL peak area were 4.0% and 6.6%, respectively, which indicated that it was unstable after being laid aside for long time at room temperature. Therefore, BPL solution should be stored at −20 °C and measured immediately after being taken out. There was no BPL detected in LHIRV purified samples, while the average level was found 6.56 μg/mL in unpurified samples with RSD of 4.0%, suggesting that relatively accurate results could still be obtained in case of minor fluctuations of the measurement conditions.

3.1.6. Accuracy
The accuracy was measured by determining the recovery of spiked samples. As Table 1 shows, the average recoveries of purified samples and unpurified samples were 103.46% and 102.65%, and the RSDs were 3.2% and 1.4%, respectively.

3.2. Application in LHIRV injection

To demonstrate the effectiveness and applicability of this method, the proposed method was applied for the analysis of LHIRV injection, including LHIRV purified samples (MPV20170401-G25, MPV20170402-G25 and MPV20170501-G25) and unpurified samples (MPV20170401-Mie, MPV20170402-Mie and MPV20170501-Mie). As shown in Table 2, BPL was not detected in three batches of purified samples and was found in three batches of unpurified samples.

3.3. BPL hydrolyzation experiments

BPL was unstable in aqueous solution and could be hydrolyzed easily to 3-hydroxypropionic acid at room temperature. The result

Table 1
Accuracy and precision of the method for analysis of BPL in vaccine samples at three spiked levels.

Vaccine samples	Spiked (μg/mL)	BPL in samples (μg/mL)	Accuracy (%)	Average accuracy (%)	RSD (%)
Purified samples	2.40	0	101.61	103.46	3.2
			104.22		
			104.76		
	3.00		95.77		
			103.07		
			103.52		
	3.60		105.21		
			105.84		
			107.19		
Unpurified samples	2.40	3.09	103.28	102.65	1.4
			102.46		
			103.28		
	3.00		101.81		
			100.49		
			101.89		
	3.60		102.11		
			105.73		
			102.85		

Table 2
Determination results of lyophilized human inactivated rabies vaccine samples.

Sample	Batch NO.	Concentration of BPL (µg/mL)
Purified samples	MPV20170401-G25	–
	MPV20170402-G25	–
	MPV20170501-G25	–
Unpurified samples	MPV20170401-Mie	3.38
	MPV20170402-Mie	3.79
	MPV20170501-Mie	3.41

showed that BPL in aqueous solution was hydrolyzed quickly and disappeared completely after 3 h (Fig. 2).

4. Discussion

At present, many kinds of vaccines are inactivated by BPL for the following reasons: First, vaccines inactivated with BPL possess good immunocompetence on account of the reservation of the virus capsid protein [8]. Next, the residual can be hydrolyzed and removed easily [8], which confirms the safety of vaccines. Finally, BPL can also destroy the DNA of stromal cells that cause contamination or remain in the vaccines [18]. Therefore, it is very necessary to consider the factors that affect the experimental efficiency.

4.1. Column selection

At the beginning of the experiment, DB-624 and HP-INNOWAX were selected to determine BPL, according to the polarity of BPL and existing literature [7,9,11]. The results showed that the analyte had a satisfactory symmetry factor and better resolution from interfering substances in samples when HP-INNOWAX capillary
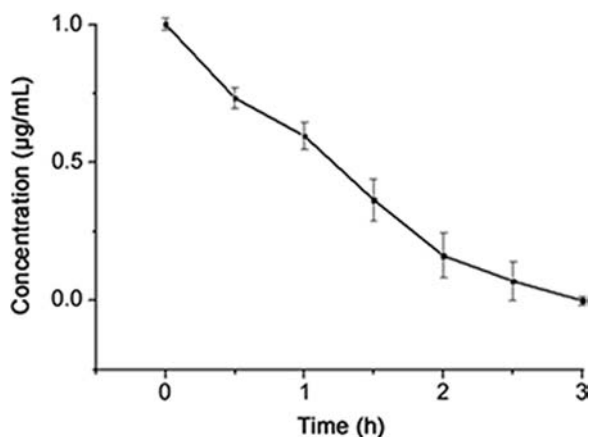

Fig. 2. Hydrolysis curve of BPL in water solution.

column was chosen and the temperature was set at 80 °C. Therefore, the analysis of BPL was operated on HP-INNOWAX at the column temperature of 80 °C.

4.2. Hydrolysis analysis

Initially, BPL was hydrolyzed directly without adjusting pH of the solution. After 4 h, BPL could still be detected. Then, we tried to explore the optimal hydrolysis condition by adjusting pH. It is reported that BPL was added to vaccines with pH of 7.2, 7.4, 7.6, 7.8 and 8.0, respectively and hydrolyzed in water bath at 37 °C for 2 h [21]. The results showed there was a decrease in content when pH increased: BPL was detected when hydrolyzed for 2 h with pH of 7.2 and 7.4; when pH was above 7.6, BPL disappeared completely. Therefore, pH value was proved to be an important factor in determining whether BPL would be completely hydrolyzed within 2 h. In this study, hydrolysis of BPL was carried out with pH of 7.6 and the concentration of BPL decreased below LOQ of 0.050 µg/mL after hydrolyzing for 3 h.

4.3. Comparison among different methods

According to the literature [7,9,11,18,21], residual BPL in vaccines was mostly determined by GC or HPLC. The comparison among different methods is shown in Table 3. First of all, acetonitrile was applied as reference attenuant dissolvent, which showed that BPL could remain stable within a short period in acetonitrile, avoiding the trouble of quick operation at low temperature with water as solvent. Moreover, the chromatographic behavior of BPL in acetonitrile and sample was the same, confirming that acetonitrile had no effect on the determination of BPL. What's more, in course of experiment, the study of Shan et al. [9] provided a reference but the present research was improved and supplemented. The advantages of the present study are summarized below.

Firstly, this study performed hydrolysis experiments, which ensured that as a common but virulent inactivator, BPL could be hydrolyzed into non-toxic 3-hydroxypropionic acid. The hydrolysis experiment made the process of inactivation and detoxification of vaccine more comprehensive and confirmed the safety of the preparation process of it.

Secondly, Shan et al. [9] determined BPL in vaccine by GC method. In this study, GC-MS was applied to obtain more accurate qualitative assay according to the structure. At the same time, matrix interference could be reduced and sensitivity could be improved with SIM module.

Thirdly, the sensitivity increased to a certain degree. Shan et al. [9] used GC method to obtain values of LOD and LOQ for 0.2 µg/mL and 1.0 µg/mL, respectively. In this study, the LOD and LOQ values obtained by GC-MS method were 0.015 µg/mL and 0.050 µg/mL, respectively, which means higher sensitivity. In the authors' opinion, an excessively large linear range had little significance for the determination of trace analytes. In this study, the linear range was narrowed appropriately without prejudice to the results, making the determination of trace analytes in biological samples more

Table 3
The comparison of different methods for determination of BPL.

Methods	Column	Attenuant dissolvent	LOD (µg/mL)	LOQ (µg/mL)	Linearity (µg/mL)	References
GC-MS	HP-INNOWAX	Acetonitrile	0.015	0.050	0.50–10.00	This study
GC	DB-624	Water	–	8.900	8.90–566.90	[7]
GC	DB-624	Acetonitrile	0.200	1.000	1.08–1082.00	[9]
GC	HP-INNOWAX	Buffer solution	0.164	–	–	[11]
GC	HP-20M	Water	0.100	–	–	[21]
HPLC	C$_{18}$	Water	–	–	–	[18]

practical. It is extremely important to increase the sensitivity for qualitative and quantitative determination of trace analytes in biological samples.

Lastly, BPL was measured by temperature-programmed GC in Shan's research [9]. In the present study, column temperature was kept constant at 80 °C. The improvement of this condition, on the one hand, simplified the instrument conditions and eliminated the process of cooling after running, and thereby shortened the running time. On the other hand, the service life of the capillary column was prolonged and the experimental cost was decreased to some extent.

5. Conclusion

In this paper, a simple, versatile and sensitive analytical method, based on GC-MS for determination of BPL in LHIRV, has been developed and validated to meet the needs of quality control of BPL in vaccines. To the authors' knowledge, such a method based on GC-MS is exploited for the first time, which has been applied to the trace determination of BPL in vaccines.

The method indicated that the purification process of the tested samples was favorable for removing BPL from the vaccine effectively. The established method provided means for validation of vaccine production process and effective experience and reference for research on the safety of biological products.

Conflicts of interest

The authors declare that there are no conflicts of interest.

References

[1] R.A. Seder, A.V. Hill, Vaccines against intracellular infections requiring cellular immunity, Nature 406 (2000) 793–798.
[2] A.C. Jackson, Diabolical effects of rabies encephalitis, J. Neurovirol. 22 (2016) 8–13.
[3] C.W. Gnanadurai, C.T. Huang, D. Kumar, et al., Novel approaches to the prevention and treatment of rabies, Int. J. Virol. Stud. Res. 3 (2015) 8–16.
[4] R. Hu, S. Zhang, Y. Liu, Suggestions on prevention and control of rabies in China, Chin. J. Zoonoses 28 (2012) 487–491.
[5] J. Wang, J. Yan, The past, present and future of human rabies vaccines, Chin. J. Epidemiol. 22 (2001) 23–25.
[6] R. Feng, D. Fan, P. Wei, et al., Experimental study on the inactivation effect of β-propiolactone on encephalomyocarditis virus, Chin. J. Vet. Med. 47 (2011) 19–21.
[7] Y. Jian, J. Gao, Q.Y. Zhang, et al., Development of gas chromatography for determination of β-propiolactone (BPL) content and analysis of BPL hydrolysis, Chin. J. Biol. 23 (2010) 323–324.
[8] J.J. Jiang, F.C. Qi, Y.L. Hu, et al., Inactivation of hepatitis A virus with β-propiolactone, Chin. J. Biol. 25 (2012) 529–530.
[9] G.Z. Shan, X. Ma, J.I. Hong, et al., Determination of residual β-propiolactone in inactivated rabies virus concentrate by gas chromatography, Chin. Pharm. 25 (2014) 2357–2359.
[10] L. Zhu, Y. Zhu, L. Gao, et al., Comparison of formaldehyde and β-propiolactone inactivation effect on coxsackievirus A16, Int. J. Epidemiol. Infect. Dis. 42 (2015) 418–420.
[11] Y. Xu, R. Wei, Y. Jiang, et al., Study on the determination of β-propiolactone in rotavirus vaccine by gas chromatography, Prog. Microbiol. Immunol. 38 (2010) 21–23.
[12] C. Fan, X. Ye, Z. Ku, et al., Beta-propiolactone inactivation of coxsackievirus A16 induces structural alteration and surface modification of viral capsids, J. Virol. 91 (2017) e00017–e00038.
[13] Y.M. She, K. Cheng, A. Farnsworth, et al., Surface modifications of influenza proteins upon virus inactivation by β-propiolactone, Proteomics 13 (2013) 3537–3547.
[14] J.P. Uittenbogaard, B. Zomer, P. Hoogerhout, et al., Reactions of beta-propiolactone with nucleobase analogues, nucleosides, and peptides: implications for the inactivation of viruses, J. Biol. Chem. 286 (2011) 36198–36214.
[15] Y. Zhang, S. Li, Z. Yang, Reactivity analysis of β-propiolactone, Acta Phys.-Chim. Sin. 15 (1999) 986–989.
[16] H. Kubinski, E.H. Szybalski, Intermolecular linking and fragmentation of DNA by β-propiolactone, a monoalkylating carcinogen, Chem. -Biol. Interact. 10 (1975) 41–55.
[17] R.K. Boutwell, N.H. Colburn, C.C. Muckerman, In vivo reactions of β-propiolactone, Ann. N. Y. Acad. Sci. 163 (1969) 751–763.
[18] W. Chen, Z.Y. Li, J.Q. Liu, et al., Application of β-propiolactone in HFRS vaccine, Chin. J. Public Health 19 (2003) 669–670.
[19] Y. Zhang, C. Gao, G. Pan, et al., Determination of β-propiolactone residues in human rabies vaccine for Vero cells, Chin. J. Biol. 11 (1998) 144.
[20] D. Pruggmayer, W. Stephan, Gas chromatographic trace analysis of β-propiolactone in sterilized serum proteins, Vox. Sang. 31 (1976) 191–198.
[21] F. Li, Z. Dou, L. Pan, Selection of optimal pH for β-propiolactone hydrolysis after inactivation of rabies vaccine, Chin. J. Public Health 15 (1999) 964.

Original Research Article

Highly sensitive LC–MS/MS method to estimate doxepin and its metabolite nordoxepin in human plasma for a bioequivalence study

Nirav P. Patel [a,b], Mallika Sanyal [b,c], Naveen Sharma [a], Dinesh S. Patel [a],
Pranav S. Shrivastav [d,*], Bhavin N. Patel [a,*]

[a] Bio-Analytical Laboratory, Cliantha Research India Ltd., Bodakdev, Ahmedabad 380054, Gujarat, India
[b] Kadi Sarva Viswavidyalaya, Sector-15, Ghandhinagar 382715, Gujarat, India
[c] Department of Chemistry, St. Xavier's College, Navrangpura, Ahmedabad 380009, Gujarat, India
[d] Department of Chemistry, School of Sciences, Gujarat University, Navrangpura, Ahmedabad 380009, Gujarat, India

ARTICLE INFO

ABSTRACT

A selective, sensitive and rugged liquid chromatography–tandem mass spectrometry (LC–MS/MS) assay has been developed for the simultaneous determination of doxepin (Dox) and its pharmacologically active metabolite, nordoxepin (NDox) in human plasma. The analytes and their internal standards (IS) were extracted from 500 μL of human plasma by liquid-liquid extraction using methyl *tert*-butyl ether. Chromatographic separation was achieved on Hypurity C$_8$ column (100 mm × 4.6 mm, 5 μm) using a mixture of acetonitrile-methanol (95:5, v/v) and 2.0 mM ammonium formate in 93:7 (v/v) ratio. Detection was accomplished by tandem mass spectrometry in the positive ionization and multiple reaction monitoring acquisition mode. The protonated precursor to product ion transitions studied for Dox, NDox, and their corresponding ISs, propranolol and desipramine, were m/z 280.1 → 107.0, 266.0 → 107.0, 260.1 → 116.1 and 267.1 → 72.1, respectively. A linear dynamic range of 15.0–3900 pg/mL for Dox and 5.00–1300 pg/mL for NDox was established with mean correlation coefficient (r^2) of 0.9991 and 0.9993, respectively. The extraction recovery ranged from 86.6%–90.4% and 88.0%–99.1% for Dox and NDox, respectively. The intra-batch and inter-batch precision (% CV) across quality control levels was ≤ 8.3% for both the analytes. Stability evaluated under different storage conditions showed no evidence of degradation and the % change in stability samples compared to nominal concentration ranged from 4.7% to 12.3%. The method was successfully applied to a bioequivalence study of 6 mg doxepin hydrochloride orally disintegrating tablet in 41 healthy Indian subjects under fasting and fed conditions.

© 2018 Xi'an Jiaotong University. Production and hosting by Elsevier B.V. This is an open access article under the CC BY-NC-ND license (http://creativecommons.org/licenses/by-nc-nd/4.0/).

1. Introduction

Tricyclic antidepressants (TCAs) are a group of drugs used mainly to treat patients suffering from major depression and other psychiatric disorders including panic disorder, obsessive-compulsive disorder, sleep disorder, eating disorders and attention deficit hyperactivity disorder [1]. Doxepin (Dox), a TCA, is widely used for the treatment of depression and has also shown anti-anxiety and anti-histamine properties [2,3]. It displays a potent central anticholinergic activity and inhibits the reuptake of noradrenalin and serotonin [4]. Among several antidepressant drugs, use of Dox is also associated with suicide and narcotic drug-related deaths [5].

Generally, lower dose of Dox has a higher selectivity for H1 receptor and is considered safe for short-term and long-term insomnia [3]. Dox is rapidly absorbed from the gastro-intestinal tract and is extensively N-demethylated to its active metabolite nordoxepin (NDox) mainly through cytochrome P450 enzyme 2C19 [6]. The pharmacological and toxicological properties of NDox are comparable with its parent drug. In addition to NDox, there are several pharmacologically inactive metabolites that are also formed, including 2-hydroxydoxepin, 2-hydroxynordoxepin and doxepine-N-oxide. Dox and NDox are widely distributed throughout the body and their plasma protein binding is about 80% [4]. Dox has a plasma life ranging from 8 to 24 h, while the half life of NDox is much longer (> 30 h) [7]. Therapeutic drug monitoring for Dox is essential due to wide inter-individual variability observed in the pharmacokinetics and in the production of active metabolite. This can help to optimize dose and thus minimize potentially life-threatening toxicity [8].

Bioanalytical methods reported for the analyses of Dox in human whole blood [9], human plasma [4,10] and cerebrospinal fluid [4] include high-performance liquid chromatography (HPLC) [10] and liquid chromatography–tandem mass spectrometry (LC–MS/MS) [4,9]. Other methods report simultaneous estimation of Dox and NDox in a variety of biological samples like whole blood [5], gastric fluids [5], bile, urine [5], cerebrospinal fluid [5], tissues [5], hair [7], urine [11] and human plasma [11–13]. A majority of these methods were developed for forensic or toxicological studies but only few of them addressed the pharmacokinetics of Dox and NDox in human plasma [11,13]. Moreover, they have limited sensitivity (lower limit of quantitation) in the range of 0.25–100 ng/mL for both the analytes. Further, assay methods for the determination of Dox together with several TCAs, other antidepressants and antipsychotic drugs using capillary electrophoresis [14], HPLC [15–19], gas chromatography–mass spectrometry (GC–MS) [20], LC–MS/MS [21,22] and ultra-performance liquid chromatography–tandem mass spectrometry (UPLC–MS/MS) [8,23–25] in biological samples have also been reported.

Based on the work reported thus far, the objective of the present work was to develop and fully validate a selective, sensitive and rugged LC–MS/MS method for the estimation of Dox and NDox in human plasma based on current regulatory guidelines. Further, there are no reports on the pharmacokinetics of Dox and NDox in Indian subjects. The method presents a competent extraction procedure based on liquid-liquid extraction (LLE) to obtain precise and quantitative recovery for both the analytes. The proposed method was successfully applied to a bioequivalence study of 6 mg of doxepin orally disintegrating tablet formulation in 41 healthy subjects under fasting and fed conditions.

2. Experimental

2.1. Chemicals and materials

Reference standards of Dox hydrochloride (99.8%) and NDox (99.2%) were procured from Toronto Research Chemicals Inc. (Ontario, Canada), while internal standards (ISs), propranolol (99.1%) and desipramine (98.9%) were purchased from Vivan Life Sciences Pvt. Ltd. (Mumbai, India). HPLC grade methanol and acetonitrile, analytical grade ammonia, ammonium acetate and ammonium formate were obtained from S.D. Fine Chemicals Ltd. (Mumbai, India). HPLC grade methyl *tert*-butyl ether (MTBE) was obtained from J.T Baker Chemicals Ltd. (Haryana, India). Deionized water used for LC–MS/MS was prepared using Milli Q water purification system from Millipore (Bangalore, India). Control buffered (K_2EDTA) human plasma was procured from Clinical Department, BA Research India Limited (Ahmedabad, India) and stored at –20 °C until use.

2.2. LC–MS/MS instrumentation and conditions

The liquid chromatography system from Shimadzu (Kyoto, Japan) consisted of an LC-10ADvp pump, an auto sampler (SIL-HTc) and an on-line degasser (DGU-14A). Chromatographic column used was Hypurity C_8 (100 mm × 4.6 mm, 5.0 μm) from Thermo Fisher Scientific Inc. (Waltham, MA, USA). Separation of analytes and ISs were performed under isocratic conditions using a mobile phase consisting of acetonitrile-methanol (95:5, v/v) and 2.0 mM ammonium formate in 93:7 (v/v) ratio, delivered at a flow rate of 1.2 mL/min. The auto-sampler temperature was maintained at 4 °C and the injection volume was 15 μL. Detection of analytes and ISs was performed on a triple quadrupole mass spectrometer, API-5500 equipped with Turbo Ion spray®, from MDS SCIEX (Toronto, Canada) in the positive ionization mode. Quantitation was done in

multiple reaction monitoring (MRM) mode to monitor protonated precursor → product ion transition of m/z 280.1→107.0, 266.0 →107.0, 260.1→116.1 and 267.1→72.1 for Dox, NDox, propranolol and desipramine, respectively. All the parameters of LC and MS were controlled by Analyst software version 1.5.1.

The source dependent mass parameters maintained for the analytes and ISs were Gas 1 (nebulizer gas): 50 psi, Gas 2 (heater gas): 60 psi, ion spray voltage: 5500 V, turbo heater temperature: 500 °C, entrance potential: 10 V, collision activation dissociation (CAD): 7, curtain gas: 30 psi. The compound dependent parameters, namely declustering potential, collision energy and cell exit potential, were set at 60 V, 27 eV and 11 V for Dox, 60 V, 29 eV and 11 V for NDox, 81 V, 25 eV and 6 V for propranolol and 26 V, 21 eV and 10 V for desipramine respectively. Quadrupole 1 and quadrupole 3 were maintained at unit resolution and the dwell time was set at 300 ms.

2.3. Preparation of standard stock and plasma samples

The calibration standards (CSs) were made at 15.0, 30.0, 60.0, 150, 300, 750, 1500, 2400, 3150 and 3900 pg/mL for Dox and 5.00, 10.0, 20.0, 50.0, 100, 250, 500, 800, 1050 and 1300 pg/mL for NDox. Quality control (QC) samples (LLOQ QC, lower limit of quantitation quality control; LQC, low quality control; MQC-1&MQC-2, medium quality control; HQC, high quality control; ULOQ QC, upper limit of quantitation quality control) were prepared at 15.0/5.00 pg/mL (LLOQ), 45.0/15.0 pg/mL (LQC), 360/120 pg/mL (MQC-2), 900/300 pg/mL (MQC-1), 3000/1000 pg/mL (HQC) and 3900/1300 pg/mL (ULOQ) for Dox/NDox, respectively.

2.4. Protocol for sample preparation

Prior to analysis, spiked plasma/subject samples were thawed and allowed to equilibrate at room temperature. The samples were adequately vortexed using a vortex mixer before pipetting. Aliquots of 500 μL plasma solutions containing 25 μL of combined working solution of Dox and NDox and 475 μL blank plasma were transferred into glass screw tubes. To which, 25 μL of methanol: deionized water (50:50, v/v), 50 μL combined working solution of ISs was added and vortexed to mix. Further, 200 μL of 100 mM ammonium acetate solution (pH 8 adjusted with ammonia) was added and vortexed again. LLE was carried out using 4.0 mL of MTBE by centrifuging the samples for 5.0 min at 1811g. After freezing the aqueous layer in dry ice bath, the organic layer was transferred in clean pre-labeled glass tubes. The samples were then evaporated to dryness at 40 °C under gentle stream of nitrogen. The dried samples were reconstituted with 300 μL of acetonitrile: methanol: 2.0 mM ammonium formate (80:10:10, v/v/v) and 15 μL was used for injection in LC–MS/MS system.

2.5. Methodology for validation

Method validation for Dox and NDox in human plasma was done following the USFDA guidelines [26] and the procedures followed were similar to our previous work [27]. The method was validated for selectivity, interference check, carryover, linearity, precision and accuracy, reinjection reproducibility, recovery, ion suppression/enhancement, matrix effect, stability, dilution integrity and ruggedness. The details are described in Supplementary Material.

2.6. Bioequivalence study design, statistical analysis and incurred sample reanalysis (ISR)

The study design comprised an open label, randomized, two period, two treatment, two sequence, crossover, balanced, single

dose, evaluation of relative oral bioavailability of test (6 mg doxepin hydrochloride orally disintegrating tablet from an Indian company) and reference (SILENOR™, 6 mg doxepin orally disintegrating tablet from Somaxon Pharmaceuticals Inc., San Diego, USA) formulations in 41 healthy Indian male subjects under fasting and fed conditions. The procedures followed while dealing with human subjects were based on International Conference on Harmonization, E6 Good Clinical Practice guidelines [28]. An ISR was also conducted by computerized selection of 264 subject samples near C_{max} and the elimination phase for both the studies as reported previously [29]. The experimental details for both the studies along with statistical analysis are given in Supplementary Material.

3. Results and discussion

3.1. Method development

The objective of the present work was to develop and validate a simple, selective and sensitive method for Dox and NDox in human plasma by LC–MS/MS for routine sample analysis. Additionally, the sensitivity of the method should be adequate to monitor at least five half lives of Dox and NDox concentration with good accuracy and precision for subject samples analysis. During method development, the electrospray ionization of the analytes and ISs was conducted in positive ionization mode using 5.0 ng/mL tuning solution as the drug and its metabolite are basic in nature due to the presence of tertiary and secondary amino groups, respectively. The analytes and ISs gave predominant singly charged protonated precursor $[M+H]^+$ ions at m/z 280.1, 266.0, 260.1 and 267.1 for Dox, NDox, propranolol and desipramine, respectively in Q1 full scan spectra. Further, fragmentation was initiated using sufficient nitrogen for CAD and by applying 30.0 psi curtain gas to break the precursor ions. The most abundant and consistent product ions in Q3 mass spectra of Dox and NDox were found at m/z 107.0, which corresponds to a highly stable hydroxy tropylium ion (Figs. S1 and S2). For propranolol and desipramine, the most stable and reproducible product ions were observed at m/z 116.1 and m/z 72.1, respectively. To reach an ideal Taylor cone for better spectral response, nebulizer gas pressure was set at 50 psi. Fine tuning of nebulizer gas and CAD gas was done to get a consistent and stable response. Ion spray voltage and turbo heater temperature did not have any significant impact on the analyte response and hence were maintained at 5500 V and 500 °C, respectively. A dwell time of 300 ms was found adequate for the quantitation of analytes and ISs. Further, no cross talk was observed between the MRMs of the analytes having identical product ions.

The chromatographic conditions were set to obtain adequate separation and resolution of analytes from the endogenous peaks. This included optimization of mobile phase, its composition, flow rate, column type and injection volume. Different combinations of acetonitrile/methanol and acidic buffers (ammonium formate/formic acid, ammonium acetate/acetic acid) of different strengths (2.0–10 mM) were tested as mobile phase. Further, mobile phase additives like formic acid and ammonium trifluoroacetate were also tried on Hypurity C_{18} (100 mm × 4.6 mm, 5 μm), ACE C_{18} (100 mm × 4.6 mm, 5 μm), Beta Hypersil C_{18} (150 mm × 4.6 mm, 5 μm) and Hypurity C_8 (100 mm × 4.6 mm, 5 μm) columns. In addition, the effect of total flow rate was also studied from 0.5 to 1.2 mL/min, which was responsible for acceptable chromatographic peak shapes and separating endogenous peaks. All C_{18} columns provided acceptable separation of analytes within 3.0 min but there was significant interference of endogenous components, especially with Dox which eluted within 2.0 min.

Additionally, the response was inconsistent at LLOQ, CS-1 (5.0 pg/mL), CS-2 (10.0 pg/mL) and LQC levels for NDox with a small peak tailing. This problem was overcome by using Hypurity C_8 column, which helped in complete separation of endogenous matrix from the analyte peaks and also provided adequate response at lower concentration levels using a mixture of acetonitrile-methanol (95:5, v/v) and 2.0 mM ammonium formate in 93:7 (v/v) ratio as the mobile phase. Addition of 2.0 mM ammonium formate was sufficient to get adequate response and also good peak shape for both the analytes. A flow rate of 1.2 mL/min ensured acceptable peaks shapes with baseline separation of analytes (resolution factor, R_s 2.45) within 5.0 min. The retention time for Dox, NDox, propranolol and desipramine were 2.87, 3.56, 3.15 and 3.77 min, respectively (Figs. 1 and 2). The maximum on-column loading (at ULOQ) of Dox and NDox per injection was 97.5 pg and 32.5 pg, respectively. The reproducibility in the measurement of retention time for Dox and NDox was ≤ 1.3% (% CV) for 100 injections on the same column. Due to unavailability of deuterated analogues, some general ISs like desipramine, propranolol, imipramine and amitriptyline having structural similarity with the analytes were tested. Based on similar extraction efficiency and chromatographic behavior, propranolol, a beta-blocker, was selected as the IS for Dox and desipramine, a tricyclic antidepressant drug, was preferred as the IS for NDox. Further, both ISs did not affect analytes recovery, sensitivity or ion suppression.

Due to lipophilic nature of Dox and NDox, a vast majority of published methods have used LLE for their isolation from biological matrices with diethyl ether-ethyl acetate [4], n-pentane-isopropanol [11], hexane-propan-2-ol/hexane-dichloromethane mixtures [12], and isoamyl alcohol in hexane [13]. In the present work, solvents like n-hexane, MTBE, dichloromethane and ethyl acetate, and their binary mixtures were used to set the optimum conditions for extraction under neutral as well as alkaline conditions. In all the solvent systems, the recovery of Dox and NDox was in the range of 62%–78% and 73%–86%, respectively under neutral conditions. However, the best recovery for both the analytes was found under mild alkaline conditions (pH 8) using MTBE. The recovery obtained was highly consistent and quantitative across all QC levels.

3.2. Assay performance and validation

3.2.1. Selectivity, carryover and interference study

The purpose of evaluating selectivity with 20 different human plasma sources was to determine the extent to which endogenous plasma components might interfere at the retention time of analytes and the ISs and thus, ensure the authenticity of the results for study sample analysis. Figs. 1 and 2 demonstrate the selectivity of the method with the chromatograms of double blank plasma, blank plasma spiked with IS, Dox and NDox at LLOQ concentration, respectively and subject samples. Carry-over evaluation was performed in each analytical run to ensure that it does not impact the accuracy and the precision of the proposed method. The experiments showed a carryover of ≤ 0.35% for Dox and ≤ 0.25% for NDox of LLOQ concentration in blank plasma sample after injection of the highest calibration standard (ULOQ) at the retention time of analytes and ISs. Further, there was no interference of commonly used medications by healthy volunteers like acetaminophen, aspirin, caffeine, chlorpheniramine, cetrizine, ibuprofen and pseudoephedrine at the retention time of the analytes and ISs.

3.2.2. Linearity, sensitivity, accuracy and precision

The calibration curves for Dox and NDox were linear over the established concentration range of 15.0–3900 pg/mL and 5.00–
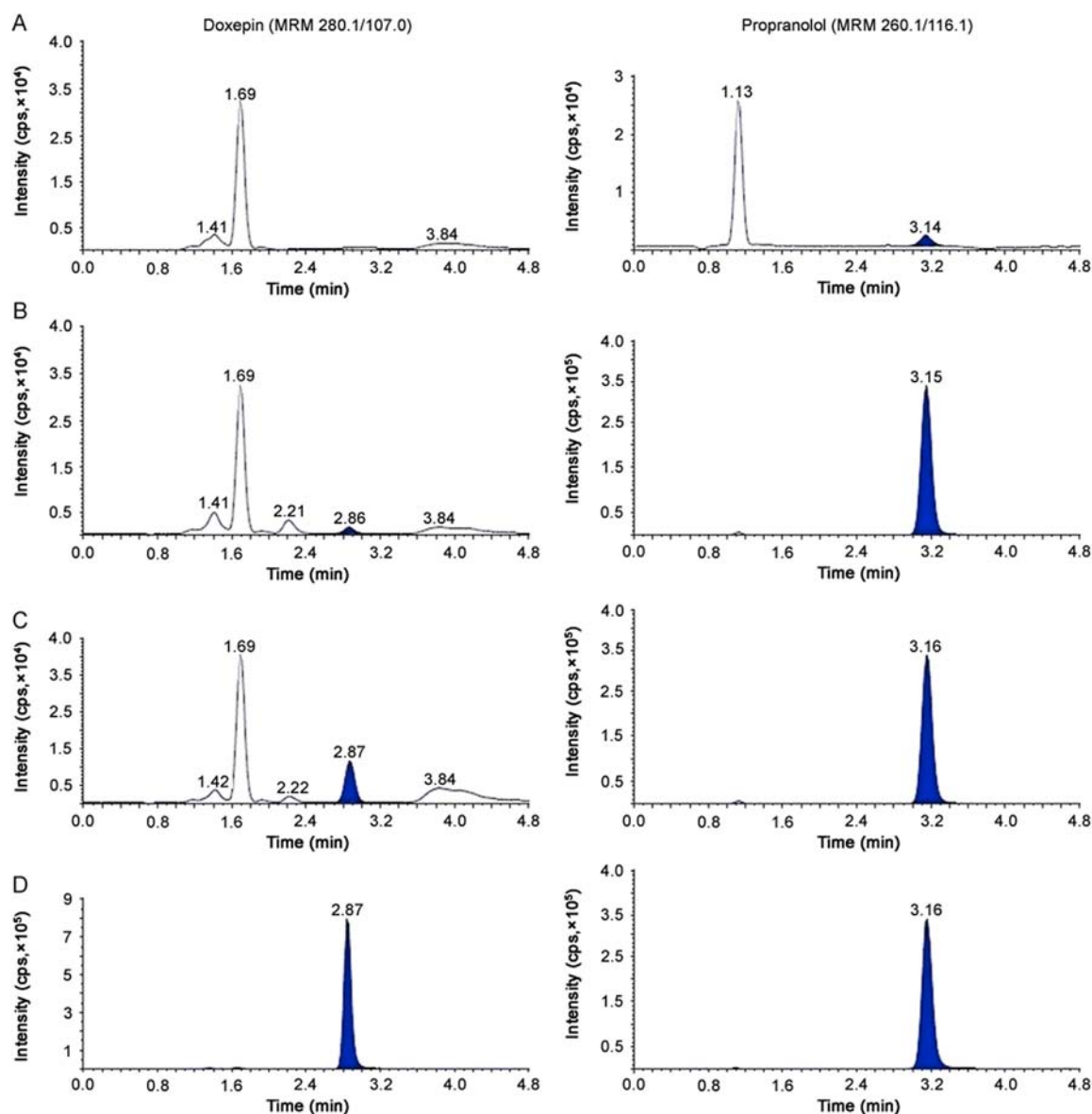
Fig. 1. MRM ion-chromatograms of doxepin (m/z 280.1 → 107.0) and propranolol (IS, m/z 260.1 → 116.1) in (A) double blank plasma (without analyte and IS), (B) blank plasma with IS, (C) doxepin at LLOQ and IS and (D) real subject sample at C_{max} after administration of 6 mg dose of doxepin.

1300 pg/mL with correlation coefficient (r^2) ≥ 0.9991 and ≥ 0.9993, respectively. The mean linear equations computed by least square regression analysis for DOX and NDox were $y = (0.00192 \pm 0.00016)x + (0.00017 \pm 0.00003)$ and $y = (0.00117 \pm 0.00021)x + (0.00026 \pm 0.00002)$, respectively, where y is the peak area ratio of the analyte/IS and x the concentration of the analyte. The accuracy and precision (% CV) observed for the CSs ranged from 94.4% to 104% and 0.8%–3.7%, respectively for Dox and 95.9%–102% and 1.1%–5.4%, respectively for NDox. The lowest concentration in the standard curves for Dox and NDox was 15.0 pg/mL and 5.00 pg/mL, respectively at a signal-to-noise ratio (S/N) of ≥ 15.

The intra-batch and inter-batch precision and accuracy results are summarized in Table 1. The intra-batch precision (% CV) and accuracy ranged from 1.0% to 8.3% and 93.1%–104.0%, respectively for both the analytes. Similarly for inter-batch experiments, the precision and accuracy varied from 3.4% to 7.2% and 91.7%–101.0% for Dox and NDox.

3.2.3. Recovery, matrix effect and post-column analyte infusion

The extraction recovery and matrix effect data for the analytes and ISs are presented in Table 2. Highly consistent recovery was obtained across QC levels for both the analytes. The IS-normalized matrix factors ranged from 1.02 to 1.05, which shows minimal interference of endogenous matrix components for Dox and NDox. Matrix effect in different plasma sources (6-K_2EDTA, 1-lipemic and 1-heamolyzed) was also evaluated at LQC and HQC levels. The precision values in different plasma sources varied from 0.3% to 3.9% for both the analytes (Table S1). Further, results of post-column analyte infusion experiment showed no regions of ion suppression or enhancement at the retention time of analytes and IS.

3.2.4. Stability, dilution integrity and ruggedness

Stability experiments were performed to evaluate the analytes stability in stocks solutions and in plasma samples under different conditions, simulating the same conditions which occurred during
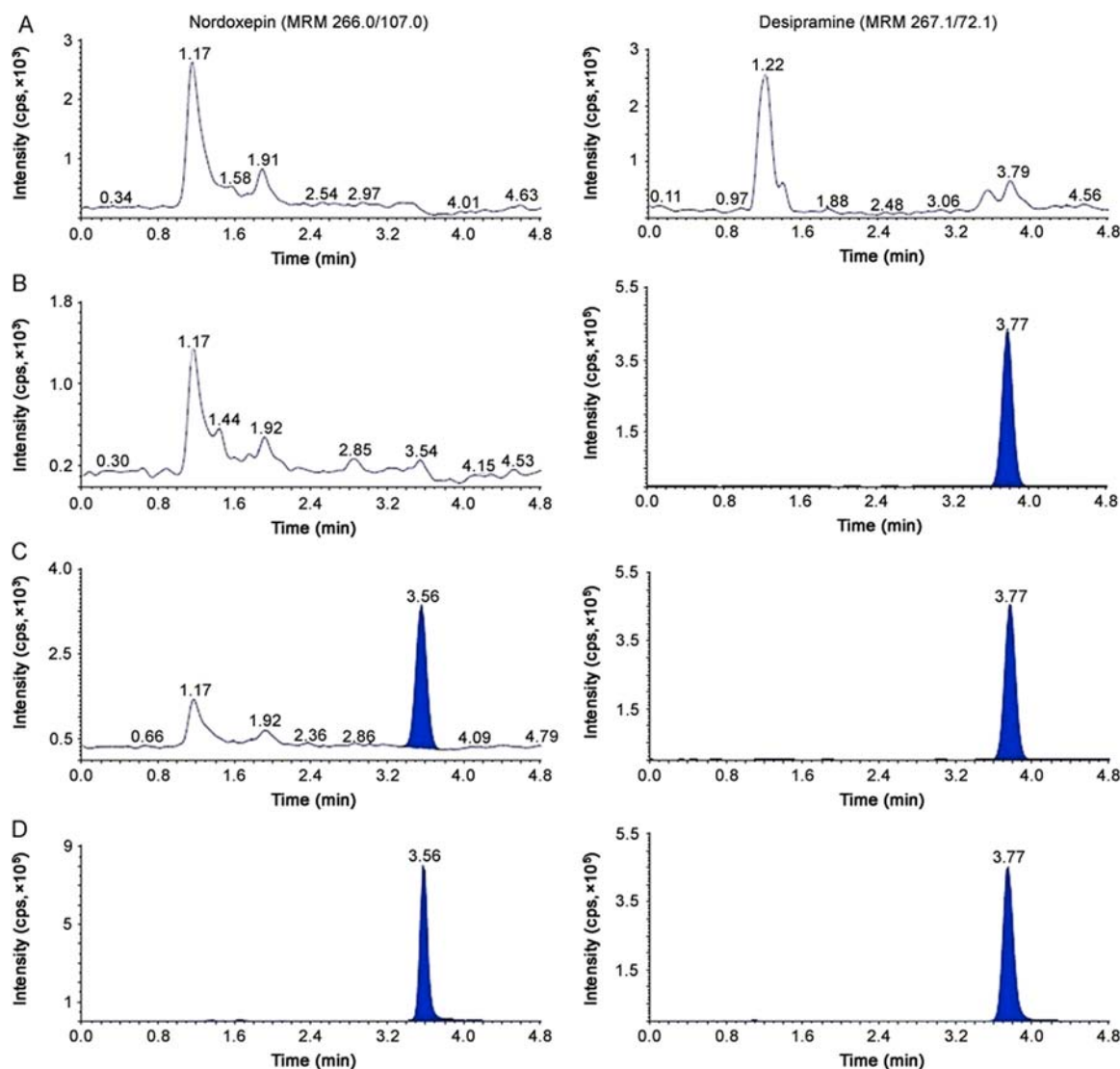
Fig. 2. MRM ion-chromatograms of nordoxepin (m/z 266.0 → 107.0) and desipramine (IS, m/z 267.1 → 72.1) in (A) double blank plasma (without analyte and IS), (B) blank plasma with IS, (C) nordoxepin at LLOQ and IS and (D) real subject sample at C_{max} after administration of 6 mg dose of doxepin.

sample analysis. Dox and NDox were found stable in controlled blank plasma at room temperature up to 24 h and for six freeze-thaw cycles. The analytes in extracted plasma samples were stable for 91 h under refrigerated conditions (2–8 °C) and for 48 h at room temperature. The spiked plasma samples of Dox and NDox stored at −20 °C for long-term stability showed evidence of degradation up to 123 days. The detailed stability results are shown in Table 3.

Dilution integrity of the method was checked to confirm dilution reliability of samples having concentration above ULOQ. The precision (% CV) value for 10-fold dilution of 19,500/6500 pg/mL for Dox/NDox was in the range of 2.2%−5.5% and the accuracy results were within 94.4%−102.0%. The results obtained were well within the acceptance limit of 15% for precision (% CV) and 85%–115% for accuracy. Similarly, the precision and accuracy for method ruggedness on two different Hypurity C$_8$ columns and with different analysts varied from 1.5% to 6.2% and 93.5%–103.0%, respectively for both the drugs.

3.3. Application of the method in healthy subjects

The validated method was applied to a bioequivalence study of Dox and NDox in 41 healthy Indian males who received 6 mg of

test and reference formulations of Dox under fasting and fed conditions. The study was performed to evaluate the impact of food on the pharmacokinetics of Dox and NDox. The method was sensitive enough to monitor their plasma concentration up to 120 h. Fig. 3 shows the plasma concentration *vs.* time profile of Dox and NDox in healthy subjects under fasting and fed conditions. Table 4 gives a comparative assessment of pharmacokinetic parameters obtained for both the studies. As evident from the results, there was minimal effect of food on the pharmacokinetics of Dox and NDox. It was not possible to compare the results obtained with reported methods [11,13] due to limited information on the pharmacokinetic studies of Dox and NDox in healthy subjects. The equivalence statistics of bioavailability for the pharmacokinetic parameters of the two formulations are summarized in Table S2. No statistically significant differences were found between the two formulations in any parameter. Approximately 5060 samples including the calibration, QC and volunteer samples were run and analyzed successfully. The % change in the measurement of selected subject samples for ISR was within ± 16%, which confirms method reproducibility.

Table 1
Intra-batch and inter-batch accuracy and precision for doxepin and nordoxepin.

Quality control level (pg/mL)	Intra-batch ($n = 6$; single batch)			Inter-batch ($n = 18$; 6 from each batch)		
	Mean conc. found (pg/mL)	Accuracy (%)	CV (%)	Mean conc. found (pg/mL)	Accuracy (%)	CV (%)
Doxepin						
LLOQ (15.0)	15.11	101.0	2.4	15.00	100.0	4.3
LQC (45.0)	44.32	98.5	1.5	43.02	95.6	3.4
MQC – 2 (360)	359.1	99.8	1.4	352.8	98.0	5.0
MQC – 1 (900)	936.7	104.0	2.8	905.1	101.0	4.7
HQC (3000)	3006	100.0	1.0	2869	95.6	5.8
ULOQ (3900)	3688	94.6	1.1	3575	91.7	4.2
Nordoxepin						
LLOQ (5.00)	4.70	93.9	8.3	4.84	96.9	5.7
LQC (15.0)	13.97	93.1	1.6	13.76	91.7	3.4
MQC – 2 (120)	116.0	96.7	1.7	114.1	95.1	5.0
MQC – 1 (300)	306.6	102.0	1.1	292.0	97.3	6.3
HQC (1000)	1032	103.0	2.1	990.0	99.0	7.2
ULOQ (1300)	1243	95.6	2.4	1235	95.0	5.3

CV: coefficient of variation; LQC: low quality control; MQC: medium quality control.
HQC: high quality control; LLOQ QC: lower limit of quantitation quality control.

Table 2
Extraction recovery and matrix factor for doxepin and nordoxepin ($n = 6$).

Quality control level (pg/mL)	Mean area response ($n = 6$)			Recovery (B/A, %)		Matrix factor		
	A (post-extraction spiking)	B (pre-extraction spiking)	C (neat samples in mobile phase)	Analyte	IS	Analyte (A/C)	IS	IS-normalized (Analyte/IS)
Doxepin								
45.0	260,239	225,421	268,564	86.6	78.0	0.97	0.95	1.02
360	2,067,205	1,838,261	2,146,630	88.9	77.2	0.96	0.92	1.04
900	5,273,665	4,766,340	5,504,869	90.4	77.3	0.96	0.91	1.05
3000	17,039,908	15,085,311	17,880,281	88.5	79.0	0.95	0.92	1.03
Nordoxepin								
15.0	72,870	65,772	68,082	90.3	84.3	1.07	1.02	1.05
120	615,922	584,171	606,222	94.8	86.5	1.02	0.99	1.03
300	1,386,867	1,374,321	1,318,315	99.1	85.7	1.05	1.00	1.05
1000	5,144,172	4,529,038	4,928,914	88.0	85.4	1.04	1.01	1.03

IS: internal standard, propranolol for doxepin and desipramine for nordoxepin.

Table 3
Stability results for doxepin and nordoxepin under different conditions ($n = 6$).

Storage condition	Quality control level	Doxepin			Nordoxepin		
		Mean stability sample (pg/mL)	CV (%)	%Change	Mean stability sample (pg/mL)	CV (%)	%Change
Bench top stability	LQC	42.98	4.7	− 4.5	15.21	3.5	1.4
(24 h, 25 °C)	HQC	2776	5.2	− 7.5	1047	6.0	4.7
Freeze-thaw stability	LQC	43.60	2.8	− 2.7	13.45	2.5	− 10.3
(6 cycles, − 20 °C)	HQC	2980	3.2	− 0.7	991.3	3.3	− 0.9
Auto-sampler stability	LQC	43.56	4.0	− 3.2	13.59	2.8	− 9.4
(91 h, 2–8 °C)	HQC	3033	4.5	1.1	991.6	1.9	− 0.8
Processed sample stability	LQC	43.61	4.2	− 3.1	13.16	2.2	− 12.3
(48 h, 25 °C)	HQC	3056	1.1	1.9	979.7	4.1	− 2.0
Long-term stability	LQC	46.43	3.8	3.2	14.24	1.3	− 5.1
(123 days, − 20 °C)	HQC	2967	4.1	− 1.1	986.1	3.3	− 1.4

LQC: low quality control; HQC: high quality control; CV: coefficient of variation.

$$\%Change = \frac{Mean\ stability\ sample - Mean\ comparison\ sample}{Mean\ comparison\ sample} \times 100$$

4. Conclusion

The present study describes a new, highly sensitive and rugged LC–MS/MS method for the simultaneous determination of Dox and NDox in human plasma, especially to meet the requirement for subject sample analysis. The LLE procedure established using MTBE gave consistent and reproducible recoveries for both the analytes. The optimized linear concentration range was adequate
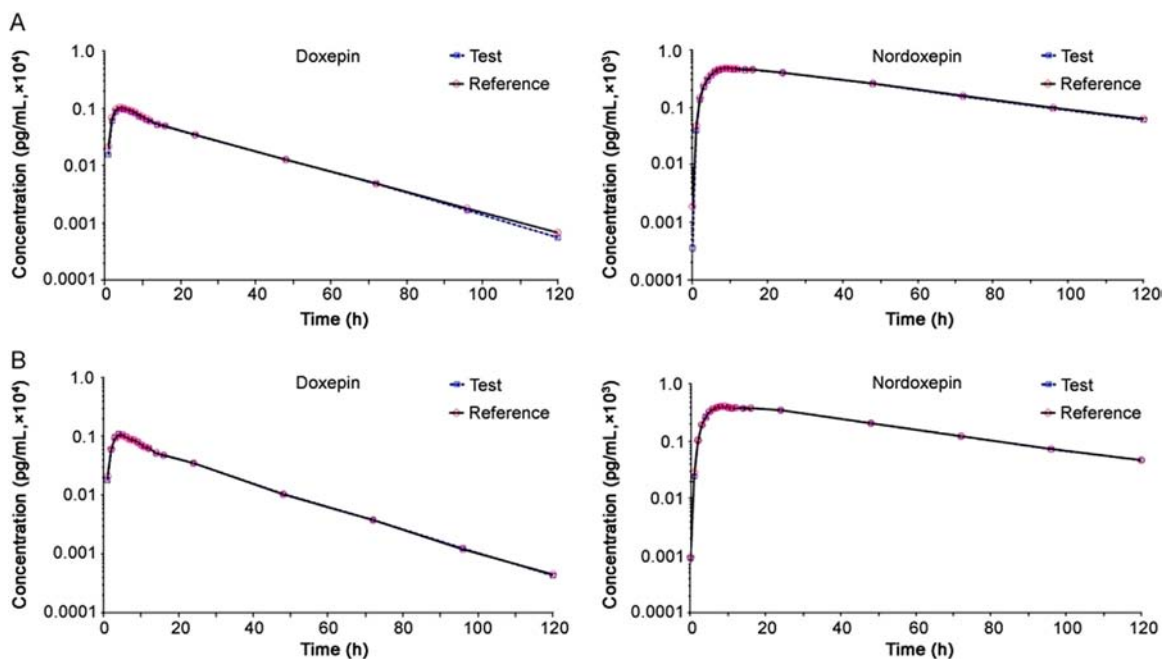
Fig. 3. Mean plasma concentration-time profile of doxepin and nordoxepin after oral administration of 6 mg doxepin orally disintegrating tablet (test and reference) formulation to 41 healthy Indian male subjects under (A) fasting and (B) fed conditions.

Table 4

Mean pharmacokinetic parameters ($\pm$ SD) following oral administration of 6 mg of doxepin hydrochloride tablet formulation on 41 healthy Indian male subjects under fasting and fed condition.

Parameter	Doxepin		Nordoxepin	
	Test	Reference	Test	Reference
Fasting				
C_{max} (pg/mL)	1044.2 $\pm$ 692.9	1094.7 $\pm$ 813.8	506.2 $\pm$ 169.0	518.9 $\pm$ 191.8
T_{max} (h)	4.85 $\pm$ 1.11	4.81 $\pm$ 1.45	11.76 $\pm$ 7.21	11.27 $\pm$ 6.36
$t_{1/2}$ (h)	16.18 $\pm$ 3.80	16.56 $\pm$ 4.06	32.96 $\pm$ 10.07	32.84 $\pm$ 9.52
$AUC_{0-120\ h}$ (h·pg/mL)	22,619.2 $\pm$ 17,826.4	23,289.3 $\pm$ 20,103.9	27,054.5 $\pm$ 13,989.8	27,579.6 $\pm$ 15,882.6
AUC_{0-inf} (h·pg/mL)	23,247.1 $\pm$ 18,137.8	24,039.6 $\pm$ 20,472.2	30,625.9 $\pm$ 19,439.3	31,498.3 $\pm$ 22,320.7
K_{el} (1/h)	0.045 $\pm$ 0.011	0.044 $\pm$ 0.011	0.023 $\pm$ 0.006	0.022 $\pm$ 0.005
Fed				
C_{max} (pg/mL)	1216.1 $\pm$ 765.5	1149.6 $\pm$ 698.1	442.4 $\pm$ 161.8	435.6 $\pm$ 160.8
T_{max} (h)	4.81 $\pm$ 1.63	4.79 $\pm$ 1.73	9.52 $\pm$ 3.18	10.02 $\pm$ 4.21
$t_{1/2}$ (h)	15.51 $\pm$ 4.30	15.94 $\pm$ 4.70	32.88 $\pm$ 6.58	32.66 $\pm$ 6.03
$AUC_{0-120\ h}$ (h·pg/mL)	22,607.9 $\pm$ 13,685.2	22,231.2 $\pm$ 13,856.0	22,785.5 $\pm$ 9097.4	22,476.1 $\pm$ 8983.4
AUC_{0-inf} (h·pg/mL)	23,229.2 $\pm$ 13,827.3	22,843.1 $\pm$ 14,088.7	25,232.5 $\pm$ 10,510.5	24,899.8 $\pm$ 10,368.1
K_{el} (1/h)	0.048 $\pm$ 0.013	0.047 $\pm$ 0.012	0.022 $\pm$ 0.004	0.022 $\pm$ 0.004

C_{max}: maximum plasma concentration; T_{max}: time point of maximum plasma concentration;
$t_{1/2}$: half-life of drug elimination during the terminal phase;
AUC_{0-t}: area under the plasma concentration-time curve from zero hour to 120 h;
AUC_{0-inf}: area under the plasma concentration-time curve from zero hour to infinity;
K_{el}: elimination rate constant; SD: standard deviation.

to monitor at least five half-lives of Dox and NDox with good accuracy and precision. The results of clinical study showed no major impact of food on the pharmacokinetics of Dox and NDox. Finally, the reproducibility of the method was adequately proved through incurred sample reanalysis of subject samples for the first time.

Conflicts of interest

The authors have declared that there are no conflicts of interest.

Appendix A. Supplementary material

Supplementary data associated with this article can be found in the online version at doi:10.1016/j.jpha.2017.06.004.

References

[1] S. Akhondzadeh, H. Faraji, M. Sadeghi, et al., Double-blind comparison of fluoxetine and nortriptyline in the treatment of moderate to severe major depression, J. Clin. Pharm. Ther. 28 (2003) 379–384.

[2] P.B. Kandagal, S. Ashoka, J. Seetharamappa, et al., Study of interaction between doxepin and human serum albumin by spectroscopic methods, J. Photochem. Photobiol. A: Chem. 179 (2006) 161–166.

[3] J. Katwala, A.K. Kumar, J.J. Sejpal, et al., Therapeutic rationale for low dose doxepin in insomnia patients, Asian Pac. J. Trop. Dis. 3 (2013) 331–336.

[4] R. Schomburg, D. Remane, K. Fassbender, et al., Doxepin concentrations in plasma and cerebrospinal fluid, J. Neural Transm. 118 (2011) 641–645.

[5] A. Gronewold, A. Dettling, H.T. Haffner, et al., Doxepin and nordoxepin concentrations in body fluids and tissues in doxepin associated deaths, Forensic Sci. Int. 190 (2009) 74–79.

[6] A. Koski, I. Ojanpera, J. Sistonen, et al., A fatal doxepin poisoning associated with a defective CYP2D6 genotype, Am. J. Forensic Med. Pathol. 28 (2007) 259–261.

[7] A. Negrusz, C.M. Moore, J.L. Perry, Detection of doxepin and its major metabolite desmethyldoxepin in hair following drug therapy, J. Anal. Toxicol. 22 (1998) 531–536.

[8] K.L. Johnson-Davis, J.M. Juenke, R. Davis, G.A. McMillin, Quantification of tricyclic antidepressants using UPLC-MS/MS, in: L.J. Langman, C.L.H. Snozek (Eds.), LC-MS in Drug Analysis: Methods and Protocols, Springer Protocols, Humana Press, 2012, pp. 175–184.

[9] F.J. Gong, S.M. Yan, Z.P. Wu, R.S. Zhang, Determination of doxepin in whole blood by SPE-LC-MS/MS, Fa Yi Xue Za Zhi 27 (2011) 350–352.

[10] M.R. Baezzat, F. Banavand, M. Tabandeh, et al., Determination of doxepin in human plasma using cloud-point extraction with high-performance liquid chromatography and ultraviolet detection, J. Sep. Sci. 38 (2015) 3192–3197.

[11] J. Yan, J.W. Hubbard, G. Mckay, et al., Stereoselective and simultaneous measurement of cis- and trans-isomers of doxepin and N-desmethyldoxepin in plasma or urine by high-performance liquid chromatography, J. Chromatogr. B 691 (1997) 131–138.

[12] V.S. Haritos, H. Ghabrial, J.T. Ahokas, et al., Stereoselective measurement of E- and Z-doxepin and its N-desmethyl and hydroxylated metabolites by gas chromatography–mass spectrometry, J. Chromatogr. B 736 (1999) 201–208.

[13] D. Badenhorst, F.C.W. Sutherland, A.D. de Jager, et al., Determination of doxepin and desmethyldoxepin in human plasma using liquid chromatography-tandem mass spectrometry, J. Chromatogr. B 742 (2000) 91–98.

[14] J. Li, F. Zhao, H. Ju, Simultaneous determination of psychotropic drugs in human urine by capillary electrophoresis with electrochemiluminescence detection, Anal. Chim. Acta 575 (2006) 57–61.

[15] V.F. Samanidou, M.K. Nika, I.N. Papadoyannis, Development of an HPLC method for the monitoring of tricyclic antidepressants in biofluids, J. Sep. Sci. 30 (2007) 2391–2400.

[16] R. Wietecha-Posłuszny, A. Garbacik, M. Woźniakiewicz, et al., Microwave-assisted hydrolysis and extraction of tricyclic antidepressants from human hair, Anal. Bioanal. Chem. 399 (2011) 3233–3240.

[17] R. Wietecha-Posłuszny, A. Garbacik, M. Woźniakiewicz, et al., Application of microextraction by packed sorbent to isolation of psychotropic drugs from human serum, Anal. Bioanal. Chem. 402 (2012) 2249–2257.

[18] F. Zare, M. Ghaedi, A. Daneshfar, Ionic-liquid-based surfactant-emulsified microextraction procedure accelerated by ultrasound radiation followed by high-performance liquid chromatography for the simultaneous determination of antidepressant and antipsychotic drugs, J. Sep. Sci. 38 (2015) 844–851.

[19] B. Fahimirad, A. Asghari, M. Bazregar, et al., Application of tandem dispersive liquid–liquid microextraction for the determination of doxepin, citalopram, and fluvoxamine in complicated samples, J. Sep. Sci. 39 (2016) 4828–4834.

[20] S. Rana, V.P. Uralets, W. Ross, A new method for simultaneous determination of cyclic antidepressants and their metabolites in urine using enzymatic hydrolysis and fast GC-MS, J. Anal. Toxicol. 32 (2008) 355–363.

[21] K. Titier, N. Castaing, M. Le-Deodic, et al., Quantification of tricyclic antidepressants and monoamine oxidase inhibitors by high-performance liquid chromatography-tandem mass spectrometry in whole blood, J. Anal. Toxicol. 21 (1997) 200–207.

[22] H. Kirchherr, W.N. Kuhn-Velten, Quantitative determination of forty-eight antidepressants and antipsychotics in human serum by HPLC tandem mass spectrometry: a multi-level, single-sample approach, J. Chromatogr. B 843 (2006) 100–113.

[23] M.M.R. Fernandez, S.M.R. Wille, N. Samyn, Quantitative method validation for the analysis of 27 antidepressants and metabolites in plasma with ultra performance liquid chromatography–tandem mass spectrometry, Ther. Drug Monit. 34 (2012) 11–24.

[24] M. Wozniakiewicz, R. Wietecha-Posłuszny, A. Moos, et al., Development of micro extraction by packed sorbent for toxicological analysis of tricyclic antidepressant drugs in human oral fluid, J. Chromatogr. A 1337 (2014) 9–16.

[25] E.E. Chambers, M.J. Woodcock, J.P. Wheaton, et al., Systematic development of an UPLC–MS/MS method for the determination of tricyclic antidepressants in human urine, J. Pharm. Biomed. Anal. 88 (2014) 660–665.

[26] Guidance for Industry, Bioanalytical Method Validation, US Department of Health and Human Services, Food and Drug Administration Centre for Drug Evaluation and Research (CDER), Centre for Veterinary Medicine (CVM), May 2001.

[27] D.S. Patel, N. Sharma, M.C. Patel, et al., Development and validation of a selective and sensitive LC–MS/MS method for determination of cycloserine in human plasma: application to bioequivalence study, J. Chromatogr. B 879 (2011) 2265–2273.

[28] Guidance for Industry: ICH E6 Good Clinical Practice, U.S. Department of Health and Human Services, Food and Drug Administration, Centre for Drug Evaluation and Research (CDER), Centre for Biologics Evaluation and Research (CBER), 1996.

[29] M. Yadav, P.S. Shrivastav, Incurred sample reanalysis: a decisive tool in bioanalytical research, Bioanalysis 3 (2011) 1007–1024.

Original Research Article

Long-term stability of gentamicin sulfate-ethylenediaminetetraacetic acid disodium salt (EDTA-Na$_2$) solution for catheter locks

Anne-Sophie Fiolet [a,1], Elise Jandot [a,1], Pauline Doucey [a,1], Coralie Crétet [a], Célia Brunel [a], Christine Pivot [a], Jean-Marc Ghigo [b], Christophe Beloin [b], David Lebeaux [b,c,d], Fabrice Pirot [a,e,*,2]

[a] Service Pharmaceutique, Plateforme FRIPHARM, Groupe Hospitalier Centre Edouard Herriot, Hospices Civils de Lyon, 5, Place d'Arsonval, F-69437 Lyon Cedex 03, France
[b] Unité de Génétique des Biofilms, Département de Microbiologie, Institut Pasteur, 28 rue du docteur Roux, F-75724 Paris Cedex 15, France
[c] Service de Microbiologie, Unité Mobile de Microbiologie Clinique, Assistance Publique-Hôpitaux de Paris, Hôpital Européen Georges Pompidou, 20 rue Leblanc, 75015 Paris, France
[d] Université Paris Descartes, 12 rue de l'Ecole de Médecine, 75270 Paris Cedex 06, France
[e] Laboratoire de Recherche et Développement de Pharmacie Galénique Industrielle, UMR 5305, Plateforme FRIPHARM,F-69373, Faculté de Pharmacie, Université Claude Bernard Lyon 1, 8, avenue Rockefeller, F-69373 Lyon Cedex 08, France

ARTICLE INFO

ABSTRACT

A lock solution composed of gentamicin sulfate (5 mg/mL) and ethylenediaminetetraacetic acid disodium salt (EDTA-Na$_2$, 30 mg/mL) could fully eradicate in vivo bacterial biofilms in totally implantable venous access ports (TIVAP). In this study, fabrication, conditioning and sterilization processes of antimicrobial lock solution (ALS) were detailed and completed by a stability study. Stability of ALS was conducted for 12 months in vial (25 °C $\pm$ 2 °C, 60% $\pm$ 5% relative humidity (RH), and at 40 °C $\pm$ 2 °C, RH 75% $\pm$ 5%) and for 24 h and 72 h in TIVAP (40 °C $\pm$ 2 °C, RH 75% $\pm$ 5%). A stability indicating HPLC assay with UV detection for simultaneous quantification of gentamicin sulfate and EDTA-Na$_2$ was developed. ALS was assayed by ion-pairing high performance liquid chromatography (HPLC) needing gentamicin derivatization, EDTA-Na$_2$ metallocomplexation of samples and gradient mobile phase. HPLC methods to separate four gentamicin components and EDTA-Na$_2$ were validated. Efficiency of sterility procedure and conditioning of ALS was confirmed by bacterial endotoxins and sterility tests. Physicochemical stability of ALS was determined by visual inspection, osmolality, pH, and sub-visible particle counting. Results confirmed that the stability of ALS in vials was maintained for 12 months and 24 h and 72 h in TIVAP.

1. Introduction

Central venous catheters (CVC) are frequently used in oncology, nephrology and intensive care units to administer medication or fluids to patients [1]. The use of CVC is complicated by the risk of colonization by pathogenic microorganisms on their surface, causing infectious complications such as catheter-related bloodstream infections (CRBSI) [2]. Optimal management of CRBSI involves systemic antimicrobial therapy and CVC removal, which might be questionable in specific clinical situations (e.g., limited vascular access or bleeding disorders) [3]. Therefore, direct instillation of a small volume of highly-concentrated antimicrobial solution into the lumen of the catheter, known as antimicrobial lock therapy (ALT), might be favored as an alternative strategy for both prevention and treatment of CRBSI [4,5]. Several studies reported the use of antibiotics such as aminoglycosides, e.g., gentamicin, [3], beta-lactams, fluoroquinolones, folate antagonists (sulfamethoxazole/trimethoprim), glycopeptides, glycylcyclines, lipopeptides, oxazolidinones, polymyxins, and tetracyclines in ALT [6]. However, surface of medical device might be colonized by a reservoir of pathogenic microorganisms forming a biofilm, a complex microbial consortium surrounded by an heterogeneous matrix composed of water, polysaccharides, proteins and deoxyribonucleic acid [6], decreasing the antibiotic efficacy [7]. Potential additives (e.g., ethylenediaminetetraacetic acid disodium salt, EDTA-Na$_2$, and sodium citrate) have shown their capacity to disrupt biofilm and to enhance bactericidal effect of current antibiotics [6,8–11]. Recent in vitro and in vivo study demonstrated the

---

beneficial effect of EDTA-Na$_2$ against *Pseudomonas aeruginosa* biofilm and the concomitant decrease of minimal inhibitory concentration of ciprofloxacin and ampicillin (30-fold) and gentamicin (two-fold) [12]. An earlier in vivo study reported that an antimicrobial lock solution (ALS) composed of gentamicin (5 mg/mL) and EDTA-Na$_2$ (30 mg/mL) in association with systemic antibiotics completely eradicated biofilms formed by *Escherichia coli*, *Pseudomonas aeruginosa*, *Staphylococcus epidermidis* or *Staphylococcus aureus* on the surface of totally implantable venous access ports (TIVAP) [13].

Gentamicin produced by *Micromonospora purpurea* is used as gentamicin sulfate which is a complex mixture of five structurally related components: *C1*, *C1a*, *C2* and *C2a* and a minor component *C2b* [14]. Previous basic stability study showed that gentamicin sulfate-EDTA-Na$_2$ antibiotic lock solution stored at 25 °C or 37 °C was visually stable for at least 72 h [3].

In the present study, a process of pharmaceutical compounding and conditioning of gentamicin sulfate-EDTA-Na$_2$ lock solution is detailed and then completed by a study of stability according to the technical requirements of International Conference on Harmonization (ICH) for registration of pharmaceuticals for human use. The physicochemical stability of ALS conditioned in glass vial was analyzed (i) over 12 months of storage at 25 °C $\pm$ 2 °C (relative humidity (RH) 60% $\pm$ 5%) and 40 °C $\pm$ 2 °C (RH 75% $\pm$ 5%), and (ii) after 24 h and 72 h of contact time in TIVAP at 40 °C $\pm$ 2 °C (RH 75% $\pm$ 5%), by high performance liquid chromatography (HPLC) evidencing the impurities and degradation products of gentamicin sulfate and EDTA-Na$_2$.

2. Materials and methods

2.1. Reagents

Gentamicin sulfate and EDTA-Na$_2$ dihydrate physico chemical properties are reported in Table 1. Ready-to-use gentamicin sulfate sterile solutions (40 mg$-$2 mL and 80 mg$-$2 mL), and EDTA- Na$_2$ dihydrate (pharmaceutical grade) were purchased from Panpharma® (Beignon, France) and Inresa (Bartenheim, France) laboratories, respectively. Nitrilotriacetic acid and trifluoroacetic acid (HPLC grade, TFA) were purchased from Carl Roth (Lauterbourg, France) and Rhône Poulenc (Lyon, France), respectively.

Hydrochloric acid (HCl) and sodium hydroxide (NaOH) were provided by Carlo Erba Reagents (Peypin, France). Hydrogen peroxide solution (3%) was purchased from Gifrer (Décines, France). Gentamicin for peaks identification (CRS, European Pharmacopoeia reference standard), gentamicin USP standard, sisomicin sulfate, EDTA disodium salt standard, ortho-phtalaldehyde (OPA), thioglycolic acid, boric acid and potassium hydroxide (KOH) were obtained from Sigma-Aldrich (Saint Quentin Fallavier, France). Acetonitrile and methanol (HPLC grade) were purchased from Merck Millipore (Molsheim, France). Copper sulfate was obtained from Cooper (Melun, France). Peptone water (0.1%) was purchased from Oxoid (Basingstoke, United Kingdom). Culture media for anaerobic bacteria (fluid thioglycollate medium), aerobic bacteria and fungi (soya bean casein digest medium), and neutralizing pharmacopoeia diluent used for the gentamicin neutralization were obtained from Biomérieux (Lyon, France). Water for injection was delivered by Lavoisier (Paris, France).
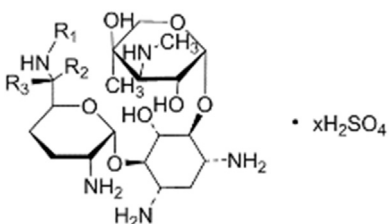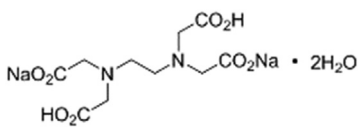
2.2. Pharmaceutical compounding and conditioning of ALS

EDTA-Na$_2$ solution (40 mg/mL) was prepared by dissolution of 22.5 g of EDTA-Na$_2$ in 562.5 mL of water for injection. Then, EDTA-Na$_2$ solution (40 mg/mL) was mixed to 187.5 mL of gentamicin sterile solution for injection (40 mg$-$2 mL). Finally, the pH value of the ALS was adjusted to 8.5 by adding few drops of 5 M NaOH solution. ALS was filtered through 0.22 µm sterile filter (Millex® GS, Millipore®, Molsheim, France), and then sampled (5 mL) in 150 individual amber type 1 glass injection vials (15 mL) hermetically sealed by bromobutyl stoppers in cleanroom. Finally, ALS vials were autoclaved at 121 °C for 20 min [15,16]. Final concentrations of gentamicin (5 mg/mL) and EDTA-Na$_2$ (30 mg/mL) in ALS were assayed by HPLC (see Section 2.6).

2.3. Storage stability testing

The environmental factors (temperature, RH) and time of storage upon degradation of gentamicin sulfate and EDTA-Na$_2$ in ALS conditioned in vials and then stored at 25 °C $\pm$ 2 °C, RH 60% $\pm$ 5% and 40 °C $\pm$ 2 °C, RH 75% $\pm$ 5% in climatic test chambers (Froilabo, Meyzieu, France) for 12 months were investigated using HPLC (see Section 2.6) [17]. Complementary physicochemical and

Table 1
Physicochemical properties of gentamicin sulfate and EDTA-Na$_2$ dihydrate (from Pubmed open chemistry database, National Institute of Health).

Physicochemical parameters	Gentamicin sulfate	EDTA-Na$_2$ dihydrate
Chemical structure		
Molecular mass (g/mol)	*C1* = 477.6 (R1 = R2 = CH$_3$; R3 = H) *C1a* = 449.5 (R1 = R2 = R3 = H) *C2a* = 463.6 (R1 = R2 = H; R3 = CH$_3$) *C2b* = 463.6 (R1 = CH$_3$; R2= R3 = H) *C2* = 463.6 (R1 = H; R2 = CH$_3$; R3 = H)	372.2
pKa	10.18, 12.55	2.0, 2.7, 6.2, 10.3
Log P (octanol-water)	$-$3.1	$-$11.70
Melting point (°C)	102–108	250
Water solubility	100 mg/mL	1 000 mg/mL
Solubility	Soluble in pyridine, dimethylformamide, in acidic media with salt formation, moderately soluble in methanol, ethanol, acetone, insoluble in benzene, halogenated hydrocarbons	–
Case number	1405–41–0	6381–92–6

microbiological controls of ALS were conducted over the period of storage (see Section 2.4). TIVAP, supplied by Perouse Medical (polysite 4000, 4008 IPS, Ivry le Temple, France), was used to test compatibility between ALS and implantable port. This medical device is made up of a chamber in titanium / polyoxymethylene and a silicone catheter. Total dead space of implantable port was 1.38 mL and internal surface of silicone catheter was 6.6 cm^2. One mL of ALS was injected into the device and left for 24 h and 72 h at 40 °C $\pm$ 2 °C, RH 75% $\pm$ 5%. To detect a potential water loss through polymeric wall, implantable port was weighted before and after filling throughout storage. Gentamicin and EDTA-Na$_2$ contents after 24 h and 72 h of contact time in chambers (n=3) were assessed by HPLC (see Section 2.6).

2.4. Physicochemical and microbiological controls of ALS

Physicochemical controls of ALS included pH measurement (EcopHtest2, Thermo Fisher Scientific, Massachusetts, USA) and determination of osmolality (Fiske®, Norwood, MA, USA). Controls of visual aspect, particulate contamination of ALS by visible particles (2.9.20 European Pharmacopoeia Monograph, 2016) and sub-visible particles (2.9.19 European Pharmacopoeia Monograph, 2016, method 1: light obscuration particle count test, Hiac/Royco 9703+, Pacific Scientific Instruments, IL, USA) were carried out after autoclaving. Microbiological assays of ALS were carried out by membrane filtration using Steritest™ closed filtration device [18] with special low-binding Durapore® membranes for products with inhibitory properties, e.g. antibiotics (Millipore, Merck KGaA, Darmstadt, Germany), peptone water (0.1%) as rinse fluid, neutralizing pharmacopoeia diluent and both soya-bean casein digest medium and fluid thioglycollate medium (2.6.1 European Pharmacopoeia Monograph, 2016).

2.5. Preparation of gentamicin sulfate and EDTA-Na$_2$ standard and ALS assay solutions

A derivatization reaction of gentamicin sulfate with OPA allowing a detection gentamicin OPA derivative was adapted from previous reports [19–21]. A stock solution of derivatizing agent was prepared by dissolving 250 mg of OPA in 1.25 mL of methanol, then addition of 23.75 mL of boric acid solution (2.47%, m/v; pH adjusted to 10.4 by 8 M KOH solution) and 0.5 mL of thioglycolic acid. Finally, the pH value of derivatizing agent solution was adjusted to 10.4 using 8 M KOH solution, for pre-column derivatization. The stock solution of derivatizing agent, stored at 4 °C and protected from light, was stable for three days. Therefore, 2.5 mL of gentamicin sulfate standard solution or ALS was then mixed with 0.5 mL of stock solution of derivatizing agent and 2.75 mL of methanol (final volume: 5.75 mL). Although usually derivatization was carried out at 60 °C constant temperature [20,22], no heating was applied to gentamicin – OPA based solution, taking into account the lack of stability of such chemical reaction and the short half-life of reaction products, as reported elsewhere [23].

The determination of EDTA-Na$_2$ in ALS was allowed by conversion to Cu(II)EDTA complex [24] using copper sulfate containing solution and subsequent separation from gentamicin, formulation excipients, impurities, and potential degradation products by HPLC (see Section 2.6). Therefore, 2.5 mL of EDTA-Na$_2$ standard solution or ALS were then mixed with 2.5 mL of copper sulfate solution (10 mg/mL) and 0.75 mL of water for injection (final volume: 5.75 mL).

Gentamicin sulfate-standard EDTA-Na$_2$ solutions were prepared daily by dissolving the appropriate amount of EDTA-Na$_2$ in water for injection, and then mixing with gentamicin sulfate sterile solution for injection (40 mg – 2 mL or 80 mg – 2 mL) to obtain, after gentamicin sulfate derivatization or EDTA-Na$_2$

complexation, final concentrations of gentamicin sulfate and EDTA-Na$_2$ in the range of 87 − 260 μg/mL and 0.52 − 1.56 mg/mL, respectively.

2.6. Stability indicating HPLC assay

An HPLC Agilent® (Agilent® 1290 Infinity Quaternary LC System, Les Ulis, France), equipped with a binary pump with integrated vacuum degasser, a thermostated column compartment (40 °C), an autosampler and a diode array detector, was used for gentamicin and EDTA dosages. The separation of gentamicin and EDTA-Na$_2$ was accomplished using SecurityGuard™ cartridge and column Kinetex™ (C$_{18}$ 100 Å, 100 mm × 4.6 mm, 2.6 μm) Core-Shell Technology (Phenomenex®, Le Pecq, France). The detection wavelength was set at 330 nm and injection volume was 10 μL. The mobile phase was a binary mixture of 100 mM TFA, used as pairing reagent in water (phase A, the pH value was adjusted to 3 by adding 5 M NaOH solution) and acetonitrile (phase B) in a gradient elution mode at a flow-rate of 1 mL/min [25,26]. The mobile phase A was filtered and degassed through nylon membranes (0.20-μm pore size) under vacuum before use. A linear gradient elution was programed as 95% A − 5% B (v/v; 0 min), 95% A − 5% B (v/v; 2 min), 50% A − 50% B (v/v; 10 min), and 40% A − 60% B (v/v; 15 min). Therefore, the resolved peaks of gentamicin sulfate OPA derivatives, C1, C1a, C2a and C2, and EDTA-Na$_2$ were identified from gentamicin for peaks identification (CRS, European Pharmacopoeia reference standard), gentamicin (216 μg/mL) USP standard solutions, and EDTA (1.3 mg/mL) standard solution. Sisomicin and nitrilotriacetic acid, as gentamicin sulfate and EDTA-Na$_2$ respective impurities, were identified from sisomicin (4.65 mg/mL) and nitrilotriacetic acid (43.5 μg/mL) standard solutions.

2.7. HPLC assay validation criteria

The HPLC-UV analytical methods for gentamicin sulfate and EDTA-Na$_2$ were validated for specificity, precision (repeatability, intermediate precision), linearity, limits of detection (LOD) and quantification (LOQ), accuracy/recovery and robustness to include the essential requirements of ICH guidelines [27,28]. The validation protocol was conducted on three consecutive days by the same operator and fresh solutions were prepared daily. Five standard gentamicin sulfate and EDTA-Na$_2$ solutions were prepared to enable the determination of drugs concentrations in ALS. Furthermore, forced degradation of ALS was investigated (i) by acidic (0.1–1 M HCl) and alkaline (0.1–1 M NaOH), (ii) heating (80 °C for 1 h) treatments, (iii) under oxidative conditions using 3% H$_2$O$_2$ then heating at 80 °C for 3 h, and (iv) from UVA (320–400 nm) irradiation for 6 h [29].

3. Results and discussion

3.1. Physicochemical and microbiological controls of ALS

Results of visual inspections for color, clarity, and particles completed by sub-visible particles counting, pH and osmolality assessments of ALS throughout the 12 months storage at 25 °C $\pm$ 2 °C, RH 60% $\pm$ 5% and 40 °C $\pm$ 2 °C, RH 75% $\pm$ 5% are summarized in Table 2. No significant macroscopic and/or microscopic alterations of ALS were evidenced. Efficiency of sterility procedure and conditioning of ALS was confirmed by the absence of microbial growth and endotoxin. No impact of autoclaving either upon particle quality or colligative property of ALS was observed. Interestingly, ALS was isosmotic to serum compared to hypoosmotic commercial gentamicin sulfate solution (Panpharma®) in favor of further easy handling in TIVAP filling and blood compatibility.

Table 2
Characterization of ALS stability over 12 months of storage at 25 °C $\pm$ 2 °C, RH 60% $\pm$ 5% (at 40 °C $\pm$ 2 °C, RH 75% $\pm$ 5%). Each data is the mean $\pm$ standard deviation of three experimental determinations. nd: Not determined.

Test	Acceptance criteria	Time of storage				
		Day 1	Month 1	Month 3	Month 6	Month 12
Appearance	Colorless (C), yellowish (Y), limpid (L)	C, L	C, L	C, L	Y, L (Y, L)	Y, L
pH	8.2 − 8.7	8.4	8.2	8.3	8.3 (8.2)	8.1
Osmolality (mOsmol/kg)	290 − 310	301	297	308	308 (310)	309
$\geq$ 10-μm particle count	< 6000/mL	nd	3	15	10	121
$\geq$ 25-μm particle count	< 600/mL	nd	0	0	0	1
Gentamicin conc. (mg/mL)	4.50 − 5.50	5.20 $\pm$ 0.10	5.20 $\pm$ 0.02	5.10 $\pm$ 0.02	5.10 $\pm$ 0.04 (5.00 $\pm$ 0,05)	4.55 $\pm$ 0.13
EDTA-Na$_2$ conc. (mg/mL)	27 − 33	29.00 $\pm$ 0.10	29.00 $\pm$ 0.36	29.00 $\pm$ 0.06	31.00 $\pm$ 0.28 (30.00 $\pm$ 0.24)	29.07 $\pm$ 0.05
Sterility	No bacterial growth	No bacterial growth	nd	No bacterial growth	No bacterial growth (nd)	No bacterial growth
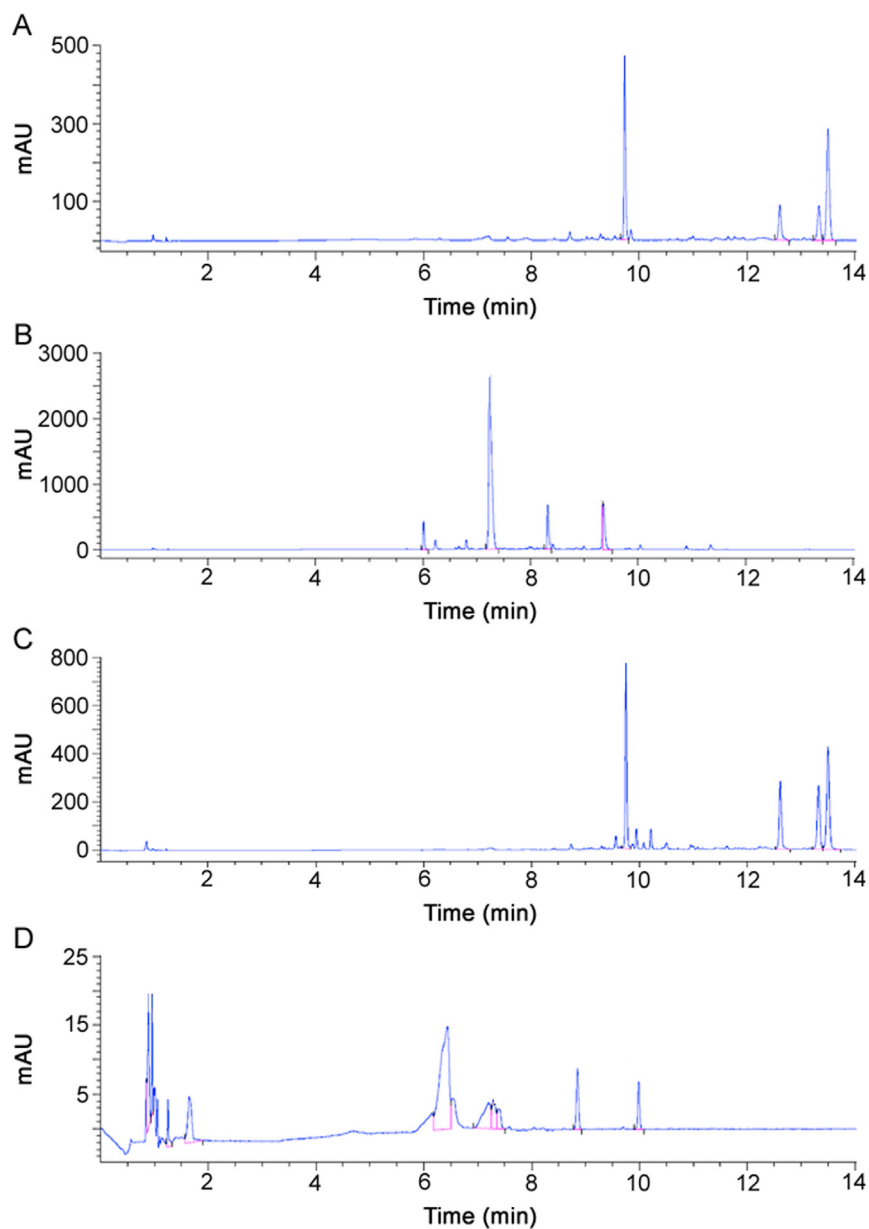
Fig. 1. (A) A typical chromatogram of gentamicin standard solution (USP) (216 μg/mL) after OPA derivatization. (B) A typical chromatogram of sisomicin after OPA derivatization (4.65 mg/mL). (C) A typical chromatogram of ALS after OPA derivatization (gentamicin 217 μg/mL). (D) Analysis of ALS (gentamicin 217 μg/mL) under oxidative conditions (3% H$_2$O$_2$, 80 °C for 3 h) after OPA derivatization.

Table 3

Identification of the gentamicin sulfate components in gentamicin USP standard solution (217 μg/mL) and in ALS according to the requirements of US Pharmacopeia USP37-NF32 monograph. Relative content (%) of each component was calculated as the area of each individual peak divided by the sum of all peak areas. The sum of all peak areas (C1a, C2 C2a, C2b and C1) corresponds to 100%. The elution order is gentamicin C1, C1a, C2a and C2.

USP37-NF32 gentamicin component relative content (%)	Gentamicin component relative content (%)	
	USP standard solution	ALS
C1: 25 – 50	37	26
C1a: 10 – 35	12	22
C2a + C2: 25 – 55	51	52

3.2. HPLC assay validation

Gentamicin sulfate and EDTA-Na$_2$ contents in ALS conditioned in amber type I glass vials were analyzed during the storage using HPLC method adapted, for a part, from US Pharmacopoeia

Monograph [22] and earlier studies [20,21,24]. The chemical structure of gentamicin reveals the lack of chromophore in the molecule, making the direct detection of the antibiotic difficult. Furthermore, besides methods based on microbiological assay [30], enzyme immunoassay, polarization fluoroimmunoassay [31,32], direct detection methods, e.g., electrochemical detection [14,33,34], evaporative light scattering detection [35,36], charged aerosol detection [26,37], direct capillary electrophoresis [38] require specific and costly instrumentation (e.g., tandem mass spectrometer, [39]) are not commonly found in quality control laboratories. In the present study, gentamicin sulfate components were assayed by UV-detection after pre-column derivatization with OPA based reagent which reacts only with three primary amines of gentamicin to form UV- absorbing fluorophores, ion-pairing chromatographic gradient and separation by a combination of electrical (charge-charge between two underivatized secondary amines of gentamicin positively charged at acidic pH of mobile phase) and hydrophobic interactions with the stationary phase and ions of the mobile phase [25]. No pre-heating of gentamicin-OPA based mixture was carried out, as described by
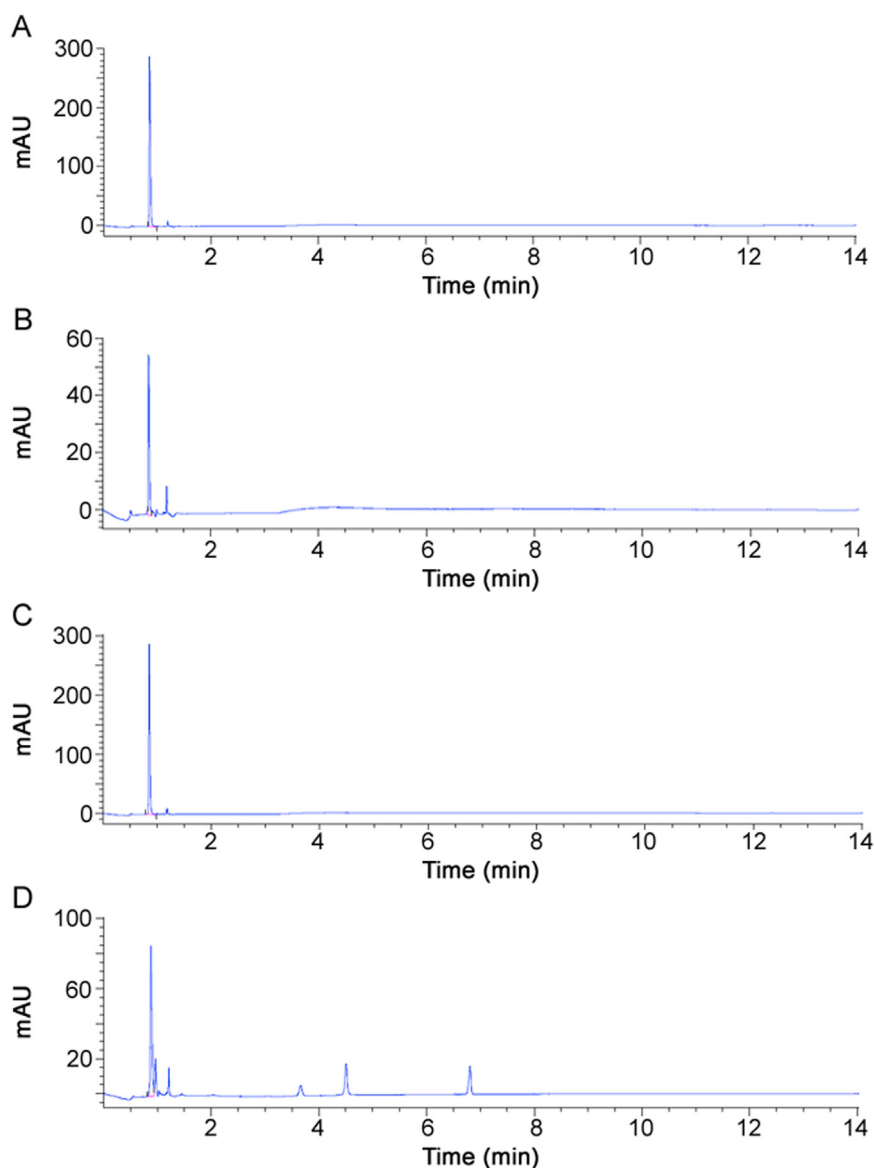

Fig. 2. (A) A typical chromatogram of EDTA-Na$_2$ (USP) (1.3 mg/mL) after CuSO$_4$ complexation. (B) A typical chromatogram of nitrilotriacetic acid (43 μg/mL) after CuSO$_4$ complexation. (C) A typical chromatogram of ALS (EDTA-Na$_2$: 1.3 mg/mL) after CuSO$_4$ complexation. (D) Analysis of ALS (EDTA-Na$_2$: 1.3 mg/mL) under stress oxidative conditions (3% H$_2$O$_2$, 80 °C for 3 h) after CuSO$_4$ complexation.
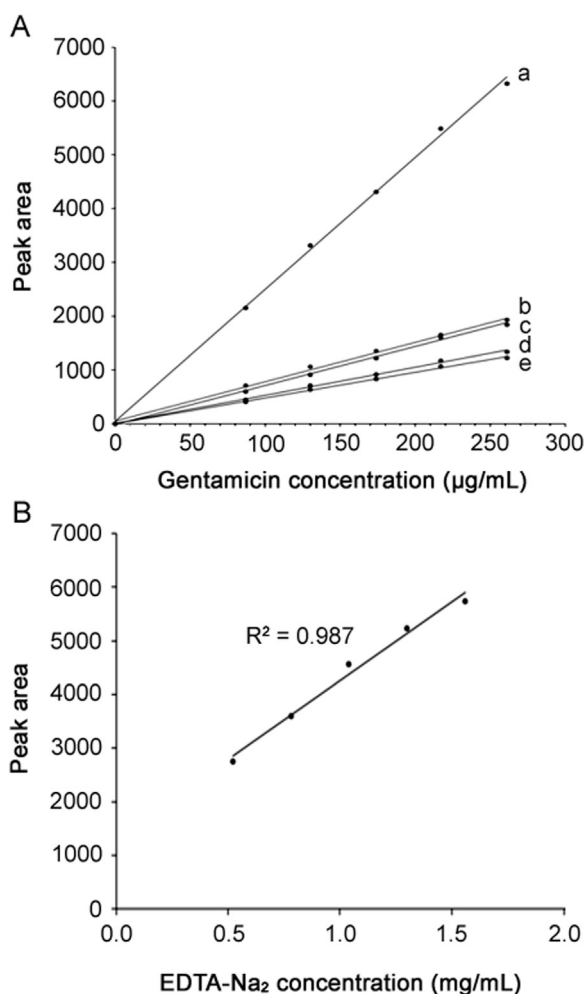
Fig. 3. (A) A typical calibration curve of the cumulative peak area (C1, C1a, C2a, C2) of gentamicin sulfate (Panpharma®) (a) and four components (b, c, d and e) ranged from 87 to 260 μg/mL. (B) A typical EDTA-Na$_2$ calibration curve ranged from 0.52 to 1.56 mg/mL.
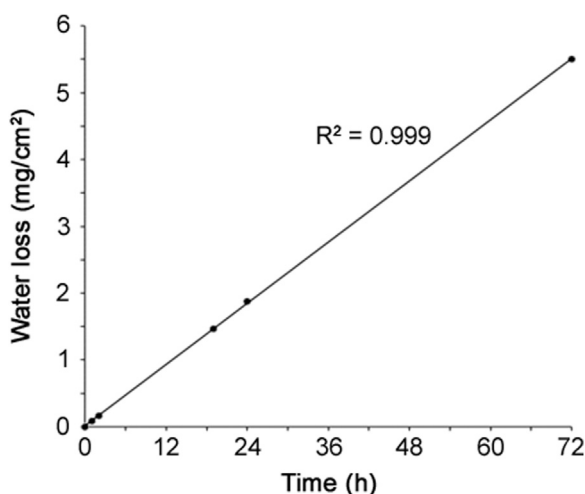

Fig. 4. Linear relationship between water loss through TIVAP and time of storage at 40 °C ± 2 °C, RH 75% ± 5%.

previous authors [19], eliminating tedious manual procedures, reducing error, and thereby increasing method reproducibility. The column was maintained at 40 °C, leading likely to more reproducible in situ derivatization of gentamicin components passing through the C$_{18}$ stationary phase.

Fig. 1A shows typical chromatogram of gentamicin standard solution. The four components of gentamicin (C1, C1a, C2a and C2) were eluted as distinct peaks with retention time of 9.7, 12.6, 13.3 and 13.5 min, respectively in the order reported by US Pharmacopoeia Monograph [22]. Gentamicin C2b component was below LOD. Furthermore, the relative content of each gentamicin component in gentamicin standard was found in agreement with US Pharmacopoeia Monograph requirements, as reported in Table 3. These findings were similar to those reported in previous study [20], in which the chromatogram of gentamicin sulfate solution (2 mg/mL) prepared from the gentamicin sulfate powder met the USP test specifications. The USP method describes the elution order as C1, C1a, C2a and C2 gentamicin with a 5 mm × 10 cm column that contains 5 μm packing L1 (octadecyl silane chemically bonded to porous or nonporous silica or ceramic microparticles, 1.5–10 μm in diameter, or a monolithic silica rod). In the present method, Kinetex™ (C$_{18}$ 100 Å, 100 mm × 4.6 mm, 2.6 μm, Core-Shell Technology) column was preferred to Luna® C$_{18}$ (2) column used by earlier authors [20]. Therefore, the elution of last gentamicin component (C2) was nearly 2.5 times shorter (13.5 min versus 31 min) in the present method than that reported previously [20], confirming that the combination of the small particle size and narrow particle size distribution coupled with the significantly shorter diffusion path resulted in a material that yielded significantly increased column efficiency and chromatographic resolution. Chromatographic separation was shortened mandatory, considering that isoindoles formed during derivatization are generally highly reactive compounds. As a result, it was considered that any derivative breakdown during chromatography would be time-dependent and that component derivatives with long retention time (C2a and C2) would be particularly affected by degradation prior to detection [40]. Previous analysis of gentamicin in raw material used column (150 mm × 4.6 mm) packed with Ultrasphere® ODS (C$_{18}$) and elution gradient (A: 5% acetic acid−25% water-70% methanol and B: 100% methanol) for faster elution of C1 (5 min) and similar elution time for C2 (13.7 min) [41]. In the present study, longer elution time for C1 (∼10 min, Fig. 1C) was preferred to elute first the most hydrophilic components of ALS (e.g., excipients from gentamicin sulfate sterile solution for injection, Panpharma®). Interestingly, it was noticed that the relative content of gentamicin components was proportional to molecular weight of C1, C1a, C2a and C2 as equimolar amounts, confirming that the sum of the areas of the four gentamicin components was a relevant measure of the gentamicin concentration. Sisomicin chromatogram shows one main peak surrounded by three minor peaks (Fig. 1B). Possible partial derivatization of one, two or three primary amines of sisomicin might explain the presence of numerous peaks.

The determination of EDTA-Na$_2$ in ALS by direct UV detection was challenging since EDTA-Na$_2$ does not contain a significant chromophore. In the present study, EDTA-Na$_2$ in ALS was assayed by ion-pairing HPLC and metallocomplex formation by using TFA in mobile phase and copper sulfate in sample preparation. Typical chromatogram of EDTA-Na$_2$ eluted as EDTA-Cu^{2+} is shown in Fig. 2A. As reported in previous study assaying EDTA-Na$_2$ in pharmaceutical formulation, EDTA-Cu^{2+}, as ionic analyte, showed minimal retention (Fig. 2C, < 1 min) through reversed-phase by using liquid chromatography with ion-pairing and elution gradient [42], and co-elution of nitrilotriacetic acid-Cu^{2+} complex (Fig. 2B).

3.3. HPLC validation criteria

3.3.1. Specificity

The specificity of the assay was conducted to evaluate the assay for potential sources of interfering peaks from the matrices used in sample preparation. No interfering peaks were seen from water

Table 4
Determination of gentamicin and EDTA-Na$_2$ concentrations in ALS after 24 h and 72 h of contact time in TIVAP. Each data is the mean $\pm$ standard deviation of three experimental determinations of concentrations in three TIVAP. Relative standard deviation (RSD) (%) of concentrations was calculated as follows: RSD (%) = (initial concentration – experimental concentration) / initial concentration.

Compounds	Volumes (μL)			Experimental concentrations (mg/mL)			Recalculated concentrations (mg/mL)	
	Initial[a]	24 h[b]	72 h[c]	Initial	24 h[d]	72 h[e]	24 h[(d × b)/a]	72 h[(e × c)/a]
Gentamicin	1000	876	637	5.00	5.40 ± 0.08 (+ 8%)	7.10 ± 1.28 (+ 43%)	4.70 ± 0.07 (− 6%)	4.60 ± 1.18 (− 9%)
EDTA-Na$_2$	1000	876	637	30.00	33.60 ± 0.38 (+12%)	44.90 ± 3.18 (+49%)	29.50 ± 0.33 (− 2%)	28.30 ± 2.00 (−6%)

used to prepare mobile phase, the mobile phase or a blank filter media. No significant macroscopic and/or microscopic alterations of ALS were evidenced in acidic (0.1–1 M HCl, at 80 °C for 1 h) and basic (0.1–1 M NaOH, at 80 °C for 1 h) conditions. ALS was found stable under heat conditions (at 80 °C) and under UVA (320–400 nm) irradiation for 6 h. Under oxidative stress conditions with 3% H$_2$O$_2$ at 80 °C for 3 h, EDTA-Na$_2$ was degraded to about 60% (Fig. 2D) while all of gentamicin sulfate was degraded (Fig. 1D). Four main degradation products were generated with retention time of 6.4, 7.2, 8.8 and 9.9 min that could correspond to the impurity A (e.g., sisomicin, Fig. 1B).

3.3.2. Precision
Repeatability and intermediate precision of gentamicin sulfate-EDTA-Na$_2$ assays were found to be 1.82% − 1.23%, and 2.16% − 1.47%, respectively, confirming the overall precision of HPLC methods involving pre-column derivatization and metallocomplex procedure.

3.3.3. Linearity
The linearity of assay was determined to have a correlation coefficient (r) for gentamicin sulfate of 0.999 (in the range of $87 − 260$ μg/mL) and for EDTA-Na$_2$ of 0.993 (in the range of $0.52 − 1.56$ mg/mL) as shown in Figs. 3A and B, respectively.

3.3.4. Accuracy
The recovery of gentamicin sulfate and EDTA-Na2 was found to be in the range of 97.96%–99.81%, and 100.72%–102.72% over all concentration range, respectively.

3.3.5. LOD and LOQ
LOD and LOQ for gentamicin were 8 μg/mL and 24 μg/mL, respectively. The LOD and LOQ for EDTA were found to be 45 μg/mL and 136 μg/mL, respectively.

3.3.6. Robustness
The robustness of the assay in terms of varied injection volume (5–15 μL) and flow rate (0.5 mL/min) did not significantly change the time retention, asymmetry and the percentage of target amounts in the samples of gentamicin sulfate and EDTA-Na$_2$.

3.3.7. Stability study of ALS in glass injection vials and in TIVAP
Stability of gentamicin sulfate and EDTA-Na$_2$ in vials stored for 12 months was confirmed by minimal variation of drug concentration in ALS, as reported in Table 2. A loss of ALS was highlighted by weighing the device throughout contact time in TIVAP. Loss solution per cm^2 of catheter is represented in Fig. 4. Solution loss was perfectly linear in function of time. After 24 h and 72 h, 124 μL and 363 μL of ALS were evaporated through polymeric wall, respectively. At the same time, HPLC assay of ALS after contact in TIVAP showed that gentamicin and EDTA concentrations increased compared to initial concentrations in ALS (Table 4). After recalculation considering the extent of water loss (124 μL for 24 h

and 363 μL for 72 h), gentamicin and EDTA concentrations were in accordance with initial concentrations in ALS (Table 4).

4. Conclusion

In this study, a process of pharmaceutical compounding and conditioning of ALS was performed. Numerous physicochemical analysis, including the development of validated HPLC methods for dual gentamicin and EDTA-Na$_2$ assays, showed a stability of ALS conditioned in amber type I glass vials for 12 months at 25 °C $\pm$ 2 °C (RH 60% $\pm$ 5%) and 40 °C $\pm$ 2 °C (RH 75% $\pm$ 5%). Furthermore, complementary findings reported satisfactory stability of ALS in TIVAP for 24 h and 72 h. At the outset, the present study confirmed the pharmaceutical relevance of gentamicin-EDTA-Na$_2$ combined solution as a new antimicrobial lock therapy.

Conflicts of interest

The authors declare that there are no conflicts of interest.

Acknowledgments

References

[1] I. Raad, H. Hanna, D. Maki, Intravascular catheter-related infections: advances in diagnosis, prevention, and management, Lancet Infect. Dis. 7 (2007) 645–657.

[2] C. Beloin, N. Fernández-Hidalgo, D. Lebeaux, Understanding biofilm formation in intravascular device-related infections, Intensive Care Med. 43 (2017) 443–446.

[3] P.B. Bookstaver, K.E.E. Rokas, L.B. Norris, et al., Stability and compatibility of antimicrobial lock solutions, Am. J. Health-Syst. Pharm. AJHP Off. J. Am. Soc. Health-Syst. Pharm., 70, (2013) 2185–2198.

[4] S. Hogan, M. Zapotoczna, N.T. Stevens, et al., In vitro approach for identification of the most effective agents for antimicrobial lock therapy in the treatment of intravascular catheter-related infections caused by Staphylococcus aureus, Antimicrob. Agents Chemother. 60 (2016) 2923–2931.

[5] L.A. Mermel, M. Allon, E. Bouza, et al., Clinical practice guidelines for the diagnosis and management of intravascular catheter-related infection: 2009 Update by the Infectious Diseases Society of America, Clin. Infect. Dis. Off. Publ. Infect. Dis. Soc. Am. 49 (2009) 1–45.

[6] J.A. Justo, P.B. Bookstaver, Antibiotic lock therapy: review of technique and logistical challenges, Infect. Drug Resist 7 (2014) 343–363.

[7] D. Lebeaux, J.-M. Ghigo, C. Beloin, Biofilm-related infections: bridging the gap between clinical management and fundamental aspects of recalcitrance toward antibiotics, Microbiol. Mol. Biol. Rev. MMBR 78 (2014) 510–543.

[8] M.G. Betjes, M. van Agteren, Prevention of dialysis catheter-related sepsis with a citrate-taurolidine-containing lock solution, Nephrol. Dial. Transplant. 19 (2004) 1546–1551.

[9] P.B. Bookstaver, J.C. Williamson, B.K. Tucker, et al., Activity of novel antibiotic lock solutions in a model against isolates of catheter-related bloodstream infections, Ann. Pharmacother. 43 (2009) 210–219.

[10] I.I. Raad, R.Y. Hachem, H.A. Hanna, et al., Role of ethylene diamine tetra-acetic acid (EDTA) in catheter lock solutions: EDTA enhances the antifungal activity of amphotericin B lipid complex against *Candida* embedded in biofilm, Int. J. Antimicrob. Agents 32 (2008) 515–518.

[11] M.C. Weijmer, M.A. van den Dorpel, P.J. Van de Ven, et al., Randomized, clinical trial comparison of trisodium citrate 30% and heparin as catheter-locking solution in hemodialysis patients, J. Am. Soc. Nephrol. 16 (2005) 2769–2777.

[12] Z. Liu, Y. Lin, Q. Lu, et al., *In vitro* and *in vivo* activity of EDTA and antibacterial agents against the biofilm of mucoid *Pseudomonas aeruginosa*, Infection 45 (2017) 23–31.

[13] A. Chauhan, D. Lebeaux, J.-M. Ghigo, et al., Full and broad-spectrum *in vivo* eradication of catheter-associated biofilms using gentamicin-EDTA antibiotic lock therapy, Antimicrob. Agents Chemother. 56 (2012) 6310–6318.

[14] Council of Europe, Gentamicin sulfate, in: Eur. Pharmacopoeia 88, 8.8, European Directorate for the Quality of Medicines & HealthCare, Strasbourg, France, 2016: 2525–2526.

[15] J.A. Ji, E. Ingham, J.Y. Wang, Effect of EDTA and methionine on preventing loss of viscosity of cellulose-based topical gel, AAPS PharmSciTech. 10 (2009) 678–683.

[16] A. Rudin, A. Healey, C.A. Phillips, et al., Antibacterial activity of gentamicin sulfate in tissue culture, Appl. Microbiol. 20 (1970) 989–990.

[17] N.D. Mullins, B.J. Deadman, H.A. Moynihan, et al., The impact of storage conditions upon gentamicin coated antimicrobial implants, J. Pharm. Anal. 6 (2016) 374–381.

[18] G.G. Christianson, T.A. Koski, A comparison of a disposable membrane filtration system with a direct inoculation system for the sterility testing of veterinary biologics, J. Biol. Stand. 11 (1983) 83–89.

[19] A.I. Al-Amoud, B.J. Clark, H. Chrystyn, Determination of gentamicin in urine samples after inhalation by reversed-phase high-performance liquid chromatography using pre-column derivatisation with o-phthalaldehyde, J. Chromatogr. B 25 (2002) 89–95.

[20] M.C. Chuong, J. Chin, J.W. Han, et al., High performance liquid chromatography of gentamicin sulfate reference standards and injection USP, Int. J. Pharm. Anal. 4 (2013) 25.

[21] P.J. Kuehl, S. De, B. Eppler, J. Marsters, et al., Development and validation of an HPLC assay for dual detection of gentamicin sulfate and leucine from a novel dry powder for inhalation, J. Anal. Bioanal. Tech. 3 (2012) 1–4.

[22] U.S. Pharmacopeial Convention, Gentamicin sulfate, in: U. S. Pharmacopoeia 37-NF32 US Pharmacopeial Conv., Rockville, USA, 2014: 3138–3139.

[23] K. Ruckmani, S.Z. Shaikh, P. Khalil, et al., A simple and rapid high-performance liquid chromatographic method for determining tobramycin in pharmaceutical formulations by direct UV detection, Pharm. Methods 2 (2011) 117–123.

[24] A.S. Kord, I. Tumanova, W.L. Matier, A novel HPLC method for determination of EDTA in a cataract inhibiting ophthalmic drug, J. Pharm. Biomed. Anal. 13 (1995) 575–580.

[25] E. Caudron, S. Baghriche, P. Prognon, et al., Simultaneous quantification of gentamicin and colistin sulfate in pharmaceuticals using ion-pairing and polarity gradient chromatography with low-UV detection, Chromatographia 76 (2013) 747–755.

[26] K. Stypulkowska, A. Blazewicz, Z. Fijalek, et al., Determination of gentamicin sulphate composition and related substances in pharmaceutical preparations by LC with charged aerosol detection, Chromatographia 72 (2010) 1225–1229.

[27] S.K. Branch, Guidelines from the International Conference on Harmonisation (ICH), J. Pharm. Biomed. Anal. 38 (2005) 798–805.

[28] G.A. Shabir, Validation of high-performance liquid chromatography methods for pharmaceutical analysis: Understanding the differences and similarities between validation requirements of the US Food and Drug Administration, the US Pharmacopeia and the International Conference on Harmonization, J. Chromatogr. A. 987 (2003) 57–66.

[29] M. Blessy, R.D. Patel, P.N. Prajapati, et al., Development of forced degradation and stability indicating studies of drugs—a review, J. Pharm. Anal. 4 (2014) 159–165.

[30] L.D. Sabath, J.I. Casey, P.A. Ruch, et al., Rapid microassay of gentamicin, kanamycin, neomycin, streptomycin, and vancomycin in serum or plasma, J. Lab. Clin. Med. 78 (1971) 457–463.

[31] J.M. Andrews, R. Wise, A comparison of the homogeneous enzyme immunoassay and polarization fluoroimmunoassay of gentamicin, J. Antimicrob. Chemother. 14 (1984) 509–520.

[32] S.A. Brown, D.R. Newkirk, R.P. Hunter, et al., Extraction methods for quantitation of gentamicin residues from tissues using fluorescence polarization immunoassay, J. Assoc. Off. Anal. Chem. 73 (1990) 479–483.

[33] V. Manyanga, O. Grishina, Z. Yun, et al., Comparison of liquid chromatographic methods with direct detection for the analysis of gentamicin, J. Pharm. Biomed. Anal. 45 (2007) 257–262.

[34] V. Manyanga, K. Kreft, B. Divjak, et al., Improved liquid chromatographic method with pulsed electrochemical detection for the analysis of gentamicin, J. Chromatogr. A 1189 (2008) 347–354.

[35] I. Clarot, P. Chaimbault, F. Hasdenteufel, et al., Determination of gentamicin sulfate and related compounds by high-performance liquid chromatography with evaporative light scattering detection, J. Chromatogr. A 1031 (2004) 281–287.

[36] N.C. Megoulas, M.A. Koupparis, Development and validation of a novel LC/ELSD method for the quantitation of gentamicin sulfate components in pharmaceuticals, J. Pharm. Biomed. Anal. 36 (2004) 73–79.

[37] A. Joseph, A. Rustum, Development and validation of a RP-HPLC method for the determination of gentamicin sulfate and its related substances in a pharmaceutical cream using a short pentafluorophenyl column and a charged aerosol detector, J. Pharm. Biomed. Anal. 51 (2010) 521–531.

[38] H. Curiel, W. Vanderaerden, H. Velez, et al., Analysis of underivatized gentamicin by capillary electrophoresis with UV detection, J. Pharm. Biomed. Anal. 44 (2007) 49–56.

[39] K. Vučićević-Prčetić, R. Cservenák, N. Radulović, Development and validation of liquid chromatography tandem mass spectrometry methods for the determination of gentamicin, lincomycin, and spectinomycin in the presence of their impurities in pharmaceutical formulations, J. Pharm. Biomed. Anal. 56 (2011) 736–742.

[40] J.F. Chissell, M. Freeman, J.S. Loran, et al., British pharmacopoeial gentamicin sulphate component ratio test by high-performance liquid chromatography. The effect of derivative breakdown on final result, J. Chromatogr. 369 (1986) 213–217.

[41] J.H. Albracht, M.S. de Wit, Analysis of gentamicin in raw material and in pharmaceutical preparations by high-performance liquid chromatography, J. Chromatogr. 389 (1987) 306–311.

[42] G. Wang, F.P. Tomasella, Ion-pairing HPLC methods to determine EDTA and DTPA in small molecule and biological pharmaceutical formulations, J. Pharm. Anal. 6 (2016) 150–156.

Original Research Article

Cytotoxic effect of *Rosa canina* extract on human colon cancer cells through repression of telomerase expression

Ibrahim Turan [a,b], Selim Demir [c,*], Kagan Kilinc [a], Serap Ozer Yaman [d], Sema Misir [d,e], Hanife Kara [d], Berna Genc [a], Ahmet Mentese [f], Yuksel Aliyazicioglu [d], Orhan Deger [d]

[a] *Department of Genetic and Bioengineering, Faculty of Engineering and Natural Sciences, Gumushane University, 29100 Gumushane, Turkey*
[b] *Medicinal Plants, Traditional Medicine Practice and Research Center, Gumushane University, 29100 Gumushane, Turkey*
[c] *Department of Nutrition and Dietetics, Faculty of Health Sciences, Karadeniz Technical University, 61080 Trabzon, Turkey*
[d] *Department of Medical Biochemistry, Faculty of Medicine, Karadeniz Technical University, 61080 Trabzon, Turkey*
[e] *Department of Biochemistry, Faculty of Pharmacy, Cumhuriyet University, 58140 Sivas, Turkey*
[f] *Program of Medical Laboratory Techniques, Vocational School of Health Sciences, Karadeniz Technical University, 61080 Trabzon, Turkey*

ARTICLE INFO

ABSTRACT

Rosa canina is a member of the genus *Rosa* that has long been used for medical objectives. Several studies have reported cytotoxic effects of different *Rosa* species, but there has been only limited investigation of the cytotoxic effect of *R. canina*. The purpose of the current study was to examine the potential effect of *R. canina* extract on cell viability, the cell cycle, apoptosis, and the expression of telomerase in human colon cancer (WiDr) cells. The cytotoxic effect of the extract was determined using MTT assay. The mechanism involved in the cytotoxic effect of the extract was then evaluated in terms of apoptosis and the cell cycle using flow cytometry. Mitochondrial membrane potential (MMP) was investigated using the fluorometric method, and expression levels of telomerase were studied using RT-PCR. *R. canina* extract exhibited a selective cytotoxic effect on WiDr cells compared with normal colon cells. The extract induced cell cycle arrest at the S phase and apoptosis via reduced MMP in WiDr cells. *R. canina* extract significantly repressed telomerase expressions at treatment times of 48 and 72 h in WiDr cells. Our results suggest that *R. canina* may have considerable potential for development as a novel natural product-based anticancer agent.

1. Introduction

Rosa canina is a member of the genus *Rosa* and the family *Rosaceae*. The genus *Rosa* contains more than 100 species widely spread over Asia, Europe, the Middle East, and North America [1,2].

Approximately 25% of all rose species are reported to grow in Turkey, especially in the regions of central and North-East Anatolia, and particularly in Gumushane and neighboring cities. *R. canina* contains many beneficial compounds, including vitamins, phenolic acids, proanthocyanidins, tannins, flavonoids, pentacyclic triterpenes, and minerals [1,3,4]. It exhibits numerous biological properties, such as antioxidant, anti-inflammatory, anti-ulcerogenic, anti-obesity, antidiabetic, diuretic, antimutagenic, anticarcinogenic, anti-arthritic, neuroprotective, and antimicrobial effects [3–6]. *R. canina* is one of the most commonly used medicinal plants in traditional medicine in both Western and Asian countries

for the treatment of colds, asthma, hemorrhoids, infections, chronic pains, arthritis, and inflammatory diseases [1,2,4]. The fruits of *R. canina* are consumed as a natural source of vitamin C in the forms of tea, snacks, jam, nectar, and dried pulp. There is also considerable interest in this species in various commercial spheres, especially the food, pharmaceutical, and cosmetic industries [2,3].

Cancer is a pathological condition characterized by excessive cell growth and deriving from loss of control over the cell cycle and/or decreased apoptosis [7]. Cancer cells exhibit characteristic features, such as avoidance of apoptosis, impaired cell cycle control, self-sufficiency in growth signaling, and telomerase activation [8,9]. Telomerase is a ribonucleoprotein consisting of human telomerase reverse transcriptase (hTERT) and human telomerase RNA (hTR) [8]. Its principal function is to synthesize telomeres using the RNA template instead of telomeric series lost during DNA replication in order to overcome the problem of end-replication [10]. Telomerase reactivation in the cell is believed to be associated with carcinogenesis and is a significant step in tumor immortalization. Telomerase is reported to be active in more than 85% of all tumors but is present at low or undetectable levels in

normal cells [8]. Telomerase plays an important role in the un-limited growth of cancer cells, and inhibition of telomerase activity potentially represents a highly selective target for the treatment of cancer [11].

Colon cancer is one of the most common types of cancers worldwide. While chemotherapy is one of the most widely used therapeutic strategies against colon cancer, it also has some limitations, such as normal cell toxicity and gradually increasing resistance in cancer cells. The discovery of new drugs for use in alternative strategies in cancer treatment is therefore highly desirable. Plants are regarded as very promising from this perspective, since they represent substantial sources of substances with various therapeutic uses. Most anticancer drugs are today produced from plants [12–14].

Various studies have investigated the cytotoxic effects of different *Rosa* species. Olsson et al. [15] demonstrated that ethanolic extract of rose-hip has a cytotoxic effect on human colon (HT-29) and breast (MCF-7) cancer cells, while Fujii et al. [16] reported that ethanolic extract of *R. canina* exhibits a cytotoxic effect on mouse melanoma cells by inhibiting tyrosinase activity. Zamiri-Akhlaghi et al. [17] reported that ethanolic extract of *R. damascena* has a concentration-dependent cytotoxic effect against human cervix cancer (HeLa) cells. Recently, Jiménez et al. [18] demonstrated that *R. canina* extracts exhibit antiproliferative effects on human colon cancer (Caco-2) cells by increasing the number of apoptotic cells and cell cycle arrest at the S phase. However, no studies have examined the relationship between telomerase and *R. canina* extract in any cancer cell lines. The objective of this study was therefore to determine the cytotoxic effect of acidified dimethyl sulfoxide extract of *R. canina* on colon cancer (WiDr) cells, coupled with the mechanism of action.

2. Experimental

2.1. Chemicals

Gentamicin and trypsin solutions were obtained from Biological Industries (Kibbutz Beit Haemek, Israel), Eagle's minimum essential medium (EMEM) from Lonza (Verviers, Belgium), and fetal bovine serum (FBS) from Biochrom (Berlin, Germany). All flow cytometry kits were purchased from Becton Dickinson (San Diego, CA, USA). All kits used for gene expression studies were purchased from Roche Diagnostics (Mannheim, Germany). The other principal chemicals used were obtained from Sigma (St. Louis, MO, USA).

2.2. Sample collection and extract preparation

Fully mature fruits of *R. canina* were harvested from Gumushane in the Eastern Anatolia region of Turkey. Samples were preserved in cool bags for transportation to the laboratory. These fruits were air-dried at 25 °C and converted into a fine powder using a blender and milling procedures. The fruit powder (1 g) was extracted with 20 mL of dimethyl sulfoxide (DMSO) plus 0.5% (v/v) hydrogen chloride (HCl) in a mechanical shaker (Shell Lab, Cornelius, OR, USA) in the dark for 24 h at 45 °C. The prepared 50 mg/mL stock acidified DMSO extract of *R. canina* was filtered with Whatman No. 1 filter paper and a 0.2 μm filter and then stored at −20 °C until used in further experiments.

2.3. Drug preparation and treatment

Cisplatin was dissolved in DMSO and used as a reference compound in cytotoxicity experiments due to its use in colon cancer treatment [19]. Final solvent concentrations of compounds were no higher than 0.5% in culture media in any experiment. That

concentration was not sufficient to affect cell morphology or viability.

2.4. Cell culture

Human colon adenocarcinoma (WiDr, ATCC-CCL-218) cancer and human colon normal epithelial cell lines (CCD 841 CoN, ATCC-CRL-1790) were supplied by the America Type Culture Collection (Manassas, VA, USA). Both cells were cultured in EMEM supplemented with 10% heat inactivated FBS and 1% antibiotic solution with a 5% CO_2 supply at 37 °C.

2.4.1. Cytotoxicity experiments

MTT assay with a 72 h treatment time was employed to measure the cytotoxic effects of *R. canina* extract and cisplatin on colon cancer and normal cells [20]. Briefly, cells were seeded into a 96-well cell culture plate at 1×10^4 cells per well. The cells were then treated with varying concentrations of *R. canina* extract (0–500 μg/mL) and cisplatin (0–10 μg/mL) for 72 h in a quadruplet manner. Subsequently, 10 μL of MTT dye (0.25 mg/mL) was placed inside each well. The crystals that emerged were then dissolved in DMSO. Finally, absorbance was measured at 570 nm with the help of a microplate reader (Molecular Devices Versamax, California, USA). Optical densities were employed to calculate percentage viabilities in treated cells compared to untreated control cells. Log-concentrations versus % cell viabilities were plotted with a logarithmic graph, which was then used to determine the IC_{50} values.

2.4.2. Flow cytometry analysis for cell cycle distribution

WiDr cells in the exponential growth phase were treated with 135, 270, 405 and 540 μg/mL concentrations of *R. canina* extract for 72 h, then harvested by trypsinization, and washed twice with buffer solution (containing sodium citrate, sucrose, and DMSO). After that procedure, 250 μL of trypsin buffer was added to each tube and incubated for 10 min. Next, 200 μL of trypsin inhibitor and RNase buffer was added to each tube and incubated for 10 min. Finally, 200 μL of cold PI stain solution was added to each tube and incubated for 10 min in the dark on ice. Data from 30,000 cells per sample were collected and analyzed on a flow cytometer (BD Accuri C6, MI, USA). The percentage of cells in cycle phases was determined using MODFIT 3.0 verity software. The results were finally compared with the untreated control cells.

2.4.3. Measurement of apoptosis using flow cytometry

WiDr cells in the exponential growth phase were treated with 135, 270, 405 and 540 μg/mL concentrations of *R. canina* extract for 72 h, then harvested by trypsinization, and washed twice with ice-cold PBS. The cells were then resuspended with 100 μL of the binding buffer. In the next stage, 5 μL of FITC Annexin V and 5 μL of propidium iodide (PI) were added to each tube and incubated for 10 min at room temperature in the dark. Finally, 400 μL of the binding buffer was added to each tube and data from 10,000 cells per sample were collected and analyzed on a flow cytometer (BD Accuri C6, MI, USA) within 1 h. The results were compared with the untreated control cells.

2.4.4. Determination of mitochondrial membrane potential (MMP)

$DiOC_6(3)$, a lipophilic cationic dye, was used to determine the changes in MMP in this study. Normally, it tends to remain in the mitochondria. A decrease in dye intensity indicates disruption of MMP [21]. Briefly, cells were seeded into a 96-well black-walled plate at 1×10^3 cells per well. The cells were then treated with different concentrations of *R. canina* extract (135–540 μg/mL) for 72 h. After treatment, the cells were washed twice with PBS and loaded with 10 nM $DiOC_6(3)$ for 30 min at 37 °C in the dark. Finally, the fluorescence measurement was performed on a

plate-reading fluorometer (Molecular Devices SpectraMax Paradigm Multi-Mode, Sunnyvale, CA, USA) with an excitation wavelength of 484 nm and an emission wavelength of 525 nm. Results were given as relative MMP compared to untreated control cells.

2.4.5. Gene expression analysis

Based on data from the cytotoxicity studies, the extract IC_{50} value (270 μg/mL) was used to investigate gene expression. WiDr cells were treated with this concentration of extract for 24, 48, and 72 h. After incubation, the cells were harvested for RNA isolation.

2.4.6. RNA isolation and RT-PCR

Total RNA isolation was performed using a highly pure RNA isolation kit in line with the manufacturer's recommmendations. RNA samples were converted to complementary DNA using a first strand cDNA synthesis kit as recommended by the manufacturer. A total of 100 ng/μL total RNA was employed for all reaction samples. Reaction compounds were incubated at 25 °C for 10 min, 50 °C for 60 min, and 85 °C for 5 min.

The RT-PCR method using UPL probes was employed to measure hTERT expression. hTERT and GAPDH amplicon dimensions were 60 and 127 bp, respectively. Forward and reverse primers of hTERT and GAPDH were 5′-CCCCGGTTTCTATAAATTGAGC-3′, 5′-CACCTTCCCCATGGTGTCT-3′, 5′-AGCCACGTCTCTACCTTGACA-3′, and 5′-CAGGTGAGCCACGAACTGT-3′, respectively. The reaction mixtures were incubated under the following conditions: pre-incubation 95 °C 10 min; amplification 95 °C 10 s 60 °C 30 s, 72 °C 1 s, 45 cycles and cooling 40 °C 30 s, in a Roche Light Cycler 480-II device (Rotkreuz, Switzerland). Measurements were calculated using an advanced relative quantification module with mRNA levels being compared against the negative control samples (cells with no test compound) following normalization to GADPH mRNA levels.

2.5. Statistical analysis

All experiments were performed at least three times, the results being expressed as mean ± standard deviation. Normal distribution was determined using the Kolmogorov-Smirnov test. One-way ANOVA was used to analyze intergroup differences. $p < 0.05$ was regarded as significant.

3. Results

R. canina extract exhibited selective cytotoxicity in the colon cancer cell line compared to normal colon cells (Table 1 and Fig. 1).

The results of the cell cycle analysis are presented in Fig. 2. All the concentrations of *R. canina* extract used (except for 135 μg/mL) significantly increased cell numbers at the S phase ($p = 0.0001$). Additionally, these concentrations of *R. canina* extract significantly reduced cell numbers at the G_0/G_1 phase compared to untreated cells ($p = 0.0001$).

The results of the Annexin V analysis are presented in Fig. 3. *R. canina* extract significantly reduced the number of viable cells and increased the number of late and early apoptotic cells compared to untreated cells in a dose-dependent manner ($p < 0.05$).

Table 1
Cytotoxic effects of test compounds and their IC_{50} values (μg/mL) ($n = 4$).

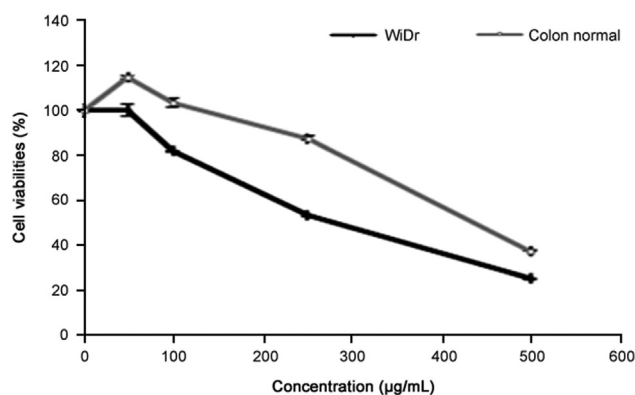| Test compound	WiDr cells	Colon normal cells
R. canina extract	270 ± 1.2	405.4 ± 3.7
Cisplatin	1.30 ± 0.02	2.86 ± 0.09

Fig. 1. The anti-growth effect using MTT assay after treatment with *R. canina* extract for 72 h against WiDr cells and colon normal cells ($n = 4$).
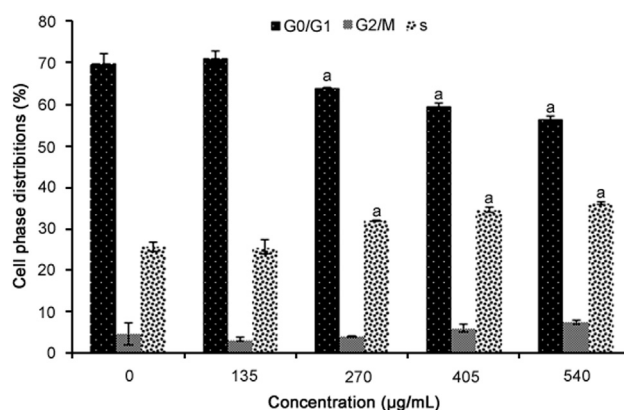

Fig. 2. Cell cycle analysis of WiDr cells treated for 72 h with *R. canina* extract at different concentrations ($n = 4$). ªRepresents significant results ($p < 0.05$) compared with untreated WiDr cells.
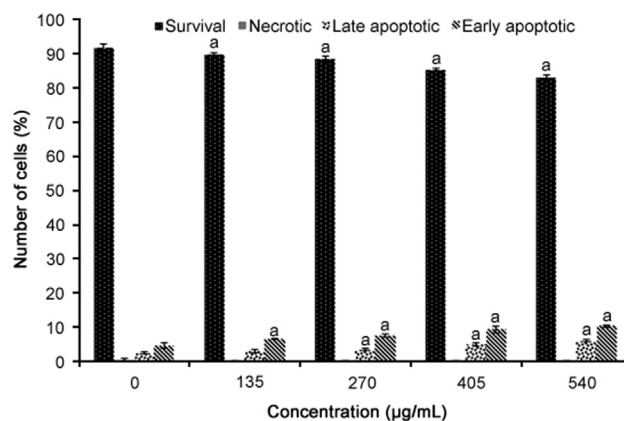

Fig. 3. Apoptosis analysis of WiDr cells treated with different concentrations of *R. canina* extract for 72 h using Annexin-V FITC and propidium iodide staining ($n = 4$). ªRepresents significant results ($p < 0.05$) compared with untreated WiDr cells.

MMP analysis results are presented in Fig. 4. All concentrations of *R. canina* extract significantly reduced the MMP in WiDr cells ($p = 0.001$). The percentage reductions in MMP caused by *R. canina* extract were 12.7%, 23.7%, 57.9%, and 62.9% for concentrations of 135, 270, 405 and 540 μg/mL of *R. canina* extract, respectively.
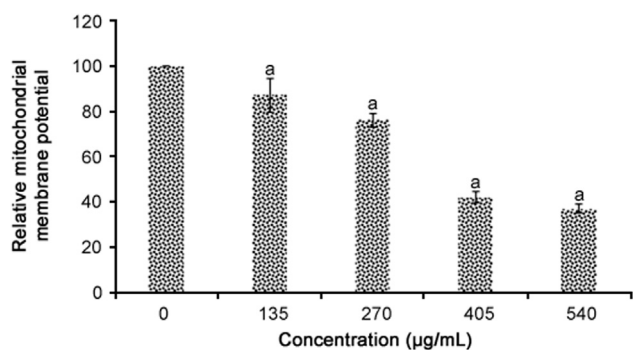
Fig. 4. DiOC$_6$ staining for *R. canina* extract-induced dissipation of mitochondrial membrane potential in WiDr cells ($n = 4$). ^{a}Represents significant results ($p < 0.05$) compared with untreated WiDr cells.
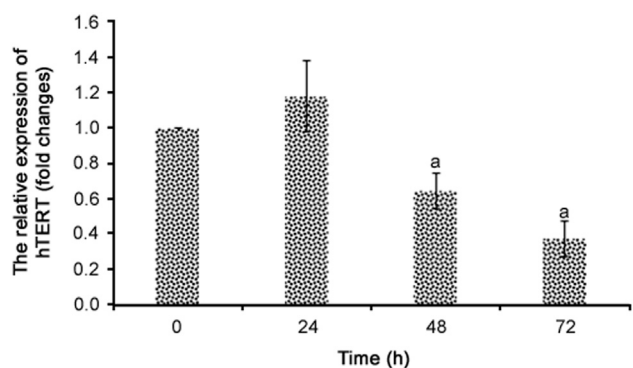

Fig. 5. Relative mRNA levels of hTERT after treatment with *R. canina* extract (270 µg/mL) at different treatment times ($n = 3$). ^{a}Represents significant results ($p < 0.05$) compared with negative control cells.

The IC$_{50}$ concentration (270 µg/mL) of *R. canina* extract significantly repressed hTERT expression at treatment times of 48 h and 72 h ($p < 0.05$) in colon cancer cells (Fig. 5). hTERT expression decreased by 36% and 63% after 48 and 72 h, respectively, compared to the negative control group. No statistically significant differences were regarded between the 48 and 72 h treatment groups ($p > 0.05$).

4. Discussion and conclusion

The use of plants to treat diseases is known as herbal medicine and is regarded as a part of traditional treatment. Traditional medicine with plants is thought to go back to very early times in human history [22]. Edible plants are rich in antioxidant molecules, such as vitamins, polyphenolic compounds and carotenoids. The fruits of *R. canina* have long been used for medical aims, and the biological functions of these fruits may be partly attributed to their phenolics and vitamin C contents [1,3].

Colon cancer is one of the leading causes of death in the USA and the second most common form of fatal cancer worldwide. Almost half of all patients diagnosed with colon cancer are reported to die. Fewer than 10% of patients of with metastatic colon cancer survive for more than 5 years. Surgical treatment, chemotherapy, radiotherapy or combinations of these are generally applied in cancers of the digestive system [13]. Chemotherapy is an effective means of treating several types of cancer, including colon cancer, but the cost represents an important public health problem in developing countries. In addition, gradual resistance developed in cancer cells to chemotherapeutic drugs and healthy cells being affected by them reduce the success levels of

chemotherapy [14]. New strategies are therefore required in order to solve these problems. More than 60% of anticancer drugs in use today are isolated from natural products of plant origin [23]. Natural product research for cancer treatment is therefore one of these new strategies due to its effectiveness against cancer cells and the fact that it is harmless to normal cells [12]. Although experimental studies have shown that phenolic compounds in particular exhibit anticancer properties, the entire mechanism involved is as yet unclear. The mechanisms that have been proposed in the context of the anticancer effect of phenolic compounds include their ability to scavenge free radicals, their ability to induce xenobiotic metabolism, their ability to regulate gene expression, and their ability to modulate DNA repair, apoptosis and cell signaling, such as cell replication and invasion [14]. However, the number of cytotoxicity studies performed with *Rosa* species is very limited [15–18]. The purpose of this study was therefore to determine the cytotoxic effect of *R. canina* extract in colon cancer cell lines, one of the most common forms of cancer worldwide, and to identify the probable mechanisms of action. In vitro analyses are first performed in determining the potential biological benefits of any compound. If positive results are obtained from that analysis, then in vivo studies are performed in the second stage [7]. The WiDr cell line is derived from a human colon carcinoma and is commonly used in cancer research involving in vitro colon cancer models [24,25]. This study was therefore planned on a colon cancer cell line (WiDr) under in vitro conditions. An effective and acceptable anticancer compound has to meet various criteria, including exhibiting no harmful effects on healthy cells [7]. Cytotoxicity experiments were therefore conducted in WiDr cells together with normal colon cells. In order to investigate the antiproliferative activity of *R. canina* extract, WiDr and colon normal cells were treated with different concentrations of extract for 72 h. *R. canina* extract exhibited reasonable selective cytotoxic effects against WiDr cells compared with normal colon cells. In terms of cytotoxic activity, Lee et al. [26] demonstrated that methanolic extracts of *R. rugosa* stem act as anti-prostate cancer agents, while Olsson et al. [15] demonstrated that ethanolic extract of rose hip has a cytotoxic effect on HT-29 and MCF-7 cells. Tumbas et al. [27] reported that quercetin, ellagic acid and vitamin C are the most abundant antioxidant compounds in *R. canina*. However, only vitamin C-free extract, which is rich in polyphenols, exhibits cytotoxic activity in three human cancer cell lines (HeLa, MCF-7 and HT-29 with IC$_{50}$ values of approximately 81, 248 and 364 µg/mL, respectively). They concluded that vitamin C and flavonoids are responsible for the antioxidant activity of *R. canina*, while only polyphenols contribute to its cytotoxic activity. Olech et al. [28] reported that teas and tinctures prepared from *R. rugosa* exhibit cytotoxic effects against human ovarian, lung, cervix, and breast cancer cells without harming human skin fibroblast cells. In another study, Guimarães et al. [29] showed that methanolic extract of *R. canina* from Portugal exhibits cytotoxic effect against human lung, colon, cervix and liver cancer cells, while no effect was observed on breast cancer cells. Artun et al. [30] recently reported that methanolic extract of *R. damascena* exhibits selective cytotoxic effects on human cervix cancer (HeLa) cells compared to normal kidney epithelial (Vero) cells. Additionally, not only the extracts of *Rosa* species but also various compounds isolated from *Rosa* species (such as bee pollen polysaccharides, phenylethanoids, and essential oils) have been reported to exhibit cytotoxic effects in colon, leukemia, liver, breast and oropharyngeal epidermoid carcinoma cell lines [13,31,32].

Loss of control of the cell cycle is reported to play a role in the development of cancer. Therefore, halting the cycle of cancer cells at any stage is one of the basic aims in the approach to treating cancer [9]. We performed cell cycle analysis to assess population cell death and to determine whether *R. canina* extract can induce

cell cycle arrest. As shown in Fig. 2, *R. canina* extract induced significant dose-dependent accumulation of cells at the S phase. Consistent with our results, Jiménez et al. [18] reported that *R. canina* extracts arrested the cell cycle of Caco-2 cells at the S phase. Cagle et al. [33] demonstrated that an 80% methanolic extract of *R. canina* exhibited antiproliferative effects on human glioblastoma cells by increasing cell cycle arrest at the G_2/M phase and blocking both the MAPK and AKT signaling mechanisms. No findings were determined concerning apoptosis in that study.

Attenuate or extinct apoptosis capacity has been identified in a range of cancer types. Raising apoptosis levels through the use of different agents is therefore another approved target mechanism component of anticancer strategies [7]. We therefore examined the capability of varying concentrations of *R. canina* extract to reduce the growth of WiDr cells by increasing levels of apoptosis using the Annexin V/propidium iodide double-staining assay. Our results showed that *R. canina* extract significantly induced cell apoptosis in a concentration-dependent manner (Fig. 3). Mitochondrial depolarization is a major component of apoptosis induction [9]. We therefore investigated alterations in MMP following *R. canina* extract treatment. As shown in Fig. 4, *R. canina* extract significantly induced loss of MMP in a concentration-dependent manner. These results suggest that the type of cell death induced by *R. canina* extract is mitochondria-dependent apoptosis. Several studies have investigated the apoptotic properties of *Rosa* species in many different cancer cells. Khatib et al. [34] reported that essential oil from *R. damascena* exhibits cytotoxic effects against a gastric cancer cell line by inducing apoptosis. Erguven et al. [35] demonstrated that ethanolic extract of *R. agrestis* exhibits concentration-dependent cytotoxic effects on human endometrial adenocarcinoma cells by inducing apoptotic cell death. Jiménez et al. [18] reported that *R. canina* extracts have cytotoxic effects on Caco-2 cells by increasing the number of apoptotic cells.

Telomerase activation is one of the characteristic features of cancer cells [8,11]. Telomerase is reported to be active in more than 85% of all tumors, but it is present at low or undetectable levels in normal cells [8]. Telomerase plays an important role in the unlimited proliferation of cancer cells, so inhibition of telomerase activity is regarded as a highly selective target for cancer treatment [11]. Moreover, increased telomerase expression has been reported in several types of epithelial cancer, including colon cancer [36]. To the best of our knowledge, no previous studies have investigated the effect of *R. canina* extract on telomerase expression in any human cancer cells. Our findings show that the IC_{50} (270 μg/mL) concentration of *R. canina* extract significantly repressed hTERT expression at treatment times of 48 and 72 h. Inhibition of telomerase in cancer cells is known to result in induction of cell death. However, there is increasing evidence that telomerase plays a key role in apoptosis regulation by changing MMP or metal homeostasis in mitochondria in a manner unrelated to its classic role [37]. Additionally, global expression profiling studies have stated that hTERT expression affects 284 genes, the function of which involves a wide range of cellular processes, including cell cycle regulation, metabolism, differentiation, apoptosis, and cell signaling [38]. Suppression of hTERT expression also causes elevated p53 and p21 transcription, and p21 mediates p53-dependent growth arrest in cancer cells [37]. Polyphenols are also capable of downregulating hTERT expression in various cancer cell lines. This confirms previous reports showing such downregulation with some polyphenols (resveratrol, apigenin, baicalein, chrysin, galangin, and kaempferol) in colon and esophageal squamous cancer cells [11,39]. We therefore think that downregulation of telomerase by *R. canina* extract (rich in polyphenols) may contribute to its apoptotic and antiproliferative activity in WiDr cells.

One limitation of this research is that in vitro studies cannot be extrapolated to potential activity in vivo. Further studies are now necessary to understand the exact interaction of the involved signaling pathways.

Conflicts of interest

The authors declare that there are no conflicts of interest.

Acknowledgments

References

[1] S. Ercisli, Chemical composition of fruits in some rose (*Rosa* spp.) species, Food Chem. 104 (2007) 1379–1384.

[2] M. Elmastas, A. Demir, N. Genç, et al., Changes in flavonoid and phenolic acid contents in some Rosa species during ripening, Food Chem. 235 (2017) 154–159.

[3] N. Demir, O. Yildiz, M. Alpaslan, et al., Evaluation of volatiles, phenolic compounds and antioxidant activities of rose hip (*Rosa* L.) fruits in Turkey, Food Sci. Technol. 57 (2014) 126–133.

[4] B.C. Cheng, X.Q. Fua, H. Guo, et al., The genus Rosa and arthritis: overview on pharmacological perspectives, Pharmacol. Res. 114 (2016) 219–234.

[5] C. Chrubasik, B.D. Roufogalis, U. Müller-Ladner, et al., A systematic review on the *Rosa canina* effect and efficacy profiles, Phytother. Res. 22 (2008) 725–733.

[6] I. Mármol, C. Sánchez-de-Diego, N. Jiménez-Moreno, et al., Therapeutic applications of rose hips from different Rosa species, Int. J. Mol. Sci. 18 (2017) E1137, < http://dx.doi.org/10.3390/ijms18061137 > .

[7] S. Demir, Y. Aliyazicioglu, I. Turan, et al., Antiproliferative and proapoptotic activity of Turkish propolis on human lung cancer cell line, Nutr. Cancer 68 (2016) 165–172.

[8] S. Saleh, A.K. Lam, Y.H. Ho, Real-time PCR quantification of human telomerase reverse transcriptase (hTERT) in colorectal cancer, Pathology 40 (2008) 25–30.

[9] S. Demir, I. Turan, Y. Aliyazicioglu, et al., *Morus rubra* extract induces cell cycle arrest and apoptosis in human colon cancer cells through endoplasmic reticulum stress and telomerase, Nutr. Cancer 69 (2017) 74–83.

[10] A.K. Khaw, J.W. Yong, G. Kalthur, et al., Genistein induces growth arrest and suppresses telomerase activity in brain tumor cells, Genes Chromosomes Cancer 51 (2012) 961–974.

[11] R.G. Jayasooriya, S.H. Kang, C.H. Kang, et al., Apigenin decreases cell viability and telomerase activity in human leukemia cell lines, Food Chem. Toxicol. 50 (2012) 2605–2611.

[12] H.M. dos Santos Júnior, D.F. Oliveira, D.A. de Carvalho, et al., Evaluation of native and exotic Brazilian plants for anticancer activity, J. Nat. Med. 64 (2010) 231–238.

[13] M. Rezaie-Tavirani, S. Fayazfar, S. Heydari-Keshel, et al., Effect of essential oil of *Rosa damascena* on human colon cancer cell line SW742, Gastroenterol. Hepatol. Bed Bench 6 (2013) 25–31.

[14] L.S. Rosa, N.J.A. Silva, N.C.P. Soares, et al., Anticancer properties of phenolic acids in colon cancer– a review, J. Nutr. Food Sci. 6 (2016) 468, < http://dx.doi.org/10.4172/2155-9600.1000468 > .

[15] M.E. Olsson, K.E. Gustavsson, S. Andersson, et al., Inhibition of cancer cell proliferation *in vitro* by fruit and berry extracts and correlations with antioxidant levels, J. Agric. Food Chem. 52 (2004) 7264–7271.

[16] T. Fujii, K. Ikeda, M. Saito, Inhibitory effect of rose hip (*Rosa canina* L.) on melanogenesis in mouse melanoma cells and on pigmentation in brown guinea pigs, Biosci. Biotechnol. Biochem. 75 (2011) 489–495.

[17] A. Zamiri-Akhlaghi, H. Rakhshandeh, Z. Tayarani-Najaran, et al., Study of cytotoxic properties of *Rosa damascena* extract in human cervix carcinoma cell line, Am. J. Phys. 1 (2011) 74–77.

[18] S. Jiménez, S. Gascón, A. Luquin, et al., *Rosa canina* extracts have antiproliferative and antioxidant effects on Caco-2 human colon cancer, PLoS One 11 (2016) e0159136, <http://dx.doi.org/10.1371/journal.pone.0159136>.

[19] L. Svihálková-Sindlerová, V. Foltinová, A. Vaculová, et al., LA-12 overcomes confluence-dependent resistance of HT-29 colon cancer cells to Pt (II) compounds, Anticancer Res. 30 (2010) 1183–1188.

[20] T. Mosmann, Rapid colorimetric assay for cellular growth and survival: application to proliferation and cytotoxicity assays, J. Immunol. Methods 65 (1983) 55–63.

[21] J. Jakubowicz-Gil, E. Langner, D. Badziul, et al., Apoptosis induction in human glioblastoma multiforme T98G cells upon temozolomide and quercetin treatment, Tumor Biol. 34 (2013) 2367–2378.

[22] S.A. Sargin, E. Akçicek, S. Selvi, An ethnobotanical study of medicinal plants used by the local people of Alaşehir (Manisa) in Turkey, J. Ethnopharmacol. 150 (2013) 860–874.

[23] A. Latif, H.M. Amer, M.E. Hamad, et al., Medicinal plants from Saudi Arabia and Indonesia: in vitro cytotoxicity evaluation on Vero and Hep-2 cells, J. Med. Plants Res. 8 (2014) 1065–1073.

[24] I. Turan, S. Demir, S. Misir, et al., Cytotoxic effect of Turkish propolis on liver, colon, breast, cervix and prostate cancer cell lines, Trop. J. Pharm. Res. 14 (2015) 777–782.

[25] A. Setiawati, H. Immanuel, M.T. Utami, The inhibition of Typhonium flagelliforme Lodd. Blume leaf extract on COX-2 expression of WiDr colon cancer cells, Asian Pac. J. Trop. Biomed. 6 (2016) 251–255.

[26] Y.H. Lee, M.G. Jung, H.B. Kang, et al., Effect of anti-histone acetyltransferase activity from Rosa rugosa Thunb. (Rosaceae) extracts on androgen receptor-mediated transcriptional regulation, J. Ethnopharmacol. 118 (2008) 412–417.

[27] V.T. Tumbas, J.M. Canadanović-Brunet, D.D. Cetojević-Simin, et al., Effect of rosehip (Rosa canina L.) phytochemicals on stable free radicals and human cancer cells, J. Sci. Food Agric. 92 (2012) 1273–1281.

[28] M. Olech, R. Nowak, R. Los, et al., Biological activity and composition of teas and tinctures prepared from Rosa rugosa Thunb, Cent. Eur. J. Biol. 7 (2012) 172–182.

[29] R. Guimarães, L. Barros, R.C. Calhelha, et al., Bioactivity of different enriched phenolic extracts of wild fruits from Northeastern Portugal: a comparative study, Plant Foods Hum. Nutr. 69 (2014) 37–42.

[30] F.Tugba Artun, A. Karagoz, G. Ozcan, et al., In vitro anticancer and cytotoxic activities of some plant extracts on HeLa and Vero cell lines, J. BUON 21 (2016) 720–725.

[31] X.M. Gao, L.D. Shu, L.Y. Yang, et al., Phenylethanoids from the flowers of Rosa rugosa and their biological activities, Bull. Korean Chem. Soc. 34 (2013) 246–248.

[32] B. Wang, Q. Diao, Z. Zhang, et al., Antitumor activity of bee pollen polysaccharides from Rosa rugosa, Mol. Med. Rep. 7 (2013) 1555–1558.

[33] P. Cagle, O. Idassi, J. Carpenter, et al., Effect of rosehip (Rosa canina) extracts on human brain tumor cell proliferation and apoptosis, J. Cancer Ther. 3 (2012) 534–545.

[34] H. Khatib, M. Rezaei-Tavirani, S.H. Keshel, et al., Flow cytometry analysis of Rosa damascena effects on gastric cancer cell line (MKN45), Iran. J. Cancer Prev. 6 (2013) 30–36.

[35] M. Erguven, S. Kultur, N. Ozsoy, Anti-proliferative effect of Rosa agrestis on endometrium cancer cells in vitro, Int. J. Focus. Eng. Res. 1 (2015) 17–23.

[36] L. Boldrini, P. Faviana, S. Gisfredi, et al., Evaluation of telomerase mRNA (hTERT) in colon cancer, Int. J. Oncol. 21 (2002) 493–497.

[37] Y. Cong, J.W. Shay, Actions of human telomerase beyond telomeres, Cell Res. 18 (2008) 725–732.

[38] S.D. Perrault, P.T. Hornsby, D.H. Betts, Global gene expression response to telomerase in bovine adrenocortical cells, Biochem. Biophys. Res. Commun. 335 (2005) 925–936.

[39] M.P. Fuggetta, G. Lanzilli, M. Tricarico, et al., Effect of resveratrol on proliferation and telomerase activity of human colon cancer cells in vitro, J. Exp. Clin. Cancer Res. 25 (2006) 189–193.

Original Research Article

Evaluation of naproxen-induced oxidative stress, hepatotoxicity and *in-vivo* genotoxicity in male Wistar rats

Mir Hilal Ahmad [a,b], Mahino Fatima [a,b], Mobarak Hossain [b], Amal Chandra Mondal [a,*]

[a] *School of Life Sciences, Jawaharlal Nehru University (JNU), New Delhi 110067, India*
[b] *Interdisciplinary Brain Research Centre, Faculty of Medicine, Aligarh Muslim University, Aligarh, India*

A B S T R A C T

Naproxen (NP), a nonsteroidal anti-inflammatory drug (NSAID), is used for the treatment of common pain, inflammation and tissue damage. Genotoxicity testing of NP is of prime importance as it represents the largest group of drugs to which humans are exposed. Not many genotoxic studies are reported on NP; therefore, the present study investigated the detailed genotoxic and oxidative stress properties of NP. Male Wistar rats were administered NP orally at the doses of 38.91 and 65.78 mg/kg body weight for 14 days. Reduced glutathione (GSH), superoxide dismutase (SOD), catalase (CAT) and lipid peroxidation (LPO) activities/levels were measured in the liver, kidney and brain tissues. The aspartate amino-transferase (AST), alanine aminotransferase (ALT), alkaline phosphatase (ALP) activities, and total bilirubin (TBIL) levels were measured in the liver tissues. Micronucleus frequency (micronucleus test MNT) and DNA damage (comet assay) were performed in the bone marrow cells and leukocytes, respectively. The results showed that NP treatment decreased the GSH levels and increased the SOD, CAT, LPO, ALT, AST, ALP and TBIL activities/levels compared to the control ($p < 0.05$). Results of MNT showed an in-creased micronucleus induction and comet assay showed a significant increase in DNA damage in the NP treated animals ($p < 0.05$). Treatment of NP resulted in the biochemical imbalance and induced oxida-tive stress that deteriorated the integrity of the cells, which caused significant damage to the genetic material and affected liver function in male Wistar rats. Therefore, NP is a potential genotoxic agent that induces genotoxicity and oxidative stress.

© 2018 Xi'an Jiaotong University. Production and hosting by Elsevier B.V. This is an open access article under the CC BY-NC-ND license (http://creativecommons.org/licenses/by-nc-nd/4.0/).

1. Introduction

NP(S)−6-(Methoxy-α-methyl-2-naphthalene acetic acid), the propionic acid derivative, is a non-steroidal anti-inflammatory drug (NSAID), widely used for the treatment of primary dysme-norrhoea, rheumatoid arthritis, osteoarthritis, ankylosing, tendi-nitis, bursitis, acute gout and juvenile arthritis [1,2]. The main mechanism of action of NP is the inhibition of COX-dependent synthesis of proinflammatory algogenic prostaglandins by in-hibiting cyclooxygenase (COX-1 and COX-2) activity [3]. NSAIDs generate free radicals resulting in the generation of reactive oxy-gen species (ROS) [4].

ROS generation induces oxidative stress and is associated with cell death [4]. Oxidative stress has been implicated as a general me-chanism in the toxicity of many NSAIDs [5]. Recent studies have re-ported that NSAIDs induce ROS production in cells [6] and elicit and/

or contribute to oxidative stress [7,8]. NSAIDs have been associated with liver injury; the mechanism is thought to be immunological idiosyncrasy [9,10]. ROS produced in the cells results in error-prone DNA repair and increased susceptibility to apoptosis, which can all lead to cytotoxic, mutagenic, or carcinogenic events [11].

Genotoxic studies on NP are rather scarce, and there is very little information on the potential genotoxic effects of NP despite its wide range of applications, which is mentioned by another author as well [12]. Nevertheless, it has been reported that NP can alter the biochemical biomarkers and genetic materials [13]. Pre-vious studies have reported a weak or no genotoxic effect of NP, employing either one or two parameters to assess the genotoxicity of NP. Further studies on this drug with additional factors are worth performing. In this milieu, a detailed study employing genotoxic and biochemical biomarkers in different organs was conducted in order to determine the possible organ-specific oxi-dative stress potential, hepatotoxicity and genotoxicity of NP. This will help to analyze its safety and efficacy, and furthermore can be interpreted and/or extended to the assessment of health risk to the humans. The set of tests used in this study can be considered as a

reliable biomarker for the evaluation of NSAIDs toxicities in humans.

2. Materials and methods

2.1. Test animals

The study was conducted after obtaining Institutional Animal Ethical Committee's clearance. All protocols and experiments were conducted in strict compliance with ethical principles and guidelines provided by CPCSEA, New Delhi, India, after approval of Institutional Animal Ethics Committee (IAEC), Central Animal House Jawaharlal Nehru Medical College, Aligarh Muslim University, Aligarh (U.P), Registration No 401/RO/c/2001/CPCSEA. Male rats (Wistar strains), 8–10 weeks old, weighing 180 ± 30 g, were brought to the laboratory one month before the start of the experiment for acclimatization to the laboratory conditions. Rats were housed in 3 different groups in separate cages, maintained under conditions of 12 h dark/light cycle under conditions of constant temperature ($22 \pm 2\,°C$) and humidity (60% – 70%). Under standard laboratory conditions, the animals were allowed to access food and water ad libitum.

2.2. Test drug

The test drug used in the present study was NP, an NSAID. NP was procured from Sigma Chemicals Co. (USA). It was dissolved in DMSO and orally administered to the animals by oral gavage method. The administered DMSO concentrations did not cause any toxicity or affect the viability of the animals.

2.3. Experimental design

Rats were divided into 3 experimental groups: control, Treatment I, and Treatment II groups (6 rats/group). The control was administered with 10% dimethyl sulphoxide (75 μL DMSO/kg b.wt) for 14 days. Treatment I group was administered with 1/8th (38.91 mg/kg b.wt) of LD_{50} of NP for 14 days. Treatment II group was administered with 1/4th (65.78 mg/kg b.wt) of LD_{50} of NP for the same duration. Rats were sacrificed by cervical dislocation, immediately dissected to obtain the bone marrow, liver, kidney and brain tissues. These tissues were utilized for biochemical estimations of GSH, SOD, CAT and LPO activities/levels. Liver function parameters such as AST, ALT, ALP activities and TBIL level were determined in the liver tissues. For genotoxic studies, bone marrow was used for micronucleus test (MNT), and leukocytes for comet assay (single cell gel electrophoresis).

2.4. Statistical analysis

All the data were subjected to statistical analysis. The values were expressed as mean $\pm$ SE. Statistical analysis was performed by one-way analysis of variance (ANOVA) followed by Tukey multiple comparison tests. p values < 0.05 were considered as significant.

2.5. Biochemical assays

Biochemical assays were conducted for determination of nonenzymatic (GSH), enzymatic (SOD, CAT) and oxidative stress (LPO) biomarkers. For the estimation of biochemical parameters, tissues were homogenized and centrifuged to separate the post-mitochondrial fraction from homogenate. The tissues were homogenized in 0.1 M phosphate buffer, pH 7.4, to obtain the 10% homogenates using a Potter-Elvehjem homogenizer, 6–8 strokes at medium speed. During this operation, the samples were kept under ice. Homogenates were centrifuged at 10,000 rpm for 20 min at 4 °C. The sediments consisted of primary mitochondrial pellets and the supernatants were kept at $-20\,°C$ until further analysis. Post mitochondrial supernatant (PMS) was used for the estimation of various biochemical analyses. Protein content in various samples was estimated by the method described by Lowry et al. [14] with bovine serum albumin (BSA) as a protein standard.

2.5.1. Nonenzymatic antioxidants

GSH was studied as a nonenzymatic antioxidant. Tissue-reduced glutathione level was estimated as total acid soluble sulf-hydryl concentrations colorimetrically at 480 nm using Ellman's reagent dithiobis 2- nitrobenzoic acid (DTNB) as per the procedure modified by Jollow et al. [15]. PMS was precipitated with sulpho-salicylic acid (4.0%) in the ratio of 1:1. The samples were kept at 4 °C for 1 h and then subjected to centrifugation at 4000 rpm for 15 min at 4 °C. The assay mixture contained 0.4 mL supernatant, 2.2 mL of 0.1 M sodium phosphate buffer (pH 7.4) and 0.4 mL DTNB making a total volume of 3 mL. The optical density of reaction product was read immediately at 412 nm on a spectrophotometer and results were calculated using a molar extinction coefficient of 1.36×10^4 M^{-1} cm^{-1} and were expressed as μmoles/gram tissue. 2.6 mL phosphate buffer and 400 μL DTNB were taken as blank.

2.5.2. Enzymatic antioxidants

SOD and CAT together are enzymatic antioxidants providing first line defense against free radicals in tissues. The activities of both the enzymes were calculated by standard techniques.

2.5.2.1. Estimation of SOD activity. SOD activity was measured according to the procedure described by Misra and Fridovich [16]. The assay mixture consisted of 0.8 mL of glycine buffer (50 mM, pH 10.4), 0.2 mL of supernatant (prepared in glycine buffer) and 20 μL of epinephrine in a final volume of 1.02 mL. SOD activity can be measured kinetically at 480 nm. The activity was measured indirectly by the oxidized product of epinephrine, i.e. adrenochrome. SOD activity was expressed as nmol of (-) epinephrine protected from oxidation by the sample compared with the corresponding reading in the blank. The activity was calculated by using its extinction coefficient (ε) 4.02×10^3 M^{-1} cm^{-1}, and expressed as nmoles of epinephrine protected from oxidation/min/mg protein.

2.5.2.2. Determination of CAT activity. CAT activity was estimated by using the method of Clairborne [17] with slight modifications. 1.95 mL of phosphate buffer (pH 7.4) was taken, and 1.0 mL of hydrogen peroxide and 50 μL of PMS were added in a 3 mL cuvette. The total volume for the assay was 3 mL. Optical density (OD) was taken via kinetic method at 240 nm in a spectrophotometer. The activity was calculated by using its extinction coefficient (ε) 39.6 M^{-1} cm^{-1}, and expressed as μmoles of H_2O_2 consumed/min/mg protein.

2.5.3. Oxidative stress

LPO occurs due to tissue exposure to free radicals and this biomarker for oxidative stress was assessed.

LPO was determined by the method of Mihara and Uchiyama [18] with slide modifications. Briefly, 0.25 mL of tissue PMS was mixed with 25 μL of 10 mM butylated hydroxytoluene (BHT). 3 mL of phosphoric acid (1%) and 1 mL of 0.67% thiobarbituric acid (TBA) were added and the reaction mixture was incubated at 95 °C for 1 h. The absorbance was measured at 535 nm. The level of LPO was expressed as μmoles of thiobarbituric acid reactive substance (TBARS) formed/g tissue using a molar extinction coefficient of 1.56×10^5 M^{-1} cm^{-1}.

2.6. Liver function test

Biochemical indices of liver function determinants include AST, ALT, ALP activities and TBIL level. The liver function test was performed in the 10% rat liver homogenate. Commercially available diagnostic test kits were used for these tests. ALT and AST activities were determined according to the method described by Reitman and Frankel [19]. The method was standardized with Kinetic Method (Standard Karmen Unit assay) for accuracy and the absorbance was taken at 505 nm. TBIL level was determined by the method described by Cherian et al. [20]. The absorbance of the color was measured at 546 nm (546 and 630 nm in bichromatic mode) which is directly proportional to the concentration of TBIL in the sample. The ALP activity was determined by the method of Kind and King [21]. The OD was measured at 510 nm.

2.7. Genotoxic assessments

Free radicals affect the genetic constituents of tissue. Detailed assays, to assess clastogenic (disruption or breakages of chromosomes), aneugenic effects and DNA strand-damaging effects because of oxidative stress, were assessed.

2.7.1. MNT

micronucleus (MN) frequency in erythrocytes was evaluated according to the method described by Schmid [22]. Both femurs were extracted from the test animals and cleared off from muscular tissues. The bone was cut open and the marrow was flushed out with 5% fetal bovine serum (FBS). The solution obtained was evenly suspended. The solution was kept for 5 min at room temperature, the supernatant was discarded and pellet was saved. The sediment was mixed with a pipette, and a small drop of cell suspension was dropped at the one end of a clean dry slide and evenly smeared and finally air dried. The staining procedure followed a combination of May-Gruenwald and Giemsa staining in succession: the slides were first covered with undiluted May- Gruenwald solution for 3 min and replaced by dilute (1:1) May-Gruenwald solution with distilled water for 2 min, followed by Giemsa staining in Giemsa for 5 min. The slides were rinsed and dried, treated with xylene and mounted in dibutylphathalate xylene (DPX). All the slides were coded and scored by a single observer for analysable MN. A total number of 2000 erythrocytes were examined for each group under a light microscope (Nikon Eclipse E200), with oil immersion at $400 \times$ magnification. Scoring of micronuclei was performed on randomized and coded slides. The MN frequency was determined as follows:

MN frequency = (No. of cells containing MN) (1000) / Total No. of cells counted.

2.7.2. Comet assay

DNA damage was assessed using an alkaline comet assay as per as the method described by Singh et al. [23] with slight modifications. All of the comet assay experiment was performed under dim light conditions to avoid additional DNA damage. Cells were homogenized with PBS-CMF, 20 mM EDTA, pH 7.4 and filtered through a 100 μm mesh strainer to get cell suspension. 2 mL PBS-CMF was added to the cell suspension, followed by centrifugation at 2000 rpm at 4 °C for 10 min. The cell pellet was collected and resuspended in PBS-CMF. The cell viability test was performed using the Trypan blue exclusion method by Anderson et al. [24] and samples showing viability 80% were considered for comet assay. The cells were suspended in 0.5% low melting agarose (LMPA) and overlaid on slides precoated with a fine layer of 1.25% normal melting agarose (NMPA). The third layer of 0.75% LMPA was poured onto the slides. Slides were immersed in lysing solution (25 M NaCl, 100 mM EDTA, 10 mM Trizma base, 0.2 mM NaOH,

1% Triton X-100 and DMSO, pH 10) for 1 h at 4 °C to lyse cells. The slides were later immersed in chill electrophoresis buffer (300 mM NaOH, 1 mM EDTA, pH > 13) for 20 min to allow DNA unwinding, followed by electrophoresis at 25 V and 300 mA current in the same buffer for 30 min. Following electrophoresis, slides were neutralized in neutralizing buffer (0.4 M Tris buffer, pH 7.5). The slides were dried and stained with ethidium bromide. Photographs were obtained at $400 \times$. A total number of 300 cells were scored per group, and 50 cells per replicate were analyzed with Cometscore™software (version 1.5, TriTek Corporation, Sumerduck). The degree of DNA damage was represented as percent DNA in the tail.

3. Results

3.1. Non-enzymatic antioxidant

GSH level decreased significantly in the liver, kidney and brain tissues in the treatment groups, when compared with the control. The trend of the decrease in GSH level of liver, kidney and brain tissues of treatment groups compared to the control is given in Fig. 1.

Brain (% change 79.71% − 40.73%), showed a maximum depletion of GSH level in the treatment groups with respect to the control followed by the liver (% change 73.33% − 54.14%). Kidney (% change 80.64% − 64.51%) showed the least decline in GSH level in the treatment groups compared to the control. The percent change was calculated as the ratio of decrease in the GSH level between the treatment groups and the control.

3.2. Enzymatic antioxidants

3.2.1. SOD

SOD activity increased significantly in the liver, kidney and brain tissues. Trends of increase in SOD activities of liver, kidney and brain tissues in the treatment groups compared to the control given in Fig. 2.

Brain (% induction 233.43%–317.65%) showed a maximum increase in SOD enzyme activity in the treatment groups with respect to the control followed by the liver (% induction 145.07%–187.111%). Kidney (% induction 149.95%–177.12%), showed the least increased SOD activity in the treatment groups compared to the control.
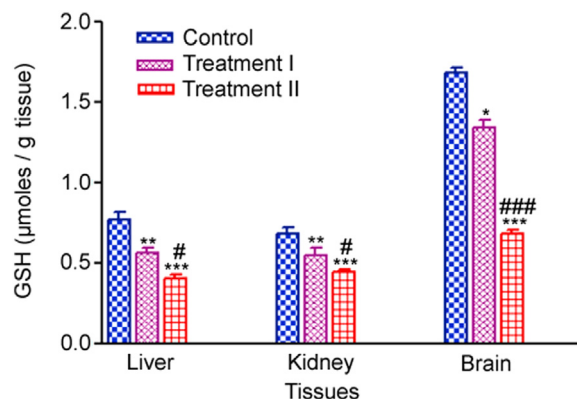

Fig. 1. Tissue-specific GSH (μmoles/g tissue) measured after 14 days oral administration of NP in Treatment I (38.91mg/ kg b.wt) and Treatment II (65.78 mg/kg b. wt) groups, and the control (75 μL DMSO/kg b.wt). Values are Mean $\pm$ SE ($n = 6$). Analysis of variance (One-way ANOVA) followed by Tukey test. Significant differences were indicated by $^{*}p < 0.05$, $^{**}p < 0.01$ and $^{***}p < 0.001$, when compared with the control while $^{#}p < 0.05$ and $^{###}p < 0.01$ were used to show the significant difference between the treatment groups.
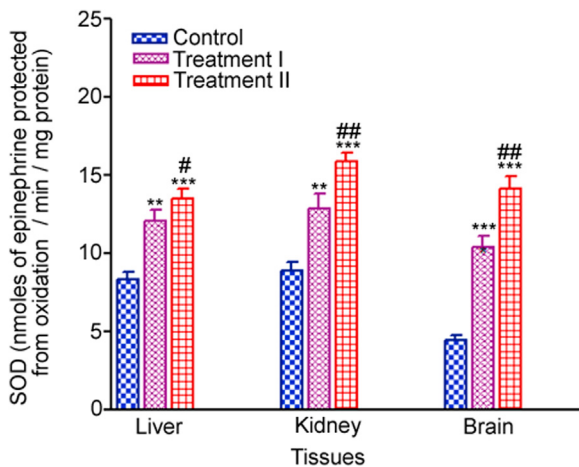
Fig. 2. Tissue-specific SOD (nmoles of epinephrine protected from oxidation/min/ mg protein) measured after 14 days oral administration of NP in Treatment I (38.91 mg/kg b.wt) and Treatment II (65.78 mg/kg b.wt) groups, and the control (75 μL DMSO/kg b.wt). Values are Mean $\pm$ SE ($n = 6$). Analysis of variance (One-way ANOVA) followed by Tukey test. Significant differences were indicated by $^{**}p < 0.01$ and $^{***}p < 0.001$, when compared with the control values while $^{\#}p < 0.05$ and $^{\#\#}p < 0.01$ were used to show the significant difference between the treatment groups.

3.2.2. CAT

CAT activity increased significantly in the liver, kidney and brain tissues in the treatment groups, when compared to the control. Trends of increase in CAT activities of liver, kidney and brain tissues in the treatment groups compared to control are given in Fig. 3.

Liver (% induction 132.43%–179.21%) showed a maximum increase in CAT activity in the treatment groups with respect to the control followed by the kidney (% induction 132.86%–172.6518%). Brain (% induction 124.51%–137.78%) showed the least increase in CAT activity in the treatment groups compared to the control.

3.3. Induction of oxidative stress

Tissue-specific disturbances in the antioxidant system were observed in all the experimental rat groups; therefore, this
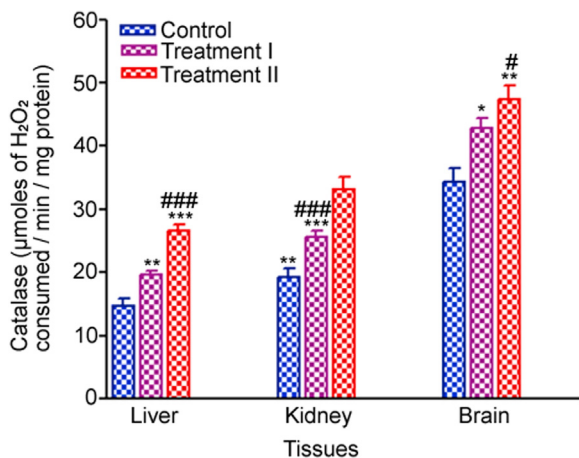

Fig. 3. Tissue-specific CAT (μmoles of H_2O_2 consumed/min/mg protein) measured after 14 days oral administration of NP in Treatment I (38.91 mg/kg b.wt) and Treatment II (65.78 mg/kg b.wt) groups, and the control (75 μL DMSO/kg b.wt). Values are Mean $\pm$ SE ($n = 6$). Analysis of variance (One-way ANOVA) followed by Tukey test. Significant differences were indicated by $^{*}p < 0.05$, $^{**}p < 0.01$ and $^{***}p < 0.001$ when compared with the control values while $^{\#}p < 0.05$ and $^{\#\#\#}p < 0.001$ level were used to show the significant difference between the treatment groups.
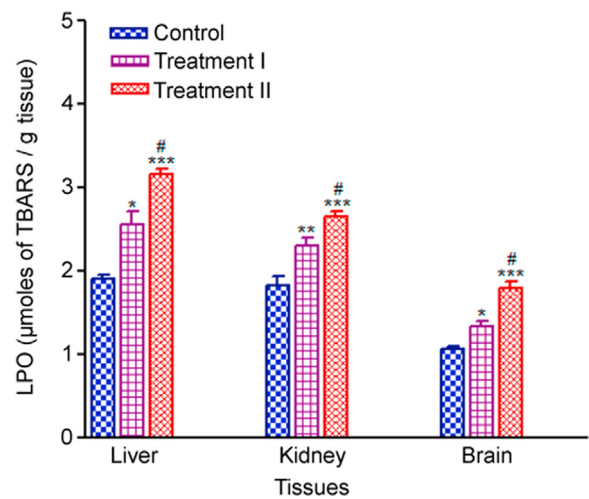

Fig. 4. Tissue-specific LPO (μmoles of TBARS/g tissue) measured after 14 days oral administration of NP in Treatment I (38.91 mg/kg b.wt) and Treatment II (65.78 mg/ kg b.wt) groups, and the control (75 μL DMSO/kg b.wt). Values are Mean $\pm$ SE ($n = 6$). Analysis of variance (One-way ANOVA) followed by Tukey test. Significant differences were indicated by $^{*}p < 0.05$, $^{**}p < 0.01$ and $^{***}p < 0.001$, when compared with the control values while $^{\#}p < 0.05$ was used to show the significant difference between the treatment groups.

generated oxidative stress, which was evaluated by estimation of LPO in the liver, kidney and brain tissues.

LPO level increased significantly in the liver, kidney and brain tissues in the treatment groups compared to the control. The trend of increase in LPO of liver, kidney and brain tissues in the treatment groups compared to the control is given in Fig. 4.

In the treatment groups, induction of LPO in the treatment groups compared to the control was significantly higher in the brain (% induction 124.91%–169.01%), followed by liver (% induction 135.40%–167.51%), and kidney (% induction 125.69%–145.38%) showed the least increase in LPO level compared to the control.

3.4. Effect of NP administration on liver function

Liver function was measured by liver-specific AST, ALT, ALP activities and TBIL level. AST, ALT, ALP activities and TBIL level significantly increased in all the NP administered rats (treatment groups), when compared to the control. The trend in the increase of ALT, AST, ALP activities and TBIL level in the treatment groups compared to the control is given in Fig. 5.

ALT showed the maximum significant increase (% induction 164.59%–208.27%) in the treatment groups compared to the control followed by TBIL (% induction 147.39%–192.17%) and ALP (% induction 164.93%–189.32%). AST activities showed the least increase in the treatment groups compared to the control (% induction 131.90%–164.70%).

3.5. Genotoxic assessments

3.5.1. Effect of NP on MN frequency

Two types of erythrocytes could be distinguished using differential staining by May-Gruenwald-Giemsa in bone marrow cells. The polychromatic erythrocytes with MN (MNPCEs) significantly increased in the treatment groups compared to the control. NP in the treatment groups induced a statistically significant increase in the percentage of PCEs with micronuclei in a dose-dependent manner, with the treatment I group showing a mean $\pm$ SE value of 1.87 $\pm$ 0.15 and treatment II group 2.54 $\pm$ 0.20, when compared to the control values (1.09 $\pm$ 0.10).

The trends in the increase of MN frequencies in the treatment groups compared to the control are given in Fig. 6. The
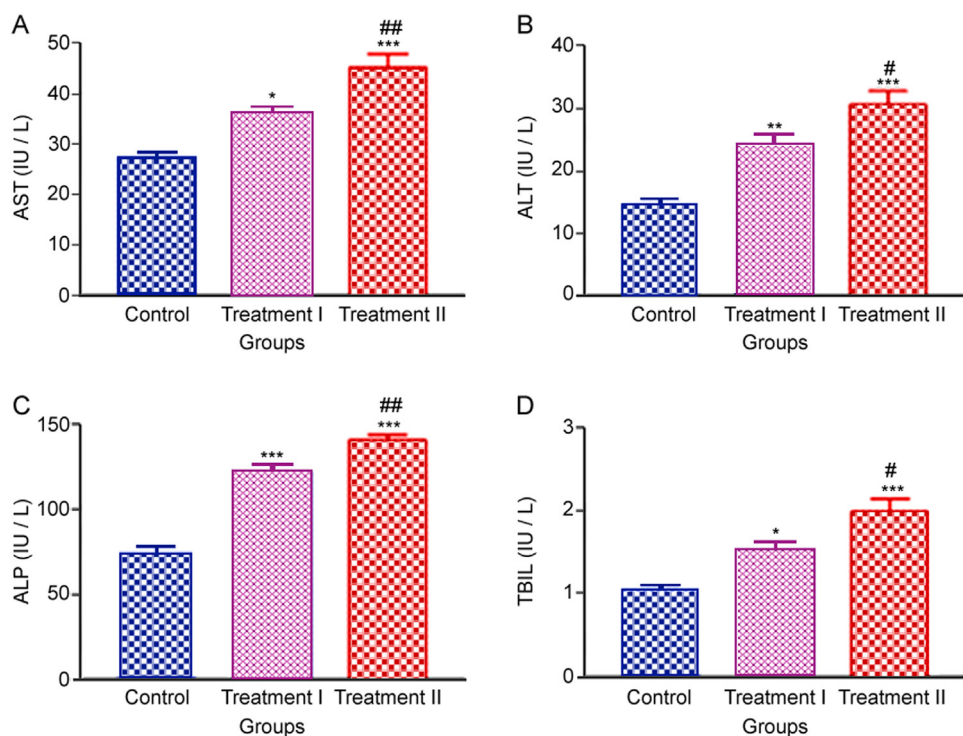
Fig. 5. Liver-specific (A) AST, (B) ALT and (C) ALP activities, and (D) TBIL levels measured after 14 days oral administration of NP in Treatment I (38.91 mg/kg b.wt) and Treatment II (65.78 mg/kg b.wt) groups, and the control (75 μL DMSO/kg b.wt). Values are Mean $\pm$ SE ($n = 6$). Analysis of variance (One-way ANOVA) followed by Tukey test. Significant differences were indicated by $*p < 0.05$, $**p < 0.01$ and $***p < 0.001$, when compared with the control values while $^{\#}p < 0.05$ and $^{\#\#}p < 0.01$ were used to show the significant difference between the treatment groups.
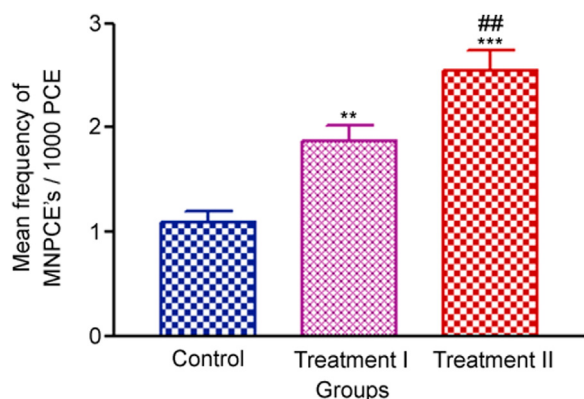

Fig. 6. Frequency of bone marrow micronuclei induction measured after 14 days oral administration of NP in Treatment I (38.91 mg/kg b.wt) and Treatment II (65.78 mg/kg b.wt) groups, and the control (75 μL DMSO/kg b.wt). Values are Mean $\pm$ SE ($n = 6$). Analysis of variance (One-way ANOVA) followed by Tukey test. Significant differences were indicated by $**p < 0.01$ and $***p < 0.001$, when compared with the control group and $^{\#\#}p < 0.01$ was used to show the significant difference between the treatment groups.

Fig. 7. Representative photomicrographs showing (A) PCEs in control and (B) MNPCEs in NP treated rats in bone marrow cells.

representative photomicrographs showing PCEs in the control and PCEs with micronucleated cells in the treatment groups are shown in Fig. 7.

3.5.2. Effect of NP administration on DNA damage

Quantification of DNA damage for each cell was calculated as the percent of the total DNA in the tail. The trend of percent DNA tail in the treatment groups compared with the control is given in Fig. 8. Results showed significant DNA damage induced by two different doses of NP in leukocytes of in vivo-treated rats as compared to the control ($p < 0.001$). The treatment groups 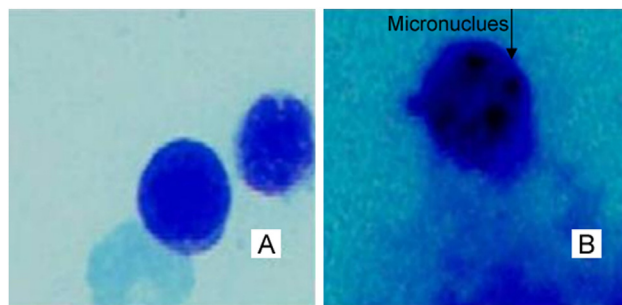showed clear induction of DNA damage. The Treatment II group showed the highest significant increase in the percent DNA tail (16.789 $\pm$ 0.606), followed by the Treatment I group (10.91 $\pm$ 0.6490), which were 24-fold and 15-fold higher, respectively, when compared with the control values (0.692 $\pm$ 0.090). The degree of damage was directly proportional to the concentrations ($p < 0.001$) used, having the highest induction factor in the Treatment II group (24.26), followed by Treatment I group (15.77) when compared with the control. The representative photomicrograph leukocytes and, percent DNA in the tail of the control, Treatment I and Treatment II groups are given in Fig. 9.

4. Discussions

In the present study, the level of GSH decreased significantly in the liver, kidney and brain tissues of treatment groups compared to the control, which confirms the oxidized state of the cells and indicates an inefficient metabolism of glutathione system in the ROS scavenging induced by NP. Our results are in line with a
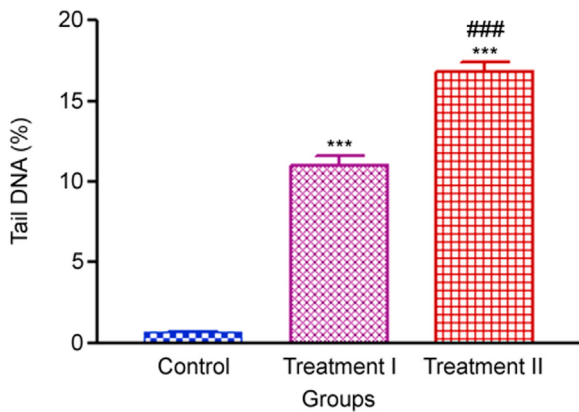
Fig. 8. % tail DNA in leukocytes measured after 14 days oral administration of NP in Treatment I (38.91 mg/kg b.wt) and Treatment II (65.78 mg/kg b.wt) groups, and the control (75 μL DMSO/kg b.wt). Values are Mean $\pm$ SE ($n = 3$). Analysis of variance (One-way ANOVA) followed by Tukey test. Significant differences were indicated by ***$p < 0.001$, when compared with the control and ###$p < 0.001$ was used to show the significant difference between the treatment groups.
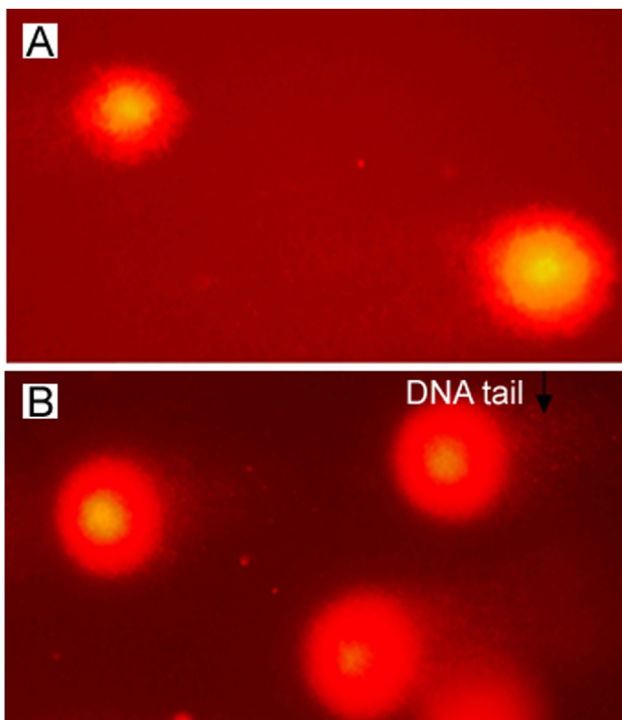

Fig. 9. Representative photmicrographs showing % tail DNA in (A) control and (B) NP treated rats in leukocytes.

previous study, where NP administration decreased the level of cardiac tissue glutathione as compared to the normal and toxic control groups in rats [25]. In the present study, NP also caused a significant increase in SOD activities in the liver, kidney and brain tissues of treatment groups compared to the control, which indicates an adaptive response to increased oxidative stress. The increased SOD activities in the present study favour the evidence of the pro-oxidant action of NP, and our results are in line with the previous study reported by Gómez-Oliván et al. [13], where NP was reported to cause increased SOD activity over 48 h NP exposures in *Daphnia magna*.

In the present study, NP treatment resulted in significant increase in CAT activities in the liver, kidney and brain tissues of treatment groups compared to the control. Similar increased CAT activities in the treatment groups were reported by Gómez-Oliván
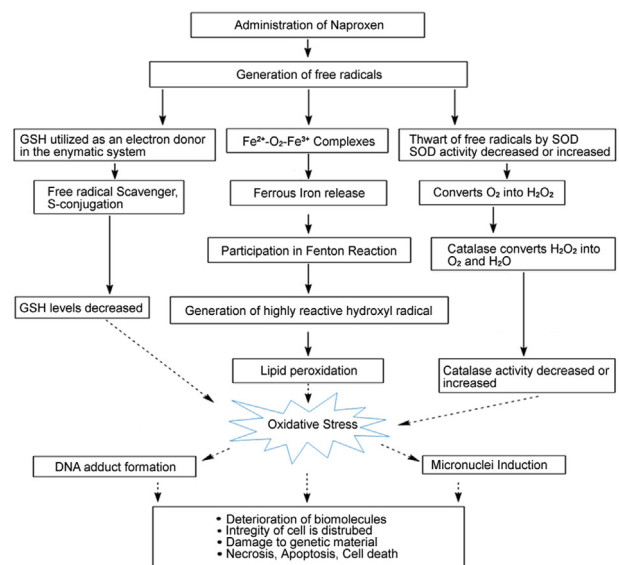

Fig. 10. Diagrammatic representation of possible mechanism of NP induced biochemical alterations, oxidative stress, hepatotoxicity and genotoxicity in male Wistar rats.

et al. [13] in *Daphnia magna* over 48 h NP exposures. This increase may also be attributed to the increased SOD activities or possibly to an increase in the formation of H_2O_2 in the cells due to the increase of ROS linked to arachidonic acid metabolism via lipoxygenase (LOX) pathway instead of COX pathway blockage by NSAIDs [26].

In this study, NP induced a significant increase in lipid peroxidation in the treatment groups, suggesting the generation of ROS. The results of the present study are in accordance with a study where NP-induced lipid peroxidation in the liver microsomes and the isolated hepatocytes of rats caused by the ROS are produced during NP oxidative metabolism [27]. Similarly, NP treatment caused elevated lipid peroxide levels in rat gastric mucosa [28]. Increased lipid peroxidation appears to be involved in the up-regulation of several antioxidant enzymes. Therefore, the increased lipid peroxidation, decreased glutathione level, increased SOD and CAT activities in the liver, kidney and brain tissues following NP treatment in the present study indicate a possible involvement of NP induced oxidative stress that altered antioxidant level in the treatment groups.

Administration of NSAIDs results in elevated ALT, AST and ALP activities and bilirubin level [9,29,30], which correlates with the present study, where treatment groups showed significant elevated liver-specific AST, ALT, ALP activities and TBIL level compared to the control after NP treatment for 14 days. The results of the present study corroborate with the previous study in rats [31]. The increased liver enzymes in the present study may also be possibly due to the fact that NP induced ROS generation since the liver is the major organ attacked by ROS [32].

Micronuclei induction in the PCEs of bone marrow cells has been regarded as one of the most sensitive biomarkers for mutagenic genotoxicity of a compound [33,34]. The increased micronuclei induction in the present study correlates with the previous study which demonstrated the cytotoxic effect of NSAIDs concentrations in the blood of *Cyprinuscarpio* and found a significant increase in micronuclei [9]. This significant increase in micronuclei induction in the present study may be due to chromosome missegregation, resulting from aneugenic and clastogenic effects elicited by NP induced ROS.

In the present study, NP caused a significant increase in the % DNA in the tail in cells of treatment groups compared to the

control. Similar results were obtained by Gómez-Oliván et al. [13], where 48 and 96 h NP exposure increased the % DNA tail in the cells of *Daphnia magna*. Similarly, significant DNA damage was present in the MG-63 osteosarcoma cells treated with NP [35]. It can be interpreted that the NP-induced DNA damage may be due to the result of ROS generated oxidative stress. Therefore, NP-induced ROS generation in the present study might be the possible mechanism for the damage to the genetic materials in Wistar rats. The possible mechanism of NP induced biochemical alterations, oxidative stress, hepatotoxicity and genotoxicity in male Wistar rats is shown in Fig. 10.

5. Conclusion

NP administration resulted in biochemical changes, like alteration of tissue sulfhydryl (GSH) levels, affecting the tissue antioxidants like SOD and CAT activities resulting in the increased oxidative stress. NP also caused elevated liver enzymes in the treatment groups, suggesting that it has some deleterious effect on the basic structure and functions of the liver. NP administration resulted in significant micronuclei inductions and damage to the genetic materials, exhibiting mutagenic activities in the male Wistar rats. From the present study, it can be concluded that NP is a potential genotoxic agent at the doses used that induces oxidative stress, hepatotoxicity and genotoxicity in vivo and thus use of this drug should be restricted.

Conflicts of interest

The authors declare that there are no conflicts of interest.

Acknowledgments

References

[1] M.H. Zuberi, U. Haroon, Y. BiBi, et al., Optimization of quantitative analysis of naproxin sodium using UV spectrophotometery in different solvent mediums, Am. J. Anal. Chem. 5 (2014) 211–214.

[2] N. Soltani, N. Tavakkoli, Z.S. Mosavimanesh, et al., Electrochemical determination of naproxen in the presence of acetaminophen using a carbon paste electrode modified with activated carbon nanoparticles, C. R. Chim. 58 (2018) 54–60.

[3] T. Hautaniemi, N. Petrenko, N. Skorinkin, et al., The inhibitory action of the antimigraine nonsteroidal anti-inflammatory drug naproxen on P2 × 3 receptor-mediated responses in rat trigeminal neurons, Neuroscience 209 (2012) 32–38.

[4] C.L. Keng, Y.C. Lin, W.L. Tseng, et al., Design of peptide-based probes for the microscale detection of reactive oxygen species, Anal. Chem. 89 (2017) 10883–10888.

[5] A. Bhattacharyya, R. Chattopadhyay, S. Mitra, et al., Oxidative stress: an essential factor in the pathogenesis of gastrointestinal mucosal diseases, Physiol. Rev. 94 (2014) 329–354.

[6] C.B.G. Ruas, S. Carvalho Cdos, H.S. Araújo, et al., Oxidative stress biomarkers of exposure in the blood of cichlid species from a metal-contaminated river, Ecotoxicol. Environ. Saf. 71 (2008) 86–93.

[7] H. Islas-Flores, L.M. Gómez-Oliván, M. Galar-Martínez, et al., Diclofenac-induced oxidative stress in brain, liver, gill and blood of common carp (Cyprinus carpio), Ecotoxicol. Environ. Saf. 92 (2013) 32–38.

[8] N. SanJuan-Reyes, L.M. Gómez-Oliván, M. Galar-Martínez, et al., Effluent from an NSAID-manufacturing plant in Mexico induces oxidative stress on Cyprinus carpio, Water Air Soil Pollut. 224 (2013) 1689–1698.

[9] P. Sriuttha, B. Sirichanchuen, U. Permsuwan, Hepatotoxicity of nonsteroidal anti-inflammatory drugs: a systematic review of randomized controlled trials, Int. J. Hepatol. 2018 (2018) 1–13.

[10] K. Kakisaka, Y. Yoshida, Y. Suzuki, et al., Serum markers for mitochondrial dysfunction and cell death are possible predictive indicators for drug-induced liver injury by direct acting antivirals, Hepatol. Res. 48 (2018) 78–86.

[11] S. García-Medina, J.A. Núñez-Betancourt, A.L. García-Medina, et al., The relationship of cytotoxic and genotoxic damage with blood aluminum levels and oxidative stress induced by this metal in common carp (Cyprinus carpio) erythrocytes, Ecotoxicol. Environ. Saf. 96 (2013) 191–197.

[12] M. Ćenanović, C. Duraković, In vivo genotoxicity testing of vitamin C and naproxen sodium using plant bioassay, Southeast Eur. J. Soft Comput. 4 (2015) 66–71.

[13] L.M. Gómez-Oliván, M. Galar-Martínez, S. García-Medina, et al., Genotoxic response and oxidative stress induced by diclofenac, ibuprofen and naproxen in Daphnia magna, Drug Chem. Toxicol. 37 (2014) 391–399.

[14] O.H. Lowry, N.J. Rosebrough, A.L. Farr, et al., Protein measurement with the Folin phenol reagent, J. Biol. Chem. 193 (1951) 265–275.

[15] D.J. Jollow, J.R. Mitchell, N. Zampaglione, et al., Bromobenzene-induced liver necrosis. Protective role of glutathione and evidence for 3,4-bromobenzene oxide as the hepatotoxic metabolite, Pharmacology 11 (1974) 151–169.

[16] H.P. Misra, I. Fridovich, The role of superoxide anion in the autoxidation of epinephrine and a simple assay for superoxide dismutase, J. Biol. Chem. 247 (1972) 3170–3175.

[17] A. Clairborne Catalase activity, R.A. Greenwald (ed), CRC Handbook of Methods for Oxygen Radical Research, CRC Press, 1985:283–284.

[18] M. Mihara, M. Uchiyama, Determination of malonaldehyde precursor in tissues by thiobarbituric acid test, Anal. Biochem. 86 (1978) 271–278.

[19] S. Reitman, S. Frankel, Colorimetric methods for aspartate and alanine aminotransferase, Am. J. Clin. Pathol. 28 (1957) 55–60.

[20] A.G. Cherian, S.J. Soldin, J.G. Hill, Automated Jendrassik-Grof method for measurement of bilirubin in serum with the Greiner Selective Analyzer (GSA II D), and comparison with the method involving diazotized 2, 4-dichloroaniline, Clin. Chem. 27 (1981) 748–752.

[21] P.R. Kind, E.J. King, Estimation of plasma phosphatase by determination of hydrolysed phenol with amino-antipyrine, J. Clin. Pathol. 7 (1954) 322–326.

[22] W. Schmid, The micronucleus test, Mutat. Res. 31 (1975) 9–15.

[23] N.P. Singh, M.T. McCoy, R.R. Tice, et al., A simple technique for quantitation of low levels of DNA damage in individual cells, Exp. Cell Res. 175 (1988) 184–191.

[24] S.L. Anderson, G.C. Wild, Linking genotoxic responses and reproductive success in ecotoxicology, Environ. Health Perspect. 102 (1994) 9–12.

[25] R.A. Pathan, B.K. Singh, K.K. Pillai, et al., Naproxen aggravates doxorubicin-induced cardiomyopathy in rats, Indian J. Pharmacol. 42 (2010) 44–49.

[26] R. Ardaillou, L. Baud, J. Sraer, Role of arachidonic acid metabolites and reactive oxygen species in glomerular immune-inflammatory process, Springer Semin. Immunopathol. 9 (1987) 371–385.

[27] H. Yokoyama, T. Horie, S. Awazu, Naproxen-induced oxidative stress in the isolated perfused rat liver, Chem. Biol. Interact. 160 (2006) 150–158.

[28] J.H. Kim, Y.S. Kim, G.G. Song, et al., Protective effect of astaxanthin on naproxen-induced gastric antral ulceration in rats, Eur. J. Pharmacol. 514 (2005) 53–59.

[29] P. Sarges, J.M. Steinberg, J.H. Lewis, Drug-induced liver injury: highlights from a review of the 2015 literature, Drug Saf. 39 (2016) 801–821.

[30] J.C. Albretsen, Oral medications, Vet. Clin. North Am. Small Anim. Pract. 32 (2002) 421–442.

[31] A.P. Adegunloye, J.O. Adebayo, D.R. Olayele, Effects of artemether-lumefantrine and naproxen combination on liver and kidney of rats, J. Pharm. Biol. Sci. 9 (2014) 19–23.

[32] V. Sánchez-Valle, N.C. Chávez-Tapia, M. Uribe, et al., Role of oxidative stress and molecular changes in liver fibrosis: a review, Curr. Med. Chem. 19 (2012) 4850–4860.

[33] F.M. Hamam, I.H. Foda, Mutagenic studies on the effect of Aldicarb "Temik" and vitamin C as antioxidant agent on the white rat: chromosomal aberrations and micronucleus tests, Egypt. J. Hosp. Med. 17 (2004) 143–154.

[34] J.A. Heddle, M. Hite, B. Kirkhart, et al., The induction of micronuclei as a measure of genotoxicity. A report of the US Environmental Protection Agency Gene-Tox Program, Mutat. Res. 123 (1983) 61–118.

[35] I. Correia, R. Arantes-Rodrigues, R. Pinto-Leite, et al., Effects of naproxen on cell proliferation and genotoxicity in MG-63 osteosarcoma cell line, J. Toxicol. Environ. Health Part A 77 (2014) 916–923.

Original Research Article

Recovery rates of combination antibiotic therapy using *in vitro* microdialysis simulating *in vivo* conditions

Jayesh A. Dhanani [a,b,*], Suzanne L. Parker [a], Jeffrey Lipman [a,b,c], Steven C. Wallis [a], Jeremy Cohen [a,b], John Fraser [d], Adrian Barnett [e], Michelle Chew [f], Jason A. Roberts [a,b,g,h]

[a] *Burns, Trauma and Critical Care Research Centre, The University of Queensland, UQ Centre for Clinical Research, Herston, Brisbane, QLD 4029, Australia*
[b] *Department of Intensive Care Medicine, Royal Brisbane & Women's Hospital, Brisbane, Australia*
[c] *Faculty of Health, Queensland University of Technology, Brisbane, Australia*
[d] *Critical Care Research Group, The University of Queensland, Brisbane, Australia*
[e] *Institute of Health and Biomedical Innovation & School of Public Health and Social Work, Queensland University of Technology, Kelvin Grove, Brisbane, Australia*
[f] *Department of Anaesthesiology and Intensive Care, and Department of Medical and Health Sciences, Linköping University, Linköping, Sweden*
[g] *School of Pharmacy, The University of Queensland, Brisbane, Australia*
[h] *Department of Pharmacy, Royal Brisbane & Women's Hospital, Brisbane, Australia*

ARTICLE INFO

ABSTRACT

Microdialysis is a technique used to measure the unbound antibiotic concentration in the interstitial spaces, the target site of action. In vitro recovery studies are essential to calibrating the microdialysis system for in vivo studies. The effect of a combination of antibiotics on recovery into microdialysate requires investigation. In vitro microdialysis recovery studies were conducted on a combination of vancomycin and tobramycin, in a simulated in vivo model. Comparison was made between recoveries for three different concentrations and three different perfusate flow rates. The overall relative recovery for vancomycin was lower than that of tobramycin. For tobramycin, a concentration of 20μg/mL and flow rate of 1.0μL/min had the best recovery. A concentration of 5.0μg/mL and flow rate of 1.0μL/min yielded maximal recovery for vancomycin. Large molecular size and higher protein binding resulted in lower relative recoveries for vancomycin. Perfusate flow rates and drug concentrations affected the relative recovery when a combination of vancomycin and tobramycin was tested. Low perfusate flow rates were associated with higher recovery rates. For combination antibiotic measurement which includes agents that are highly protein bound, in vitro studies performed prior to in vivo studies may ensure the reliable measurement of unbound concentrations.

© 2018 Xi'an Jiaotong University. Production and hosting by Elsevier B.V. This is an open access article under the CC BY-NC-ND license (http://creativecommons.org/licenses/by-nc-nd/4.0/).

1. Introduction

Combination antibiotic therapy is commonly used in clinical practice due to an increase in multidrug resistant bacterial infections [1,2]. Consequently, antibiotic pharmacokinetic data is essential to developing accurate dosing regimens which can achieve effective antibiotic concentrations at the site of infection which is mostly the interstitial fluid of tissue [3,4]. This principle is fundamental for not only optimal microbiological and clinical outcome, but also for minimizing the risk of microbial resistance

[5–9]. Moreover, it is the free (unbound) drug concentrations at the site of infection that are relevant with dosing challenges prominent because tissue interstitial space fluid penetration can differ substantially for some drugs [10].

Microdialysis is a minimally invasive sampling technique used to measure unbound drug concentrations in the interstitial space fluid of different tissues [11,12], both in animals and humans [13]. The pharmacokinetic data from in vivo microdialysis studies can be used to design antibiotic dosing guidelines [14]. The details of the microdialysis technique have been described elsewhere [15–18]. Briefly, the probe has a semipermeable membrane tip, which is perfused with a physiological solution (perfusate) at a slow flow rate. According to the concentration gradient, molecules with a size less than that of the membrane pore size will diffuse from the tissue interstitial space fluid (C_{tissue}) into the perfusate and collect as the microdialysate ($C_{dialysate}$).

Peer review under responsibility of Xi'an Jiaotong University.

* Corresponding author at: Burns, Trauma and Critical Care Research Centre, The University of Queensland, UQ Centre for Clinical Research, Herston, Brisbane, QLD 4029, Australia.

E-mail address: jadhanani@hotmail.com (J.A. Dhanani).

For most substances, the full equilibrium cannot be achieved i.e. $C_{tissue} > C_{dialysate}$. The term 'recovery' is used to describe the relationship between C_{tissue} and $C_{dialysate}$. The ratio of $C_{dialysate}$ to C_{tissue} is termed 'relative recovery'. This factor is then used to calculate the actual drug concentration in the tissue interstitial space fluid. Knowing the drug concentration in the solution, in vitro recovery studies could be used to investigate the effect of parameters such as perfusate flow rate, membrane characteristics, membrane length and drug characteristics on recovery [19]. Furthermore, data from these studies could inform subsequent in vivo studies.

With combination antibiotic therapy, a number of issues can affect drug recovery with in vivo studies [15]. In vitro microdialysis recovery studies using combination drugs can provide preliminary data on drug recovery and likely in vivo calibration [15]. Despite this there are very few microdialysis studies investigating relative recovery of antibiotics, let alone a combination of antibiotics, despite how commonly they are used clinically [20]. Furthermore, for combination antibiotics therapy, previous in vitro microdialysis recovery studies have not fully accounted for in vivo conditions [20].

Microdialysis catheters may have individual variation in membrane permeability. Diffusion through the microdialysis membrane follows Fick's law. Hence, factors such as partition coefficient, particle size and surface area of the substance will affect the drug permeability through the membrane [21]. This necessitates individual probe calibration [22].

The feasibility of using microdialysis for different drugs depends on the physico-chemical characteristics of the substance, e.g. lipophilic and high molecular weight compounds are less likely to diffuse through the microdialysis catheter membrane and may be less feasible for microdialysis [23]. High molecular weight is associated with lower diffusion coefficients through the microdialysis membrane, thus resulting in decreased recovery [23].

Vancomycin has protein binding of approximately 55% [24] and a molecular weight of ~ 1.5 Da. The molecular weight of tobramycin is 467 Da with low serum protein binding ($< 30\%$) [25]. Both drugs are also hydrophilic and suitable for microdialysis studies.

Therefore, the aim of this study was to assess the relative recovery of concomitant vancomycin and tobramycin in an in vitro model simulating in vivo conditions. The study assessed the effect of different perfusate flow rates and the concentrations of the antibiotic solutions on the relative recoveries.

2. Materials and methods

2.1. Chemicals and standards

Vancomycin hydrochloride was obtained from Aspen Pharmacare (St Leonards, Australia), tobramycin sulphate was obtained from Pfizer (Perth, Australia), and compound sodium lactate IV solution was obtained from Baxter (Old Toongabbie, Australia). The chemical structures for vancomycin and tobramycin are shown in Fig. 1.

Acetonitrile was of HPLC-gradient grade (Merck, Darmstadt, Germany), while dichloromethane (Merck, Darmstadt, Germany), formic acid (Ajax, Taren Point, Australia), heptafluorobutyric acid (HFBA, Fluka, Castle Hill, Australia) and trichloroacetic acid (Sigma-Aldrich, Castle Hill, Australia) were of analytical grade. Ultrapure water was obtained using a Permutit system (resistivity at 25 °C at least 18 ΩM.cm). Drug-free human plasma was obtained from the Royal Brisbane and Women's Hospital blood bank (Brisbane, Australia).
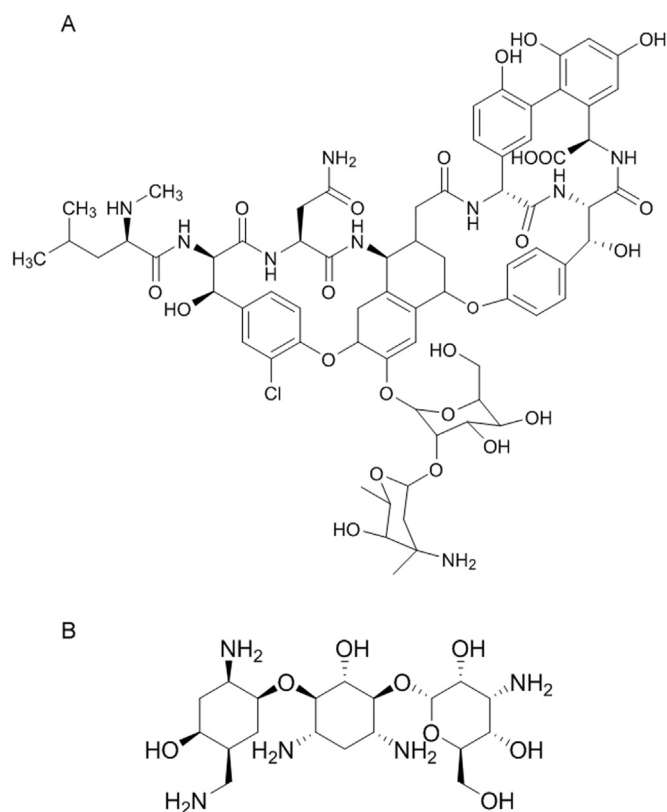

Fig. 1. Structures of vancomycin (A) and tobramycin (B).

2.2. Microdialysis in vitro model

Commercially available microdialysis probes CMA 63 (CMA Microdialysis AB, Stockholm, Sweden) with a molecular weight cut-off of 20 kDa, an outer diameter of 0.6 mm and a membrane length of 30 mm were used. Probes were perfused with lactated Ringer's solution at flow rates of 1 and 2 μL/min by using a precision microinfusion pump CMA 107 (CMA Microdialysis AB, Stockholm, Sweden). To enable perfusion at 1.5 μL/min, a Cole-Parmer two-syringe infusion pump 230 VAC CE (John Morris Group, Chatswood, Australia), was used.

2.3. Stock and standard solution preparation

A stock solution was freshly prepared by dissolving tobramycin in compound sodium lactate IV solution at 2 mg/mL and stored at −80 °C. A stock solution was freshly prepared by dissolving vancomycin in compound sodium lactate IV solution at 2 mg/mL and stored at −80 °C. These stock solutions were serially diluted with compound sodium lactate IV solution to produce a standard solution containing 200 μg/mL of both vancomycin and tobramycin, and a standard solution containing 20 μg/mL of both vancomycin and tobramycin.

2.4. Plasma sample solutions

The study plasma solutions were prepared using the stock solutions containing both vancomycin and tobramycin and drug-free plasma, to yield plasma sample solutions containing vancomycin and tobramycin of 0.5, 5.0 and 20 μg/mL.

2.5. Recovery experiments

Microdialysis probes were fully immersed in four separate 100 mL beakers. The beakers contained either 0.5, 5 or 20 μg/mL of vancomycin and tobramycin plasma sample solution, or drug-free plasma. A magnetic stirrer was used to simulate in vivo conditions as previously described [26]. Temperature and pH of each of the study solutions were recorded to ensure consistency of these variables.

The microdialysis probe was connected to the precision pump and perfused at 5 μL/min with compound sodium lactate IV solution for 10 min to flush the air out of the system. Following this, the probe was perfused at 1 μL/min for 1 h to enable equilibration. At the end of the equilibration period the following perfusate flow rates were used for 100 min each, with sampling occurring at 20-min intervals ($n = 5$ sampling points): 1.0, 1.5 and 2 μL/min. Samples were then stored at $-80\,^\circ$C for analysis.

The percent relative recovery was calculated using the recovery-by-gain formula as follows:

Relative recovery (%) = ($C_{dialysate}$ /$C_{solution}$) × 100

Where $C_{dialysate}$ is the mean concentration in the microdialysate ($n = 5$); $C_{solution}$ is the mean concentration in the study solution ($n = 5$).

2.6. Instrument and analytical method

Vancomycin and tobramycin in plasma and microdialysate matrices were measured using validated liquid chromatography-tandem mass spectrometry (LC-MS/MS) methods. Drug-free compound sodium lactate IV solution and drug-free plasma solution were used to prepare calibration standards used in the assay.

The LC-MS/MS used two Perkin Elmer LC-200 micro-pumps and a CTC PAL autosampler equipped with an Applied Biosystems API2000 mass spectrometer detector. An electro-spray ionization (ESI) source interface operating in positive-ion mode was used for the multiple reaction monitoring (MRM) LC-MS/MS analysis. The interface settings consisted of the nebulizing gas flow of 40 L/min, turbo gas of 50 L/min, curtain gas of 30 L/min, ion-spray voltage of 4500 V, a turbo-gas temperature of 400 $^\circ$C, and the interface heater on. Two MRMs were monitored and summed for vancomycin, m/z of 725–144 and 725–99, whilst tobramycin was monitored at m/z of 468–163.

Chromatographic separation of vancomycin, tobramycin and the internal standard (teicoplanin) was achieved using a Waters Xterra C_{18} column (2.1 mm × 150 mm, 5 μm) using a gradient of mobile phases consisting of (a) 0.1% formic acid with 10 mM HFBA and (b) 80% methanol in 0.1% formic acid with 10 mM HFBA. The mobile phase was operated using a concentration gradient for methanol, ranging from 5% to 80%. The analytical method for tobramycin was similar to that used in other studies [27–29].

Vancomycin and tobramycin in plasma were assayed separately. For the extraction of vancomycin from plasma, 100 μL of plasma was treated with 400 μL of acetonitrile to precipitate proteins, with 600 μL of dichloromethane subsequently added to remove both the acetonitrile and lipids. For the extraction of tobramycin from plasma, 200 μL of plasma was treated with the addition of 50 μL of 30% trichloroacetic acid. Both vancomycin and tobramycin were assayed simultaneously in microdiaysate, with 10 μL of sample being diluted with 40 μL of internal standard (teicoplanin, 100 μg/mL) for direct injection onto the instrumental analysis.

Calibration standards were prepared using sequential dilution to obtain concentrations of 0.1, 0.2, 0.5, 1, 2, 5, 10, 20 and 50 μg/mL. The chromatographic calibration was linear for vancomycin from 0.1 to 50 μg/mL in plasma (LLOQ 0.0917 ± 0.011 (mean ± SD)) and 0.2–50 μg/mL in microdialysate (LLOQ 0.196 ± 0.010,) and for tobramycin from 0.2 to 50 μg/mL in plasma (LLOQ 0.205 ± 0.012), and 0.1–20 μg/mL in microdialysate (LLOQ 0.111 ± 0.004). Quality control samples were prepared at three concentrations 0.6, 2 and 16 μg/mL with precision and accuracy within 15% for all analyses. All analyses passed the batch acceptance criteria. The assay was validated according to an international FDA guideline [30] in terms of stability, specificity, linearity, precision and accuracy.

2.7. Statistical analysis

A linear regression model was used, with recovery as the dependent variable and flow rate and concentration as independent variables. This allowed us to examine if the recovery changed when the flow rate or concentration was altered. To estimate the variation in recovery we fitted the linear regression model using a Bayesian paradigm and modelled the result of a new test, using the 95% credible interval to estimate the likely range in percent recovery for a new test. As we assume a constant variance across dose, flow rate, and sample number, this credible interval will apply to any mean. We used 10,000 Markov chain Monte Carlo iterations with a burn-in of 10,000 thinned by 3. All analyses were made using R version 3.0.2 (www.r-project.org) with the Bayesian analysis in WinBUGS version 3.1.4 [31].

3. Results

The temperature of all the study solutions was constant at room temperature (24.0 $^\circ$C ± 0.5). The pH of all the study solutions was 7.40 ± 0.04. The mean (± SD) concentrations of vancomycin and tobramycin are summarized in Table 1. Table 2 presents the mean (± SD) relative recoveries of vancomycin and tobramycin, respectively.

3.1. Stability of relative recovery during in vitro microdialysis

There was no significant inter-experiment variation in relative recovery. Relative recovery appeared stable for each microdialysis probe over the 100-min sampling period. The variations were ± 11% for tobramycin and ± 14% for vancomycin (using the Bayesian 95% credible intervals (CI)).

Table 1

Mean (± SD) vancomycin and tobramycin concentrations (μg/mL) in microdialysate at different microdialysis flow rates (1, 1.5, and 2 μL/min).

Plasma concentrations (μg/mL)	Vancomycin (μg/mL)			Tobramycin (μg/mL)		
	1	1.5	2	1	1.5	2
20	5.36 (± 0.50)	5.06 (± 0.32)	4.29 (± 0.50)	13.7 (± 0.44)	13.7 (± 0.57)	11.68 (± 0.31)
5	1.63 (± 0.09)	1.37 (± 0.09)	1.03 (± 0.05)	3.45 (± 0.18)	3.47 (± 0.09)	3.03 (± 0.19)
0.5	< LLOQ	< LLOQ	< LLOQ	0.39 (± 0.01)	0.32 (± 0.01)	0.32 (± 0.01)

LLOQ= lower limit of quantification (LLOQ for vancomycin = 1 μg/mL).

Table 2
Mean (± SD) vancomycin and tobramycin relative recovery (%) at different microdialysis flow rates (1, 1.5, and 2 μL/min).

Plasma concentrations (μg/mL)	Vancomycin (%)			Tobramycin (%)		
	1	1.5	2	1	1.5	2
20	26.8 (± 0.50)	25.3 (± 0.32)	22.2 (± 050)	68.5 (± 2.23)	70.0 (± 2.89)	58.4 (± 1.55)
5	32.6 (± 0.09)	27.5 (± 0.09)	20.7 (± 0.04)	69.0 (± 3.74)	69.5 (± 3.47)	60.7 (± 3.8)
0.5	NC	NC	NC	78.53 (± 3.13)	65.9 (± 2.70)	65.0 (± 1.70)

NC = Not calculated.

Table 3
Multiple regression analysis for relative recovery rates (mean (%) and 95% confidence interval (CI)) of vancomycin and tobramycin for different concentrations and perfusate flow rates (For vancomycin, reference level is 1.0 μL/min flow rate and concentration 5.0 mg/mL. For tobramycin, reference level is 1.0 μL/min flow rate and concentration 0.5 μg/mL).

Parameter	Vancomycin			Tobramycin		
	Mean (%)	95% CI	P value	Mean (%)	95% CI	P value
Intercept	29.2	23.7, 34.7	< 0.001	71.0	67.2, 74.8	< 0.001
Concentration						
5.0 μg/mL				2.2	− 1.9, 6.4	0.286
20 μg/mL	1.0	− 4.7, 6.7	0.712	5.7	1.6, 9.9	0.008
Flow rate						
1.5 μL/min	− 6.1	− 12.7, 0.5	0.070	− 5.7	− 9.8, − 1.5	0.009
2.0 μL/min	− 11.6	− 18.9, − 4.3	0.003	− 12.0	− 16.2, − 7.9	< 0.001

3.2. Flow rate dependence on relative recovery

As shown in Table 2, the relative recoveries for vancomycin were higher at the 1.0 μL/min and 1.5 μL/min flow rates (mean 29.7% and 26.4%, respectively), compared with the 2.0 μL/min flow rate group (mean 21.4%). The regression model in Table 3 shows that a flow rate of 2.0 μL/min had a significantly lower relative recovery than the reference flow rate of 1.0 μL/min. The relative recoveries remained stable for the duration of sampling, i.e. 100 min.

In Table 2, relative recoveries for tobramycin were seen to be comparable at the 1.0 μL/min and 1.5 μL/min flow rates (means 72.0% and 68.5%, respectively), but decreased at 2.0 μL/min (61.4%). There were no significant variations in the results over the duration of the study. Table 3 shows the regression model demonstrating the differences in the effect of flow rate on the relative recoveries, with a significantly lower relative recovery for flow rates of 1.5 and 2.0 μL/min compared with 1.0 μL/min.

3.3. Concentration dependence relative recovery

As shown in Table 2, the relative recoveries for vancomycin were higher for the 5.0 μg/mL concentration (range 20.664%–32.69%) compared with the 20 μg/mL concentration (range 21.7%–27.3%). Importantly, the microdialysate in the 0.5 μg/mL group did not yield any results, as the concentrations were less than the lower limit of quantification of the assay (0.2 μg/mL). For tobramycin, the range of relative recoveries is shown in Table 2 and was the highest for concentration of 0.5 μg/mL (range 63.3%–81.66%).

3.4. Combined effect of drug concentration and flow rate

For vancomycin (Table 3) there was no statistical difference between the concentrations, but there was a lower relative recovery for flow rate of 2.0 μL/min compared with flow rate of 1.0 μL/min (mean difference − 11.6%, 95% CI: − 18.9 to − 4.3, P value = 0.003). The highest relative recovery was for the concentration of 5.0 μg/mL and flow rate of 1.0 μL/min (mean recovery 32.6%, 95% CI: 24.8%–35.7%).

For tobramycin (Table 3), there was a higher relative recovery for the concentration of 20 μg/mL compared with 0.5 μg/mL, with a mean increase of 5.7% (95% CI 1.6%–9.9%, P value = 0.008). Flow rates of 1.5 μL/min and 2.0 μL/min had lower relative recoveries than the flow rate of 1.0 μL/min, with P value 0.009 and < 0.001, respectively. The highest relative recovery was for a concentration of 0.5 μg/mL and flow rate 1.0 μL/min (mean 78.53%, 95% CI: 73.0%–80.6%).

4. Discussion

Though in vitro microdialysis studies have been performed previously to examine probe recovery, to the best of our knowledge, this is the first study simulating in vivo conditions and examining the relative recoveries for a combination of antibiotics in plasma. Knowledge of potential drug effects on microdialysis recovery is essential as combination antibiotic therapy is commonly used clinically and if not accounted for in relative recovery, may have the risk of under- or over-estimating drug concentrations in interstitial space fluid in in vivo studies. In vitro studies provide an ideal platform to study this effect and thus allow useful calibration for in vivo studies. Although there were inter-experiment differences in the relative recovery, its practical relevance is negligible. In general, for a drug, inter-experiment relative recovery variations of 20% are acceptable under in vivo conditions [12].

Nosocomial infections due to methicillin-resistant *Staphylococcus aureus* (MRSA) and *Pseudomonas spp* are prevalent [32] and hence most therapies, both empirical and specific, would include vancomycin and tobramycin as part of the regimen [33]. Hence, for our study, we chose these two antibiotics. Interstitial space fluid concentrations of antibiotics could be affected by a number of factors during in vivo microdialysis. For vancomycin, the reported values in the microdialysis samples have been variable with a wide range [34–36]. For tobramycin, there is dearth of data in the microdialysis samples but Bernardi et al.[37] report a lung microdialysis study using tobramycin and Rodvold et al.[38] report a range of lung penetration ratio for tobramycin. Hence, the three concentrations chosen for the study would encompass a wide range of possible values.

In comparison to a previous study [20], our study showed that relative recoveries for vancomycin were lower (26% *vs.* 50%) across all flow rates and concentrations. Considering that MacVane et al. [20] performed their study in a non-protein medium, our results could be explained by the protein binding of vancomycin. However, perfusate composition, membrane characteristics and other factors may also play a role in this phenomenon.

For both drugs and all concentrations, we found improved relative recovery at lower flow rates. Hence, where possible, lower

microdialysis flow rates should be preferred for optimal recovery. However, decreasing the flow rate could reduce the ability to sample frequently, due to the increased time required to collect the sample volume required for the assay. Less frequent sampling may adversely affect the temporal resolution of the data. Studies using drugs with narrow therapeutic index or in conditions with temporal fluctuations of drug concentration are likely to produce significant differences. Therefore, choosing a flow rate appropriate for the desired sampling frequency is an important consideration of all studies. In future and with improved analytic techniques, where measurement in a low volume is possible, this may not be an issue.

Careful consideration of the expected interstitial space fluid concentration should be taken into account when performing studies. Here, the lower recovery rates caused the microdialysate concentration to fall below the lower limit of the assay, as we encountered in the group of low vancomycin concentrations. Therefore, in vitro calibration can help prevent loss of clinical samples from the same issue.

5. Limitations

The exact composition of the interstitial space fluid is likely to be different between individual tissues and could be different in illness [39]. Moreover, in critical illness the increased inflammation could lead to changes in the interstitial space fluid protein content [39]. We were unable to obtain interstitial fluid, hence plasma was used for the study as the surrogate medium. Plasma offers a reasonable surrogate for this experiment, while the protein concentrations are higher at around 60–80 g/L in a healthy adult, compared to interstitial fluid with protein content 24–32 g/L (interstitial fluid to serum protein ratio $\sim$ 0.4)[40], this offers an insight into the conditions of a patient during critical illness where capillary leak syndrome may elevate the protein content in the interstitial fluid. Although we have attempted to mimic in vivo conditions, our study focussed on only two factors, drug concentration and perfusate flow rate, which affects relative recovery. There is currently no data on the effect of different concentrations of one antibiotic on the recovery rate of another antibiotic during combined antibiotic therapy. Our study did not investigate this effect, but it remains a worthy subject for better characterisation of relative recoveries in this context. Processes such as pressure gradients, extracellular–microvascular exchange, metabolism, and tissue diffusion of the drug can affect the relative recovery of the drugs. In vivo recovery may be affected by experimental and/or disease conditions [19]. Besides these, microdialysis probe related factors such as membrane length, material and surface area, perfusate composition and temperature; tissue factors such as blood flow and temperature; the tissue- drug-probe material interactions could affect the drug concentrations, resulting in even lower concentrations of the drug in the microdialysate [19]. With this study, we have attempted to establish a minimum set of conditions to be fulfilled for microdialysis-based studies. When possible, future studies should include in vivo calibration for recovery calculations.

6. Conclusion

In this simulated in vivo model, the in vitro relative recoveries for vancomycin and tobramycin varied with the perfusate flow rate and drug concentration. We suggest that a low perfusate flow rate $\leq$ 1 μL/min should be used to achieve optimal relative recovery.

Furthermore, we recommend performing in vitro recovery studies simulating in vivo conditions to accurately calibrate the microdialysis system prior to in vivo studies, to establish the most accurate combination of flow rate and drug concentration. Performing studies in plasma for moderate-to-highly protein bound drugs may better replicate in vivo conditions. Based on our study results, vancomycin and potentially other molecules of larger size and/or high protein binding need additional consideration for improving the relative recovery.

Conflicts of interest

The authors declare that there are no conflicts of interest.

Acknowledgments

References

[1] J. Caballero, J. Rello, Combination antibiotic therapy for community-acquired pneumonia, Ann. Intensive Care 1 (2011) 48.
[2] A. Kumar, R. Zarychanski, B. Light, et al., Early combination antibiotic therapy yields improved survival compared with monotherapy in septic shock: a propensity-matched analysis, Crit. Care Med. 38 (2010) 1773–1785.
[3] O.M. Klibanov, R.H. Raasch, J.C. Rublein, Single versus combined antibiotic therapy for gram-negative infections, Ann. Pharmacother. 38 (2004) 332–337.
[4] American Thoracic Society, and Infectious Diseases Society of America, Guidelines for the management of adults with hospital-acquired, ventilator-associated, and healthcare-associated pneumonia, Am. J. Respir. Crit. Care Med. 171 (2005) 388–416.
[5] C. Lamer, V. de Beco, P. Soler, et al., Analysis of vancomycin entry into pulmonary lining fluid by bronchoalveolar lavage in critically ill patients, Antimicrob. Agents Chemother. 37 (1993) 281–286.
[6] M.S. Engineer, D.H. Ho, G.P. Bodey, Comparison of vancomycin disposition in rats with normal and abnormal renal functions, Antimicrob. Agents Chemother. 20 (1981) 718–722.
[7] D. Farin, G.A. Piva, I. Gozlan, et al., modified HPLC method for the determination of vancomycin in plasma and tissues and comparison to FPIA (TDX), J. Pharm. Biomed. Anal. 18 (1998) 367–372.
[8] G.R. Matzke, G.G. Zhanel, D.R. Guay, Clinical pharmacokinetics of vancomycin, Clin. Pharmacokinet. 11 (1986) 257–282.
[9] R. Kitzes-Cohen, D. Farin, G. Piva, et al., Pharmacokinetics of vancomycin administered as prophylaxis before cardiac surgery, Ther. Drug Monit. 22 (2000) 661–667.
[10] M. Muller, H. Stass, M. Brunner, et al., Penetration of moxifloxacin into peripheral compartments in humans, Antimicrob. Agents Chemother. 43 (1999) 2345–2349.
[11] C. Joukhadar, H. Derendorf, M. Muller, Microdialysis. A novel tool for clinical studies of anti-infective agents, Eur. J. Clin. Pharmacol. 57 (2001) 211–219.
[12] M. Muller, Science, medicine, and the future: microdialysis, BMJ 324 (2002) 588–591.
[13] A. de la Pena, P. Liu, H. Derendorf, Microdialysis in peripheral tissues, Adv. Drug Deliv. Rev. 45 (2000) 189–216.
[14] C. Joukhadar, M. Muller, Microdialysis: current applications in clinical pharmacokinetic studies and its potential role in the future, Clin. Pharmacokinet. 44 (2005) 895–913.
[15] L. Stahle, P. Arner, U. Ungerstedt, Drug distribution studies with microdialysis. III: extracellular concentration of caffeine in adipose tissue in man, Life Sci. 49 (1991) 1853–1858.
[16] W.F. Elmquist, R.J. Sawchuk, Application of microdialysis in pharmacokinetic studies, Pharm. Res. 14 (1997) 267–288.
[17] C.S. Chaurasia, In vivo microdialysis sampling: theory and applications, Biomed. Chromatogr. 13 (1999) 317–332.
[18] P. Lonnroth, P.A. Jansson, U. Smith, A. microdialysis method allowing characterization of intercellular water space in humans, Am. J. Physiol. 253 (1987) E228–E231.
[19] E.C.M.Lange, Recovery and calibration techniques: toward quantitative microdialysis, in microdialysis in drug development, M. Müller, Ed., Springer New York: New York, 2013: 13–33.
[20] S.H. MacVane, S.T. Housman, D.P. Nicolau, In vitro microdialysis membrane efficiency of broad-spectrum antibiotics in combination and alone, Clin. Pharmacol. 6 (2014) 97–101.

[21] J. Kehr, A survey on quantitative microdialysis: theoretical models and practical implications, J. Neurosci. Methods 48 (1993) 251–261.

[22] P. Abrahamsson, O. Winso, An assessment of calibration and performance of the microdialysis system, J. Pharm. Biomed. Anal. 39 (2005) 730–734.

[23] T.S. Shippenberg, A.C. Thompson, Overview of microdialysis, Curr. Protoc. Neurosci. (2001) 1–27, Chapter 7.

[24] H. Sun, E.G. Maderazo, A.R. Krusell, Serum protein-binding characteristics of vancomycin, Antimicrob. Agents Chemother. 37 (1993) 1132–1136.

[25] R.C. Gordon, C. Regamey, W.M. Kirby, Serum protein binding of the aminoglycoside antibiotics, Antimicrob. Agents Chemother. 2 (1972) 214–216.

[26] B.B. Ba, A. Bernard, A. Iliadis, et al., New approach for accurate simulation of human pharmacokinetics in an in vitro pharmacodynamic model: application to ciprofloxacin, J. Antimicrob. Chemother. 47 (2001) 223–227.

[27] M.X. Guo, L. Wrisley, E. Maygoo, Measurement of tobramycin by reversed-phase high-performance liquid chromatography with mass spectrometry detection, Anal. Chim. Acta 571 (2006) 12–16.

[28] J.B. Arsand, L. Jank, M.T. Martins, et al., Determination of aminoglycoside residues in milk and muscle based on a simple and fast extraction procedure followed by liquid chromatography coupled to tandem mass spectrometry and time of flight mass spectrometry, Talanta 154 (2016) 38–45.

[29] L. Chen, H. Chen, M. Shen, Hydrophilic interaction chromatography combined with tandem mass spectrometry method for the quantification of tobramycin in human plasma and its application in a pharmacokinetic study, J. Chromatogr. B Anal. Technol. Biomed. Life Sci. 973C (2014) 39–44.

[30] Center for drug evaluation and research, Federal drug administration guidance for industry: bioanalytical method validation, 2001.

[31] D.J. Lunn, A. Thomas, N. Best, et al., WinBUGS–a Bayesian modelling framework: concepts, structure, and extensibility, Stat. Comput. 10 (2000) 325–337.

[32] E.R. Sydnor, T.M. Perl, Hospital epidemiology and infection control in acute-care settings, Clin. Microbiol. Rev. 24 (2011) 141–173.

[33] P.D. Tamma, S.E. Cosgrove, L.L. Maragakis, Combination therapy for treatment of infections with gram-negative bacteria, Clin. Microbiol. Rev. 25 (2012) 450–470.

[34] M. Bue, H. Birke-Sorensen, T.M. Thillemann, et al., Single-dose pharmacokinetics of vancomycin in porcine cancellous and cortical bone determined by microdialysis, Int. J. Antimicrob. Agents 46 (2015) 434–438.

[35] S.T. Housman, A.A. Bhalodi, A. Shepard, et al., Vancomycin tissue pharmacokinetics in patients with lower-limb infections via in vivo microdialysis, J. Am. Podiatr. Med. Assoc. 105 (2015) 381–388.

[36] K. Skhirtladze, D. Hutschala, T. Fleck, et al., Impaired target site penetration of vancomycin in diabetic patients following cardiac surgery, Antimicrob. Agents Chemother. 50 (2006) 1372–1375.

[37] P.M. Bernardi, F. Barreto, T. Dalla Costa, Application of a LC-MS/MS method for evaluating lung penetration of tobramycin in rats by microdialysis, J. Pharm. Biomed. Anal. 134 (2017) 340–345.

[38] K.A. Rodvold, W.W. Hope, S.E. Boyd, Considerations for effect site pharmacokinetics to estimate drug exposure: concentrations of antibiotics in the lung, Curr. Opin. Pharmacol. 36 (2017) 114–123.

[39] H. Wiig, M.A. Swartz, Interstitial fluid and lymph formation and transport: physiological regulation and roles in inflammation and cancer, Physiol. Rev. 92 (2012) 1005–1060.

[40] G. Rutili, K.E. Arfors, Protein concentration in interstitial and lymphatic fluids from the subcutaneous tissue, Acta Physiol. Scand. 99 (1977) 1–8.

Original Research Article

Novel ligand-based docking; molecular dynamic simulations; and absorption, distribution, metabolism, and excretion approach to analyzing potential acetylcholinesterase inhibitors for Alzheimer's disease

Subramaniyan Vijayakumar [a,*], Palani Manogar [a], Srinivasan Prabhu [a],
Ram Avadhar Sanjeevkumar Singh [b]

[a] Computational Phytochemistry Laboratory, PG and Research Department of Botany and Microbiology, AVVM Sri Pushpam College (Autonomous) Poondi, Thanjavur (Dist), Tamil Nadu, India
[b] Computer Aided Drug Design and Molecular Modeling Laboratory, Department of Bioinformatics, Alagappa University, Karaikudi 630004, Tamil Nadu, India

ARTICLE INFO

ABSTRACT

Acetylcholinesterase (AChE) plays an important role in Alzheimer's disease (AD). The excessive activity of AChE causes various neuronal problems, particularly dementia and neuronal cell deaths. Generally, anti-AChE drugs induce some serious neuronal side effects in humans. Therefore, this study sought to identify alternative drug molecules from natural products with fewer side effects than those of conventional drugs for treating AD. To achieve this, we developed computational methods for predicting drug and target binding affinities using the Schrodinger suite. The target and ligand molecules were retrieved from established databases. The target enzyme has 539 amino acid residues in its sequence alignment. Ligand molecules of 20 bioactive molecules were obtained from different kinds of plants, after which we performed critical analyses such as molecular docking; molecular dynamic (MD) simulations; and absorption, distribution, metabolism, and excretion (ADME) analysis. In the docking studies, the natural compound rutin showed a superior docking score of -12.335 with a good binding energy value of -73.313 kcal/mol. Based on these findings, rutin and the target complex was used to perform MD simulations to analyze rutin stability at 30 ns. In conclusion, our study demonstrates that rutin is a superior drug candidate for AD. Therefore, we propose that this molecule is worth further investigation using in vitro studies.

1. Introduction

Alzheimer's disease (AD) is an irreversible neurodegenerative disease of brain neurons. The term Alzheimer's was first used by the German physician Alois Alzheimer in 1906 [1]. According to the World Health Organization (WHO), AD is the commonest cause of dementia, and it affects approximately 25 million people worldwide [2]. Acetylcholine (ACh) is an organic substance involved in the transfer of neuronal signals in the brain. Its hydrolysis into a cholineacetyl group is catalyzed by acetylcholinesterase (AChE) [3], which is a well-known enzyme that plays an important role in the central nervous system (CNS) [4]. The most important etiological factor in AD is not yet known; however, some established abnormal brain pathologies such as AChE over-expression and extracellular accumulation of "mysterious" β-amyloid plaques are the trademark of this disease.

Currently, four drugs that act as inhibitors of AChE are used in patients with AD, which are tacrine, dopenzil, galantamine, and rivastigmine [5–8]. These drugs are known to induce several side effects such as gastrointestinal disturbances, and they have low bioavailability. Hence, it is urgent to develop better inhibitors of AChE from natural sources to treat AD without any side effects. Currently, plants are used to enhance memory and to alleviate other problems associated with AD. Natural products and their derivatives are known to have efficient biological activities against numerous diseases, including CNS disorders [9]. Numerous plant-derived substances that may be considered as potential AChE drug molecules belong to different classes of compounds characterized by their structures [10].

Generally, medicinal plant-derived secondary metabolites such as alkaloids, flavonoids, tannins, saponins, and other phytochemicals show promising activities when they are consumed. They are also produced as part of the defence mechanisms against various

---

disorders and some highly pathogenic diseases. These active substances have been found to be beneficial for numerous therapeutic uses [11]. Recently, numerous plant-derived drugs have been investigated in clinical phase trials, and the trials of some molecules against globally challenging diseases have been successfully completed [12].

Currently, patients are seeking plant-based drug treatments for their health needs because these drugs are believed to have fewer side effects. Most individuals take only crude extracts for their health complaints which can never let them know the scientific background. Many research studies have isolated bioactive compounds from natural sources, but comprehensive studies are required to determine their molecular interactions. Therefore, in this study, we investigated the efficacy of some bioactive molecules using molecular docking and confirmed their mode of interaction with AChE.

2. Tools and methods

2.1. Modeling platform

The entire computational analysis was carried out using the Schrodinger suite using the Maestro10.2 version packages including LigPrep, Glide XP docking, grid generation, free energy calculations, absorption, distribution, metabolism, and excretion (ADME) toxicity, and MD simulations. Centos Linux was used as the operating system.

2.2. Biological data

In this study, 20 bioactive molecules were retrieved from the chemical database [13]. The AChE target was taken from the Protein Data Bank [14], and its databank alpha-numeric identity is PDB: 1B41.

2.3. Preparation of the protein

The protein was prepared using the wizard tool in Maestro version 10.2. During the process, the missing side and back chains were included [15]. The tool has two gears, namely, preparation and refinement. The X-ray crystallography structure of the protein molecules was occasionally bound and tangled with water molecules. The water molecule occupying the protein structure was not suitable for the docking study and, therefore, it was removed. Finally, the optimization and minimization processes were completed in this step [16].

2.4. Ligand preparation

All the ligand molecules were prepared using LigPrep2.4 [17], which can generate a number of structures from each input structure with various ionization states, tautomers, stereochemical characteristics, and ring conformations to eliminate molecules on the basis of various criteria such as molecular weight or specified numbers and types of functional groups with correct chiralities for each successfully processed input structure. The OPLS 2005 force field was used for the optimization, which produced the low-energy isomer of the ligand [18]. Finally, all the ligand molecules formed in the complex structure for input were docked.

2.5. Molecular docking

First, to test the docking parameters, all the ligand molecules were docked into the binding site of AChE using the Grid glide-based ligand docking program of Schrödinger suite [19,20]. In this study, the Maestro10.2 version tool was used to perform rigid, flexible docking for predicting the binding affinity, ligand efficiency, and inhibitory constant to the target [21]. The ligands were docked to the active site of AChE using Glide Extra precision (XP), which docks to determine the ligand's flexibility. Only the active small molecule would have available access to avoid the penalties and receive favourable docking scores with accurate hydrophobic contact between the protein and ligand. The electrostatic energy interaction of the hydrogen bonds involved both the side and back chains, hydrophobic contact, and Salt bridge contacts [22].

2.6. MD simulation

MD simulations were carried out using the Desmond software [23,24]. The optimized potentials for the liquid simulations (OPLS)-2005 force field were used in this system to determine the protein (AChE) interactions with efficient ligand molecules, which was solvated with the simple point charged (TIP4P) water model [23]. The orthorhombic water box was used to create a 10 Å buffer region between the protein atoms and box sides. Overlapping water molecules were deleted, and the systems were neutralized with Na^+ ions. The OPLS-2005 force field was used for energy calculation. The temperature was maintained constant at 300 K, and a 2.0 fs value was obtained in the integration step. We executed MD simulations for the complex structure of the protein as well as the target with position restraints for 6000 ps to allow the water molecules to remain in the system. Finally, the root mean square deviation (RMSD) was calculated to monitor the stability of the AChE protein in its native motion. The synchronize file was saved every 5000 ps for up to 30 ns and the result was scrutinized using the method described by Nagasundaram et al. [25].

2.7. Prime molecular mechanics-generalized born surface area (MM-GBSA) calculations

The ligand binding energy of each of the 20 phytocompounds required to inhibit AChE was estimated using the prime molecular mechanics-generalized born surface area (MM-GBSA) module in the Schrodinger Suite 2014 [26,27]. The total free energy binding (digibind, kcal/mol) was estimated as follows using the software:

$$\Delta G_{bind} = G_{complex} - \left(G_{protein} + G_{ligand} \right)$$

Where each energy term is a combination of G=molecular mechanics energies (MME)+GSGB (SGB solvation model for polar solvation)+GNP (non-polar solvation) [28] coulomb energy, covalent binding energy, Vander Waals energy, lipophilic energy, GB electrostatic solvation energy, prime energy, hydrogen-bonding energy, hydrophobic contact, and self-contact correction [29]. We then used this score to rank the ligand-protein Glide XP docked complex.

2.8. ADME toxicity

This approach has been very useful in drug discovery, especially in determining the mechanism of action of molecules [30]. A set of ADME-related properties was calculated for each of the 20 natural compounds using the QikProp program (Schrödinger software), which was run in the normal mode. QikProp generates physically relevant descriptors, and the toxicity of a ligand is considered important for it to act as an effective drug in new drug development [31,32].

3. Results and discussion

3.1. Molecular docking simulations and validation of docking protocol

The current study aimed to exploring the excessive activity of AChE inhibition bioactive molecules. The AChE target had a sequence length of 539 amino acids with a resolution of 2.76 Å. Descriptive hydrogen atoms were added to all the inhibitors to ensure they had all-atom structures, followed by energy minimization. After the preparation process, the protein was ready for molecular docking. This procedure shows the potential of the drug molecules to bind with the protein pocket and their hydrogen bond interactions. The complexes of each of the 20 bioactive molecules docked with the AChE protein. The molecular docking method has produced ligand docking scores with generating their H-bond distance values between ligand and target, and the consequent glide energy was also generated.

In this computational analysis, rutin had a higher docking score than that of the other ligand molecules. Furthermore, it showed a better binding affinity for the target than the other small molecules did. The bioactive molecule of rutin comes under the groups of flavonoids, and it has also exhibited admirable pharmacological and biological activities in numerous experimental studies. Recently, Ganeshpurkar and Saluja [33] reported that rutin shows effective pharmacological potential against the majority of diseases and conditions including neuroinflammation, and it promotes neuralcrest cell survival and has sedative, anticonvulsant, and anti-AD activities. Furthermore, it has been used in treatment of conditions such as hyperkinetic movement disorder, depression, and stroke.

In the present study, most of the bioactive molecules exhibited docking scores above −9.0 Among them, rutin had a superior docking score of −12.335, followed by hesperidin, which had a score of −10.708. At the end of this analysis, the computational tool showed some important outputs such as the ligand glide energy value and the MM-GBSA calculations (Table 1). Recently, numerous studies have used the molecular docking method because it identifies suitable drug molecules for the target

of interest [34–36]. In this study, the phytocompounds showed good measurable binding affinities for the target residues. The binding affinities were indicative of the ligand's contribution to and flexibility for the target. The present study also showed the H-bond distances and their contacts types for each molecule.

3.1.1. Rutin

The AChE protein residues interacted with the ligand atoms, and the surfaces were controlled by a complex array of intermolecular interactions. Such interactions depend on both specific interactions at the bindings site and the non-specific forces outside the target binding pocket. Here, the pattern of interaction between AChE and rutin in the complex is shown. We examined the site at which rutin bound to the target and found that it robustly interacted with the AChE residue to form a hydrogen bond. The Asp264, Asn564, His436, Arg327, Pro399, and Glu344 residues were in contact with the ligand atoms. Furthermore, Pro399 formed covalent hydrogen back chain contacts. Asn 264 formed H-bond back chain contacts with the rutin molecule. Arg327, Asn564, His436, and Glu344 formed H-bond side chain contacts with the ligand. His436 formed contacts with the side chain and π-π stacking contacts with rutin. It had a superior docking score to that of the other bioactive molecules, which is shown in Table 1. The ligand molecule residue contacts, hydrogen bond distances, and the types of contacts are shown in Fig. 1.

3.1.2. Hesperidin

Among the 20 ligands, hesperidin showed a docking score that was close to that of rutin at −10.708, and its glide energy values are shown in Table 1. The docked complex was examined, and the residue contacts with the ligand atoms were observed. The interaction plot shows the residue interactions of Thr269, Asp264, Gly265, Arg327, His436, and Pro399. The contacts formed involved different kinds of bonding lines and were back and side chain contacts, as well as hydrophobic contacts with rutin. Complete residues were formed only with the H-bond back chain contacts, except for the His436 residues because it connected the π-π stacking contacts with the ligand. The scrutinized docked complex

Table 1

Docking results of 20 bioactive molecules (ligands) and the energy generated by the active site of acetylcholinesterase (AChE).

S. no.	Compound name	Glide XP docking score	Glide XP energy (kcal/mol)	Glide XP emodel	MM-GBSA d Gbind (kcal/mol)
1.	Rutin	−12.335	−76.583	−90.567	−73.313
2.	Hesperidin	−10.708	−65.317	−85.199	−76.888
3.	5-O-[(2E)-3-(4-hydroxyphenyl)2-pro-penoyl]pentofuranosyl-(1–3)pentopyr-anosyl-(1–4)pentose	−10.512	−61.189	−63.749	−64.286
4.	Narirutin	−10.121	−61.981	−57.486	−65.786
5.	Glycyrrhizin	−9.954	−76.800	−61.064	−71.220
6.	Procyanidin B2	−9.691	−57.812	−78.705	−69.145
7.	Chlorogenic acid	−9.568	−50.985	−58.412	−64.789
8.	Zanamivir	−9.534	−48.060	−52.536	−52.115
9.	Mangiferin	−9.445	−51.920	−32.795	−50.071
10.	(R)-(+)-rosmarinic acid	−9.101	−54.367	−52.925	−54.433
11.	Ecdysterone	−7.786	−45.813	−55.997	−58.151
12.	D-(+)-Catechin	−6.944	−37.972	−50.899	−74.389
13.	D-(-)-Mannitol	−6.835	−34.461		−40.552
14.	Cidofovir	−6.744	−43.076	−46.260	−42.374
15.	rac 8-Prenylnaringenin	−6.584	−46.158	−42.355	−57.609
16.	Epicatechin	−6.582	−36.594	−55.853	−57.653
17.	(-)-Andrographolide	−6.324	−34.059	−51.453	−58.033
18.	Trifluridine	−6.276	−33.924	−42.160	−55.218
19.	(+)-[6]-Gingerol	−6.192	−40.933	−60.933	−41.552
20.	3-hydroxy-2,3-dihydropyrrolo[2,1b]quinazolin-9(1H)-one	−6.163	−50.509	−55.345	−58.090

Fig. 1. Rutin: Residues and hydrogen bond contacts (yellow dotted line) with their distance values (pink values), and the 2D template representing the types of contacts formed between the ligand and target.

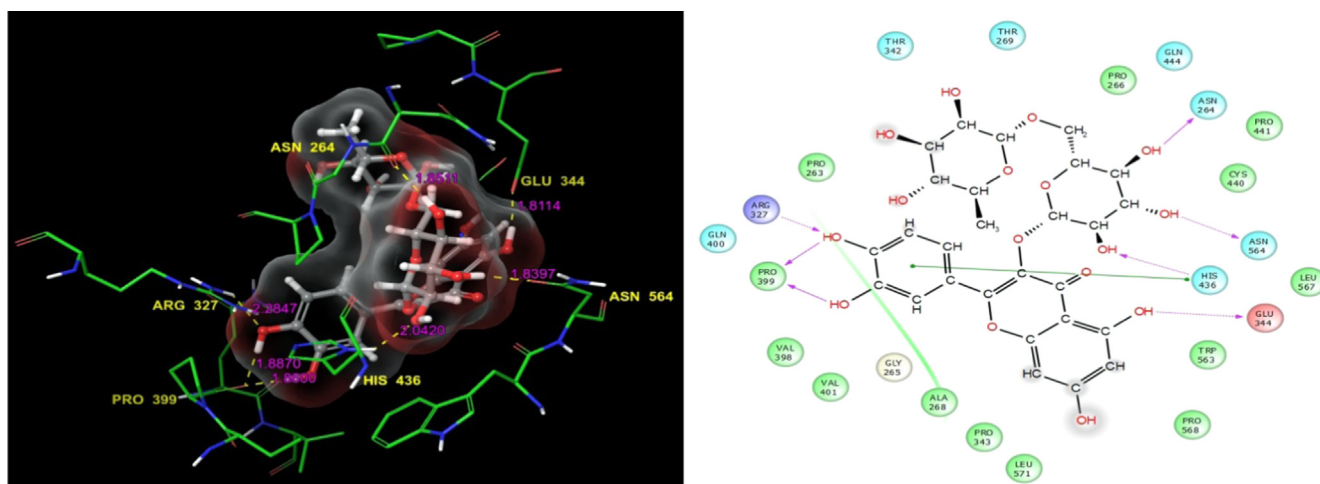**Fig. 2.** Hesperidin: Residues and hydrogen bond contacts (yellow dotted line) with their distance values (pink values), and the 2D template representing the types of contacts formed between the ligand and target.

Fig. 3. 5-O-[(2E)-3-(4-hydroxyphenyl)2-propenoyl]pentofuranosyl-(1-3)pentopyranosyl-(1-4)pentose: Residues and hydrogen bond contacts (yellow dotted line) with their distance values (pink values), and the 2D template representing the types of contacts formed between the ligand and target.
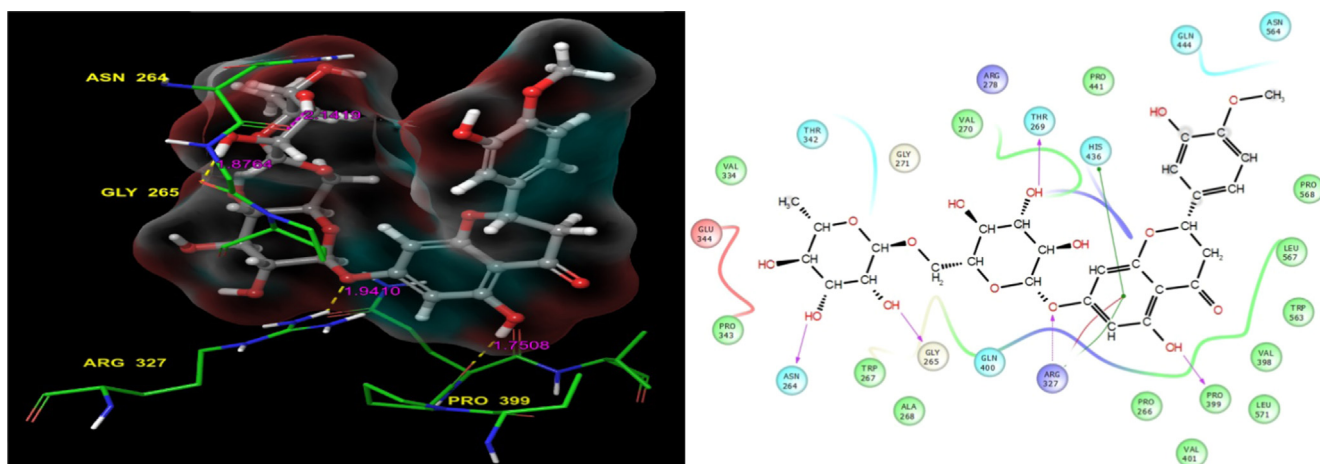
details such as the H-bond distance values, and the types of contacts are shown in Fig. 2. Previously, Remya et al. [37] conducted molecular docking studies of AChE using bioactive molecules, which showed that the hesperidin molecule had good binding affinities for AChE. It also had the second highest docking score in this study, similar to the results of this computational analysis. In addition, the anticoagulant activity of hesperidin has been investigated in vitro studies [37,38].

Fig. 4. Narirutin: Residues and hydrogen bond contacts (yellow dotted line) with their distance values (pink values), and the 2D template representing the types of contacts formed between the ligand and target.
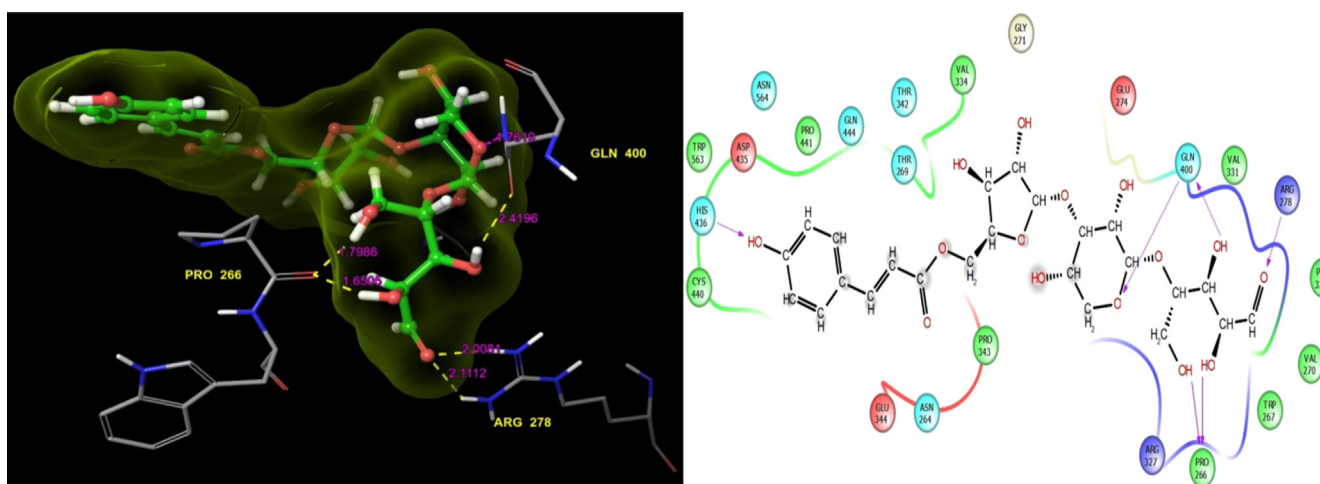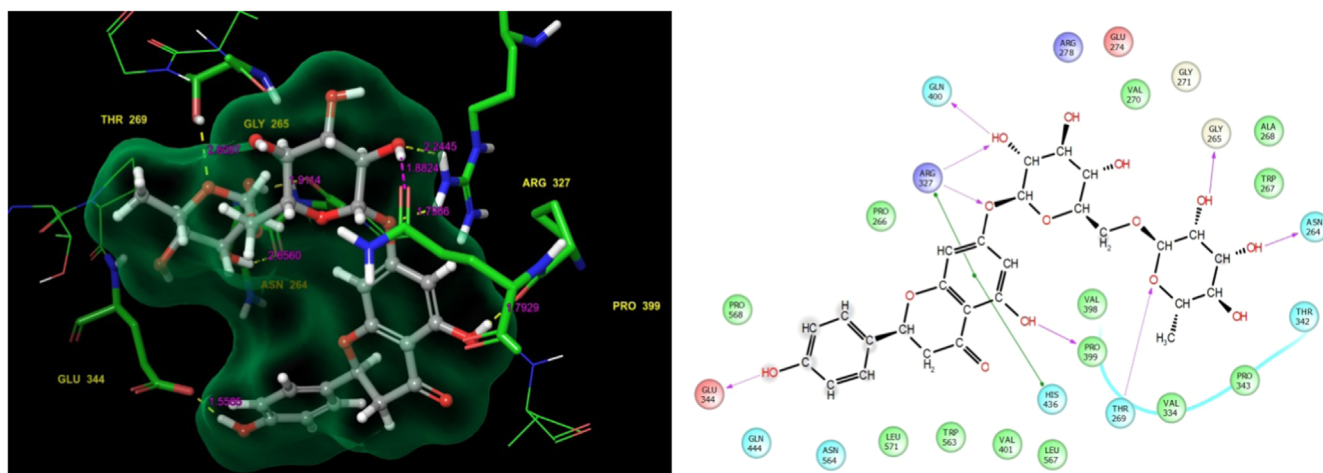

Fig. 5. Glycyrrhizin: Residues and hydrogen bond contacts (yellow dotted line) with their distance values (pink values), and the 2D template representing the types of contacts formed between ligand and target.
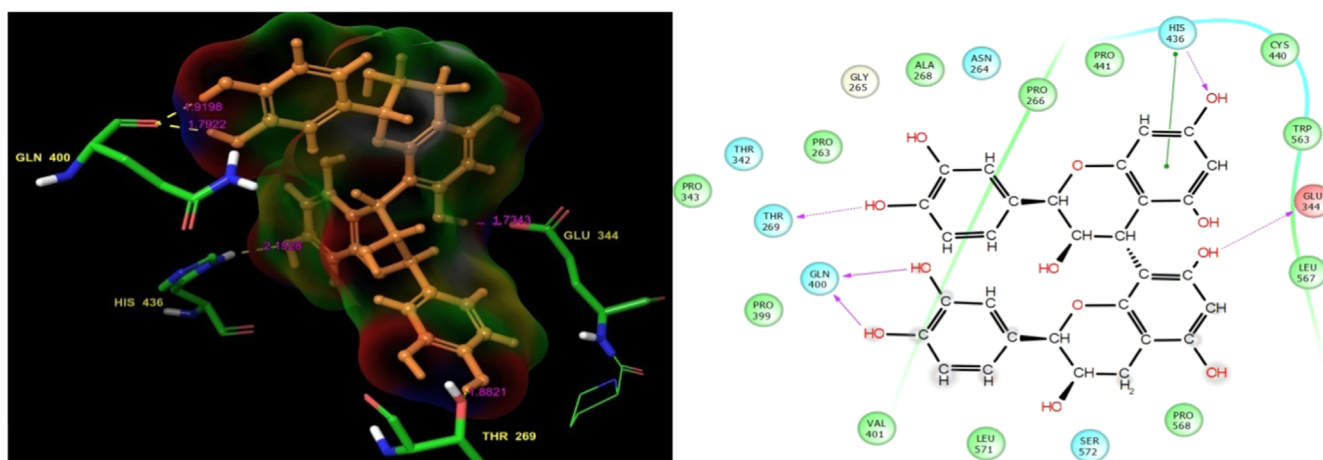
Fig. 6. (+)-Procyanidin B2: Residues and hydrogen bond contacts (yellow dotted line) with their distance values (pink values), and the 2D template representing the types of contacts formed between the ligand and target.
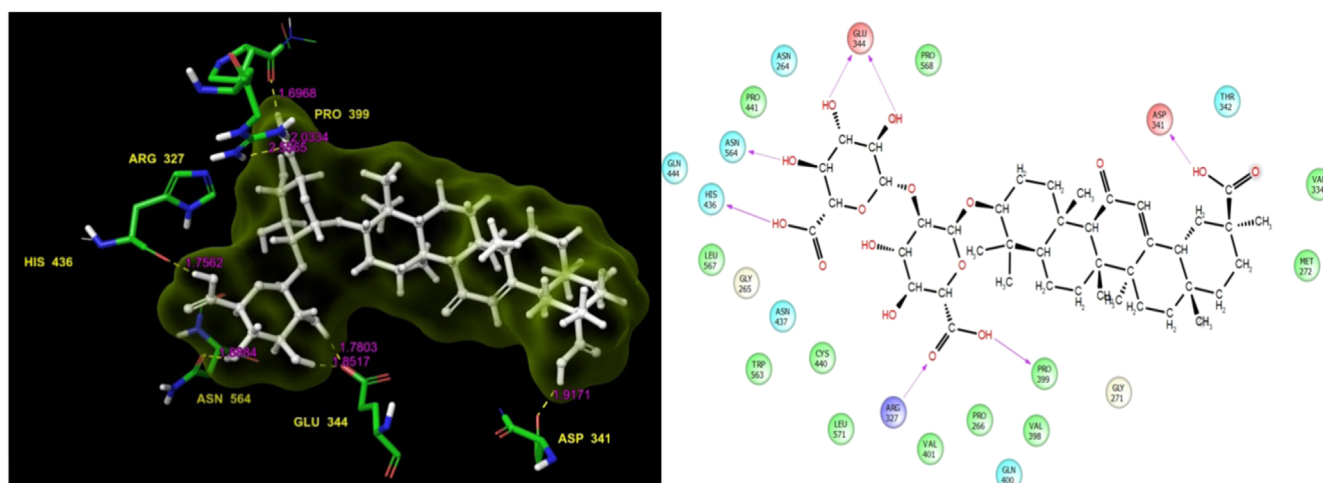
3.1.3. 5-O-[(2E)-3-(4-hydroxyphenyl)2-propenoyl]pentofuranosyl-(1-3)pentopyranosyl-(1-3.5.4)pentos

The bioactive molecular 5-O-[(2E)-3-(4-hydroxyphenyl)2-propenoyl]pentofuranosyl-(1-3)pentopyranosyl-(1-3.5.4)pentose showed the third most valuable docking score (−10.512) with good glide energy value (Table 1). The docked complex examination showed the residue was in contact with the ligand. His436, Gln400, and Pro266 formed H-bond back and side chain contacts

Table 2
Acetylcholinesterase (AChE) enzyme residue contacts with 20 bioactive molecules.

S. no.	Phytocompounds	Residues interactions and their distances	Types of bond formation	
			H-bond back chain	H-bond side chain
1.	Rutin	Pro 399 (1.86, 1.88), Arg 327 (2.28), Glu 344 (1.81), Asn 264 (1.85), Asn 564 (1.83), His 436(2.04)	Arg 327, Glu 344, Asn 564, His 436	Pro 399, Asn 264
2.	Hesperidin	Pro 399 (1.75), Asn 264 (2.14), Gly 265(1.87), Arg (1.94)	Arg 327 (1.94)	Pro 399 (1.75), Asn 264 (2.14), Gly 265 (1.87), Arg 278, Glu 400, His 436
3.	5-O-[(2E)-3-(4-Hydroxyphenyl) 2-propenoyl]pentofuranosyl-(1–3) pentopyranosyl-(1–4)pentose	Pro 266 (1.65), (1.79), Arg 278 (2.11, 2.08), Glu 400 (2.41), His 436 (2.44)	Pro 266 (1.65)	
4.	Narirutin	Glu 344 (1.55), Gln 400 (1.88), Gly 265 (1.91), Asn 264 (2.65), Thr 296 (2.60) and Pro 399 (1.79)	Glu 344, Gln 400, Gly 265, Thr 269	Asn 264, Pro 399
5.	Glycyrrhizin	Glu 344 (1.85), Asp 341(1.78), Asn 564 (1.88), His 436 (1.75), Arg 327 (2.55, 2.03), Pro 399(1.69)	Glu 344, Asp 341, Asn 564, Arg 327	His 436, Pro 399
6.	(+)-ProcyanidinB2	Gln 400 (1.79), Thr 269 (1.92), Glu 344 (1.23), His 436 (2.75)	Thr 269, Glu 344, His 436	Gln 400
7.	Chlorogenic acid	Asn 564 (1.85), Asn 264 (1.94), His 436 (1.89, 1.94), Pro 399 (2.03), Glu 344 (2.15)	Asn 564, His 436, Glu 344	Asn 264, Pro 399
8.	Zanamivir	His 436 (2.14), Asn 564 (2.21), Asn 264 (1.87), Glu 344 (1.92, 1.98), Gln 444 (1.78)	His 436, Asn 564, Asn 264, Glu 344	Gln 444
9.	Mangiferin	Gln 444 (1.63), Asn 564 (1.79), Thr 269 (1.93), Gln 400 (2.15)	Gln 444, Asn 564, Gln 400	Thr 269
10.	(R)-(+)-rosmarinic acid	Asn 264 (2.04), His 436 (1.95), Asn 564 (1.89), Pro 399 (1.97), Arg 327 (2.49)	Asn 564, Pro 399, Arg 327	Asn 264, His 436
11.	Ecdysterone	Asn 264 (1.88, 2.02), Arg 327 (2.38), Gln 400 (2.21, 2.16)	Arg 327, Gln 400	Asn 264
12.	D-(+)-Catechin	Gln 444 (2.03), Asn 264(2.37), Trp 563(1.63), Pro 399 (1.95)	Asn 264, Trp 563, Pro 399	Gln 444
13.	D-(-)-Mannitol	Glu 344 (1.92), Asn 264 (1.64), Gln 444 (2.14), Asn 564 (2.05)	Glu 344, Gln 444, Asn 564	Asn 264
14	Cidofovir	Pro 399 (2.11), Gln 400 (2.08, 2.04), Asn 564 (1.71), His 476 (1.78, 2.13)	Pro 399, Asn 564, His 476	Gln 400, His 476
15	rac 8-Prenylnaringenin	Asn 564 (1.74), His 436 (2.20), Gln 400 (1.93), Glu 344 (2.03)	Asn 564, His 436, Glu 344	Gln 400
16	Epicatechin	Glu 344 (1.89, 2.11), Asn 564 (1.96), Trp 563 (1.87)	Glu 344, Asn 564	Trp 563
17	(-)-Andrographolide	Asn 564 (1.72, 1.82)	Asn 564	–
18	Trifluridine	His 436 (2.05), Pro 399 (1.85), Arg 327 (1.97)	His 436, Arg 327	Pro 399
19.	(+)-[6]-Gingerol	Arg 327 (2.22, 2.70), Pro 399 (1.88), His 436 (1.95)	Arg 327	Pro 399, His 436
20.	3-Hydroxy-2,3-dihydropyrrolo [2,1-b]quinazolin-9(1H)-one	Glu 163 (1.93)	–	Glu 163

with the ligand. Specifically, the Gln400 residue was covalently bound to the ligand at the side chain contacts, and one end was connected to the ligand oxygen group while the other end was connected to the functional group of the ligand. The remaining Pro266 was covalently bound with the ligand functional group. The ligand molecule residue contacts, hydrogen bond distance values, and the types of contacts are shown in Fig. 3.

3.1.4. Narirutin

Narirutin had the fourth highest docking score of −10.121 and its glide energy value is shown in Table 1. It showed good binding affinities with the target residues. The scrutinized docked complex clearly showed the residue contacts. Specifically, Glu344, Gln400, Arg327, Thr269, Gly265, and Asn264 formed contacts with various atoms of narirutin. The interaction plot clearly shows the residue contacts with the side chain, back chain, and π-π stacking. Gly265 and Asn264 formed H-bond back chain contacts. The remaining residues, Glu344, Gln400, Arg327, and Thr269, formed H-bond side chain contacts with narirutin. Arg327 formed covalent H-bond contacts with the ligand. One end was connected to the ligand functional group while the other was an oxygen group. The π-π stacking bond contact formation was also shown. The ligand molecule residue contacts, hydrogen bond distance values, and the types of contacts are shown in Fig. 4. Murata et al. [39] evaluated the biological potential of narirutin, and found that it showed a significantly strong anti-degranulating activity.

3.1.5. Glycyrrhizin

Glycyrrhizin showed the fifth highest docking score of −9.954 and a good glide energy value, which was the highest

in this study (Table 1). It also showed good binding affinity. The docked complex showed a higher level of residue interactions than did the other ligand interaction patterns in this study. Specifically, Asn564, His436, Glu344, Arg327, Pro399, and Asp341 formed different kinds of H-bond contact lines with glycyrrhizin as well as the target. Asn564, Glu344, Arg327, and Asp341 were involved in the H-bond side chain contacts with glycyrrhizin. The Glu344 residue formed covalent contacts with the functional groups of the ligand and its molecule residue contacts, hydrogen bond distance values, and the types of contacts are shown in Fig. 5.

3.1.6. (+)-Procyanidin B2

(+)-Procyanidin B2 had the sixth highest docking score of −9.691 and a good glide energy value (Table 1). However, it showed a lower binding affinity than those of the previously listed small molecules. The docked complex interaction template showed it had residue interactions with Thr269, Gln400, His436, and Glu344. Moreover, Thr269, His436, and Gln344 were involved in side chain contacts with (+)-procyanidinB2 while Gln400 formed H-bond back chain contacts. It was also covalently bound with the functional groups of the ligand. Surprisingly, the His436 residue was involved in the H-bond side chain and π-π stacking contacts. The ligand molecule residue contacts, hydrogen bond distance values, and the types of contacts are shown in Fig. 6. The AChE residue interactions, H-bond distance values, and their contacts are shown in Table 2.

Similar to our study, Shruthika and Jency [40] previously performed molecular docking studies. However, they studied bioactive molecules against AD targets. They also screened 13 bioactive
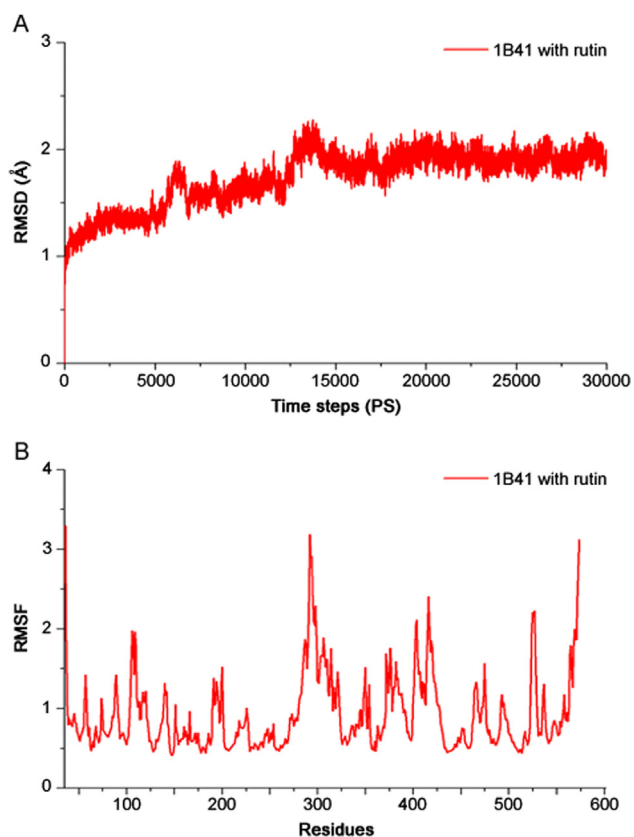
Fig. 7. Molecular dynamic (MD) simulations: (A) Root mean standard deviation (RMSD) of rutin with acetylcholinesterase (AChE) complex as a function of simulation time. (B) Root mean square fluctuation (RMSF) values of complex AChE residues with rutin.

molecules to determine their docking scores, binding energy, and number of bonds formed. Based on their research, the bioactive molecules docked against AChE. However, this research outcome represents bioactive molecules that showed superior docking scores and higher maximum binding affinities than those of the molecules reported previously [40].

3.2. MD

The MD simulation was performed for AChE and rutin complex to evaluate the structural constancy using the Desmond software. We ran MD simulations for the AChE protein and rutin for 30 ns. Initially, the RMSD plot showed that the complex deviated for a certain period and attained equilibrium at 17 ns. Subsequently, it remained stable throughout the simulation time for up to 30 ns (Figs. 7A and B).

3.3. ADME analysis

In this study, the ADME properties of 20 bioactive molecules were analyzed using the QikProp tool. This analysis presents the physicochemical properties of both synthetic and organic molecules and their biological functions. Based on the previous analysis, the physicochemical and biological properties we analyzed included the bioactive molecules, molecular formula, molecular weight, volume, SASA, acceptor H-bond, donor H-bond groups, the number of ring atoms, QPlogPw (-2 to 6.5), percentage human oral absorption, and CNS effects. These are all listed in Table 3. The ADME-based analysis is an important method for analyzing the efficacy of drug molecules. Much more information is recently available from studies related to ADME toxicity analysis of ligands including donor and acceptor hydrogen bonds, QPlogPw, percentage human oral absorption, and molecular weight [39].

4. Conclusion

AChE is one of the vital enzymes involved in regulating neuronal signaling. The excessive activity of this enzyme in patients with AD causes memory loss and impaired cognitive ability. Patients with AD are currently administered synthetic drugs that affect the organs and induce side effects. Therefore, our research study sought to identify alternative drugs from naturally available plants and their products. Of the bioactive molecules we screened, 20 showed potential and were selected. Their activity against the AChE target was analyzed to determine their suitability as drug molecules for treating AD by using computation. Most of the tested ligands exhibited effective docking

Table 3
Physicochemical properties and biological functions of 20 bioactive molecules analyzed using QuikProp.

S. no.	Molecular formula	Molecular weight (Da)	Volume	SASA	Acceptor H-bond groups	Donor H-bond groups	Number of ring atoms	QPlogPw (-2 to 6.5)	% Human oral absorption	CNS	Rule of five
1.	$C_{27}H_{30}O_{16}$	610.524	1552.483	778.079	20	9	28	-2.557	0.000	-2	3
2.	$C_{28}H_{34}O_{15}$	610.568	1671.132	866.924	20	7	28	-1.354	0.000	-2	3
3.	$C_{24}H_{32}O_{15}$	560.508	1568.806	821.477	22	7	17	-3.007	0.000	-2	3
4.	$C_{27}H_{32}O_{14}$	580.541	1611.303	837.282	19	7	28	-1.397	0.000	-2	3
5.	$C_{42}H_{62}O_{16}$	822.942	2190.041	1057.957	21	6	34	1.884	0.000	-2	3
6.	$C_{30}H_{26}O_{12}$	578.528	1519.296	807.567	10	10	32	0.453	0.000	-2	3
7.	$C_{16}H_{18}O_9$	354.313	995.503	553.076	9	6	12	-0.515	14.088	-2	3
8.	$C_{12}H_{20}N_4O_7$	332.313	963.976	535.187	12	9	6	-2.426	0.000	-2	1
9.	$C_{19}H_{18}O_{11}$	422.345	1127.265	634.363	13	7	20	-1.760	0.000	-2	2
10.	$C_{18}H_{16}O_8$	360.320	1094.899	637.616	7	5	12	-0.957	35.097	-2	2
11.	$C_{27}H_{44}O_7$	480.640	1443.524	746.044	9	6	17	-2.223	61.286	-2	0
12.	$C_{15}H_{14}O_6$	290.272	856.481	503.931	5	5	16	0.427	61.480	-2	1
13.	$C_6H_{14}O_6$	182.173	595.353	369.932	10	6	0	-3.079	28.264	-2	0
14.	$C_8H_{14}N_3O_6P$	279.189	794.879	616.277	12	5	6	-1.245	21.969	-2	1
15.	$C_{20}H_{20}O_5$	340.375	1093.897	466.636	2	2	16	3.323	88.020	-2	0
16.	$C_{15}H_{14}O_6$	290.272	834.190	477.400	5	5	16	0.286	60.152	-2	0
17.	$C_{20}H_{30}O_5$	296.203	1041.592	547.798	3	3	15	1.289	78.344	-2	0
18.	$C_{10}H_{11}F_3N_2O_5$	294.390	836.626	516.586	3	3	11	-0.359	53.875	-2	0
19.	$C_{17}H_{26}O_4$	234.821	1057.263	587.815	1	1	6	3.561	100.000	-2	0
20.	$C_6H_{11}O_6$	179.056	1037.142	526.327	6	5	13	-1.693	0.000	-2	0

SASA: Solvent Accessible Surface Area; QPlogPw: Solvation free energy in water; CNS: Central Nervous System.

scores with good binding affinities. In particular, rutin showed a superior docking score to that of the other bioactive molecules against AChE. Based on the outcome, we further evaluated the residue interaction with rutin and found it showed the maximum level of binding affinities. The other promising bioactive molecules, hesperidin, narirutin, glycyrrhizin and (+)-procyanidin B2 also showed good binding affinities in this analysis. Based on these results, we concluded that rutin is an effective and favourable potential anti-AChE drug and it may be a suitable drug candidate for AD. Further, in vitro studies on the purified rutin molecule are ongoing using various concentrations in neuronal cell lines.

Conflicts of interest

The authors declare that there are no conflicts of interest.

Acknowledgments

References

[1] A.K. Singhal, V. Naithani, O.P. Bangar, Medicinal plants with a potential to treat Alzheimer and associated symptoms, Int. Nutr. Pharmacol. Neurol Dis. 2 (2012) 84–91.

[2] C. Qiu, M. Kivipelto, E. von Strauss, Epidemiology of Alzheimer's disease: occurrence, determinants, and strategies toward intervention, Dialogues Clin. Neurosci. 11 (2009) 111–128.

[3] A. da Silva Goncalves, T.C. Franca, O. Vital de Oliveira, Computational studies of acetylcholinesterase complexed with fullerene derivatives:a new insight for Alzheimer disease treatment, J. Biomol. Struct. Dyn. 34 (2016) 1307–1316.

[4] M.B. Colovic, D.Z. Krstic, T.D. Lazarevis Pasti, Acetylcholinesterase inhibitors: pharmacology and toxicology, Curr. Neuropharmacol. 11 (2013) 315–335.

[5] P.J. Whitehouse, Cholinergic therapy in dementia, Acta Neurol. Scand. Suppl. 149 (1999) 42–45.

[6] C.A. Kelly, R.J. Harvey, H. Cayton, Drug treatments for Alzheimer's disease, Br. Med. J. 314 (1997) 693–694.

[7] L.J. Scott, K.L. Goa, Galantamine: a review of its use in Alzheimer's disease, Drugs 60 (2000) 1095–1122.

[8] M.D. Gottwald, R.I. Rozanski, Rivastigmine, a brain region selective acetylcholinesterase inhibitor for treating Alzheimer's disease: review and current status, Expert Opin. Investig. Drugs 8 (1999) 1673–1682.

[9] G.P. Kumar, F. Khanum, Neuroprotective potential of phytochemicals, Pharmacogn. Rev. 6 (2012) 81–90.

[10] K. Rashed, A.C.C. Sucupira, J.M.M. Neto, et al., Evaluation of acetylcholinesterase inhibition by Alnus rugosa L. stems methanol extract and phytochemical content, Int. J. Biomed. Adv. Res. 4 (2013) 366.

[11] A.G. Atanasov, B. Waltenberger, E.M. Pferschy-Wenzig, et al., Discovery and resupply of pharmacologically active plant-derived natural products: a review, Biotechnol. Adv. 33 (2015) 1582–1614.

[12] L. Ghribia, H. Ghouilaa, A. Omrib, et al., Antioxidant and anti-acetylcholinesterase activities of extracts and secondary metabolites from Acacia cyanophylla, Asian Pac. J. Trop. Biomed. 4 (2014) S417–S423.

[13] ⟨http://www.chemspider.com⟩.

[14] ⟨http://www.rcsb.org⟩.

[15] S.K. Tripathi, M. Ravikumar, Sanjeev Kumar Singh, extra precision docking, free energy calculation and molecular dynamics simulation studies of CDK2 inhibitors, J. Theor. Biol. 334 (2013) 87–100.

[16] LigPrep, version 2.5, Schrödinger, LLC, New York, 2011.

[17] K.K. Kakarala, K. Jamil, V. Devaraji, Structure and putative signaling mechanism of protease activated receptor 2 (PAR2)– a promising target for breast cancer, J. Mol. Graph. Model. 53 (2014) 179–199.

[18] Glide, version 5.7, Schrödinger, LLC, New York, 2011.

[19] K.M. Elokely, R.J. Doerksen, Docking challenge: protein sampling and molecular docking performance, J. Chem. Inf. Model. 53 (2013) 1934–1945.

[20] T.A. Binkowski, W. Jiang, B. Roux, et al., Virtual high-throughput ligand screening, Methods Mol. Biol. 1140 (2014) 251–261.

[21] X.Y. Meng, H.X. Zhang, M. Mezei, et al., Molecular docking: a powerful approach for structure-based drug discovery, Curr. Comput. Aid. Drug Des. 7 (2011) 146–157.

[22] Desmond, version 3.0, Schrödinger, LLC, New York, 2011.

[23] J.J. Blessy, D.J. Sharmila, Molecular simulation of N-acetylneuraminic acid analogs and molecular dynamics studies of cholera toxin-Neu5Gc complex, J. Biomol. Struct. Dyn. 33 (2015) 1126–1139.

[24] W.L. Jorgensen, D.S. Maxwell, J.T. Rives, Development and testing of the OPLS All-atom force field on conformational energetics and properties of organic liquids, Am. Chem. Soc. 118 (1996) 11225–11236.

[25] N. Nagasundaram, H. Zhu, J. Liu, et al., Analysing the effect of mutation on protein punction and discovering potential inhibitors of CDK4: molecular modelling and dynamics studies, PLoS One 8 (2015) e0133969.

[26] Prime, version 2.1, Schrödinger, LLC, New York, 2011.

[27] J.M. Hayes, G. Archontis, MM-GB(PB)SA calculations of protein-ligand binding free energies, molecular dynamics - studies of synthetic and biological macromolecules, L. Wang (Ed.), InTech, DOI: http://dx.doi.org/10.5772/37107.

[28] K.K. Kakarala, K. Jamil, Protease activated receptor-2 (PAR2): possible target of phytochemicals, J. Biomol. Struct. Dyn. 33 (2015) 2003–2022.

[29] M.S. Lee, M.A. Olson, Comparison of volume and surface area non polar solvation free energy terms for implicit solvent simulations, J. Chem. Phys. 139 (2013) 044119.

[30] T. Katsila, G.A. Spyroulias, G.P. Patrinos, et al., Computational approaches in target identification and drug discovery, Comput. Struct. Biotechnol. J. 14 (2016) 177–184.

[31] QikProp, version 4.3, Schrödinger, LLC, New York, 2014.

[32] F. Ntie-Kang, L.L. Lifongo, J.A. Mbah, et al., In silico drug metabolism and pharmacokinetic profiles of natural products from medicinal plants in the Congo basin, In Silico Pharmacol. (2013), ⟨http://dx.doi.org/10.1186/2193-9616-1-12⟩.

[33] A. Ganeshpurkar, A.K. Saluja, The pharmacological potential of rutin, Saudi Pharm. J. 25 (2017) 149–164.

[34] S. Subhani, A. Jayaraman, K. Jamil, Homology modelling and molecular docking of MDR1 with chemotherapeutic agents in non-small cell lung cancer, Biomed. Pharm. 71 (2015) 37–45.

[35] J. Sharma, K. Ramanathan, R. Sethumadhavan, Identification of potential inhibitors against acetylcholinesterase associated with alzheimer's diseases: a molecular docking approach, J. Comput. Method Mol. Des. 1 (2011) 44–51.

[36] S. Roy, A. Kumar, M.H. Baig, et al., Virtual screening, ADMET profiling, molecular docking and dynamics approaches to search for potent selective natural molecules based inhibitors against metallothionein-III to study Alzheimer's disease, Methods 83 (2015) 105–110.

[37] C. Remya, K.V. Dileep, I. Tintu, et al., Flavanone glycosidesas acetylcholinesterase inhibitors: computational and experimental evidence, Indian J. Pharm. Sci. 76 (2014) 567–570.

[38] V. Kuntic, I. Filipović, Z. Vujić, Effects of rutin and hesperidin and their Al (III) and Cu (II) complexes on in vitro plasma coagulation assays, Molecule 16 (2011) 1378–1388.

[39] K. Murata, S. Takano, M. Masuda, et al., Anti-degranulating activity in rat basophil leukemia RBL-2H3 cells of flavanone glycosides and their aglycones in citrus fruits, J. Nat. Med. 67 (2013) 643–646.

[40] A. Shruthika Ravel, S. Jency, QSAR and docking studies on phytocompounds as lead molecule against Alzheimer's disease, Int. J. Curr. Res. 5 (2013) 1198–1201.